2014

Acta carsologica, Volume 43, Issue 1, 2014

Franci Gabrovšek
Karst Research Institute, ZRC SAZU, Slovenia, gabrovsek@zrc-sazu.si

ACTA CARSOLOGICA

43/1 · 2014

ACTA CARSOLOGICA
ISSN 0583-6050

Naslov uredništva / Editor's address:
Inštitut za raziskovanje krasa ZRC SAZU - Karst Research Institute ZRC SAZU
SI - 6230 Postojna, Titov trg 2, Slovenija
Fax: +386 (0)5 700 19 99; e-mail: gabrovsek@zrc-sazu.si

Vsebina je prosto dostopna na spletnem naslovu / The content is freely available at: http://ojs.zrc-sazu.si/carsologica/

Sprejeto na seji IV. razreda SAZU 18. 2. 2014 in na seji predsedstva SAZU 25. 2. 2014.

Distribucija in prodaja / Ordering address:
Založba ZRC/ZRC Publishing
Novi trg 2, P.O.Box 306, SI-1001 Ljubljana, Slovenia
Fax: +386 (0)1 425 77 94; e-mail: zalozba@zrc-sazu.si; http://zalozba.zrc-sazu.si

Acta Carsologica izide trikrat letno / Acta Carsologica is published three times a year

Cena / Price
Posamezni izvod / Single Issue
Individual / Posameznik: 15 €
Institutional / Institucija: 25 €

Letna naročnina / Annual Subscription
Individual / Posameznik: 25 €
Institutional / Institucija: 40 €

Slika na naslovnici: Gravitacijsko odprte razpoke v pobočjih gore MeBreda, nad vadijem Shehah, Združeni Arabski Emirati (gl. članek Al Farray *et al.*).

Cover figure: Gravitational crevices on the slopes of MeBreda above Wadi Shehah (see: Al Farray *et al.*).

ACTA CARSOLOGICA

43/1
2014

SLOVENSKA AKADEMIJA ZNANOSTI IN UMETNOSTI
ACADEMIA SCIENTIARUM ET ARTIUM SLOVENICA
Razred za naravoslovne vede – Classis IV: Historia naturalis

ZNANSTVENORAZISKOVALNI CENTER SAZU
Inštitut za raziskovanje krasa – Institutum carsologicum

LJUBLJANA 2014

ACTA CARSOLOGICA je vključena / *is included into:* THOMSON SCIENTIFIC Science Citation Index Expanded, Journal Citation Reports – Science Edition, Zoological Records / Elsevier SCOPUS / Current Geographical Contents / *Ulrich's* Periodicals Directory / COS GeoRef / BIOSIS Zoological Record.

ACTA CARSOLOGICA izhaja s finančno pomočjo / *is published with the financial support of:*
Agencije za raziskovalno dejavnost RS / *Slovenian Research Agency in* Slovenske nacionalne komisije za UNESCO / *Slovenian National Commission for UNESCO*

CONTENTS

VSEBINA

INTERVIEW WITH ANDREJ KRANJC

conducted by Nataša Ravbar

Andrej Kranjc is a world-recognized karstologist and speleologist for his achievements in karst geomorphology, hydrology, cave research, karst terminology and history of karst science. In 2013 he celebrated his 70th anniversary. As his student and colleague I took this opportunity to present some highlights of his life and work.

Despite being retired already since 2010, he is currently a Vice-President of the Slovenian Academy of Sciences and Arts. During our relaxing and amusing conversation in his office over a cup of coffee the present interview arose.

Andrej, how did you get acquainted with karst and became close to it?

Oh, this was a long time ago. I knew well Stane Pirnat who was living in the neighbourhood and we hang out together. When he was already a caver, he invited me to join him caving in Matjaževa jama under Šmarna gora close to Ljubljana. This was the first non-tourist cave I visited. Later, when I was already in high school, Dušan Novak, a geologist, made publicity of caving and speleological section of Planinsko društvo Železničar (Mountaineering Club Železničar). I decided to join it.

In the frame of this section I often went with Jože Bole and Boštjan Kiauta who were spelebiologists, collecting snails into caves in the surrounding of Domžale and Moravče (N and NE of Ljubljana). I had to carry textile bags and gather soil where Bole was searching for snails. Sometimes I also joined Dušan Novak at a field work carrying samples of rocks.

So, I got involved in caves and caving. With the cavers from the speleological section I learned basics of caving and cave mapping. This then led me to get acquainted with cave biology which in the beginning interested me the most. I even wanted to study biology to specialize myself to cave biota. However, I also like travelling. And just before I enrolled in University I changed my mind and decided for geography, because somehow I thought if I study geography, there will be more chances for travel.

In 1959 I was already a caver. Nada Čadež Novak and later Peter Habič worked on tracer experiments. I joined their teams for manual sampling, because at that time there were no automatic samplers. We were sampling at the Rižana, Lintvern and other springs. Every year I spent about a month in the field, camping near the springs and taking samples when necessary. I liked this very much and a lot of interesting things happened.

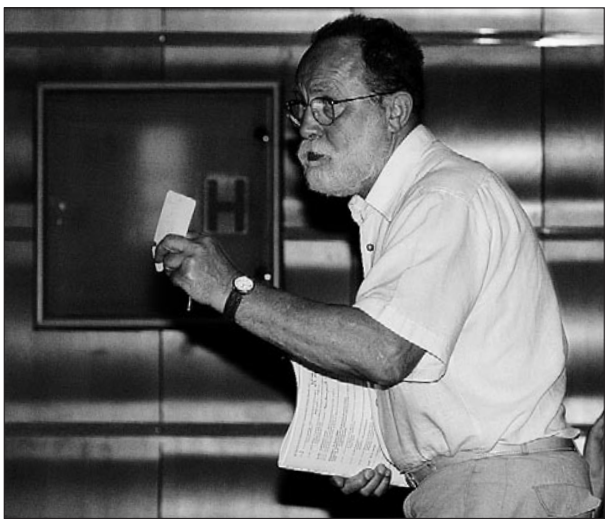

Andrej Kranjc chairing a session at the 14th International Karstological School "Classical Karst" in Postojna in 2006 (Karst Research Institute Archives).

Your scientific work is entirely devoted to karst and caves, from the diploma, master and doctoral thesis, to the most recent scientific and popular publications. Your doctoral thesis from 1987, was dedicated to the fluvial transport in karst. Unfortunately, the work was rather overlooked, unacknowledged and mostly not known in that time. Yet the citations, mostly in foreign literature, show that the work received some international response. What, on your opinion, is the highest achievement of your thesis?

This is difficult to say. At that time the research trend was to study fluvial or recent cave sediments. In England there was Peter Bull, who made thorough studies on fluvial transport in karst. On my opinion the highest value of my thesis was that similar studies have not been done in Slovenia. And my research was the first –

that was important. Another aspect was the presentation how the transported material, the pebbles form. I think this was very interesting. I emphasized their origin and role in speleogenesis. For example, in Škocjanske jame at the beginning, where Reka River enters the cave system a lot of flysch pebbles are present and then downwards towards the siphon there is less and less of these pebbles, and they are smaller and smaller.

Your mentor was prof. Ivan Gams, one of the leading persons of the international karstology. What did you learn from him?

A lot, but to summarize – I started to work under prof. Gams in 1965 for the preparations of the 4th International Speleological Congress that was held in Postojna and Ljubljana. He needed somebody for help. He asked students and I applied. I must say that I was not automatically accepted, but had to pass typing test. I worked four months for organization of this congress.

Then when I studied geography, prof. Gams just started to give lectures at the university. Before that he was employed at the Karst Research Institute in Postojna. I was in the first generation of his students. He introduced me to karst geomorphology and geography of karst. He impressed me with his enthusiastic lectures that were much more interesting in comparison to others. He also organized long and interesting geomorphological excursion going from Slovenia across Alps to France. The trip lasted for two or three weeks. We were a small group of 15 to 20 students and we had lectures practically in the field. At that occasion we learned a lot.

Prof. Gams was my supervisor for master and doctoral thesis. We often met for discussions. When meeting him he also introduced me to his colleagues Valter Bohinec, Svetozar Ilešič and Roman Savnik, all being eminent Slovene geographers. Gradually I was brought to their company and had the opportunity to discuss with them.

The period of your professional work is imbued with the Karst Research Institute (KRI) from Postojna that would without you not have the importance in world karstology as it has today. Did prof. Gams bring you to KRI in 1966 where you stayed employed until your retirement?

No, it was dr. Peter Habič. That was after I finished working for the Speleological Congress, it was decided to publish all the presentations and discussions from the Congress that have been recorded to tape recorder. That is how my part-time employment at the KRI started. This was rather ungrateful work, because the recording was of bad quality, it was impossible to recognize who is talking, the recorded sections were mixed. So, after all, most of the records were not published.

In summer 1966 I guided tours of foreign speleologist or karstologists who came to visit the cradle of karstology. A year later I was full time employed and was tasked to make preparation research for the motorway route between Postojna and Vrhnika. This was one of the first applied projects KRI was working on. My job was to map all the dolines that were in the route and to evaluate how much sediment there is on the bottom of these dolines. Every day I went mapping and occasionally drilling the bottoms of these dolines with a hand auger. A lot of material and data on dolines characteristics was gathered and I am very sorry that none of these was ever published. In quite some dolines that we selected even the whole material has been excavated and a lot of money invested so that we were able to see how the bottoms looked like. A lot of pictures and measurements were taken.

In 1972 you made specialization in France, under the supervision of dr. Alain Mangin. What experience did you gain there?

There were in fact two, on my opinion, very precious experiences. On one hand I absorbed a lot of knowledge on regional karst. Bernard Gèze, a very well known French speleologist and karstologist, together with dr. Mangin, organized a thorough trip across French karst for prof. Bleahu from Romania to show him most spectacular phenomenon. Luckily, it was possible for me to join them. The trip took us three weeks altogether and I experienced a lot.

On the other hand, I got the experience to see and feel, how research institutions abroad work. In that time working at a foreign institute was rarity and not a lot of my colleagues had such an opportunity. I must say that the manner of education and specialization in France was much different than in Yugoslavia.

My primary institution abroad was Laboratoire souterraine in Moulis, which was important institute. Dr. Mangin organized that I visited some other centres and professors in France who worked on karst. I visited prof. Nicod with whom I still have very good contacts, I can say we are friends. Dr. Renault who was specialized in sediments took me to Vercors Plateau for two days and we discussed sediments, because this was my specialization, and he explained me some aspects. Many of eminent professors I met gave me their doctoral thesis that I still keep at home.

In connection to your basic research you focused on the karst geomorphology, hydrology and cave climate. More than with the theoretical aspects you dealt with environmental issues, protection and conservation of karst. In later years, you devoted more to karst terminology and history of karstology. You are also known as a good expert in regional karstology. You

have visited most of the famous karst places. Is there a region that you haven't been but you would still like to visit?

Oh yes, of course. I like travelling. This means that I would like to go everywhere where it is possible, not just to karst regions. Once, it is probably tens of years ago, I counted caves that I have been to, including very small ones, and I reached a number of 1,000 to 1,200.

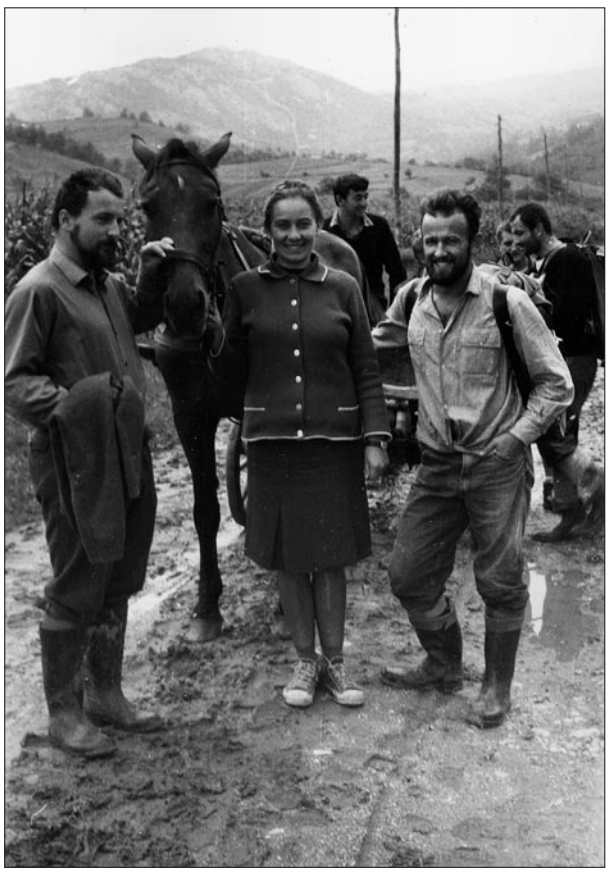

Andrej Kranjc, local girl and Boris Sket on the way from Ohaba- Șura Mare cave in Romania, August, 1968 (Andrej Kranjc archives).

And it is true, I visited karst areas in the whole continents, except in Antarctica, of course. I can say that I visited karst for example in North America, but the continent is so large that I only visited a small part of karst there. In South America I was three times in Brazil and at least two times I visited the same caves. I would still like to visit Magellan Strait and Tierra del Fuego to see the karst in marbles.

Between 1988 and 1995 you were the head of the KRI. Among others in 1993 following your initiative KRI started to organize International Karstological Schools that later grew into the main annual karstological events in the world. How do you remember this period? Some of our colleagues remember you as a very strict boss.

I wish I would have been stricter boss. I do not think I was strict enough. In general, I do not have nice memories on this period. There were problems with money. Also for Acta Carsologica printing we had high depths. At that time I did not sleep well, because I always had fear and worries, whether we would get projects or not. Because we did not have enough projects I had to fire some of very capable young colleagues.

And then there were also some disagreements among colleagues about the orientation, vision and priorities of the KRI. Some did not see it necessary to focus also on biological studies, even though it turned out that it would be good that we also oriented at least to ecology. I had the vision that a truly good research institution should be expanding not shrinking its capacities and that we should support young researchers, to educate and skill them, to ensure inheritance of our work.

For me it is better not to remember those days. But at least I managed that KRI did not go bankrupt or declined.

Regarding the International Karstological Schools it was actually dr. Zofija Klemen Krek, a Director of the Bureau of Slovenian National Commission for UNESCO, who took the initiative. At that time we were preparing proposal for Kras to be included in the UNESCO world heritage, so I had very frequent contacts with her. She offered financial help and Slovene "UNESCO" is still the sponsor of the School.

Related to your research work and publications including your large international connections, you were invited to join different international organizations, such as World Commission on Protected Areas, The World Conservation Union – Task Force for Caves and Karst, International Association of Hydrogeologists, Karst Commission of International Geographical Union, which chair you were, International Speleological Union, International Quaternary Research Association and others. Why do you think you were trusted such honourable, but responsible functions?

I considered these functions very seriously. I never tried to promote my research and ideas in these circles and forcing my mind. If necessary I told my opinion. Of course, if somebody needed my help, I was willing to do so, for example also to find results of other researchers, not only mine. Still now I am active in different committees and boards.

Between 1993 and 2010 you were the Editor-in-chief of the leading karstological journal Acta Carsologica (AC). In 2007 you succeeded that the journal

was included in the SCI (Thomson) bibliometrical system. How did you see the journal's mission then?

I think that especially in that time the journal developed from internal journal, publishing mostly results of the KRI, to what is now. Previously the authors were mostly researchers from the KRI, articles published almost entirely in Slovene. It was not a yearly publication, but only when there were enough papers. Presently AC cannot be called an international journal, because it is not: the editors, financers and most important driving wheels of the journal are Slovenes and it is published in Slovenia after all. But I think it has an international reputation, it is accepted by the distinguished authors and they like to have papers published in AC, despite the impact factor is not very high. It has the authors from all over the world, it is published in English. Now, you know better than me, that AC Editorial has problems of too many submitted manuscripts. So, I think AC really developed well. Also the appearance changed completely and I like it very much.

International and national recognition of your work is shown through the chairs or memberships of steering committees and boards, through awards like French Chévalier des Palmes Académiques, Award for research in Slovene identity, Golden medal of Slovene Geographical Society, membership of the Slovenian Academy of Sciences and Arts and through invitation to be a member of different scientific and editorial boards of leading journals on karst. Apart from the professional you performed a number of functions, primarily related to research and professional activities of the local, municipal to the republic level. However, many of readers probably do not know that you are also a war veteran.

Yes, I was a soldier in Yugoslav national army. During the Slovene independence war in 1991 I was involved in territorial defence and I was assigned a group for mobilization. One year before I had to report all my absence from Postojna because of this, and I was forbidden to leave Postojna a week before the war started.

During the war Yugoslav army wanted to get all the registers of people who can be mobilized from the communities. In Postojna this register was hidden in the KRI in my office for one week. Our commander and a soldier were also sleeping in my office for two nights, because Yugoslav army was searching it intensively. However, the register was safely hidden. At that time I also had to wear weapon, which did not make me feel very well. I am sorry that I have never seen or heard that KRI is thanked for this as an institution, although this thing was really very important.

Thanks to your vision and initiation, and to your persistence, the Postgraduate study of Karstology, unique of its kind was introduced in 2001. Did it take a lot of effort from the idea to the realization?

Its history is very long. At the KRI I made the proposal already at the end of 70ies that it would be good if we can have a study of Karstology in Slovenia. Many times at different political constellations we proposed it to different institutions like ministries, universities, research authorities and so on. I also informed the director of the Research Centre of the Slovenian Academy of Sciences and Arts, a part of which KRI is, dr. Oto Luthar and it was him who passed the idea to the newly established Faculty of Humanities in Koper. He was very tightly engaged in its organization and the Faculty tried to offer something different than the rest of the Slovene universities. Later, in 2003, the programme was moved to the University of Nova Gorica.

Andrej Kranjc in Jama v grapi, 1971 (Photo: France Habe, Andrej Kranjc Archives).

In addition, I would like to emphasize that I just came back from China, from the meeting of the Scientific Committee of the International Research Centre on Karst under auspices of UNESCO at Guilin. A very old

idea of mine is that KRI becomes an UNESCO's Karst research centre or that the programme Karstology of the University at Nova Gorica becomes an UNESCO Chair on Karstology. We started the procedure already years ago but I am afraid that we are too slow. As I recognized now in Guilin China and Hungary are in front of us already, which is a pity.

Andrej Kranjc, Janja Kogovšek and Alojz Vadnjal, 1976, in one of the Institute's field trips to Voje valley, Bohinj, Slovenia (Andrej Kranjc Archives).

You also gave lectures at other faculties and have been a mentor to many researchers at home and abroad. What is the most important that you wanted to pass on to them, on to us?

The most important thing I wanted to teach my students is to be good, responsible and competent karstologist. I always said: You cannot know all the details, but you have to know karst, what it is, how it originates, where it is, who works on karst. And if the doctors of karstology are in circles discussing about karst, it is not important on which topic, either it is tourism in caves, paleomagnetic research or speleobiology, he or she has to know it, understand it and has to be able to be involved in the discussion. Of course nobody is specialist and knows everything, but a student of karstology has to have the general level of knowledge about karst quite high. This is the most important than he or she can become specialized for whatever interests him/her.

What are your present responsibilities in the role of the Secretary-General of the Academy?

Nothing special. I am a part of the Executive Board. That means that I help the things at the Academy are going on. Academy is not very flexible, not very fast in reacting. In any case I am trying to combine this small occupation with my professional work. Sometimes it is possible to join and sometimes Academy helps me to go to the field or to participate professional meetings. For example this year I took part at the Academy exchange with Czech Academy in Prague and I combined it with the participation in International Speleological Congress at Brno. It was the same two or three years ago. When I made exchange with Russian Academy in Moscow, I visited northern Russia gypsum karst.

Besides karst what attracts you as well?

At home, I like wood chopping. In this way I can relax from office work. But my great passion, my hobby are books. My father in law was expert on Slavic languages and he had practically all modern Slovene literature and some foreign literature as well. I upgraded his collection. We now have too many books already. Practically everywhere in our house, where possible there are bookshelves, so books are everywhere. We decided at home that we will not buy books anymore, but just yesterday I saw an interesting book in a bookshop nearby and I will most probably buy it.

Besides this I initiated postcard collection in our family. I now handed over my relatively small collection to my son and I help him replenishing it. Especially when I am going somewhere, I always send him postcards. And I am also collecting stamps, but with karst and cave motives. The other motives I collect are birds. However, I am not a very serious collector.

If you look at all these 70 years, what would you put in the forefront?

I have very little memory of my early, school ages. I have to say that I never enjoyed school very much. I had such traumatic experience that even ten years after I started to work I was afraid of Mondays. So, working was much more relaxing and I am happy that I could work on what delighted me.

Andrej, thank you very much for your time and I wish you health and many more years to come.

Thank you. I hope only that my mind will serve me – it does not matter how long.

COBISS: 1.01

LOWER- TO MIDDLE PLEISTOCENE FLANK MARGIN CAVES AT CUSTONACI (TRAPANI, NW SICILY) AND THEIR RELATION WITH PAST SEA LEVELS

SPODNJE DO SREDNJE PLEISTOCENSKE JAME TIPA FLANK MARGIN PRI CUSTONACI (TRAPANI, SZ SICILIJA) IN SPREMINJANJE MORSKE GLADINE

Rosario RUGGIERI[1,2] & Jo DE WAELE[3*]

Abstract UDC 551.435.8:551.468(450.82)"628.62"

Rosario Ruggieri & Jo De Waele: Lower- to Middle Pleistocene flank margin caves at Custonaci (Trapani, NW Sicily) and their relation with past sea levels

The peninsula of San Vito Lo Capo, 50 km West of Palermo (Sicily), is characterised by the presence of a wide set of evidences of past sea level changes, such as marine terraces, notches, marine and coastal caves with phreatic overgrowths on speleothems, and continental and marine deposits. The exceptional good preservation of these landforms and deposits has been used by different authors for the reconstruction of sea level changes and neotectonic movements. Among the many caves discussed by previous authors, most are of marine origin and can preserve signs of old sea level highstands such as notches and marine or continental sediments. However, two caves in particular, Fantasma Cave and Falesia Rocca Rumena I cave, show evidences to be flank margin caves. Both caves are records of rising and falling sea level, and their position and the correlation with marine terraces suggest them to be around 0.8 and 1.1–1.2 Ma old respectively. This study shows that not all sea level high stands are preserved in the stratigraphical and geomorphological record.

Keywords: telogenetic limestones, coastal karst, mixing zone speleogenesis, sea level changes, Quaternary.

Izvleček UDK 551.435.8:551.468(450.82)"628.62"

Rosario Ruggieri & Jo De Waele: Spodnje do srednje pleistocenske jame tipa flank margin pri Custonaci (Trapani, SZ Sicilija) in spreminjanje morske gladine

Za polotok San Vito Lo Capo 50 km zahodno od Palerma so značilne številne sledi preteklega spreminjanja morske gladine: morske terase, niše, morske in obalne jame s freatičnimi prerastki na sigi ter kopenski in morski sedimenti. Na osnovi izjemno ohranjenih oblik in sedimentov, so v preteklosti različni avtorji določili spreminjanje morskega nivoja in neotektonske premike. Med številnimi obravnavanimi jamami jih je večina morskega izvora, z ohranjenimi nišami in morskimi oz. kopenskimi sedimenti. Dve jami, Fantasma in Falesia Rocca Rumena I, pa kažeta značilnosti jam tipa flank margin. Obe jami imata sledove dviganja in spuščanja morske gladine. Njun položaj, z ozirom na morske terase, kaže na starost med 0,8 in 1,1-1,2 Ma. Naša študija pokaže, da v stratigrafskem in geomorfološkem zapisu niso ohranjeni vsi visoki nivoji morske gladine.

Ključne besede: telogenetski apnenec, obalni kras,speleogeneza v območju mešanja, spremembe morske gladine, kvartar.

[1] Centro Ibleo di Ricerche Speleo-Idrogeologiche, Via Carducci 165, Ragusa, Italy, e-mail: info@cirs-ragusa.org.
[2] University of Nova Gorica
[3] Italian Institute of Speleology, Department of Biological, Geological and Environmental Sciences, Via Zamboni 67, 40126 Bologna, Italy, e-mail: jo.dewaele@unibo.it
* Corresponding author

Received/Prejeto: 02.10.2012

INTRODUCTION

Carbonate coasts are among the most important littoral landscapes where geomorphological evidences of past sea level oscillations and stillstands are likely to be preserved better than in other lithologies. Unlike in other rocks, limestones exhibit a set of typical landforms that are shaped at or close to sea level, such as notches and caves, and morphologies related to biocorrosion (e.g. lithophaga borings) or bioconstruction (e.g. vermetid reefs) in the intertidal range. Together with other sea level indicators such as marine terraces, continental and marine sediments, this extremely various set of geomorphological markers allows these coastal carbonate areas to be used worldwide for sea level reconstructions (Lambeck *et al.* 2004; Suric *et al.* 2005; 2009; Dorale *et al.* 2010; Tuccimei *et al.* 2010; van Hengstum *et al.* 2011).

Also solutional caves can indicate the position of sea level at the time of their formation (Mylroie & Carew 1988; Florea *et al.* 2007). There are four types of caves that can form at or near a relatively stable sea level: littoral caves (also called sea caves), conduit-flow stream caves, flank margin caves (Mylroie *et al.* 2008), and "Quintana Roo"-type mixing dissolution caves (Smart *et al.* 2006). The first caves form by wave action within the tidal range, causing mechanical breakdown and erosion of almost any type of rock. The wave energy exploits weaknesses in the rock mass, and chemical action of saltwater and compression of air through cracks and voids can increase the destructive action of the waves. Conduit-flow stream caves are formed by inland waters that flow underground reaching the sea in subterranean estuaries. Nice examples of such caves are the Puerto Princesa Subterranean River in Palawan, Philippines (Piccini & Iandelli 2011), Bue Marino and Bel Torrente caves in the Gulf of Orosei (De Waele 2004; De Waele *et al.* 2009), just to name a few. Many of these caves are now underwater, since these rivers tend to carve their floors in response to sea level drops. Their floors are also often covered with sediments that hide the original bedrock. In many cases the elevation of the caves itself is not a reliable sea level indicator, but the erosional and corrosional features within the passages might give a closer approximation of past sea level. Especially close to the sea, notches formed in the tidal range, or biocorrosion marks (e.g. lithophaga borings) can be good indicators of past mean sea level (Carobene 1978; Carobene & Pasini 1982; Furlani *et al.* 2011; Evelpidou *et al.* 2012). Flank margin caves form at the top and the bottom of the freshwater lens in coastal karst areas by mixing dissolution (Mylroie & Carew 1990). This very special type of caves has been reported especially in eogenetic limestones of carbonate islands such as the Bahamas and Bermuda (Mylroie *et al.* 1995), Guam (Mylroie *et al.* 2001), the Mariana Islands (Jenson *et al.* 2006), and in Kangaroo Island, Australia (Mylroie & Mylroie 2009), but also in mature limestones of New Zealand (Mylroie *et al.* 2008), in carbonate talus breccia on the Island of Cres in Croatia (Otoničar *et al.* 2010). Flank margin caves are much more reliable sea level indicators than coastal conduit-flow stream caves, showing clear evidence of dissolution at the fresh-salt water boundary, often very close to sea level, especially in areas where fresh water lenses are thin.

"Quintana Roo"-type caves represent an intermediate between true flank margin and epigene conduit-flow stream caves. Close to the coast the pattern is typically anostomosing, and sometimes spongework and ramiform, due to extensive mixing-corrosion processes, while in the upstream part the passages are typically dendritic, similar to conduit-flow stream caves. In these caves dissolution is driven by mixing of fresh and saline water over a very wide coastal zone (Smart *et al.* 2006).

In this paper we describe two flank margin caves, located 100 and 70 m a.s.l. respectively, constraining their timing of formation based on a series of correlations with dated marine terraces, geomorphological observations, and dated speleothems and their phreatic biogenic overgrowths.

STUDY AREA

San Vito Lo Capo is a peninsula that extends northward into the Tyrrhenian sea for about 10 km, between Trapani and Palermo (NW Sicily) (Fig. 1).

The geology of the area is characterised by a series of two east and southeast oriented stacked tectonic units overthrusted one upon the other. These units have been formed during the collisional tectonics that characterised this area from Lower Miocene to Middle Pleistocene (Abate *et al.* 1991, 1993; Catalano *et al.* 2011). Rocks are mostly composed of Mesozoic dolostones, limestones and dolomitic limestones, and Eocene-Miocene limestones, marly limestones, marls and clays. Since Upper Pliocene the region is slowly uplifting and fragmenting the area in blocks along NW-SE, N-S, and NE-SW faults.

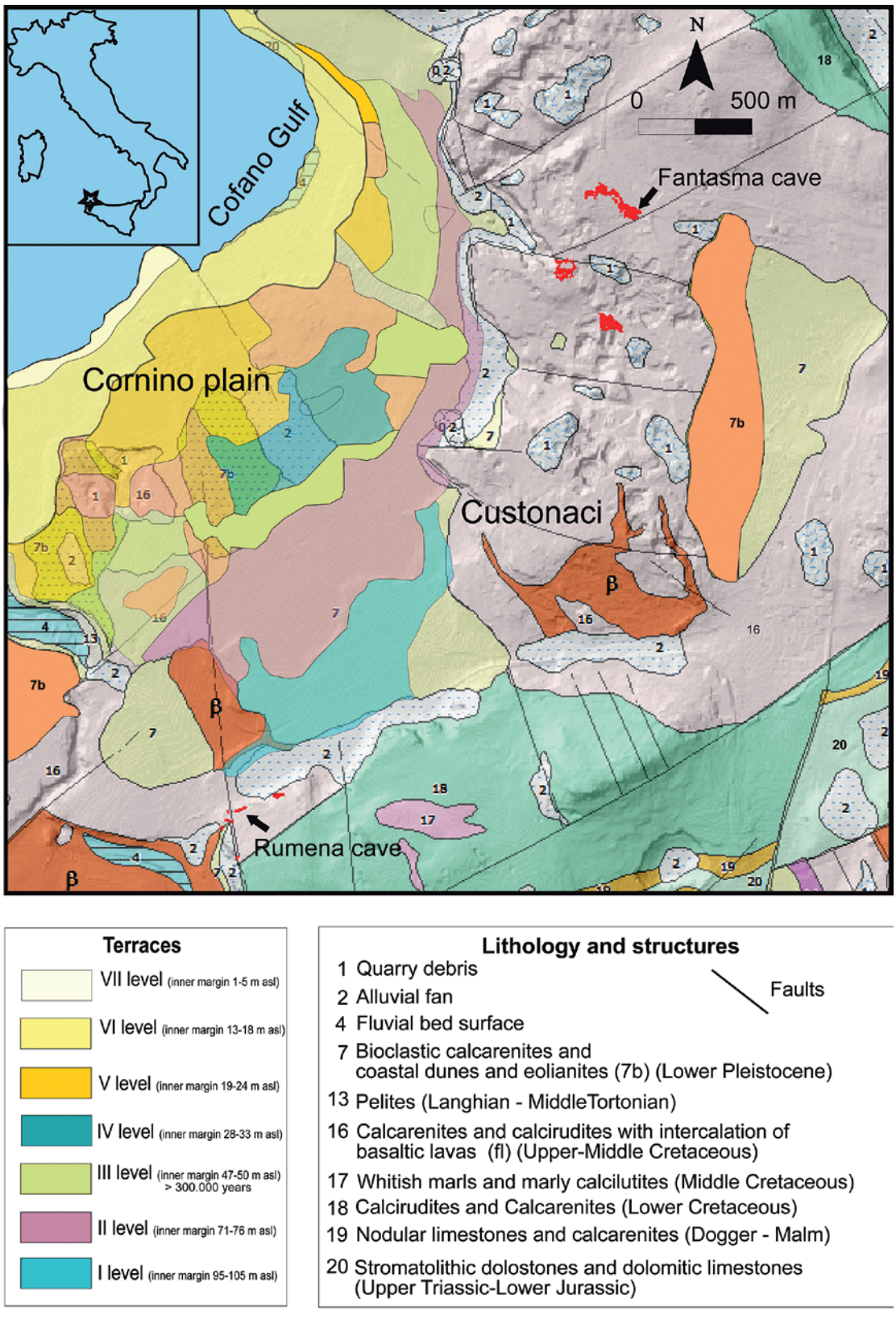

Fig. 1: Geology of the study area and location of the mentioned caves (from Di Maggio et al. 1999).

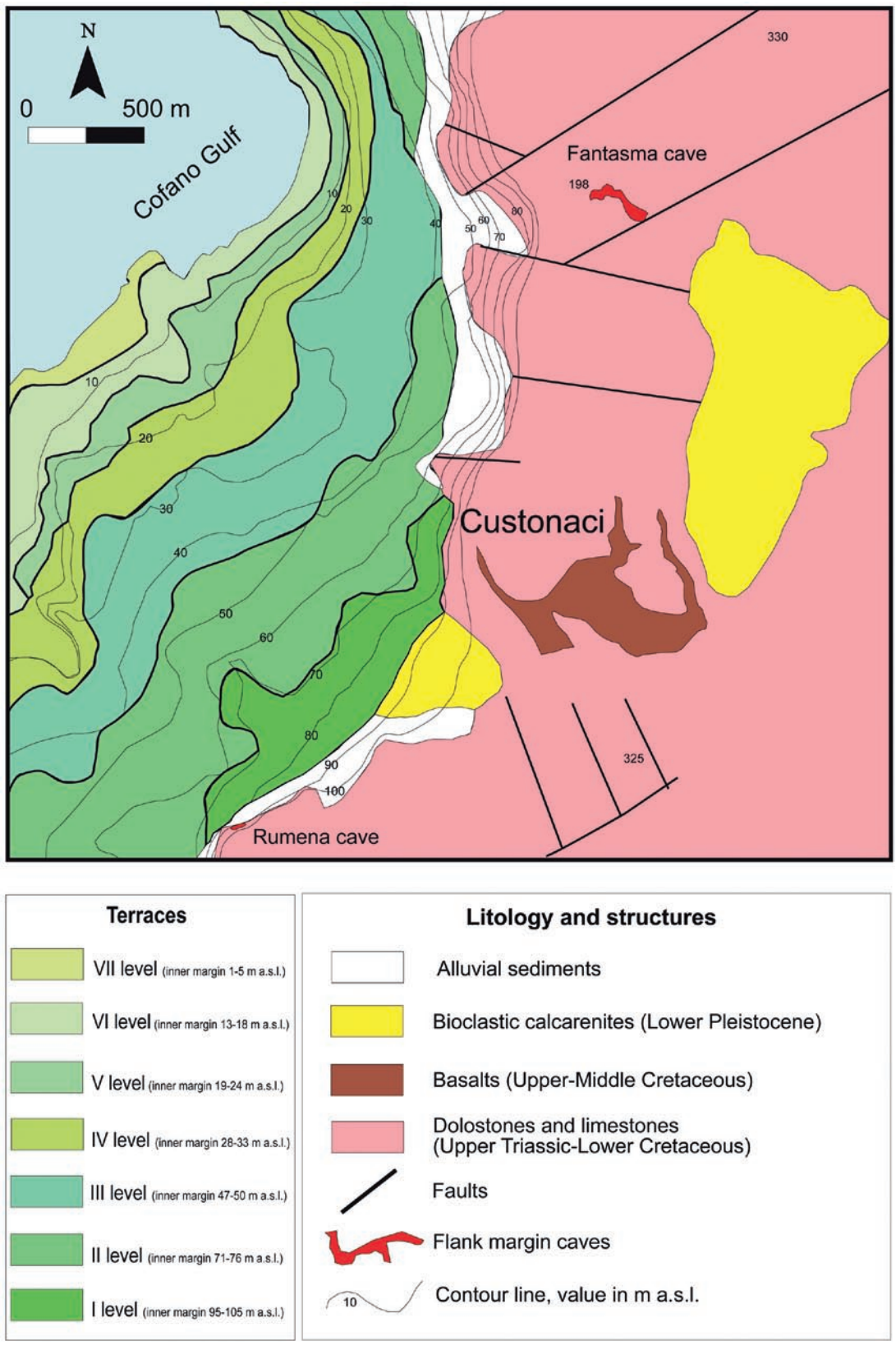

Fig. 2: Simplified geological scheme of the San Vito Lo Capo peninsula (modified from Di Maggio et al. 1999).

The tectonic activity of the last 500 ka is expressed by dislocation along normal and wrench faults of Middle Pleistocene and younger marine deposits outcropping at different altitudes along the coastal plain (Abate *et al.* 1993; Nigro & Renda 2002). Extensive continental, transitional, and marine Pleistocene deposits, mostly composed of calcarenites (Di Maggio *et al.* 1999), are present along the coastal plains.

The Cornino-Custonaci Plain, where both Fantasma and Rocca Rumena I caves are located (Ruggieri & Messina Panfalone 2011), is surrounded by high cliffs of Cretaceous limestones (Fig. 1). Seven marine terraces are present between altitudes of 0 and 105 m a.s.l. (Di Maggio *et al.* 1999) (Fig. 2). The age of these terraces has been estimated based on stratigraphical and paleontological evidences. The marine terrace VI, with upper boundary at 13–18 m a.s.l., contains the typical warm fauna with *Strombus bubonius* and can be attributed to MIS 5e. A speleothem sampled at 8 m a.sl. in a notch related to this terrace at San Vito Lo Capo has given a U/Th age of 19,625 ± 5,300 years BP, confirming this terrace to be older than the Last Glacial Maximum (LGM) (Antonioli *et al.* 1999a). The presence of *Elephas falconeri* in some continental deposits at elevations higher than 40 m a.s.l., roughly corresponding to terraces III or IV, confirms their age comprised between MIS 9 and 17 (Di Maggio *et al.* 1999). A speleothem that covered the notch at 42 m a.s.l. at San Vito Lo Capo is beyond the U/Th radiometric dating method and indicates terrace III to be older than 300 ka BP (Antonioli *et al.* 1999a). Based on these abovementioned observations, terrace VII has thus be related to MIS 5a or 5c, while terrace V was attributed to MIS 7, terrace IV to MIS 9, terrace III to MIS 11, terrace II to MIS 13, and finally the highest terrace to MIS 15 or older. There is a possibility that some of these highstands have erased the traces of marine terraces or deposits, shifting the terraces to older interglacial intervals. It can therefore not be excluded that the highest terrace is related to MIS 15 or even older.

CAVE MORPHOLOGY

Many caves are known in the Cretaceous limestones surrounding the Cornino plain, but only some of these caves show evidences of past sea levels. The most interesting of these are the Fantasma and Falesia Rocca Rumena I caves (Fig. 3).

Fantasma Cave opens at 198 m a.s.l. in the area of Contrada Marcato Gnarosa, intensively exploited for its "marbles" in several quarries. The cave has clearly formed along two main fault systems, the first striking NE-SW with inclination of 75° toward the SE, on which the entire first part of the cave is developed, and the second with WNW-ESE direction and dipping 80° toward the SSW that influences the deepest part of the cave. While the first part is characterised by narrow fissure-like dissolutionally widened voids descending rapidly and with many indices of recent tectonic activity (broken columns and deflected stalagmites), at 120 m depth (around 80 m a.s.l.) the cave starts to show wall rock features such as rounded passages and cupolas characteristic for dissolution in phreatic conditions. Ten metres lower these metre wide tubes end in a large room called "Sala del Fantasma". This room has an ellyptical shape, is 50 m long and 25 m wide and has a height between around 6 and 10 m. Its central part is occupied by a large heap of old bat guano, and large white and corroded speleothems stand out from the dark background (Fig. 4A). The northern part of this chamber is formed along a WNW-ESE fault with reddish mylonite (Fig. 4C), creating a perfectly straight wall up to 10 m high (Fig. 3A).

In general the roof and walls have extremely well rounded shapes, and at around 70 m a.s.l. the walls are perforated by up to several decimetre wide rounded tubes, forming a sort of perfectly horizontal notch (Fig. 4B–C). At the same altitude several metre wide rounded passages create loops on the southeastern side of the main chamber. Some of these passages tend to taper out and terminate with dead ends toward the East. The room is decorated with large calcite speleothems such as stalagmites, columns and stalactites. Most of these are intensively corroded, and are covered with an over 1 cm thick layer of white powder. These corrosion phenomena are most intense at 70 m a.s.l., corresponding to the altitude of the aforementioned notch. The general corrosion of cave walls and speleothems, very intense around and above the guano heap, is probably related to condensation water created by the slow exothermic transformation of the bat guano. The presence of taranakite [$H_6K_3Al_5(PO_4)_8 \cdot 18H_2O$] and apatite [$Ca_5(PO_4)_3 \cdot (OH)$] show the guano to be relatively old and diagenised.

The major corrosion at 70 m a.s.l. along a perfectly horizontal plane indicates an influence of a stable water level. The guano-related condensation corrosion appears to be the most recent process, overprinting the older mi-

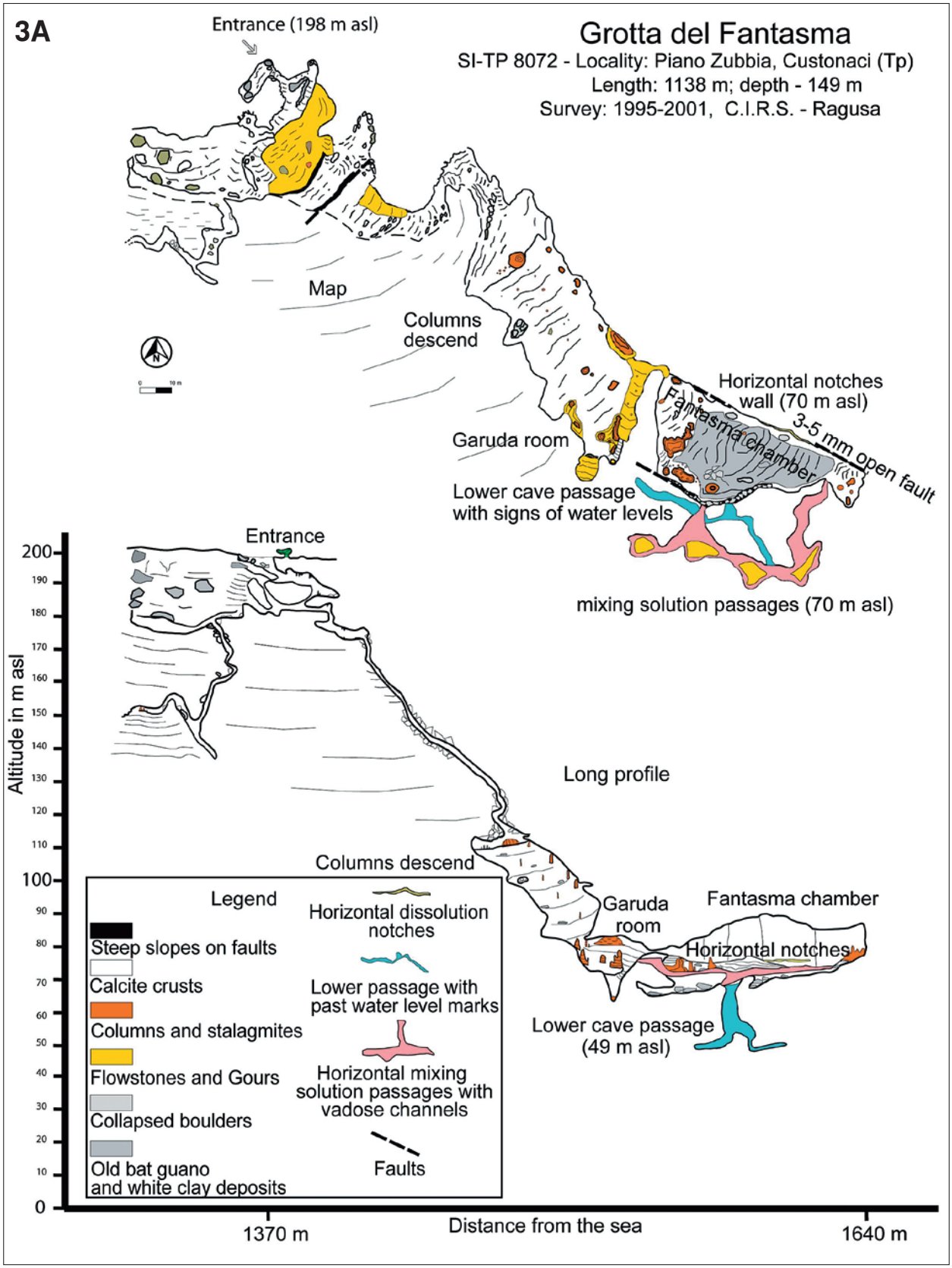

Fig. 3: Cave surveys: A) Fantasma cave B) Falesia Rocca Rumena I cave.

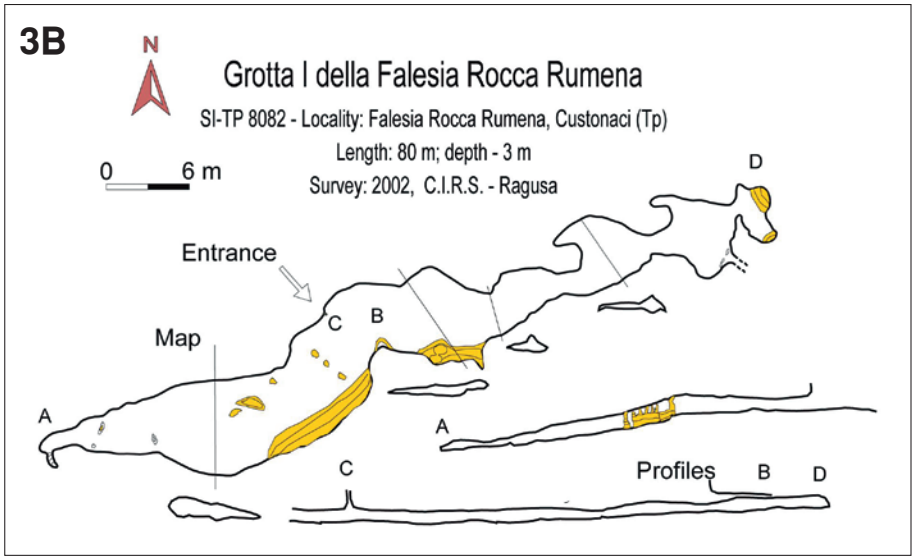

xing corrosion phenomena. One small descending conduit develops 40 metres further towards SSW reaching an altitude of 49 m a.s.l. In this passage several traces of old water levels, visible as horizontally mud stained cave walls, are clearly recognisable (Antonioli & Ruggieri 2000). Nowhere in the cave there are fluvial sediments, and the walls are always smooth and do not reveal any scallops or similar forms.

Grotta Falesia Rocca Rumena I is a small mostly horizontally developed cave formed at the foot of the 20 m high Pleistocene coastal cliff. Its entrance opens at 100 m a.s.l. in correspondence of a not well-defined notch and a clear level of lithophaga borings. It is composed of a series of small chambers and passages with rounded forms, small tubes and pillars. The passages develop parallel to the cliff wall, mostly along fractures and bedding planes, but tend to tighten gradually going away from the cliff (Fig. 3B). The roof and part of the walls are covered with organogenic crusts, mostly scleractinian corals that also fill part of the lithophaga holes. Also speleothems are covered with these corals and are perforated by lithophaga (Rosso *et al.* 2012). One stalactite in particular shows three growth hiatuses, suggesting submersion at least three times. U/Th dating of this stalactite were beyond the range of the method. The corals have been dated using $^{87}Sr/^{86}Sr$ ratio and appear to be 1,100 ± 200 ka years old (Antonioli *et al.* 2012). δO^{18} measurements on the continental stalactite layers and comparison with marine and continental records suggest this speleothem to be formed somewhere during MIS 31–37 (Antonioli *et al.* 2014).

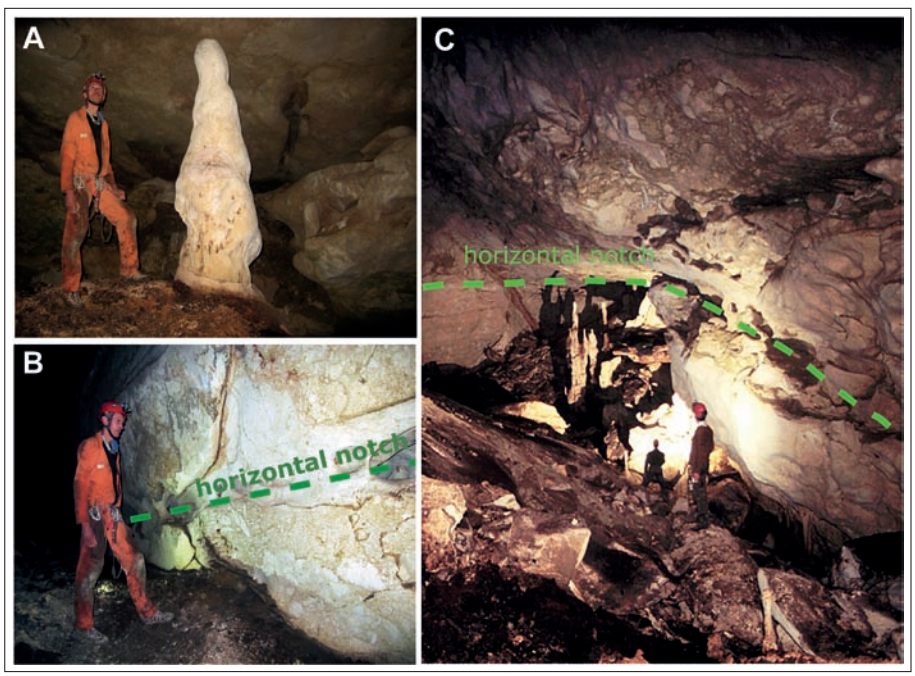

Fig. 4: Cave morphologies: a) The "Fantasma" speleothem, an old stalagmite modified by condensation-corrosion processes, probably related to organic decay of guano (dark material at its base); b) The very evident corrosion notch at 70 m a.s.l., that borders the entire Fantasma Chamber. These are formed by mixing corrosion at the former sea level. c) Panoramic view of the Fantasma Chamber looking East: the corrosion notches are clearly visible to the right ("swiss cheese" morphologies), while in the back of the room (left of the stalagmites) the reddish dark strip is the mylonite of the northern wall fault. Also note the abundant guano on the floor in the front of the picture (Photographs by Rosario Ruggieri).

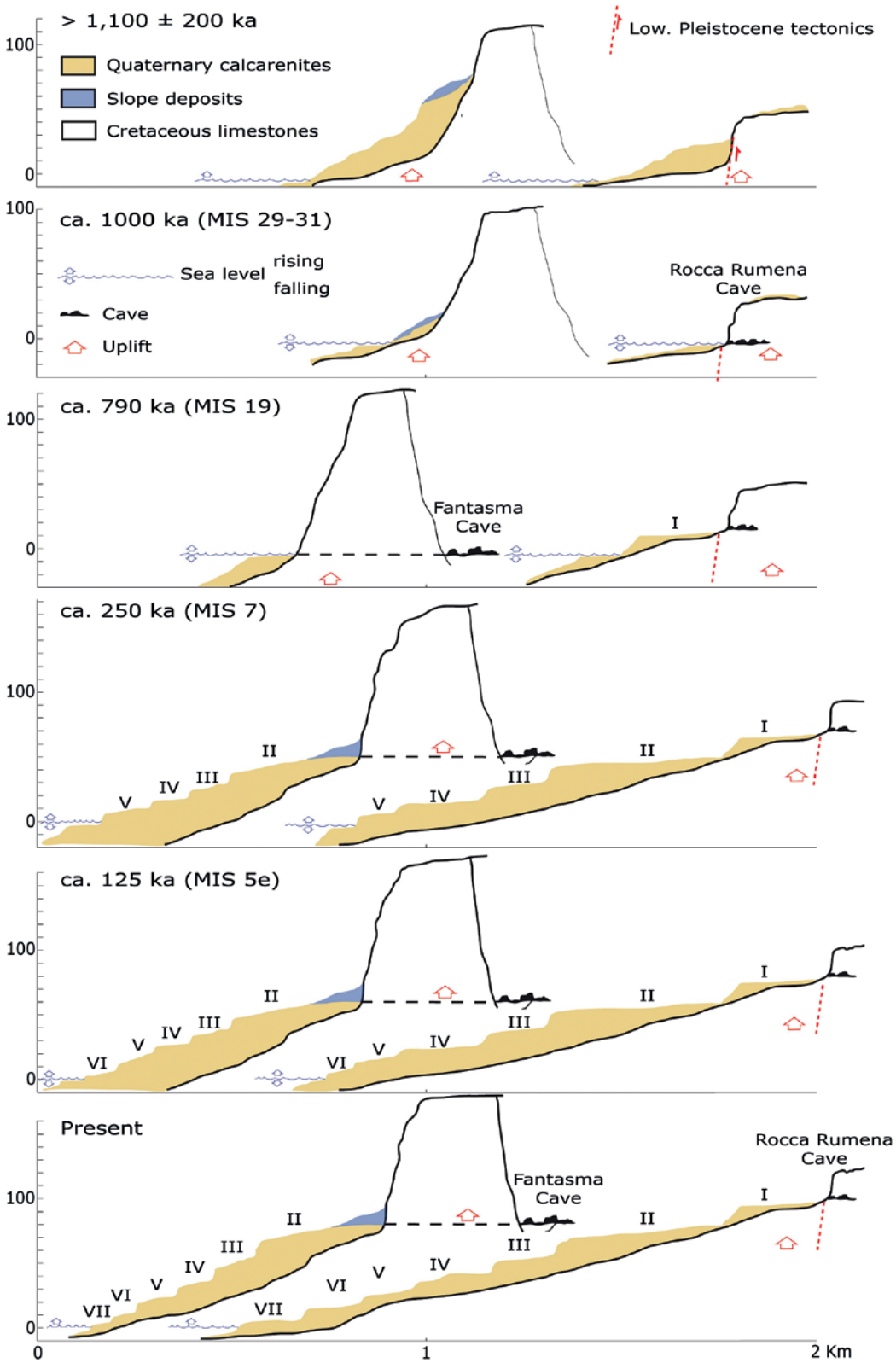

Fig. 5: Scheme showing the hypothesis of formation of the caves and the coastal terraces. See text for explanation.

DISCUSSION AND CONCLUSIONS

The coastal area of NW- Sicily and San Vito Lo Capo in particular has been studied for over 20 years by many authors for the reconstruction of Pleistocene-Holocene sea level changes (Antonioli *et al.* 1994 Mauz *et al.* 1997; Antonioli *et al.* 1999a, 1999b; Di Maggio *et al.* 1999; Antonioli *et al.* 2002). The presence of a wide and various set of sea level markers, such as marine terraces, marine and continental sediments and their palaeontological contents, coastal caves, notches, lithophaga borings, etc., well preserved thanks to the relatively slow uplift rate of the entire peninsula, has made these reconstructions rather reliable. Also coastal caves show signs of past sea level still stands through the presence of typical corrosion features or biological markers (Antonioli & Ruggieri 2000; Ruggieri 2013).

Many of the caves used for reconstruction of sea levels are marine caves, formed by the mechanical action of waves on fracture or bedding plane permeability pathways. Some of the caves, however, have typical morphologies of flank margin caves in telogenetic limestones (Mylroie *et al.* 2008). The lack of stream sediments and of stream flow morphologies such as scallops, and the typical morphology of interconnected rounded cave passages and chambers that tend to taper and terminate blindly going inland, confirm some of the coastal caves to be flank margin caves. The two described flank margin caves are especially interesting for the reconstruction of past sea level high stands (Fig. 5).

The Fantasma Cave is in reality an enlarged Middle Pleistocene – Holocene fissure that intercepts a Pleistocene flank margin cave at 80 m a.s.l. with signs of mixing corrosion down to 49 m a.s.l. The over 30 metre interval in which mixing corrosion seems to have operated in this cave is a sign of a rising (or falling) sea level over this range. In a slowly uplifting area it is more likely that the part of the cave with features related to mixing corrosion was developed during a period in which sea level stayed in this altitude interval for a long time, such as during the shift from rising to falling sea level, with a major stillstand. The main level of mixing corrosion, corresponding to the longest stable position of the sea level, is now located at 70 m a.s.l.

Falesia Rocca Rumena I cave is located at 100 m a.s.l., and based on the age of corals that cover its walls is older than 1,100 ± 200 ka (Antonioli *et al.* 2012). Since the cave itself, being a flank margin cave, developed at or near sea level, the coral age is a fairly good minimum estimate of the age of cave formation. The cave formed during an interglacial period, with relatively high sea level, probably during MIS 29 or MIS 31 (during which sea level was probably highest) (Shackleton 1995). Based on the stalactite, covered by the corals and showing at least three phases of growth interruption, the cave was probably close to sea level for a significant time span and experienced at least three subsequent subaerial and subaqueous phases (Antonioli *et al.* 2012, 2014).

This estimated age seems to indicate that not all sea level high stands have been preserved in the stratigraphical and geomorphological record in this area. This fact might easily be explained considering that the geomorphological and biological features related to less high stillstands have been subsequently entirely eroded during the higher sea-level stillstands. In the past million years this appears to have occurred at least twice, with two of the five interglacial stages between MIS 9–24 being undistinguishable or reworked in later deposits (Mauz *et al.* 1997).

To have a rough idea of the age of these caves we can use the tectonic uplift rates calculated using the MIS 5e notch and other geomorphological constraints (Di Maggio *et al.* 1999). For the Cornino-Custonaci area the uplift rate is comprised between 0.07 and 0.11 m/ka. This rate is calculated using the estimated age of Falesia Rocca Rumena I cave 1100–1200 ka (MIS 29–31), actually located at 100 m a.s.l., and the elevation of the MIS 5e notch at 16 m a.s.l. Using these ages and an average uplift rate of 0.09 mm/ka, the horizontal maze-like chamber and conduits of Fantasma cave might thus have been created by the mixing corrosion of fresh and salt water probably around 780 ka ago (ca. MIS 19). This means that half of the interglacial stages in the past 1200 ka years did not leave clear signs in the coastal landscape, probably eroded by successive highstands.

ACKNOWLEDGEMENTS

Many thanks to Davide Vito Messina Panfalone for his logistical help and assistance during our cave expeditions to Custonaci. Mineralogical analysis of the Fantasma cave samples have been carried out by Prof. Ermanno Galli from Modena and Reggio Emilia University. Suggestions and comments from Bojan Otoničar have been greatly appreciated.

REFERENCES

Abate, B., Di Maggio, C., Incandela, A. & P. Renda, 1991: Nuovi dati sulla geologia della penisola di Capo San Vito (Sicilia nord-occidentale).- Memorie della Società Geologica Italiana, 47, 15–25.

Abate, B., Di Maggio, C., Incandela, A. & P. Renda, 1993: Carta geologica dei Monti di Capo San Vito, scale 1:25,000 (1:25,000): Dipartimento di Geologia e Geodesia, University of Palermo.

Antonioli, F. & R. Ruggieri, 2000: Geomorfologia e speleogenesi nell'area carsica di Monte Palatimone (Custonaci, Tp) ed interconnessioni con il livello di base marino, I Seminario di Studi sul Carsismo negli Iblei e nell'area sud Meditterranea, Eremo della Giubiliana, Ragusa, 9–11 Aprile 1999, Centro Ibleo di Ricerche Speleo-Idrogeologiche Ragusa, p. 213–223, Ragusa.

Antonioli, F., Puglisi, C., Reitano, G. & S. Tusa, 1994: Geomorphological evolution of S. Vito lo Capo promontory (Sicily, Italy) during Pleistocene: relationship between neotectonic, eustatism and prehistorical remains – Memorie descrittive della Carta Geologica d'Italia, 52, 337–360.

Antonioli, F., Cremona, G., Puglisi, C., Silenzi, S., Valpreda, E. & V. Verubbi, 1999a: Quantitative assessment of post Tyrrhenian differential crustal movements in a Mediterranean coastal area (S. Vito-Sicily-Italy).- Physics and Chemistry of the Earth Part a-Solid Earth and Geodesy, 24, 343–347.

Antonioli, F., Silenzi, S., Vittori, E. & C. Villani, 1999b: Sea level changes and tectonic mobility: precise measurements in three coastlines of Italy considered stable during the last 125 ky.- Physics and Chemistry of the Earth (A), 24, 337–342.

Antonioli, F., Cremona, G., Immordino, F., Puglisi, C., Romagnoli, C., Silenzi, S., Valpreda, E. & V. Verrubbi, 2002: New data on the Holocenic sea-level rise in NW Sicily (Central Mediterranean Sea).- Global and Planetary Change, 34, 121–140.

Antonioli, F., Montagna, P., Caruso, A., Ruggieri, R., Lo Presti, V., Silenzi, S., Frank, N., Douville, E. & C. Pierre, 2012: Investigation of marine and continental layers in a stalactite older than 1 million years (Custonaci, north-western sector of Sicily), SLALOM 2012, Athens 19–22 March 2012, p. 57–58, Athens.

Antonioli, F., Ruggieri, R., Montagna, P., Pepe, F., Caruso, A., Stocchi, P., Renda, P., Lo Presti, V., Frank, N., Douville, E., Pierre, C., Messina Panfalone, D., 2014: The geosite Rumena cave a unique paleoclimate and sea level archive in the Mediterranean area (north-western Sicily). In abstract 4th International Symposium, Karst Geosites, Favignana 30 maggio – 2 giugno, 64–66.

Carobene, L., 1978: Valutazione di movimenti recenti mediante ricerche morfologiche su falesie e grotte marine del Golfo di Orosei.- Memorie della Società Geologica Italiana, 19, 641–649.

Carobene, L. & G. C. Pasini, 1982: Contributo alla conoscenza del Pleistocene superiore e dell'Olocene del Golfo di Orosei (Sardegna orientale).- Bollettino della Società Adriatica di Scienze, 64, 5–35.

Catalano, R., Agate, M., Basilone, L., Di Maggio, C., Mancuso, M. & A. Sulli, 2011: Note illustrative della Carta Geologica d'Italia alla scala 1:50.000, Foglio 593 Castellammare del Golfo. ISPRA, Servizio Geologico D'Italia, Roma.

De Waele, J., 2004: Geomorphologic evolution of a coastal karst: the Gulf of Orosei (Central-East Sardinia, Italy).- Acta Carsologica, 33, 37–54.

De Waele, J., Brook, G. A. & A. Oertel, 2009: Monk Seal (Monachus Monachus) bones in Bel Torrente cave (Central-East Sardinia) and their paleogeographical significance.- Journal of Cave and Karst Studies, 71, 16–23.

Di Maggio, C., Incandela, A., Masini, F., Petruso, D., Renda, P., Simonelli, C. & G. Boschian, 1999: Oscillazioni eustatiche, biocronologia dei depositi continentali quaternari e neotettonica nella Sicilia nord-occidentale (Penisola di San Vito Lo Capo – Trapani).- Il Quaternario, 12, 25–50.

Dorale, J. A., Onac, B. P., Fornós, J. J., Ginés, J., Ginés, A., Tuccimei, P. & D. W. Peate, 2010: Sea-Level Highstand 81,000 Years Ago in Mallorca.- Science, 327, 860–863.

Evelpidou, N., Kampolis, I., Pirazzoli, P. A. & A. Vassilopoulos, 2012: Global sea-level rise and the disappearance of tidal notches.- Global and Planetary Change, 92–93, 248–256.

Florea, L. J., Vacher, H. L., Donahue, B. & D. Naar, 2007: Quaternary cave levels in peninsular Florida.- Quaternary Science Reviews, 26, 1344–1361.

Furlani, S., Cucchi, F., Biolchi, S. & R. Odorico, 2011: Notches in the northern Adriatic Sea: genesis and development.- Quaternary International, 232, 158–168.

Jenson, J. W., Keel, T. M., Mylroie, J. R., Mylroie, J. E., Stafford, K. W., Taborosi, D. & C. Wexel, 2006: Karst of the Mariana Islands: The interaction of tectonics, glacio-eustasy, and freshwater/seawater mixing in island carbonates.- In: Harmon, R.S. & Wicks, C.M. (eds.). *Perspectives on Karst Geomorphology, Hydrology, and Geochemistry*. Geological Society of America Special Paper, 404, 129–138, Boulder, Colorado.

Lambeck, K., Antonioli, F., Purcell, A. & S. Silenzi, 2004: Sea-level change along the Italian coast for the past 10,000 yr.- Quaternary Science Reviews, 23, 1567–1598.

Mauz, B., Buccheri, G., Zoller, L. & A. Greco, 1997: Middle to Upper Pleistocene morphostructural evolution of the NW-coast of Sicily: Thermoluminescence dating and palaeontological-stratigraphical evaluations of littoral deposits.- Palaeogeography Palaeoclimatology Palaeoecology, 128, 269–285.

Mylroie, J. E. & J. L. Carew, 1988: Solution Conduits as Indicators of Late Quaternary Sea-Level Position.- Quaternary Science Reviews, 7, 55–64.

Mylroie, J. E. & J. L. Carew, 1990: The flank margin model for dissolution cave development in carbonate platforms.- Earth Surface Processes and Landforms, 15, 413–424.

Mylroie, J. E., Carew, J. L. & H. L. Vacher, 1995: Karst development in the Bahamas and Bermuda.- In: H. A. Curran & B. White (eds.) *Geological Society of America Special Paper*. Geological Society of America, pp. 251–267, Boulder, Colorado.

Mylroie, J. E., Jenson, J. W., Taborosi, D., Jocson, J. M. U., Vann, D. T. & C. Wexel, 2001: Karst features of Guam in terms of a general model of carbonate island karst.- Journal of Cave and Karst Studies, 63, 9–22.

Mylroie, J. E. & J. R. Mylroie, 2009: Caves as Sea Level and Uplift Indicators, Kangaroo Island, South Australia.- Journal of Cave and Karst Studies, 71, 32–47.

Mylroie, J. E., Mylroie, J. R. & C. S. Nelson, 2008: Flank margin cave development in telogenetic limestones of New Zealand.- Acta Carsologica, 37, 15–40.

Nigro, F. & P. Renda, 2002: From Mesozoic extension to Tertiary collision: deformation patterns in the units of the North- Western Sicilian chain.- Bollettino della Società Geologica Italiana, 121, 87–97.

Otoničar, B., Buzjak, N., Mylroie, J. & J. Mylroie, 2010: Flank Margin Cave Development in Carbonate Talus Breccia Facies: An Example from Cres Island, Croatia.- Acta Carsologica, 39, 79–91.

Piccini, L. & N. Iandelli, 2011: Tectonic uplift, sea level changes and Plio-Pleistocene evolution of a coastal karst system: the Mount Saint Paul (Palawan, Philippines).- Earth Surface Processes and Landforms, 36, 594–609.

Rosso, A., Sanfilippo, R., Ruggieri, R., Maniscalco, R. & A. Vertino, 2012: Associazioni di substrato roccioso da una grotta sottomarina del Pleistocene (Sicilia occidentale), Giornate di Paleontologia XII edizione, Catania 24–26 May 2012, p. 32–33, Catania.

Ruggieri, R. 2013: Speleological and Speleogenetic aspects of the Monti di Capo San Vito karst area (north-western Sicily): influence of morpho-tectonic evolution. Ph. D. thesis, University of Nova Gorica, 300 pp.

Ruggieri, R. & D. Messina Panfalone, 2011: Dentro e fuori la Montagna. Priulla, Palermo, pp. 182.

Shackleton, N.J., 1995: New data on the evolution of Pliocene climatic variability.- In: Vrba, E.S., Denton, G.H., Partridge, T.C. & L.H. Burckle, (eds.) P*aleoclimate and evolution with emphasis on human origins*. Yale University Press, p. 242–248, New Haven.

Smart, P.L., Beddows, P.A., Coke, J., Doerr, S., Smith, S. & F.F. Whitaker, 2006: Cave development on the Caribbean coast of the Yucatan Peninsula, Quintana Roo, Mexico. In: Harmon, R.S. & C.M. Wicks, (eds.). *Perspectives on Karst Geomorphology, Hydrology, and Geochemistry*. Geological Society of America Special Paper, 404, 105–128, Boulder, Colorado.

Suric, M., Juracic, M., Horvatincic, N. & I. K. Bronic, 2005: Late Pleistocene-Holocene sea-level rise and the pattern of coastal karst inundation: records from submerged speleothems along the Eastern Adriatic Coast (Croatia).- Marine Geology, 214, 163–175.

Suric, M., Richards, D. A., Hoffmann, D. L., Tibljas, D. & M. Juracic, 2009: Sea-level change during MIS 5a based on submerged speleothems from the eastern Adriatic Sea (Croatia).- Marine Geology, 262, 62–67.

Tuccimei, P., Soligo, M., Ginés, J., Ginés, A., Fornós, J., Kramers, J. & I. M. Villa, 2010: Constraining Holocene sea levels using U-Th ages of phreatic overgrowths on speleothems from coastal caves in Mallorca (Western Mediterranean).- Earth Surface Processes and Landforms, 35, 782–790.

van Hengstum, P. J., Scott, D. B., Grocke, D. R. & M. A. Charette, 2011: Sea level controls sedimentation and environments in coastal caves and sinkholes.- Marine Geology, 286, 35–50.

COBISS: 1.01

KARST IN RAS AL-KHAIMAH, NORTHERN UNITED ARAB EMIRATES

KRAS V RAS AL-KHAIMAHU, SEVERNI DEL ZDRUŽENIH ARABSKIH EMIRATOV

Asma AL-FARRAJ[1], Tadej SLABE[2], Martin KNEZ[2], Franci GABROVŠEK[2], Janez MULEC[2], Metka PETRIČ[2], Nadja ZUPAN HAJNA[2]

Abstract UDC 551.435.8(536.2)

Asma Al-Farraj, Tadej Slabe, Martin Knez, Franci Gabrovšek, Janez Mulec, Metka Petrič, Nadja Zupan Hajna: Karst in Ras Al-Khaimah, Northern United Arab Emirates

This paper presents karstological prospecting of selected areas in Ras Al-Khaimah Emirate, UAE. Several locations in Musandam Mountains have been explored for caves, karst springs and surface karst features. Two karst springs, Khatt and MeBreda, were analyzed for basic physical, chemical and microbiological parameters. Although they are both recharged from karst aquifers, they differ significantly. The first one is a thermal spring in which infiltrated rain water is mixed with more saline and mineralized water from greater depths. The location of the second one at the high altitude of 710 m a. s. l. is conditioned by the existence of a less permeable zone within a carbonate aquifer with a larger share of dolomite. There were increased concentrations of nitrates probably due to grazing goats around the spring but on the other hand there was surprisingly low number of total bacterial counts; however detected *Escherichia coli* indicated probable fecal contamination. None of the water from any of the tested sites matched the ISO criteria for direct human consumption. Surface rock relief resulted from different karst processes was studied in river beds and side walls of wadis and on the mountain plateaus. The slopes of the wadis are often dissected by large recesses, relatively rare subsoil forms, and karren with microrills and rain flutes. More extensive karren are found on the tops of the mountains. The rocky riverbeds of wadis were shaped by rapid water currents and corrosion at the contact with sediment. In the study area at the northern slopes of mountains no big cave was found. The largest discovered cave was in fact tectonic fracture which was extended due to the gravitational sliding of part of a mountain along a fissure. But several small (10–20 m long) solutional caves have been discovered and surveyed on the wadis slopes. They exhibit relatively simple assemblage of dominantly dead-end passages. Caves are vertically distributed at several levels

Izvleček UDK 551.435.8(536.2)

Asma Al-Farraj, Tadej Slabe, Martin Knez, Franci Gabrovšek, Janez Mulec, Metka Petrič, Nadja Zupan Hajna: Kras v Ras Al-Khaimahu, severni del Združenih Arabskih Emiratov

V članku predstavljamo preliminarne krasoslovne raziskave izbranih območij emirata Ras Al-Khaimah, ZAE. Na več lokacijah v Musandamskem gorovju smo raziskovali jame, kraške izvire in kraško površje. Kemične in mikrobiološke analize voda dveh kraških izvirov (Khatt in MeBreda) kažejo na precejšnjo razliko obeh vodozbirnih območij. Khatt je termalni izvir, za katere je značilno mešanje infiltrirane deževnice in globokih mineraliziranih voda. Izvir MeBreda se nahaja na nadmorski višini 710 m in iztekanje vode je pogojeno z manj prepustno dolomitizirano plastjo. Zaradi gorske paše je v vodi precej nitratov, vendar presenetljivo malo celokupnih bakterij. Prisotnost E. coli vseeno nakazuje verjetno fekalno onesnaženost. Nobena analizirana voda ne ustreza ISO standardom za neposredno uporabo za pitno vodo. Na gorskih planotah, pobočjih in koritih vadijev smo proučevali kraške skalne oblike. Pobočja vadijev so pogosto razčlenjena z velikimi vdolbinami, razmeroma redkimi podtalnimi oblikami ter škrapljami z mikrožlebiči in žlebiči. Obsežnejše škraplje so na vrhovih gora. Kamnite struge vadijev so oblikovali hitri vodni tokovi in korozija ob stiku z naplavino. Na severnih pobočjih obravnavanega območja nismo našli večjih jam. Največja odkrita jama je v sistemu razpok, ki so nastale zaradi gravitacijskega drsenja dela gore v dolino. V dolinah vadijev smo našli več pravih kraških jam (dolžina 10 do 20 m). Največkrat gre za enostavno, slabo razvejano geometrijo. Rovi se povsem slepo končajo. Jame so vertikalno razporejene po različnih nivojih glede na dno vadija. Skalne oblike kažejo na paragenetski razvoj. Več jam je povsem ali delno napolnjenih z rumenim klastičnim sedimentom. Našli smo tudi plasti sige ter kristale kalcita in sadre. Mineraloška analiza je pokazala precej podobno sestavo vzorcev. V njih smo v različnih razmerjih določili združbo kremena, sadre, kaolini-

[1] UAE University, UAE, e-mail: asma@uaeu.ac.ae

[2] Karst Research Institute ZRC SAZU, Titov trg 2, 6230 Postojna, Slovenia,
E-mails: slabe@zrc-sazu.si (Tadej Slabe), petric@zrc-sazu.si (Metka Petrič), zupan@zrc-sazu.si (Nadja Zupan Hajna), gabrovsek@zrc-sazu.si (Franci Gabrovšek), knez@zrc-sazu.si (Martin Knez), janez.mulec@guest.arnes.si (Janez Mulec), asma@uaeu.ac.ae (Asma Al Farray)

Received/Prejeto: 03.05.2013

above the wadis. The rocky relief of the caves indicates the paragenetic development of the caves. Some of the studies caves were fully and some partially filled with yellow clastic sediments. Also few layers of flowstone, calcite crystals and gypsum crystals were found. Mineralogical analyses shows very similar composition of sediments: different minerals such as quartz, gypsum, kaolinite, smectite, illite, calcite and palygorskite in various proportions. Calcite and gypsum represent precipitates from the cave (crusts, crystals, cements) and the other minerals were brought to the cave most probably by water or wind from eroded rocks and/or soils from wadis catchment areas.
Key words: karst in arid climate, wadi, karst springs, caves, rock features, United Arab Emirates.

ta, smektita, ilita, kalcita in paligorskita. Kalcit in sadra sta se verjetno izločila v jami, ostali minerali so produkti preperevanja kamnin s širšega območja vadija, v jame so preneseni z vodo in/ali vetrom.
Ključne besede: kras v aridni klimi, vadi, kraški izviri, jame, skalne oblike, Združeni Arabski Emirati.

INTRODUCTION

Dominated by a north-south alignment of mountain ridges, the Oman Mountains are the highest area in the UAE; the highest picks of the mountains reach above 2,000 m a.s.l. Our study area is located in Ras Al-Khaim-

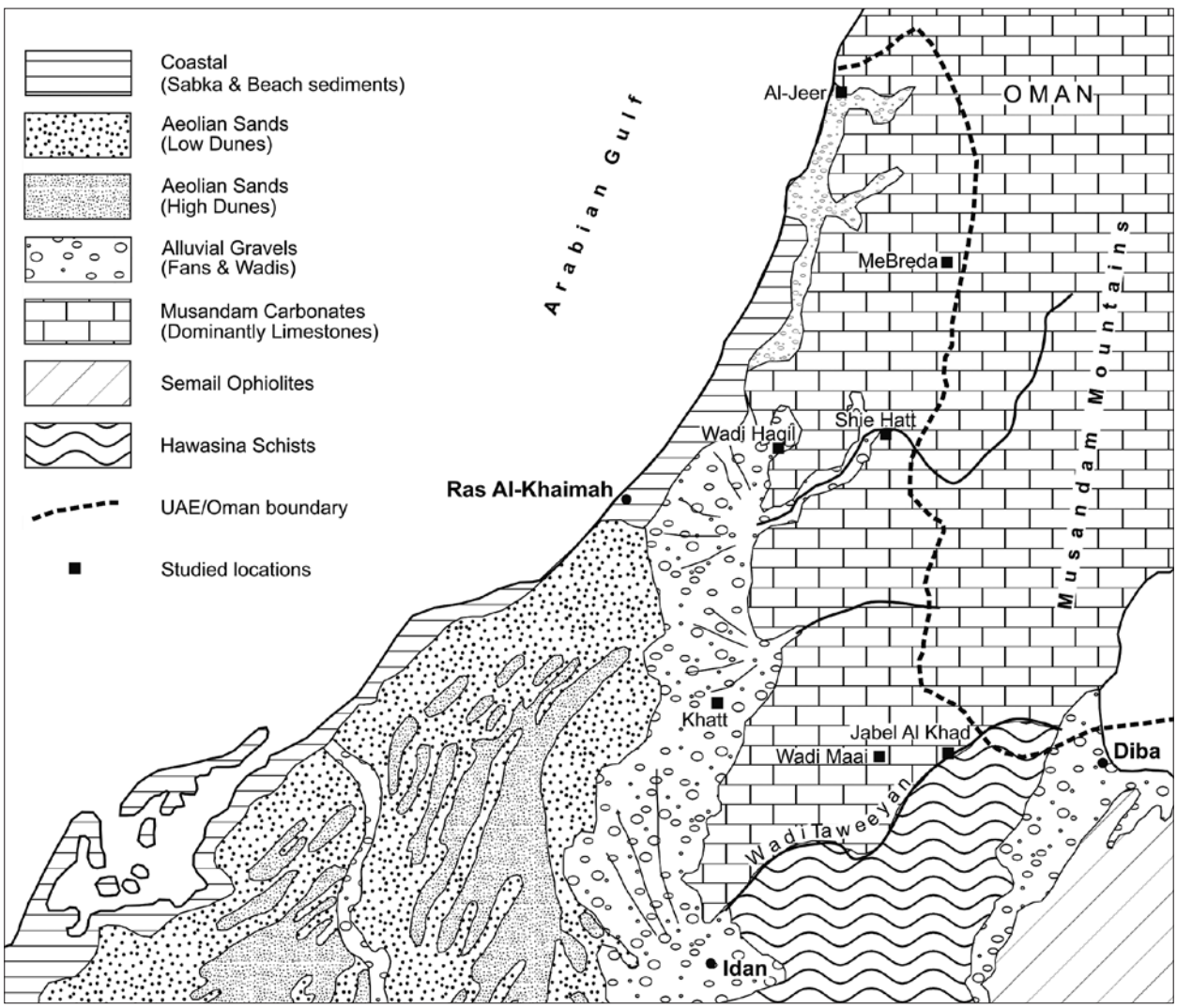

Fig. 1: Locations of the study areas with major lithology (adopted from The National Atlas of the United Emirates, 1993).

ah in northern UAE (Fig. 1) in the Musandam Mountains.

The present climate of the northern UAE is highly arid, with summer temperatures reaching 50 °C and winter temperatures rarely below 14 °C. Rain is irregular and infrequent and occurs mainly in winter. The average annual rainfall is 135 mm on the W side of the mountains and 129 mm in Dibba (E side), but can be higher at higher altitudes, e.g., 166 mm in Wadi Al-Bih (Ministry of Communications 1996). The mean annual surface run-off is 19 mm in Wadi Al-Bih (Ministry of Agriculture 1993). Flash floods occur once or twice a year in wadis such as Wadi Al-Bih. In other wadis they may be as rare as once every ten years (Meigs 1952).

Several studies have been done on caves and karst in the Arabian Peninsula. The most extensive research has been done in Saudi Arabia (Edgell 1990; Forti *et al.* 2005; Kempe & Dirks 2008). In Oman, most recent studies were done on speleothems related to climate change studies (e.g., Fleitmann & Matter 2009; Fleitmann *et al.* 2003; Burns *et al.* 1998, 2001; Sadiq & Nasir 2002; Embabi & Ali 1990).

Karst and caves in the United Arab Emirates (UAE) are poorly explored (Zupan Hajna *et al.* 2013). The existing studies have been mainly undertaken by the Emirates Natural History Group in Jebel Hafit (e.g., Jeannin 1992; Waltham & Jeannin 1998; Fogg *et al.* 2002; Aspinall & Hellyer 2004). In the northern UAE little investigation has been done on caves or karst as is seen from existing literature. Swiss expedition in the beginning of 90's reported minor speleological findings (Jeannin 1992).

This paper presents findings and observations of January 2011 field campaign aiming to locate, explore and map new caves and other karst features in northern UAE, more precisely in northern slopes of Musandam Mountains (Fig. 1). One of the goals of our study was also to look for karst areas or locations with potential use for tourism. The exploration and study areas were on the northern slopes of Mount Al Jeer; in Wadi Haqil; in the area of Wadi Bih and its tributaries Wadi Shehah (Me-Breda) and Wadi Shie Haft; and in area of Wadi Taweeyan and its tributary Wadi Maai (Fig. 1).

A BRIEF GEOLOGICAL OVERVIEW

Oman and the UAE are located on the NE margin of the Arabian plate (Ricateau and Riche 1980; Kusky *et al.* 2005). This plate is bounded to the south and SW by the active spreading axes of the Gulf of Aden and Red Sea. On the east and west its border is marked by transcurrent fault zones. Northern edge of the plate is marked by a complex continent–continent to continent–ocean collision boundary along the Zagros and Makran fold and thrust belts. The Northern Oman Mountains were formed by two distinct orogenic events separated by a period of tectonic quiescence. These events are the Late Cretaceous ophiolite obduction tectonics of the Oman Mountains and the Dibba zone, and the Cenozoic thrusting phase associated with the Zagros orogeny, which took place predominantly during the Oligocene-Miocene (Searle *et al.* 1983; Searle, 1988). As a result, the present Northern Oman Mountains consist of several major tectono-stratigraphic units (sensu Breton *et al.* 2004) as a pre-Permian Basement, the Hajar Unit, the Hawasina Nappes, the Samail Ophiolite and metamorphic sole, and the postnappe structural units.

The Musandam Mountains, which represent northeast part of Oman Mountains spreded east of Dibba fault zone. The Musandam Carbonates were deposited in shallow water on the Arabian continental margin. The Samail Ophiolite represents a portion of the Tethyan ocean crust formed at a spreading center of Middle Cretaceous age (Cenomanian). During the late Cretaceous the ocean closed and the Musandam Carbonates and Semail Ophiolites were tectonically shifted over the Hawasina Unit (Glennie *et al.* 1974).

The present-day topography is believed to have developed during a later Cenozoic orogenic event (Breesch *et al.* 2009). The emergence and uplift of the Musandam Peninsula in the Miocene caused the initiation of the drainage network in the northern UAE. However, the UAE–Oman mountain range has only been a barrier for the last fifteen to twenty million years, which has also influenced the climatic conditions there.

In the Pleistocene, huge terraces of alluvial sediments accumulated in wadis at the feet of the Musandam Mountains (Al-Farray & Harvey 2000, 2004). The limestone mountain ranges are dissected by wadis of various sizes ranging from smaller gorges to large valleys, which present a unique image of fluvial relatively densely dissected karst. Unique caves with characteristic rock relief forms developed in their slopes.

Our studied areas were dominated by carbonate rocks of the Musandam Group (Lower, Middle, Upper Musandam limestone) of Upper Jurassic to Lower Cretaceous age; carbonates of the Russ al Jibal Group (Bih dolomites, Haqil limestone, Ghail limestones) of Middle Permian to Middle Triassic age; and of the Elphinstone Group (Milaha limestone, Ghalilah limestones and mud

Tab. 1: Calcimetric Complexometric data on rock from the slopes of Mount Al Jeer, Wadi Tawiyeen, Jebel Al Khab area and Wadi Maai.

Rock sample	*CaO (%)*	*MgO (%)*	*Dolomite (%)*	*Calcite (%)*	*Total carbonate (%)*	*CaO/MgO*	*Insoluble Residue (%)*
Al Jeer 1-1	55.29	0.12	0.55	98.38	98.93	460.75	2.07
Al Jeer 1-2	47.78	4.75	21.76	73.44	95.20	10.05	4.80
Al Jeer 1-3	33.87	15.40	70.45	22.21	92.66	2.20	7.34
Tawiyeen 3-1	48.51	1.29	5.90	84.37	89.27	37.60	10.73
Tawiyeen 3-2	52.66	0.40	1.84	92.97	94.81	131.65	5.19
Tawiyeen 3-3	49.79	0.32	1.74	88.78	89.52	155.59	10.48
Tawiyeen 3-4	51.31	0.60	2.76	90.06	92.82	85.52	7.18
Tawiyeen 3-5a	54.17	0.64	2.95	95.06	98.01	84.46	1.99
Tawiyeen 3-5b	49.07	0.40	1.84	86.57	88.41	122.67	11.59
Jebel Al Khab 4-1	55.18	0.32	1.47	96.49	98.98	172.43	1.02
Jebel Al Khab 4-2	54.84	0.36	1.66	96.96	98.62	151.55	1.38
Maai 5-1	54.62	0.24	1.11	96.70	97.81	227.58	2.19
Maai below 5-2	55.01	0.68	3.13	95.47	99.60	80.89	0.40
Maai above 5-2	54.79	0.64	92.95	0.88	99.12	85.61	0.88

stones) of Upper Triassic to Lower Jurassic age (Hudson & Chattan 1995; Hudson 1960).

Thirty-nine samples were taken at 6 study areas to make fifty-nine microscopic thin-sections that were examined from the petrological and lithostratigraphic aspects to study the causes of selective karstification at lithostratigraphic contacts of the rock and to see if there were any significant ones. All samples were also subjected to calcimetric complexometric analyses. The limestone at **Mount Al Jeer** is homogeneous mudstone, intramicrite with quartz inclusions, with some dolomitized layers with more than 70% dolomite content (Tab. 1). The main structures of limestones at **Wadi Haqil** are oolites and pisolites which can be traced throughout almost the entire profile (grainstone to packstone, oobiopelintrasparite to oobiopelintramicrite). It is only in the upper part that the oolite-pisolite limestones changes into slightly dolomitized micrite to microsparite rock with a slightly lower content of total carbonate and a significantly increased percentage of dolomite and insoluble residues. Limestones from **Wadi Tawiyeen** were homogeneous and compact (mudstone, micrite), and its profile shows no distinct changes. Some samples show younger calcite fillings. All of them, however, contain a significant percentage of insoluble residues that in most cases pertain to quartz. Oolite limestone at **Jebel Al Khab** (grainstone to packstone, oosparite to oomicrite) contains a high amount of calcium carbonate (Tab. 1). Ooids are usually 15 to 40 μm in diameter in the layer below the contact and 40 to 70 or 90 μm in the layer above the contact along which initial karstification is evident. Strongly recrystallized limstones were found in the **Wadi Maai** (grainstone to packstone, biointrapelmicrite to biointrapelsparite), The calcite content below the bedding plane along which the pocket formed is above 95% (Tab. 1). The rock above this bedding plane has largely the same properties as the rock below it but displays intensive dolomitization. In the area of the MeBreda spring we studied a cave in **Wadi Shehah** that opened during a recent slide of the slope. The profile has alternating layers of mudstone, wackestone, and packstone or intrapelbiomicrite, intrabiomicrite, and intrabiopelmicrosparite, respectively, up to one meter thick. Only the highest section of the studied profile of the rock displays a high content of calcite (Tab. 1).

The main result was that the samples contain shallow sea carbonates which were partly recrystallized and dolomitized and there was no emphasises influence on karstification of the surface or formation of first initial cavities.

HYDROGEOLOGICAL CHARACTERISTICS AND WATER QUALITY

Hydrogeological characteristics of the UAE are significantly influenced by low amount of precipitation and high potential evaporation. Practically all rain water drains as surface flow in a form of seasonal floods, and according to some estimations only 2 to 3% of it recharges the groundwater (Rizk & Alsharhan 2003).

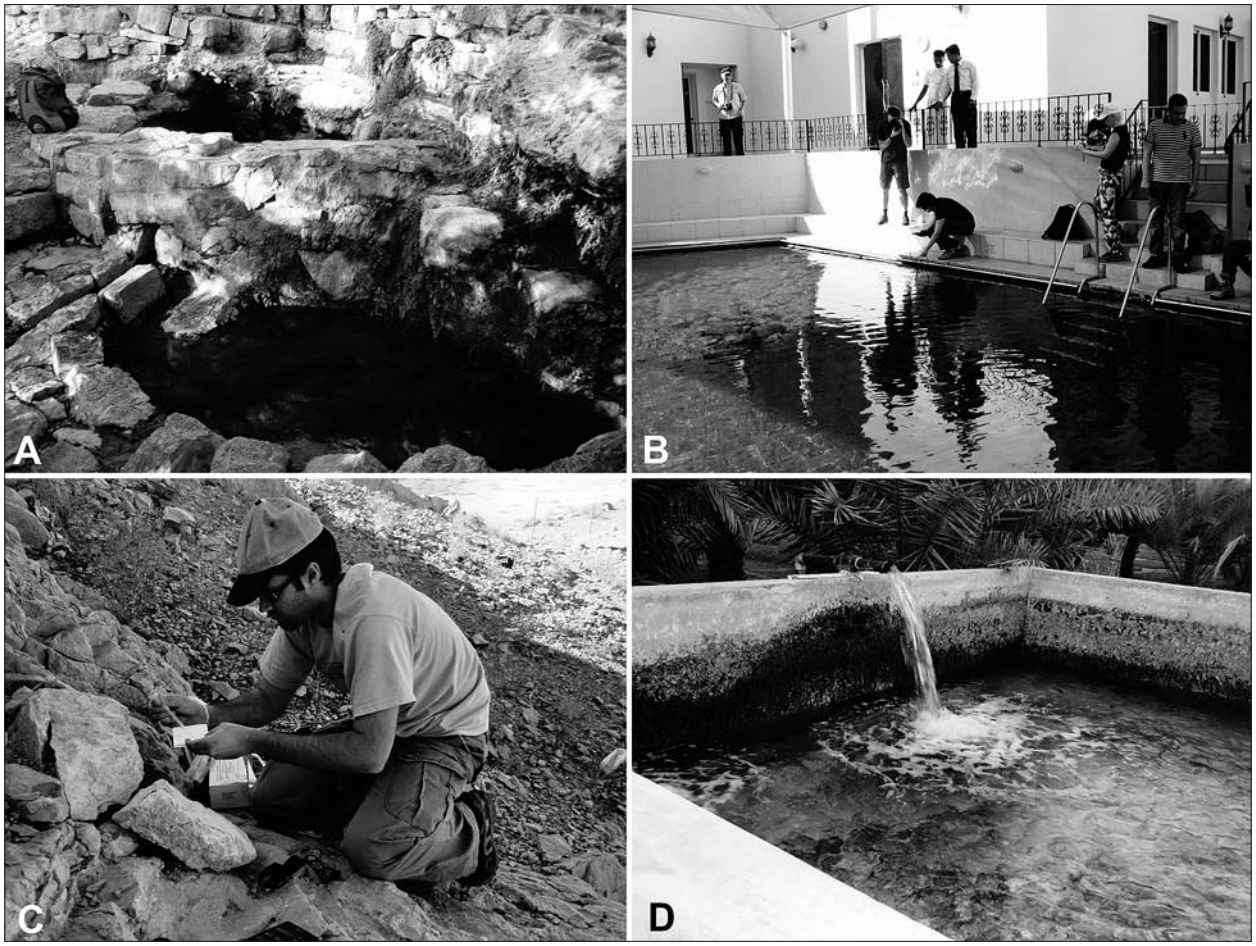

Fig. 2: Sampling sites: a) Two pools of the MeBreda spring in desert mountains above the Wadi Shehah. b) Spa resort at the Khatt spring. c) Sampling from a rainwater trap in the Wadi Haqil, and d) Water pumped from a gravel aquifer in the Wadi Haqil.

Groundwater is stored in four main types of aquifers: karst in carbonate rocks, fissured in ophiolites, and intergranular in gravel and sand dunes. Karst aquifers of rocky slopes and intergranular aquifers of alluvial deposits are characteristic for wadis. The surface water that drains through wadis represents the main source of recharge of the intergranular aquifers in Quaternary alluvial deposits, which are composed of gravel and sand with thin interbeds of silt and clay (Rizk & Alsharhan 2003). The karst aquifers are composed of limestone and dolomite. They are recharged by infiltration of rain and discharged through karst springs at the contact with less permeable rocks or directly into the sea.

Karst springs named Khatt and MeBreda (Fig. 1), which differ significantly in their hydrogeological characteristics, were studied in more detail during our field work. For the comparison only, the basic physical and bacteriological parameters of samples taken at the pumping station in an intergranular aquifer and in a small collector of surface water in a rocky slope of the Wadi Haqil (Fig. 1) were defined additionally.

The Khatt spring with two main outflows Khatt north and Khatt south is located 15 km south of the town Ras al-Khaimah at the extreme east of the gravel plains at the foot hills of the Musandam Mountains. The gravel aquifer in the plain overlies very poorly permeable Cretaceous marls and shales with variable admixtures mixtures of coarse detrital debris of chert, basic igneous rocks, and limestone. The karst recharge area of the spring is composed of Jurassic and Cretaceous dolomitic limestone and limestone. In the period from 1979 to 2004, the average annual discharge of the Khatt north spring ranged between 1 and 60 L/s, and of the Khatt south spring between 4 and 55 L/s (Wycisk *et al.* 2008). Discharge oscillations clearly reflect the precipitation intensity distribution. In dry years with low amount of rain, the discharges were significantly lower. The spring with the water temperature of approximately 39 °C is used for balneological purposes (Fig. 2B). Additionally, the water is drained into an intricate system of lined channels and falajs to support a substantial cultivation of date palms or other crops.

In the MeBreda area in the rocky slope of the Wadi Shehah (a tributary to the Wadi Al Bih) a karst spring is situated at the altitude of 710 m a. s. l. The name MeBreda is used also for the spring. A group of local people built in 1925 two pools for collecting water at the point of a small permanent outflow of water through a fissure in dolomite. The location of the spring is most likely conditioned by the existence of a less permeable zone within the carbonate sequence. This enables the water storage in a small perched aquifer, which recharges a perennial spring with the discharge of several L/s. Water flowing out of the fissure is first collected in the upper pool (our local guide used it as drinking water), and then flows in the lower pool (water used by goats and for irrigation of a small plantation, see Fig. 2A).

Several small holes, which are artificially arranged as collectors of rain water, were seen in the rocky slope of the Wadi Haqil. One of them (in a form of a channel with the cross-section 25 × 25 cm and the depth of 85 cm; Fig. 2C) was partly filled with water in the time of our visit. Stored water is probably used by herds and goats as drinking water. In the nearby pumping station (Fig. 2D), the groundwater is pumped from a gravel aquifer and used for irrigation of agricultural land, mostly for cultivation of date palms.

MEASUREMENT OF PHYSICAL AND CHEMICAL PARAMETERS

Temperature (T) and electrical conductivity (EC) were measured *in situ* with a WTW MultiLine P4 conductometer and pH with the use of pH-indicator strips (EMD, Germany). At the Khatt and MeBreda springs the water samples (0.5 L) were taken and later analyzed in the chemical laboratory of the Karst Research Institute in Postojna. Carbonate, calcium, and magnesium contents were determined using the titrimetric method, of chlorides using the standard methods with mercury nitrate, of sulfates using the standard turbidimetric method, of ophosphates using the method with tin chloride (Clesceri *et al.* 1998), and of nitrate using a method employing sodium salicylate.

Two indexes (Lee & Song 2007), which are often used for the assessment of the salt water intrusion, were calculated. The Revelle index (Revelle 1941) is based on the ionic ratio $Cl^-/(CO_3^{2-} + HCO_3^-)$ in meq/L. The values below 0.5 indicate no influence of salt water, the values between 0.5 and 6.6 a moderate influence, and the values higher than 6.6 are characteristic for waters affected by salinization. The ratio SO_4^{2-}/Cl^- of sea water is approximately 0.1.

ASSESSMENT OF BACTERIOLOGICAL INDICATORS

Drinking water in arid areas is of great concern. Because of its scarcity, its quality for human consumption is of even higher importance. For the assessment of water quality several microbiological parameters are used by the International Organization for Standardization (ISO) what is covered in the section "Water quality ICS 13.060": colony count of culturable microorganisms, sulfide-reducing anaerobes (clostridia), intestinal enterococci, *Escherichia coli*, coliforms and thermotolerant coliform bacteria, bacteriophages, *Legionella*, *Cryptosporidium* oocysts and *Giardia* cysts, thermotolerant *Campylobacter* species, and *Salmonella* spp. and *Pseudomonas aeruginosa* (www.iso.org). To assess eventual microbiological contamination in different water bodies in the UAE which are presumably used for human and/or agricultural consumption Ridacount test plates were used (R-biopharm, Germany, www.r-biopharm.com). Ridacount test plates were already successfully applied for microbiological assessment of microbiological load in different habitats during expeditions in the karst underground (Mulec *et al.* 2012, Mulec e*t al.* 2013). The ISO standards can be adopted also when using Ridacount test plates. We used the following ISO standards for drinking water quality during our expedition: the number of *Escherichia coli* and coliform bacteria must not exceed 0 colony-forming units (CFU) in a 100-mL sample of water (SIST EN ISO 9308-1) and the total number of mesophilic bacteria at 37 °C must be under 100 CFU per mL (SIST EN ISO 6222). For quantitative microbial detection we calculated total counts of heterotrophic aerobic bacteria (Ridacount Total Aerobic Count), conventional total coliform bacteria and *Escherichia coli* (Ridacount *E. coli*/Coliform).

To avoid carrying microbiological samples in cool boxes and later inoculation in a lab at the sites we aseptically inoculated microbiological media with 1 mL of fresh water sample. Coliforms and *E.coli* are usually screened in a volume of 100 mL, but due to limitation of lab equipment during field work, we applied 1 mL of water sample on microbiological media. After inoculation, test plates were placed in an incubator. Reading of results was carried out after 24 hours of cultivation at 37 °C (www.r-biopharm.com) and expressed as CFU/mL (Tab. 2).

RESULTS OF THE WATER ANALYSIS

Already the comparison of basic physical parameters shows very different types of analyzed waters. The EC value of groundwater from the gravel aquifer is very high due to salinization. In the small collector of rain water

Tab. 2: Sampling sites with examined physical and bacteriological parameters (nd - no data).

Date (dd/mm/yy)	Site	Water use	Ecosystem type	Temperature T (°C)	pH	Conductivity SEC (µS/cm)	Total bacteria (CFU/mL)	E.coli / Coliforms (CFU/mL)
24/01/11	Wadi Haqil, collected rainwater	livestock	lentic	19.8	6.5	1,710	24	3/3
24/01/11	Wadi Haqil, water pumped from a gravel aquifer	agriculture	lotic	30.0	5.0	14,400	0	0/0
27/01/11	Wadi Shehah, MeBreda spring	drinking	lotic	nd	nd	nd	28	0/4
27/01/11	Wadi Shehah, MeBreda spring, upper pool	agriculture, drinking	lentic	nd	7.0	738	375	0/64
27/01/11	Wadi Shehah, MeBreda spring, lower pool	agriculture	lentic	nd	nd	nd	1,271	6/553
25/01/11	Spa Khatt, spring	balneology	lotic	38.5	7.5	2,340	22	0/2

Tab. 3: Chemical parameters of water samples taken in the MeBreda and Khatt springs.

Spring	Carbonates (meq/L)	Ca^{2+} (meq/L)	Mg^{2+} (meq/L)	Cl^- (mg/L)	NO_3^- (mg/L)	SO_4^{2-} (mg/L)	PO_4^{3-} (mg/L)	Revelle index	SO_4^{2-}/Cl^- (–)
MeBreda	3.3	3.1	2.0	64	19.4	93	<0.01	0.5	1.1
Khatt	3.9	4.8	2.1	595	8.1	165	<0.01	4.3	0.2

in the rocky slope of the Wadi Haqil stagnant water was sampled, which has been altered by some additional influences.

The results show that although both, the MeBreda and Khatt springs, are recharged from karst aquifers, they differ significantly. The anions arranged according to their decreasing concentrations are $HCO_3^- > SO_4^{2-} > Cl^- > NO_3^-$ in the MeBreda spring and $HCO_3^- > Cl^- > SO_4^{2-} > NO_3^-$ in the Khatt spring. The springs have significantly different T, EC, and concentrations of anions. Relatively low EC, the chemical composition of water, and the ratio $Ca^{2+}/Mg^{2+} = 1.6$ in the MeBreda spring indicate an outflow from a carbonate aquifer with a larger share of dolomite. Increased concentrations of nitrates are due to grazing goats around the spring.

According to its high temperature of 38.5 °C the Khatt spring can be characterized as a thermal spring with deep groundwater circulation. For other springs in the northern part of the UAE the temperatures of springs range from 25 °C to 32 °C (Wycisk *et al.* 2008). The chemical composition of water reflects recharge from a karst aquifer composed of dolomite and limestone, and higher value of EC, higher concentrations of chlorides and sulfates, and the values of the Revelle index and the ratio SO_4^{2-}/Cl^- indicate a moderate influence of salinization. Probably the infiltrated rain water is mixed with more saline and mineralized water from greater depths.

Viable microbes on Ridacount test plates were retrieved from all sampling sites except from water pumped from the underground which had high conductivity. Surprisingly, the traditionally collected rainwater in natural crack had low number of total bacterial count; however detected *E. coli* indicated probable fecal contamination of water from pasturing goats. Water taken directly from the orifice of karst spring in Wadi Al Bih had the lowest bacterial counts in all three bacterial indicator groups (total bacteria, coliform bacteria, *E. coli*) compared to downstream samples. Water captured in pools had higher bacterial counts which can be free used only for agriculture as colonies of *E.coli* were already detected in one mL of a sample.

Considering two ISO standards SIST EN ISO 9308-1 (coliforms and *E. coli*) and SIST EN ISO 6222 (total bacteria) none of the water from any of the tested sites matched the ISO criteria for direct human consumption.

CHARACTERISTICS OF CAVES AND CAVE SEDIMENTS

Only few references report on caves and karst phenomena in the UAE (Jeannin 1992, Waltham & Jeannin 1998, Fogg *et al.* 2002).Our primary target region were mountainous in the NE part of the Ras Al-Khamaih Emirate. Close to the border with Oman, on the slopes of **Mount Al-Jeer**, several cave entrances were reported by local people. All these entrances came out to be small cavities narrowing from the entrance inwards and ending after a few meters. They have developed in thin-layered limestone in places alternating with layers of dolomite (Fig. 3); the bads are inclined at an average of 50° and are folded and broken. Faults occurred along numerous bedding planes due to tilting and folding, resulting in faster karstification in these sections. Karstified areas occur at contacts between individual strata especially along moved bedding planes. The depth of karstified contacts between individual beds is only about five meters, and the average diameter of cave entrances is about one square meter. The cave floors are covered with autogenic breakdown material, light grey clay, bones, and larger plant seeds. The surface of the rock is finely and shallowly corroded exhibiting many solution pans with outflow channels.

Several more caves and areas with caves were reported to us by locals as information on our work was well spread.

North East from Ras Al-Khaimah a large number of small cavities and that characterize the slopes at the mouth of Wadi Haqil (Fig. 4A) where a quick look at the hill resembles to a block of limestone characterized by spongework porosity. The rocks in the vicinity of the cave in **Wadi Haqil** were studied in detail. The average thickness of the strata is 30 cm and their dip 80/85. The selected strata lie between two stronger fault zones that are parallel to the stratification. The karstified area is limited to a segment of strata between stronger tectonically substantially broken zones of rock more than ten meters thick. However exploration revealed that cavities are mainly unlinked. The only cave longer than 10 m is shown on Fig. 4A. It is a simple uniform (blind!) channel with oval cross-section. Cavities contain a substantial amount of clastic sediment. Some are fully and some partially filled with yellow clastic sediments. Fine grained yellow sediment is mostly cemented and includes well visible gypsum crystals. Below and in between the clastic sediments, crusts with calcite crystals and layered flowstone were observed. Samples of clastic sediments from 4 different locations on the hill were taken. Three of them were part of so called Profile 1 (Fig. 4C, Tab.4): SNo1 grey sediment from bottom of the profile, SNo 2 laminated sediment above flowstone, and SNo 3 red sediment below flowstone. On top of the hill was taken sample SNo 4 of yellow sediment from already unroofed channel. From the middle of the hill, from profile of sediment in the wall, was taken sample SNo 5 of grey sediment with gypsum crystals. From Meander Cave sample SNo6 was taken from the brown sediment profile at the end of the cave. In caves in Wadi Haqiul mouse-tailed bats (Rhinopomatidae) were observed which belong to the species *Rhinopoma cystops*.

All samples were analyzed by x-ray diffraction method in the Laboratory of Physical Methods at Institute of Geology CAS in Prague. All samples contain quartz, gypsum and kaolinite, almost all of them also calcite, palygorskite, smectite and illite (Tab. 4). In sample SNo5 was in traces present also K-feldspar and in SNo1 and 2 also chlorite. Calcite and gypsum represent precipitates in the cave /crusts and/or cements) and other minerals were brought to the cave most probably by water from eroded rocks and/or soils from wadi catchment area. Palygorskite and smectite often occur in des-

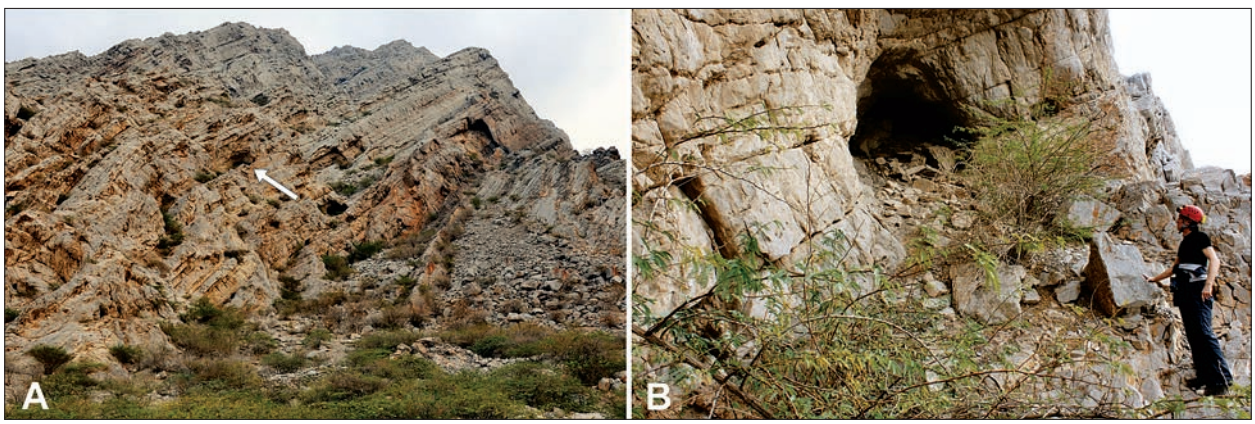

Fig. 3: a) Numerous voids developed along bedding planes of the rocky slope in the Al Jeer Mount An arrow indicates the entrance shown on Fig. 3B. b) A closer look to one of the entrances, which appeared to be a small chamber.

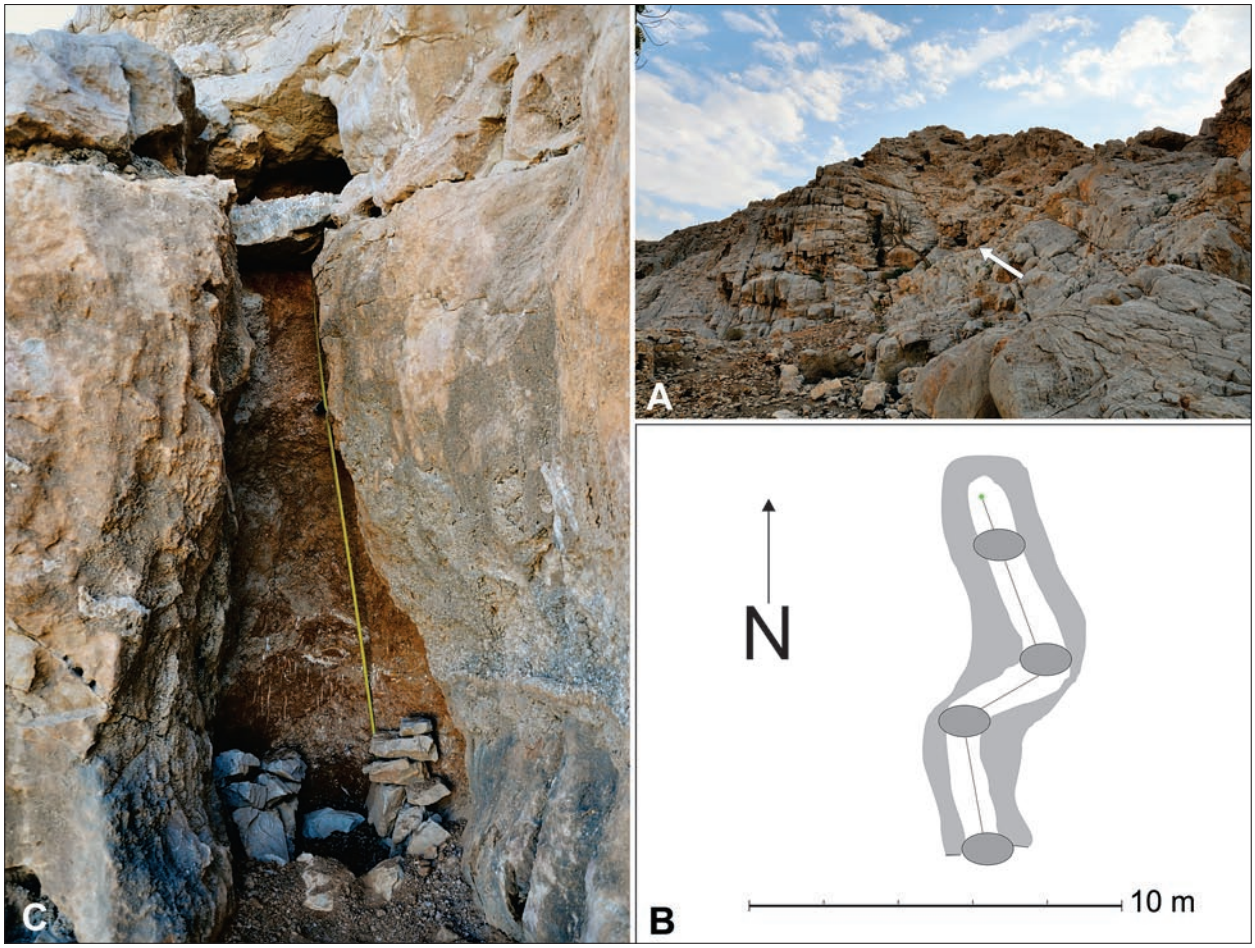

Fig. 4: a) Detail of the right bank of Wadi Haqil close to its entrance. An arrow indicates the entrance to the cave shown in a plan view on Fig. 4B. b) Plan view of the longest l cave found on the slope above Wadi Haqil. c) Profile 1, where sediments SNo1-SNo5 were sampled.

Tab. 4: Mineral identification in bulk samples.

Sediment sample	***Mineral composition***
SNo 1	gypsum, quartz, calcite, palygorskite, kaolinite, smectite
SNo2	calcite, quartz, kaolinite, smectite, illite, palygorskite, gypsum
SNo3	quartz, calcite, gypsum, smectite, kaolinite, palygorskite
SNo4	calcite, quartz, gypsum, kaolinite, palygorskite
SNo5	gypsum, calcite, quartz, palygorskite, smectite, kaolinite, illite
SNo6	quartz, gypsum, kaolinite, smectite, illite

ert types of soils or sediments connected with arid and semi-arid depositional settings (Murray *et al.* 2011).

In the wider area of the **Wadi Tawiyeen** the rocks were thinly stratified, in places thinly laminated laterally. The strata are in average 10 cm thick and with dip of 160/25. Along **Wadi Tawiyeen** many cavities can be ob-

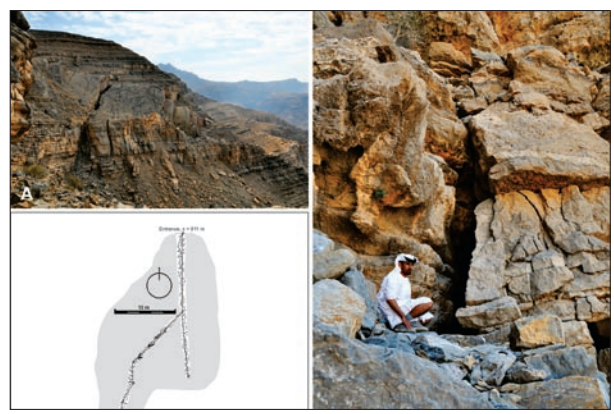

Fig. 5: Notch at the foot of Wadi Tawiyeen.

served in several places. One of them is in the foot of the wadi, and probably represents a notch (Fig. 5). The cave floor is full of gravel, sand and clay. Sample SNo7 of fluvial fine-grained orange sand was taken here. Quartz prevailed in the sample with the presence of calcite, al-

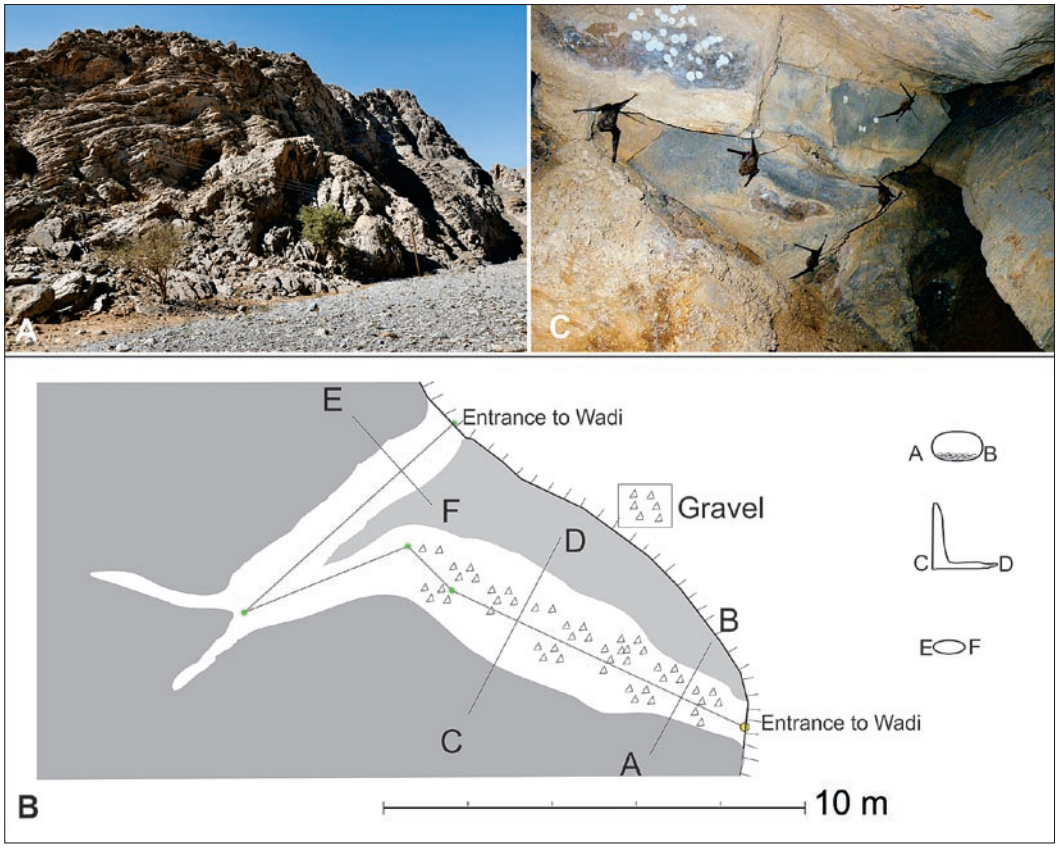

Fig. 6:
a) Detail of the right bank of the middle part of Wadi Tawiyeen with entrance to the cave about 30 m above the bottom.
b) Cave plan.
c) Mouse-tailed bats (Rhinopomatidae).

Fig. 7:
a) Rocky slope above Jebel Al Khab with a cave entrance marked by an arrow.
b) Rectangular shaped entrance.
c) Plan of the cave.

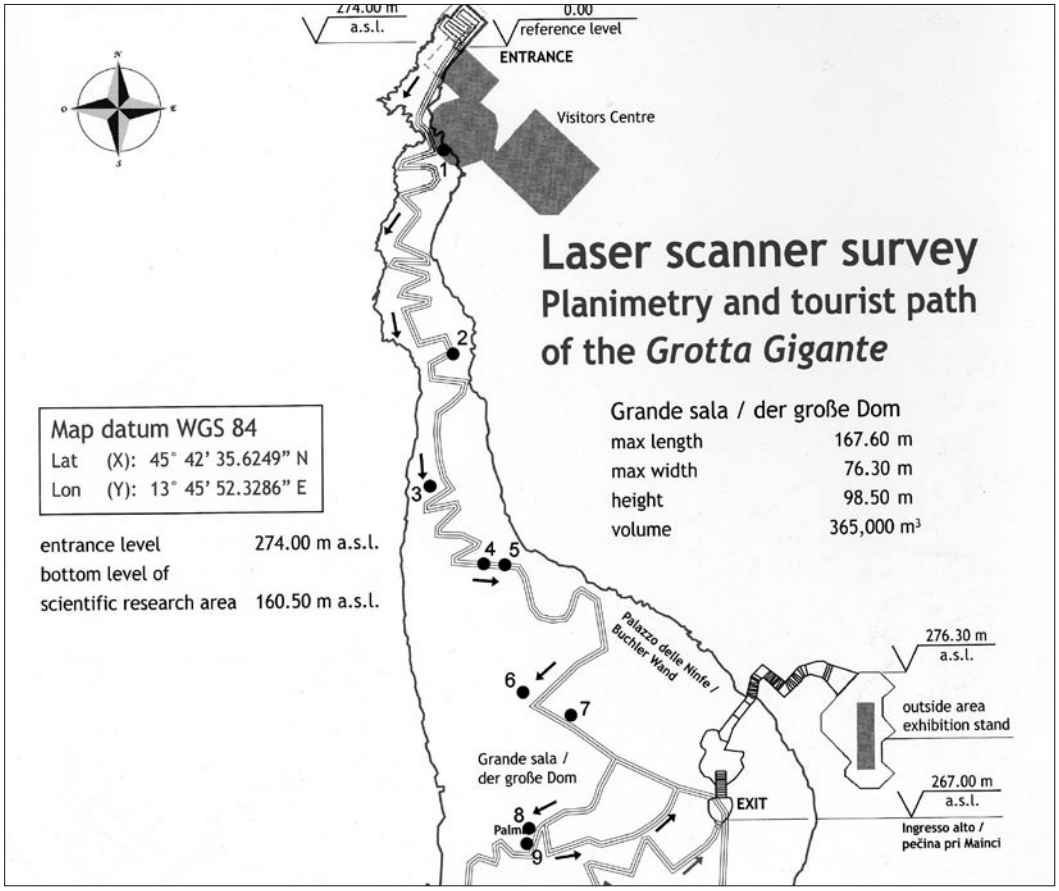

Fig. 8:
a) The slopes above Wadi Maai with numerous voids;
b) An rntrance to the largest cave.
c) A plan view (left) and extended elevation (right) of the cave.

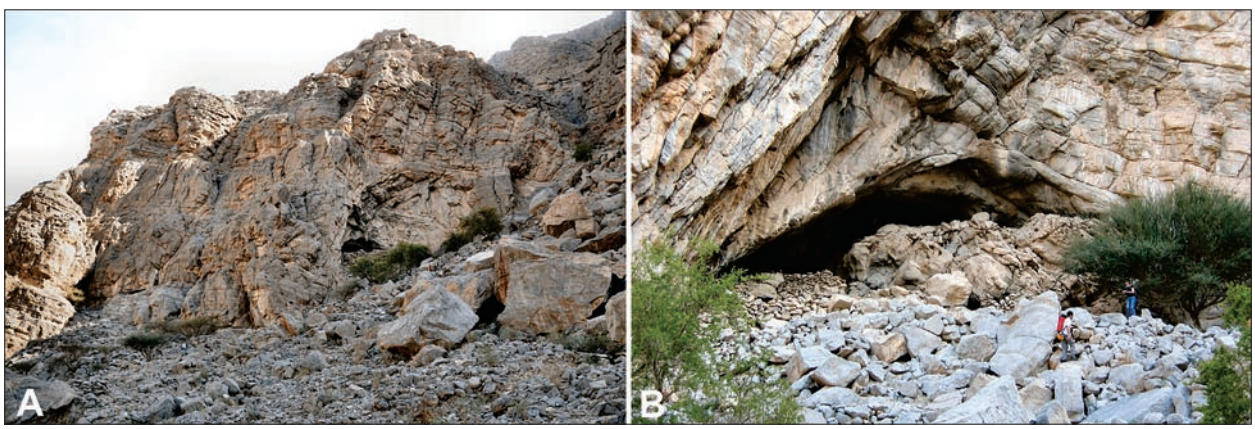

Fig. 9: a) Slopes above wadi Shie Haft with two entrances. b) One of the entrances where the potential continuation is completely filled with blocks and loam.

bite, orthoclase and rutile. Few kilometers upstream, a cave shown on Figure 6 was surveyed (25°34'N, 56°07'E). The entrance is 30 m above the bottom of the wadi. The main channel changes from an oval shaped entrance to an L-shaped channel with increasingly distinct ceiling channel. The channel ends with two blind branches and a rounded conduit leading to a second entrance in the wall of the wadi.

In the area of **Jebel Al Khab**, the upper part of the wadi widens. About 100 m above the surface of the most extensive plain, a cave entrance (Fig. 7A) can be seen at the side of a tributary gorge (25°46'36"N, 56°08'29"E). The cave is formed in 15 cm thick layers with a dip of 190/15. In upper and lower part of the profile the layers are thick, up to one meter. They are tectonically crushed and tend to disintegrate intensely due to their smaller thickness at

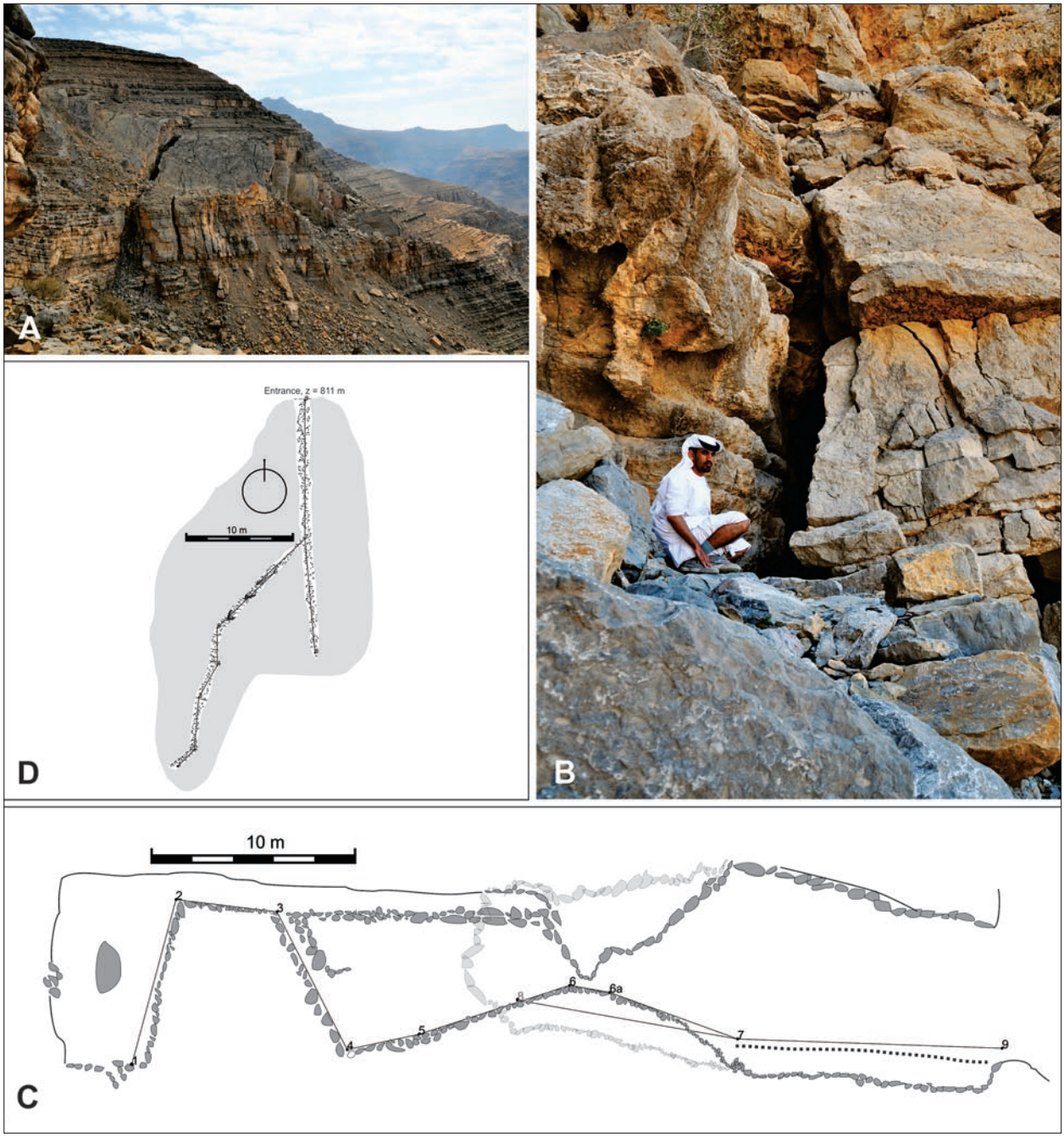

Fig. 10: a) Slopes on MeBreda above Wadi Shehah. Due to the gravity slide a large block has separated resulting in formation of numerous tensile fractures crevasses and breakdowns. The arrow indicates the position of the entrance. b) A closer look to the entrance. c) Extended elevation of the cave; d) Plan of the cave.

the edge of the wall. The entrance is rectangular shaped, 2 × 3 m in size (Fig.7B). It continues with about 10 m long channel with well-expressed ceiling channels and side pockets (Fig. 7C). The channel branches into several smaller channels, one of them exiting at the side wall. Fine-grained sediments with high organic content (including fungi) cover the floor.

About 4 km east, numerous voids and several small caves were observed along the slopes of Wadi Maai (Fig. 8A). Strongly recrystallized limstones are folded and tectonically heavily broken in the vicinity of the karstified pockets. Dip of the beds is 0/20 in the area of the cave. The biggest cave (Fig. 8C) (25°36'58"N, 56°06'13"E) is about 10 m above wadi's bottom. The cave developed

at the contact of non-dolomitized and dolomitized rock. The entrance (10 m wide, 2–4 meters high) continues with a large channel with side niches, pockets and several leads. One of these extents vertically and continues for several meters. Other passage, leading from where the entrance chamber ends, up to another chamber with several blind sub vertical channels. Clays mixed by breakdown gravel cover the floor.

In **Wadi Al Bih** two tributary wadis were prospected for eventual caves. In **Wadi Shie Haft**, relatively large cave entrance is located on the wadi slope. A possible continuation was blocked for further exploration by a large accumulation of breakdown material and clay (Fig. 9).

A cave (825 m a. s. l) very different in comparison with others is positioned close to the top of **MeBreda** above Wadi Shehah (tributary to Wadi Al Bih). In the wider vicinity, the heavily tectonically broken and recrystallized rock has a general dip of 300/80. The cave follows a set of vertical fractures disrupted by active breakdowns with absolutely no dissolutional features. A broader perspective (Fig. 10A) reveals that the cave is a *tectonic cave*. It is part of a (dominantly tensile) fracture system that formed as a consequence of a gravity slide. The sliding is active along a discontinuity which dips slightly towards the valley; a large block of stone of several hundred million cubic meters in size is in the process of breaking off. We observed constant mass movements of rock and rock fragments in the studied fissure/cave.

ROCK RELIEF

Characteristic rock relief dissects the circumference of the special caves forming in the walls of the wadis that were studied comprehensively for the first time. The slopes of the wadis are often dissected by large recesses, relatively rare subsoil forms, and karren with microrills and rain flutes. Karren-like rock surface also occurs between wadis, and rock forms are found on rocks that have broken off from the slopes as well as on and in the sediments covering the bottoms of the wadis. More extensive karren are found on the tops of the mountains. The rocky riverbeds of wadis were shaped by rapid water currents and corrosion at the contact with sediment. Rock forms are an important trace of the formation and development of caves and karst surfaces.

ROCK RELIEF OF CAVES

Caves in wadis are located just above the sediment level and are therefore periodically flooded and dry at various levels above it. They also share similar rock relief. Ceiling pockets are found on the ceilings of niches that developed at the contacts of passages and at their sharp bends in areas of emphasized swirling of water. As a rule, their diameters do not exceed one meter but they are usually deeper, with a 1:3 ratio, and wider in the upper part. In places, pockets are also found on walls, but their lower parts are flat and their upper parts are vaulted (Fig. 11A). The lower parts were frequently covered by sediment that protected the rock from dissolving and erosion and therefore grew upwards and sideways. The walls of passages are smooth and rounded. The mechanical erosive action of water currents carrying material appears to play an important role in their formation. The ceilings of passages are usually characterised by above-sediment channels (Fig. 11B) that along with the parageneticaly raised cross sections of passages indicate the frequent filling of caves with sediments and the flow of smaller quantities of water above them. The largest reach depth of one meter, the consequence of the relatively long-term formation of caves of this kind and their filling with sediment. Along-sediment wall notches, up to one meter deep, indicate periodic partial filling of the caves and a long lasting sediment level in the cave. Along-sediment rock forms are the trace of relatively frequent filling of wadis with sediment and its removal.

ROCK RELIEF OF WADI RIVERBEDS

Potholes, sub-sediment pockets, and sub-sediment channels are the dominant forms found in rocky riverbeds and on rocks in smaller wadis. In places, potholes located at the edge of the rock grew into tubes one meter or more in diameter. Tubes (Fig. 11C) one or two meters in length and from a few tens of centimeters to one meter or more in diameter are also found in the walls. They could be seen as the beginning of characteristic caves. Only the lowest parts of the riverbed are usually smoothed by erosion, while sub-sediment pockets and sub-sediment flutes (Fig. 11D) are found higher up, the traces of a periodically flooded riverbed.

ROCK FORMS ON WADI SLOPES, ON ROCKS AND IN THE SEDIMENT, AND ON MOUNTAIN TOPS

Large pockets (Fig. 11E) on the walls of the wadis are one of their most characteristic forms. In places they

dissect the majority of rocky wadi slopes, elsewhere their larger part, or only individual sections, in short, anywhere they have not been transformed due to the decomposition of the rock or shaped by rapid water flows in the river beds. The pockets are found on vertical, inclined, and overhanging surfaces. Their diameter and depth are measured in meters. Relative to their size, the openings are either shallow or deep. Along fissures and bedding planes their cross sections are most frequently elliptical. Above-horizontal or gently sloping bedding planes they are as a rule developed only in the stratum of the rock above them. They are either single or composite. Some of the pockets display dominant characteristic forms indicating their formation along sediment. As a rule, the lower sections of their circumferences are more or less horizontal while the upper parts are semi-circular or narrow towards the top (Fig. 11F) . The bottom sections of the pockets are often wide. On the tops or on the walls there are straight or winding channels that most probably formed due to the water flowing at the contact with sediment. The circumference of their upper parts, especially those that widen upwards, is dissected by smaller bell-shaped ceiling pockets that formed when the water flowed through a fissure into a pocket filled with the sediment. In most cases, the edge of the opening of large pockets is thin, measuring only a few centimeters. Behind it the pocket widens. Their bottom sections are usually open. Large pockets are dominated by the paragenetic formation of ceiling pockets in the locally flooded zone. The water constantly fills them with sediment that makes them widen and grow upward (Slabe 1995). With the lowering of the water level that permeates the sediment, the water flows downward along the walls, often opening the pockets in the process. This indicates that when the pockets are denuded the rock weathers at a faster rate and are therefore shaped or transformed by the "cavernous weathering process" (Goudie 2009). In shallow circular pockets with a distinctive thin outer edge, this process, accelerated by various salts present in the rock, wind, and microclimatic characteristics in the pocket (Goudie 2009), could be the dominant one. The rock surface of the majority pockets displays fine weathering. Is this how the large or deep pockets formed? Does this mean the faster weathering of the rock in the upper part and the deposit of weathered debris in the bottom part resulting in the asymmetrical shape of the pockets? Can we speak about tafoni in all such cases? In some pockets, a honeycomb of tiny holes developed on the upper edge that could be the consequence of the rapid disintegration of the rock due to "evaporite cooling of the saline solution in the cavity" (Rodríguez-Navarro *et. al* 1999 in Goudie 2009) or they could have developed at the contact with sediment as in caves. In the wadi Haqil, pockets are found at the end of smaller caves filled with sediment or they reach the size of smaller caves themselves. The water often flowed along a bedding plane into the rock and paragenetically transformed it. In places, the thin edges of pockets are extended by flowstone that in all probability was deposited on the contents of the pocket; today, however, it is dissolving and decomposing. All the walls in the wadi caves display clear traces of long-term filling with sediment. Hunt (1996) and Goudie (2009) explains such pockets on Malta as originally subsoil in character and later transformed by "subaerial weathering processes." At this stage we can conclude that these are mostly composite rock forms with traces of frequent dominance by one of the factors of their formation, along-sediment factors being the most distinctive. These are important questions, because these forms are characteristic of this karst and give it a distinctive and unique appearance.

Rocks in the sediment also display sub-sediment channels up to one meter in diameter. The upper parts of subsoil channels are open or semi-pocket-like at the sediment level. They are shaped by water that flows from the surface of the sediment and percolates downwards along the contact with the rock. There are also s-hallow along-sediment notches at the sediment level.

Subsoil cups and subsoil channels developed on rock that was covered by soil or sediment to a large degree or only in places (Slabe & Liu 2009). On horizontal or inclined surfaces denuded pockets are transformed into shallow solution pans. Networks of smaller subsoil channels developed into belts of shallow and elongated notches that were covered for a longer time by sediment or soil in the direction of inclination of the surface. Smaller and winding channels developed when water flowed from higher lying soil or sediment.

On bare rock there are microrills (Figs. 11G, H) that are mainly characteristic of relatively recently denuded rock surfaces and as a rule are the first and most frequent rock forms on such surfaces. They are found on the slightly inclined surfaces of wadi slopes, on the rocks on their bottoms, and on the karren between wadis. They are composed of small cups linked in a linear fashion (Gómez-Pujol & Fornos 2009). They are carved by thin film of capillary-guided moisture that crumbles the rock. The film of water or rain then removes pieces of the rock (Gómez-Pujol & Fornos 2009, 83). On the slopes of the wadis or on the rocks in them, the microrills measure several decimeters in length. They are relatively straight and distinctly oriented downward but not all of them are linear. Some meander slightly on the typical rock surface, which most often has previously undergone subsoil transformation. On the walls of the riverbeds of smaller wadis, one meter or more above the

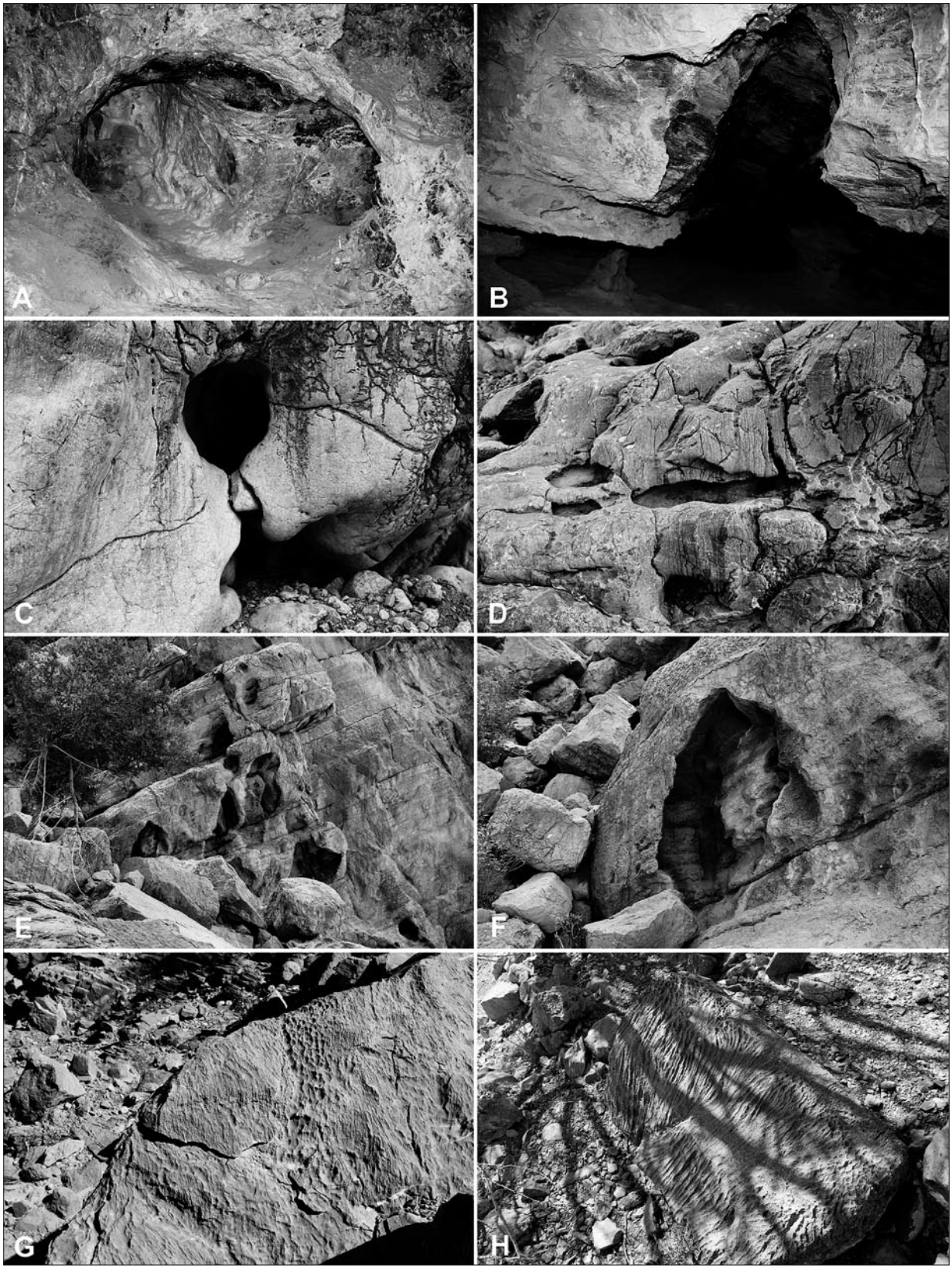

Fig. 11: Rock forms; a) Ceiling pocket. b) Above the sediment channel. c) Tubes in wadi beds. d) Sub sediment flutes. e,f) Large pockets on the wadi slopes. g,h) Microrills.

bottom where the lower walls have been smoothed by erosion, the microrills are woven in a dense network. They are periodically flooded by water that appears to deposit thin-grained sediment in them. Cups often form on horizontal or gently sloping tops of rocks, and microrills are found on inclined surfaces below them. These are rain pits. Some appear to be of subsoil origin. Larger rocks display networks of rain flutes and rain pits (Fig. 11H) as well as microrills on the surface between them, that is, on the sections of the rock that were covered by sediment or soil for a longer period. Scallops are found on overhanging walls and are the traces of water creeping over a larger surface. Although rain flutes are relatively rare, individual rocks can be completely covered with them. Channels where water flows from rain flutes are found in notches.

DISCUSSION

Several areas in Ras Al-Khaimah emirate on the Musandam Peninsula were surveyed in aspect of water quality and finding of new caves. At all described locations physical and chemical parameters were measured and basic bacteriological analyses were done, because drinking water in arid areas is of great concern. Already the comparison of basic physical parameters shows very different types of analyzed waters which indicate the local influences of geology, climate and population.

During exploration we found several small caves, but no big cave was found. In an area, with an average annual precipitation only slightly above one hundred millimeters and small infiltration ratio, karst surface forms, caves and springs are rare.

Detailed geological studies have shown that the significant factors for the karstification and the growth of the caves in the studied wadis were like everywhere: bedding planes and slips along them, older tectonically broken zones in the carbonate rocks, occurrence of large concentrations of calcite, contacts between dolomitized and non-dolomitized rocks, and last but not least, recent fissures and faults.

The described caves along with several smaller ones show some common characteristics that could point to their origin. The passages are generally round with well expressed ceiling channels, wall and ceiling pockets, and dead ends. There are no obvious flow paths along which caves developed. In some areas the vuggy porosity resembles that found in caves of hypogene origin. However, we did not observe any other typical indicators of hypogene origin. The dimensions of passages decrease from the entrance toward the interior of caves. Most caves end with solid walls with no leads continuing into the massif. Scallops are rare or non-existent.

At this stage we do not have firm arguments for any mechanism behind the origin of these caves; however, some of the characteristics mentioned above indicate that the caves originated from near-surface processes. We found and studied mainly clastic sediments. Speleothems are rare, probably due to the arid climate and the very low and diffuse infiltration from the surface. Sediment samples differ in content due to their origin in different rock. Along with fluvial cave sediments, eolian sediments and sediments of organic origin (guano, bones, seeds) are also present.

Cave rock relief and surface rock relief indicate the major significance of along-sediment and subsoil formation of the wadis and the karst between them. We can observe the development of wadis through extensive filling with sediment and rocks from the slope, the shaping of rock at the contact with sediment, and the emptying or distinct change of the sediment level. The majority of caves, including those currently located high above any sediment, were filled with sediment over a longer period. The walls on the sides of wadis commonly exhibit individual or linked cavities that resemble tafoni (Rodriguez-Navarro *et al.* 1999) of various sizes. Some of these, although rare, are large enough to enter.

Cave rock relief and surface rock relief indicate the major significance of along-sediment and subsoil formation of the wadis and the karst between them. We can observe the development of wadis through extensive filling with sediment and rocks from the slope, the shaping of rock at the contact with sediment, and the emptying or distinct change of the sediment level. The majority of caves, including those currently located high above any sediment, were filled with sediment over a longer period. The walls on the sides of wadis commonly exhibit individual or linked cavities that resemble tafoni of various sizes. Some of these, although rare, are large enough to enter.

The general morphology of caves can be linked to floodwater patterns (e.g., Palmer 2007). The flow patterns in bed sediments of wadis are known to be very complex. The carbonate bedrock at the side of the wadis is therefore exposed to dissolution by both superficially flowing water and water flowing within the sediments. The dissolution could occur along the sediment-bedrock

contact resulting in cave geometry defined by the combined action of dissolution and sediment morphology. This suggests that caves could form as the wadis develop. However, this hypothesis needs further field and theoretical verification. The lack of fluvial sediments in the caves surely raises doubts about the genesis.

CONCLUSIONS

We didn't find any big caves.

One possible explanation of why there are not many caves in the studied area of Ras Al-Khaimah is that little water penetrates the steep karst slopes of wadis, which does not create ideal conditions for the development of caves, especially in recent climate conditions.

The annual precipitation values here are very low and most of the precipitation falls in the form of downpours causing major surface runoff in the mountainous areas due to large inclination of slopes and the thin-layered impure limestone with marl layers.

Despite that the findings reported here seem insignificant, we believe that the arid karst areas deserve more research attention than they receive now. Speleogenetic and morphogenetic processes in wadis are to a large extent still unresolved and further, more focused research campaigns will surely bring new important scientific findings.

ACKNOWLEDGEMENTS

In January 2011, following the invitation of Prof. Dr. Asma Al-Farraj, a team from the Karst Research Institute at the Research Centre of the Slovenian Academy of Sciences and Arts went to study the karst and caves in the mountainous regions of the northeastern Emirate of Ras al-Khaimah in the United Arab Emirates. Dr. Al-Farraj was interested in the largely unstudied entrances of relatively inaccessible caves located in the middle of mountain slopes that inspired various legends circulating among the local population. The research was also supported by Saud bin Saqr Al Qasimi, sheikh of the RAK emirate. His staff visited our team during the field work and were particularly interested in Dr. Al-Farraj's suggestion that one of the potentially suitable caves to be developed for tourism and that part of the local karst area to be protected as a national park. The team employed an interdisciplinary approach to study the local karst and caves as effectively as possible in the short time available. Primož Presetnik helped to identify bat species. Research was included in Research Programme Karst Research and UNESCO IGCP project No. 598.

REFERENCES

Al-Farraj, A. & A.M. Harvey, 2000: Desert pavement characteristics on wadi terrace and alluvial fan surfaces Wadi Al-Bih UAE and Oman.- Geomorphology, 35, 279–297.

Al-Farraj, A. & A.M. Harvey, 2004: Late Quaternary interactions between aeolian and fluvial processes: a case study in the northern UAE.- Journal of Arid Environments, 56, 2, 235–248.

Aspinall, S. & P. Hellyer, 2004: *Jebel Hafit, A Natural History.* pp. 220, Abu Dhabi.

Breesch, L., Swennen, R. & B. Vincent, 2009: Fluid flow reconstruction in hanging and footwall carbonates: Compartmentalization by Cenozoic reverse faulting in the Northern Oman Mountains (UAE).- Marine and Petroleum Geology, 26, 113–128.

Breton, J.P., Béchennec, F., Le Métour, J., Moen-Maurel, L. & P. Razin, 2004: Eoalpine (Cretaceous) evolution of the Oman Tethyan continental margin: insights from a structural field study in Jabal Akhdar (Oman Mountains).- GeoArabia, 9, 41–58.

Burns, S.J., Fleitmann, D., Matter, A., Neff, U. & A. Mangini, 2001: Speleothem evidence from Oman for continental pluvial events during interglacial periods.- Geology 29, 623–626.

Burns, S.J., Matter, A., Frank, N. & A. Mangini, 1998: Speleothem-based paleoclimate record from northern Oman.- Geology, 26, 499–502.

Clesceri, L.S., Greenberg, A.E. & A.D. Eaton, 1998: Standard methods for the examination of water and wastewater. 20th Edition, American Public Health Association, Washington.

Edgell, H.S., 1990: Karst in Northeastern Saudi Arabia.- J.K.S.A.U, Earth Science, Special issue: 1st Saudi symposium on Earth Science, 3, 81–94.

Embabi, N.S. & A.A. Ali, 1990: *Geomorphology of depressions in the Qatar Peninsula* (in Arabic).- Qatar University, pp. 357, Al-Ahleia.

Fleitmann, D. & A. Matter, 2009: External geophysics, climate and environment, The speleothem record of climate variability in Southern Arabia.- C. R. Geoscience, 341, 633–642.

Fleitmann, D., Burns, S.J., Neff, U., Mangini, A. & A. Matter, 2003: Changing moisture sources over the last 330,000 years in northern Oman from fluid-inclusion evidence in speleothems.- Quaternary Research, 60, 223–232.

Fogg, T., Fogg, P. & T. Waltham, 2002: Magharet Jebel Hafit – a significant cave in the United Arab Emirates.- Tribulus Journal of the Emirates Natural History Group, 12, 1, 5–14.

Forti, P., Galli, E., Rossi, A., Pint, J. & S. Pint, 2005: *Cave Minerals Of Some Limestone Caves Of Saudi Arabia. Hellenic Speleological Society.*- Research made within the MIUR 2002 Project "Morphological and Mineralogical Study of speleothems to reconstruct peculiar karst environments", Kalamos, Hellas.

Glennie, K.W., Boeuff, M.G.A., Hughes-Clarke, M.W., Moody-Stuart, M., Pilaar, W.H.F. & B.M. Reinhart, 1974: Geology of the Oman Mountains.- Kon. Ned. Geol. Minnhoukundia Genoot. Vern., 33, 423.

Goudie, A., 2009: Cavernous weathering.- In: Gines, A. *et al.* (eds.) *Karst rock features: Karren sculpturing.* Carsologica 9. ZRC Publishing, pp. 89–103, Ljubljana.

Gomez-Pujol, L. & J.J. Fornos, 2009: Microrills.- In: Gines, A. et al. (eds.) *Karst rock features: Karren sculpturing.* Carsologica 9. ZRC Publishing, pp. 73–85, Ljubljana.

Hudson, R.G.S. & M. Chattan, 1959: The Musandam Limestone (Jurassic to lower Cretaceous) of Oman Arabia.- Notes Memoirs. Moyen-Orient., 3, 69–93.

Hudson, R.G.S., 1960: The Permian and Trias of the Oman peninsula, Arabia.- GeologicaMagazine, 97, 299–308.

Hunt, C.O., 1996: Tafoni (pseudokarst features) in the Maltese Islands.- Cave and Karst Science, 23, 2, 57–62.

Jeannin, P. Y., 1992: Expedition suisse aux Emirats Arabes Unis.- Stalactite (Switzerland), 42, 1, 47-55.

Kempe, K. & H. Dirks, 2008: Layla Lakes, Saudi Arabia: The World-wide largest lacustrine Gypsum Tufa.- Acta Carsologica, 37, 1, 7–14.

Kusky, T., Robinson, C. & F. El-Baz, 2005: Tertiary–Quaternary faulting and uplift in the northern Oman Hajar Mountains.- Journal of the Geological Society, 162, 871–888.

Lee, J.Y. & S.H. Song, 2007: Evaluation of groundwater quality in coastal areas: implications for sustainable agriculture.- Environmental Geology, 52, 7, 1231–1242.

Meigs, P., 1952: Arid and semi-arid climatic types of the world. *Procedings, eighth general assembly and seventeenth international congress,* International Geographical Union, 135–138, Washington.

Ministry of Agriculture, Soil and water departments, 1993, Hydrology report, N3, 265–269.

Ministry of Communications, 1996, U.A.E. Climate. Pp. 237.

Mulec, J., Krištůfek, V. & A. Chroňáková, 2012: Comparative microbial sampling from eutrophic caves in Slovenia and Slovakia using RIDACOUNT test kits.- International Journal of Speleology, 41, 1, 1-8.

Mulec, J., Krištůfek, V. & A. Chroňáková, 2013: Monitoring of microbial indicator groups in caves through the use of RIDA®COUNT kits.- Acta Carsologica, 42, 2–3, in press.

Murray, H.H., Pozo, M. & E. Galán, 2011: An Introduction to Palygorskite and Sepiolite Deposits—Location, Geology and Uses.- Developments in Clay Science, 3, 85–99.

Palmer, A.N., 2007: *Cave Geology.*- Cave Books, pp. 454, Dayton.

Revelle, R., 1941: Criteria for recognition of sea water in groundwaters.- Transactions - American Geophysical Union, 22, 593–597.

Ricateau, A. & P.H. Riche, 1980: Geology of the Musandam peninsula (Sultanate of Oman) and its surroundings.- Journal of petroleum geology, 2, 3, 139–152.

Rizk, Z.S. & A.S. Alsharhan, 2003: Water resources in the United Arab Emirates.- In: Alsharhan, A.S. & W.W. Wood (eds.) *Water Resources Perspectives: Evaluation, Management and Policy.* Elsevier, pp. 245–264, Amsterdam.

Rodriguez-Navarro, C., Doehne, E. & E. Sebastian, 1999: Origins of honeycomb weathering: The role of salts and wind.- Geological Society of America Bulletin, 111, 8, 1250–1255.

Sadiq, A.M. & S.J. Nasir, 2002: Middle Pleistocene karst evolution in the State of Qatar, Arabian Gulf.- Journal of Cave and Karst Studies, 64, 2, 132–139.

Searle, M.P., 1988: Structure of the Musandam culmination (Sultanate of Oman and United Arab Emirates) and the Straits of Hormuz syntaxis.- Journal Geological Society, 145, 831–845.

Searle, M.P., James, N.P., Calon, T.J. & J.D. Smewing, 1983: Sedimentological and Structural evolution of the Arabian continental margin in Musandam Mountains and Dibba zone, U.A.E.- Geological Society of America, Bulletin, 94, 1381–400.

Slabe, T., 1995: *Cave rocky relief and its speleogenetical significance.*- Zbirka ZRC 10, ZRC Publishing, pp. 128, Ljubljana.

Slabe, T. & H. Liu, 2009: Significant Subsoil Features.- In: Gines, A. *et al.* (eds.) *Karst rock features: Karren sculpturing.* Carsologica 9. ZRC Publishing, pp. 123–137, Ljubljana.

Waltham, A.C. & P.Y. Jeannin, 1998: Forum: Caves in the United Arab Emirates.- Journal Cave and Karst Science, 25, 3, 149–155.

Wycisk, P., Al Assam, M., Akram, S., Al Mulla, M., Schlesier, D., Sefelnasr, A., Al Suwaidi, N.B., Al Mehrizi, M.S. & A. Ebraheem, 2008: Three-dimensional geological and groundwater flow modelling of drought impact and recharge potentiality in Khatt springs area, Ras Al Khaimah Emirate, UAE.- In: *WASTA 8th Gulf Water Conf.,* Proceedings, 1–14, Bahrain.

Zupan Hajna, N., Al Farraj Al Ketbi, A., Gabrovšek, F., Petrič, M., Slabe, T., Knez, M. & J. Mulec, 2013: Cave and karst prospection in Ras Al-Khaimah Mountains, Northern United Arab Emirate.- In:

Filippi, M. & P. Bosak (eds.) *16th International Congress of Speleology,* 21st– 28th July 2013, Brno, Czech Republic, International Union of Speleology, Czech Speleological Society, 3, 164–169.

COBISS: 1.01

HOLOCENE SEDIMENTARY RECORDS OF THE KATARRAKTES CAVE SYSTEM (NORTHERN GREECE): A STRATIGRAPHICAL AND ENVIRONMENTAL MAGNETISM APPROACH

RAZISKAVE HOLOCENSKE SEDIMENTACIJE V JAMI KATARRAKTES (SEVERNA GRČIJA) S STRATIGRAFSKIMI IN MAGNETNIMI METODAMI

Christos PENNOS[1], Elina AIDONA[2], Sophia PECHLIVANIDOU[1] & Konstantinos VOUVALIDIS[1]

Abstract UDC 551.44:551.3.051(495)"628.64"

Christos Pennos, Elina Aidona, Sophia Pechlivanidou & Konstantinos Vouvalidis: Holocene sedimentary records of the Katarraktes cave system (northern Greece): a stratigraphical and environmental magnetism approach

The Katarraktes cave system is located in northern Greece and is a complex of a rockshelter and a cave formed on the south river bank of Krousovitis River canyon (Serres, Macedonia region). The archaeological site area is well known as one of the most important archaeological sites in SE Europe since it hosts numerous archaeological findings dating back to the Early Bronze Age. Detailed stratigraphic analysis of three archaeological sections was performed in order to define the depositional conditions of the cave entrance facies sediments. Mineral magnetic properties were performed to enhance the paleoenvironmental interpretations and to detect sediment origins. Magnetic susceptibility (k_{lf}) obtained in high and low frequency as well as remanence parameters, such as saturation isothermal remanent magnetization (SIRM) and S-ratio, were measured in samples collected from the archaeological sections. Results indicate a significant variability in the magnetic signal stored in the sedimentary record of Kataraktes cave system distinguishing between natural and anthropogenic sequences. The combination of the stratigraphic and magnetic results along with the archaeological data reveals that flood events of Krousovitis River and sediment accumulation from slackwater in the rockshelter area occurred around 3000 yr BC and were possibly the key factor for the abandonment of the prehistoric settlement.

Keywords: Katarraktes cave system, Greece, Mid-Holocene flood events, slackwater deposits, environmental magnetism.

Izvleček UDK 551.44:551.3.051(495)"628.64"

Christos Pennos, Elina Aidona, Sophia Pechlivanidou & Konstantinos Vouvalidi: Raziskave holocenske sedimentacije v jami Katarraktes (Severna Grčija) s stratigrafskimi in magnetnimi metodami

Jamski sistem Katarraktes, ki ga sestavljata velik spodmol in podzemni rovi, leži na južnem obrežju kanjona reke Krousovitis (Serres, Makedonija, Severna Grčija). Kraj je eno najpomembnejših arheoloških najdišč v JV Evropi. Številne najdbe segajo v zgodnjo bronasto dobo. Na osnovi podrobne stratigrafske analize treh arheoloških profilov smo sklepali o sedimentacijskih pogojih na območju jamskega vhoda. Z raziskavami magnetnih lastnosti mineralov smo določali izvor sedimentov in značilnosti paleookolja. V vzorcih smo merili magnetno susceptibilnost pri visoki in nizki frekvenci ter parametre remanentnega magnetizma, kot sta izotermni remanentni magnetizem po nasičenju (SIRM) in S-količnik. Na osnovi variabilnosti magnetnega signala v sedimentih smo ločili obdobja naravnih in antropogenih plasti. Rezultati arheoloških, stratigrafskih in magnetnih raziskav kažejo, da so opustitev prazgodovinske naselbine povzročile poplave reke Krousovitis in sedimentacija iz poplavne vode približno 3000 let pred našim štetjem.

Ključne besede: jama Katarakktes, Grčija, holocenske poplave, poplavni sedimenti, geomagnetizem.

[1] Aristotle University of Thessaloniki, School of Geology, Department of Physical Geography
[2] Aristotle University of Thessaloniki, School of Geology, Department of Geophysics, e-mail: pennos@geo.auth.gr, sophiap@geo.auth.gr, aidona@geo.auth.gr, vouval@geo.auth.gr

Received/Prejeto: 19.08.2013

INTRODUCTION

The paleoenvironmental significance of rockshelters and caves has long been recognized since these well protected environments act as important sediment traps that record past environmental conditions (Colcutt 1979; Karkanas 2001; Woodward & Goldberg 2001). Sedimentary sequences preserved at the entrance of these cave systems usually contain materials formed directly at the site (autogenic), such as coarse debris derived from roof collapse, as well as materials introduced from off-site sources (allogenic), such as fine-grained sediments transported by wind and water and coarser particles transported by slope processes (Sroubek *et al.* 2001). Changes in the flux of the fine-grained allogenic sediments are often related to changes in the off-site environment and thus the study of the fine-grained component considered assessing local and regional environmental changes (Woodward *et al.* 2001). In addition, many cultural sequences and archaeological artifacts are well preserved in rockshelter and cave sediment records and can be effectively used for paleoenvironmental interpretation. Karstic sites were attractive locations for human activity since they provided protection. In the broader area of the Mediterranean numerous records concerning the prehistoric cultures of the region have been derived from archaeological remains excavated from these environments (e.g. Gamble 1986; Straus *et al.* 1996; Bailey *et al.*1999).

During the last decades, paleoenvironmental interpretation of sedimentary sequences preserved at rockshelters and caves around the Mediterranean region is being conducted by employing a variety of methodologies such as sedimentological, geochemical and micromorphological analysis (e.g. Karkanas 1999; Courty & Vallverdu 2001; Straus *et al.* 2001; Woodward *et al.* 2001; Angelucci 2003; Turk & Turk 2010), as well as paleontological analysis (Chatzopoulou *et al*. 2001; Toškan 2009). Also, long term and short term climate fluctuations have been documented from high-resolution isotopic speleothem records (e.g. Frisia *et al.* 1998; Bar-Matthews *et al.* 1999; Bar-Matthews & Ayalon 2005).

Furthermore, mineral magnetic properties (e.g. magnetic susceptibility, remanence ratios such as ARM/SIRM and S ratio) have been successfully used to reconstruct paleoenvironmental and paleoclimatic conditions in rockshelter and cave sites (e.g. Ellwood *et al.* 1996, 2004; Sroubek *et al.* 1998, 2001, 2007; Zupan *et al. 2010*). Environmental magnetism techniques allow a rapid, low cost and sensitive characterization of sediments and can be applied in a wide range of environments (Thompson & Oldfield 1986). Magnetic properties of unconsolidated cave sediments serve as paleoclimatic proxies, since climate is the main factor controlling the magnetic signal of the source sediments, mainly as the result of pedogenesis. Pedogenic processes outside the cave produce abundant magnetic minerals such as maghemite, magnetite, hematite, and possibly greigite during periods when climate is relatively warm and wet. This increases the magnetic signature of sediments, which are protected from further pedogenesis and biological disturbance once redeposited inside caves (Ellwood *et al.* 2001).

In the present study we investigate the sedimentary record of three archaeological sections in the Katarraktes Cave system (Serres, Macedonia region, northern Greece), which is one of the most important archaeological sites in SE Europe. During the last eight years, the Ephorate of Paleoanthropology and Speleology of Northern Greece excavated numerous archaeological findings dating back to the Early Bronze Age. Previous studies have focused on the geoarchaeological setting of the karstic system (Pennos *et al.* 2008), while a paleoclimatic reconstruction of the site during human occupation has been performed, using isotopic fingerprints of carbonate sediments (Psomiadis *et al.* 2009). However, little attention has been given to the paleoenvironmental signal of the clastic sediments deposited at the entrance of the Katarraktes Cave system. In the present work we attempt an assessment of the paleoenvironmental conditions under which the deposition of the entrance facies sediments took place, coupling geomorphological, stratigraphical and environmental magnetism methods. The approach followed in this study enables a clear distinction between the natural and the anthropogenic signal stored in the sedimentary record of the Katarraktes Cave system. Moreover, a link between the detected environmental changes and the archaeological phases evidenced in the sedimentary record is provided.

STUDY AREA

GEOLOGICAL SETTING

The Katarraktes cave system is located at the southern banks of the Krousovitis River canyon, approximately 2 km northwest of Sidirokastro city (northern Greece), at an altitude of 94 m above mean sea level (Fig. 1). The elevation of the Karstic site is approximately 10 m above the

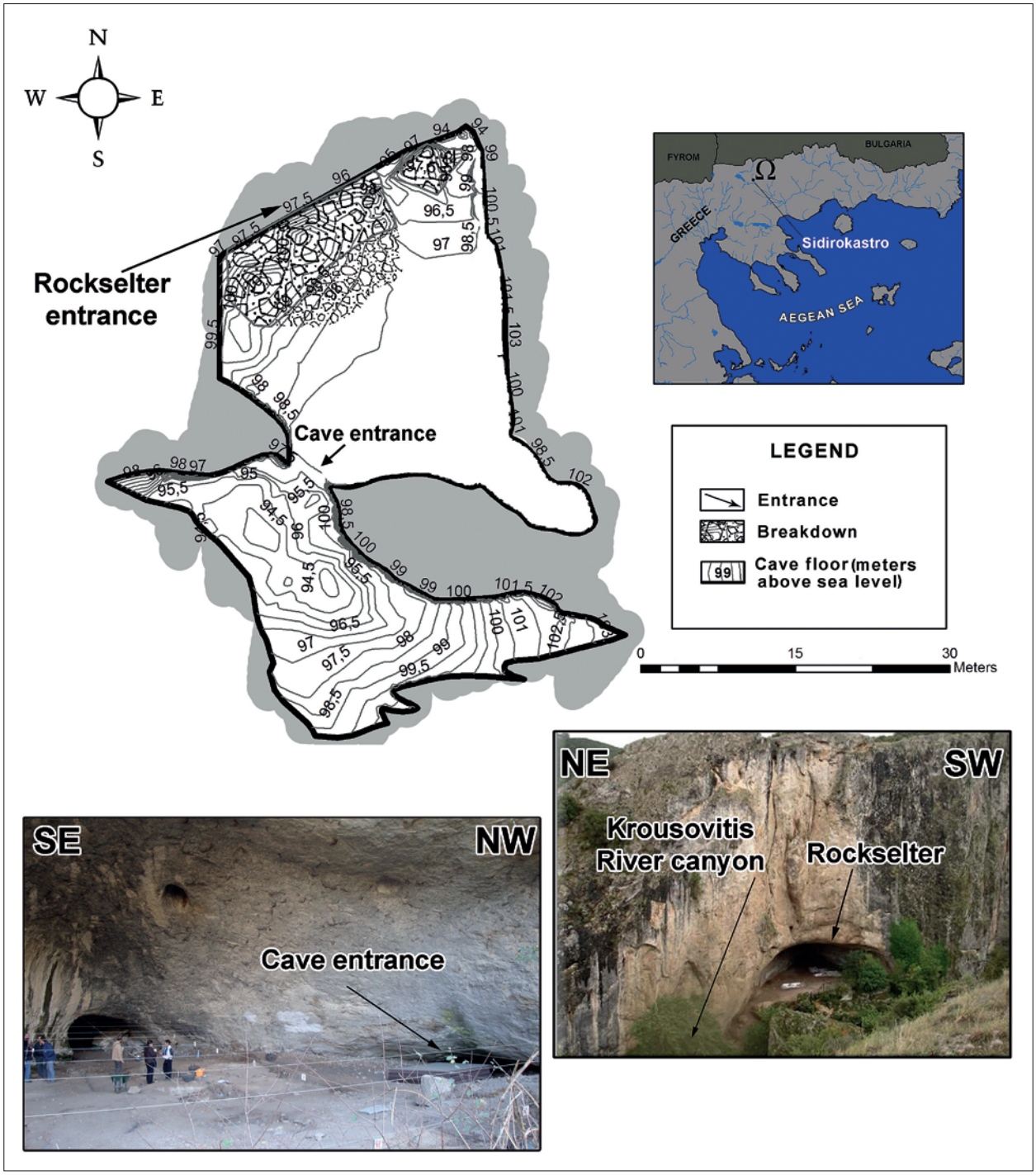

Fig. 1: Geographical setting of the Kararaktes cave system and ground plan of the site.

present river level. The total surface area of the Krousovitis River basin reaches almost 300 km^2 and it is characterized by high geomorphological relief since it is part of the tectonic graben of Serres (Papafilippou-Pennou 2004). The broader area belongs to the Rhodope massif consisting of gneiss and marbles, while sediments of Neogene age, mainly conglomerates of granitic composition and silty sands, are superimposed at the bedrock. The Krousovitis River forms a canyon created due to intense tectonic uplift during the Early Neogene – Late Pliocene. Quaternary tectonic movements produced new, but less intense uplifts, which seem to have shaped the structure of the canyon during the Middle – Late Pleistocene (Psilovikos *et al.* 1981). Furthermore, quantitative geomor-

phological analysis revealed that the tectonic activity is still intense and numerous caves at each side of the river bank likely indicative of older levels of the river flow are closely related to the tectonic regime of the area (Papafilippou-Pennou 2004).

KATARRAKTES CAVE SYSTEM MORPHOLOGY AND SPELEOGENESIS

Katarraktes cave system comprises a complex of a rockshelter and a cave (Fig. 1). The rockshelter has a vaulted shape and it is approximately 34 m wide and 22 m deep. The surface area of the site reaches ~620 m^2. The central part of the rockshelter is characterized by low relief (ground slopes are ~0–7%), while close to the entrance of the rockshelter the

relief is significant higher (ground slopes > 45%) (Fig. 2, from Pennos *et al.* 2008). This morphology favors the deposition of fine sediments (fine sand, silt and clay) at the central part of the rockshelter and also the drainage of the cave during flood events of the Krousovitis River following the general slope of the floor to the north. Erosional surfaces observed in many archaeological sections, as well as deposition of fine sediments, granitic pebbles, shingles and breccias along with anthropogenic materials and charcoal deposits at the entrance of the cave system point to high-energy events connected with the fluvial action of the Krousonitis River. Moreover, eroded calcite deposits overhanging portions of the cave entrance at an altitude of 1 m higher above the cave floor wall were also observed, indicating sediment outflow due to flood events and erosional phenomena of the palaeo-floor surface (Pennos *et al.* 2008).

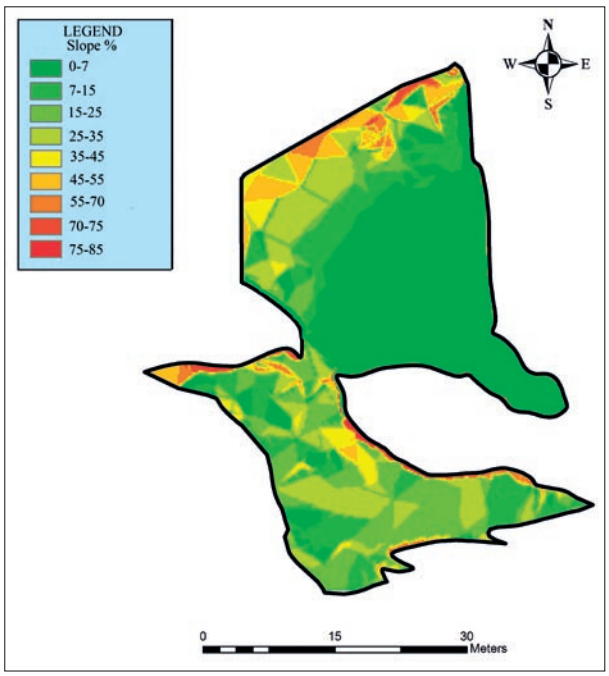

Fig. 2: Slope map of the Kataraktes cave system (from Pennos et al. 2008).

Katarraktes cave has formed at the epiphreatic zone in limestone conglomerate while it passed at the vadose zone possible due to the tectonic uplift of the region during the Middle – Late Pleistocene. The cave is developed along a group of subvertical joints in a NW – SE direction that are the major speleogenetic factor, which control the orientation of cave passages. The whole cave system is closely linked to the karst hydrological network and thus it can be described as an active karst setting (Woodward & Goldberg 2001). Seasonal water flows, dripping vadose waters and inwashing of fine sediments through conduits in the host bedrock are some of the key features of the Katarraktes cave system. Moreover, numerous carbonate deposits are present in the interior facies of the site, revealing a rather 'fresh' and rapid precipitation of carbonate material, indicated mainly by their porous texture (Psomiadis *et al.* 2009). At the entrance of the cave colluvial deposits are present, formed due to the regressive erosion and back stepping landslides of the canyon slopes.

ARCHAEOLOGICAL DATA

Archaeological research in the Katarraktes cave system started in 2004 and is continuing until 2013. Fig. 3 shows a plan view of the excavation site at the Katarraktes rockshelter. Excavations have revealed numerous archaeological finds, such as pottery and tools, dating back to the Early Bronze Age (Syros *et al.* 2008). Recent archaeological findings revealed two main prehistoric phases of occupation (named A and B phase), in contrast to previous archaeological studies where three phases of occupation had been proposed (Poulaki-Pantermali *et al.* 2006; Syros *et al.* 2008).

Both prehistoric phases of occupation (A and B phase) are mainly characterized by earthen floors interrupted by a thick clayey deposit, which is marked by the absence of any archaeological remains. The oldest archaeological phase (B phase) is detected more than half a meter below the surface and radiocarbon dating on charcoals revealed a range of ages between 3341 to 2915 cal yr BC (Syros & Miteletsis 2012 in press). Moreover, ceramics date this phase approximately at the end of the 4th millennium (~3000 yr BC) and suggest a close relation to the Sitagroi IV (Sherratt 1986) and Dikili Tash IIIA (Seferiades 1983) phases of eastern Macedonia. The youngest archaeological phase (A phase) includes mainly disturbed superficial layers. Charcoal deposits reveal an absolute age of 2880–2573 cal yr BC (Syros

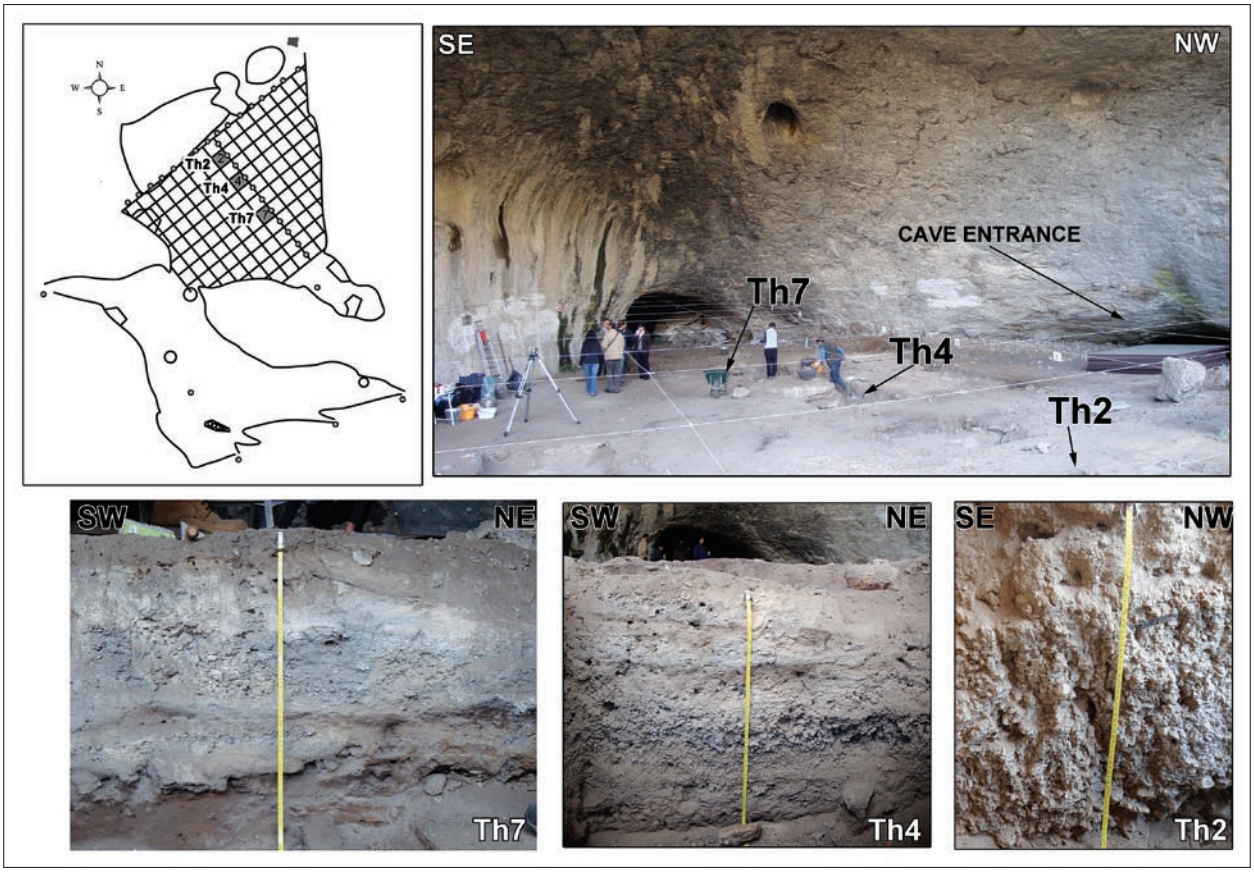

Fig. 3: Plan view of the excavation site at the Katarraktes rockshelter, with location and photographs of the studied archaeological sections, Th2, Th4 and Th7.

& Miteletsis 2012 in press). This period is characterized by the phases Sitagroi V (Sherratt 1986) and Dikili Tash IIIB (Seferiades 1983) for eastern Macedonia and Ezero B for Bulgaria.

SAMPLING AND METHODOLOGY

Three archaeological sections (Th2, Th4 and Th7) located at the central part of the Katarraktes rockshelter have been studied in detail (Figs. 3 and 4). Each archaeological trench is 2 × 2 m while the profile depth extent varies from 50 cm to 63 cm. The selected profiles are considered as the most representative among the remaining archaeological sections of the site, since they provide the best preserved stratigraphical and archaeological record. Profiles were cleared from loose debris and detailed logging of the stratigraphy was carried out before sampling. Bulk sampling was performed continuously throughout the three profiles and samples were packed in plastic boxes ($2 \times 2 \times 1.6$ cm^3).

In the laboratory, low field volume magnetic susceptibility measurements (k_{lf}) were obtained from each collected sample with a Bartington MS2 meter (resolution: 2×10^{-6} SI on 0.1 range) and a Bartington MS2B dual frequency sensor at low (0.465 kHz ±1%) and high (4.65 kHz ±1%) frequency. Low-field susceptibility (k_{lf}) is a concentration-depended magnetic parameter, indicating the concentration of the ferrimagnetic minerals (magnetite/maghemite) (Evans & Heller 2003). The dual frequency enabled the estimation of the frequency depended magnetic susceptibility (k_{fd}) which indicates the presence of ferrimagnetic grains close to the superparamagnetic stable single domain (SP) transition. Saturation isothermal remanent magnetization (SIRM) was imposed by applying a maximum field of 1 T DC-field in a Pulse Magnetizer, while a reverse field (–300 mT) was applied to evaluate the S_{-300} ($IRM_{-300mT}/SIRM_{1T}$) ra-

tio (King & Channell 1991). S_{-300} ratio is a widely used proxy of the magnetic mineralogy, with values close to unity suggesting that magnetite controls the magnetic signal (Stober & Thompson 1979). Measurements of both $SIRM_{1T}$ and IRM_{-300mT}, were performed using a Molspin magnetometer.

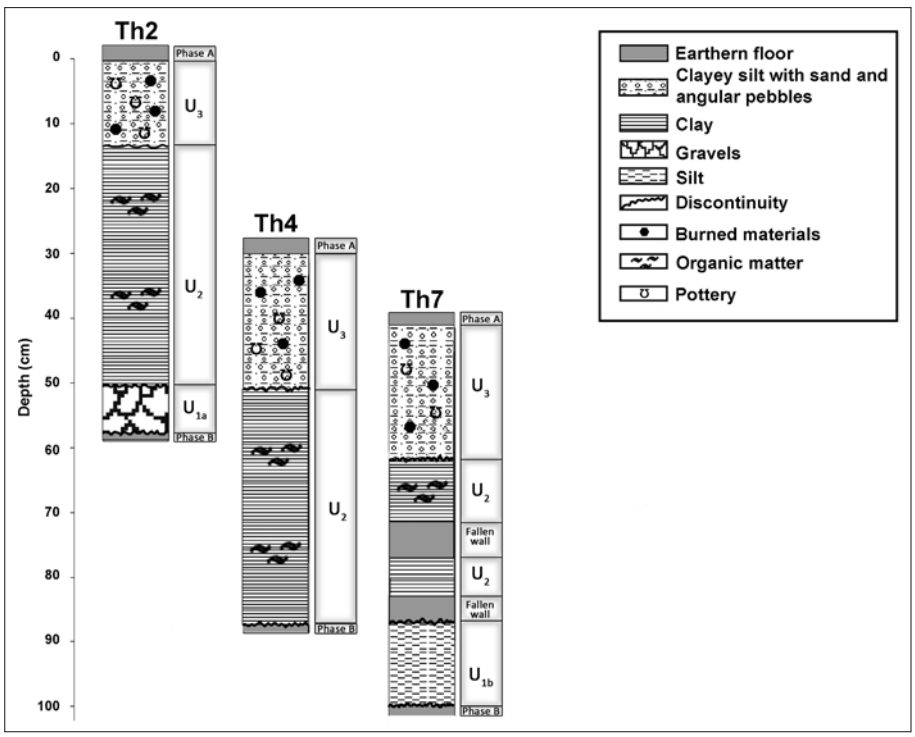

Fig. 4: Stratigraphic columns of the archaeological sections Th2, Th4 and Th7.

RESULTS

DETAILED STRATIGRAPHY

Archaeological sections Th2, Th4 and Th7, show a rather similar stratigraphic architecture; sequences of clayey sediments alternating with silty and sandy layers with scattered gravels are found between the two clayey archaeological floors, corresponding to the archaeological phases A και B. The detailed stratigraphic study revealed three successive depositional units, which can be described as follows (Fig. 4):

The first unit (U_1) is found at the deepest parts of Th2 and Th7 profiles. It overlies an archaeological floor composed of packed clay, which corresponds to the archaeological phase B. U_1 is subdivided into two distinct depositional units, U_{1a} and U_{1b}. U_{1a} is found in Th2 profile at ~50 cm depth and has a maximum thickness of ~7 cm. It consists of coarse material, mainly poorly sorted gravels and angular pebbles. U_{1b} is found in Th7 profile at 87 cm depth and is composed of fine grained sediments (fine sand, silt and clay), with a maximum thickness of ~15 cm.

The second unit (U_2) overlies uncomfortably U_1 in Th2 and Th7 profiles, while it is found directly above the lowest archaeological floor (archaeological phase B) in Th4 profile. The sediment texture of this unit is mainly composed of light grey silty clay. Mineralogical analysis (XRD) of representative samples has shown that the main phase of the studied material is calcite. Quartz and feldspars were contained in smaller quantities, while dolomite, micas and clays were found in minor amounts. Organic residuals, mainly plant remains, are also scattered throughout the sediment. The thickness of this unit varies from 37 cm in Th2 profile to 27 cm in Th7 profile. In addition, two clayey insertions that have been recognized as parts of a fallen wall (Syros & Miteletsis 2012 in press) are noticeable in Th7 profile, between the depth ranges 72–78 cm and 83–87 cm.

The third unit (U_3) is found at the upper parts of Th2, Th4 and Th7 profiles, overlying uncomfortably U_2. It has a maximum thickness of approximately 20 cm and includes poorly sorted sandy silt and silty clay with an-

gular pebbles. Pottery, burned seeds and cereals are noticeable, pointing to anthropogenic origins for these sediments. At the upper part of this unit an archaeological floor consisting of packed clay is present, corresponding to the youngest archaeological phase A.

MAGNETIC PROPERTIES

The variation with depth of all the magnetic parameters examined for the studied archaeological sections Th2, Th4 and Th7 are shown in Fig. 5. In Th2 profile (Fig. 5A) magnetic susceptibility (k_{lf}) shows a generally increasing trend from the lowest part of the section (50 cm depth) to its upper part. Mean k_{lf} values are approximately 80×10^{-5} SI across U_2 below 12.5 cm depth, while they are significantly higher at the upper part of the profile across U_3, reaching mean values of $\sim 223 \times 10^{-5}$ SI. The SIRM log follows a similar trend as the magnetic susceptibility; lower SIRM values (mean ~3 A/m) are found between 50 cm and 12.5 cm depth (U_2), while higher SIRM values (mean ~6.5 A/m) characterize the upper part (U_3) of the Th2 profile. S_{-300} depict a slightly opposite trend with values > 0.85 for U_2 which are decreasing upwards (< 0.85) across U_3. Moreover, percentage of frequency dependence susceptibility (k_{fd} %) yields relatively low values (mean ~3%) for both units U_2 and U_3.

Th4 profile shows a similar magnetic signature with Th2, with an increasing trend towards the surface for k_{lf} and SIRM parameters that also distinguish between U_2 and U_3 (Fig. 5B). Lower k_{lf} and SIRM values are observed at the interval between 90 cm and 50 cm across U_2 (mean $\sim 70 \times 10^{-5}$ SI and ~3.6 A/m, for k_{lf} and SIRM, respectively), while higher k_{lf} and SIRM values (mean ~ 140×10^{-5} SI and ~6.5 A/m, for k_{lf} and SIRM, respectively) are found at the interval between 50 cm and 30 cm, across U_3. Moreover, the k_{fd} % pattern mimics the variation of magnetic susceptibility and SIRM with depth and shows a significant increase above 6% between 60 cm and 50 cm depth. S_{-300} is almost constant ranging from 0.9 to 0.98 with an exception occurs at 50 cm showing a lower value of 0.84 that indicates possible presence of high coercivity minerals (e.g. hematite).

For the Th7 profile the variation of the magnetic parameters is more complex (Fig. 5C). At the lower part of the Th7 profile across U_{1b} (below 90 cm depth) k_{lf} depicts high values (mean $\sim 200 \times 10^{-5}$ SI). Going upwards to U_2, k_{lf} values are significant lower (mean $\sim 93 \times 10^{-5}$ SI) and are interrupted by two observed peaks at the depths of 88 cm and 75 cm (k_{lf} values are 275×10^{-5} SI and $\sim 240 \times 10^{-5}$ SI, respectively). These layers correspond to the two fallen walls, also observed in the archaeological record. k_{lf} values exhibit again relatively high values (mean $\sim 200 \times 10^{-5}$ SI) for the upper part of the section above 60 cm depth, within U_3. SIRM show a similar trend as the magnetic susceptibility emphasizing in the two peaks of the fallen walls. Furthermore, S_{-300} ratio is rather constant along the profile with no values lower than 0.83. Finally, the k_{fd} % shows increased values of 6% up to 80 cm depth followed by lower values in the range of about 4% until the end of the profile.

DISCUSSION

Stratigraphic analysis of the archaeological sections Th2, Th4 and Th7, allowed the subdivision of the Katarraktes sedimentary sequence into three depositional units; U_1, U_2 and U_3, also supported by observed mineral magnetic properties. These units were deposited under different palaeoenvironmental conditions, showing both natural and anthropogenic origins. U_1, consists of natural deposits found at the lower parts of the archaeological sections Th2 and Th7 and corresponds to the sedimentation phase that took place after the archaeological phase B, dated back at 3341–2915 cal yr BC. Magnetic analysis of U_1 was performed only in section Th7, since in section Th2 the observed subunit U_{1a} consists of coarse grained sediments (gravels and pebbles), making it impossible to sample. These coarse deposits are most likely part of the debris cone that was formed at the entrance of the rockshelter, as a result of the wall regression of the canyon. Nevertheless, mineral magnetic analysis of subunit U_{1b} indicates a relatively high concentration of magnetic minerals, revealed by high k_{lf} and SIRM values. A possible explanation for the observed magnetic signals within subunit U_{1b} could be the influence from the underlying archaeological phase B and a probable mixing with magnetically enhanced materials. Archaeological soils are generally characterized by large amounts of magnetic minerals, depicting relatively high magnetic susceptibility values (Thompson & Oldfield 1986; Evans & Heller 2003; Dalan 2008). Fluvial processes could have caused the mixing with the underlying archaeological remains; the unconformity found at the lowest part of subunit U_{1b} points to a period of erosion, reinforcing the suggestion of fluvial influence.

Similar magnetic signals are observed for the U_3, which is clearly identified at the upper parts of the pro-

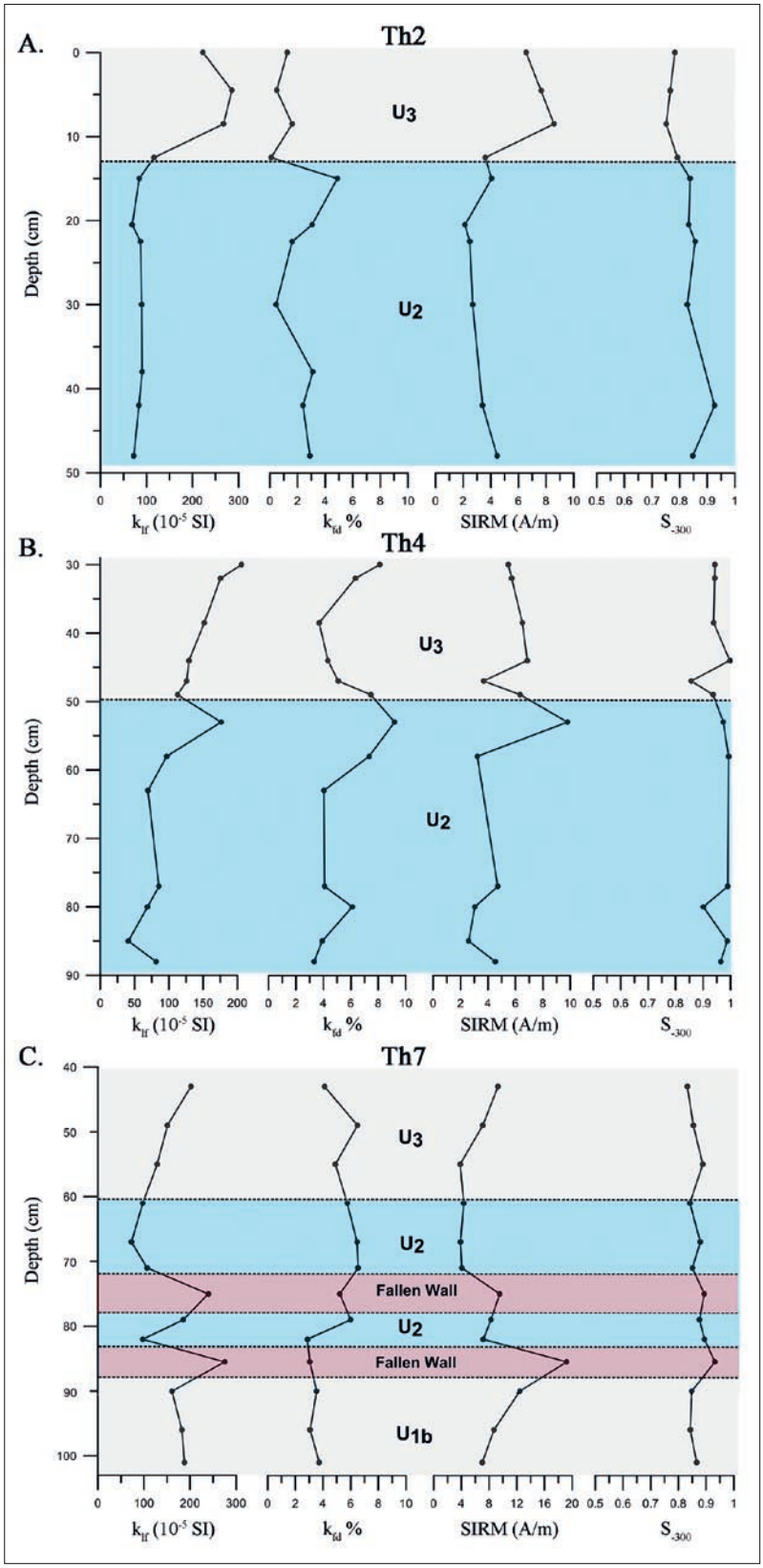

Fig. 5: Variation of mineral magnetic properties, klf (10^{-5} SI), kfd %, SIRM and S_{-300}, along the three profiles (For details see in the text).

files Th2, Th4 and Th7, below the earthen floor that corresponds to the youngest archaeological phase A (2880–2573 cal yr BC). Pottery, burnt seeds and other archeological remains reveal human interference and also account for the high k_{lf} and SIRM values.

In contrast, U_2 shows a clearly different magnetic behavior compared to the other two units. Magnetic susceptibility (k_{lf}) and SIRM yield lower values, indicating a low concentration of magnetic minerals. This could be due to dilution of minerogenic matter caused by increased organic sedimentation, since a considerable amount of organic matter is observed throughout U_2. Furthermore, the percentage of k_{fd} % shows a slightly increasing upwards trend through this unit, reaching values close to 6% that point to the possible presence of ultra-fine superparamagnetic (SP) magnetite grains (Dearing *et al.* 1996). Weymouth (2003) reported similar peak values of k_{fd} % in archaeological trenches and concluded that these are indicative of a soil development period, probably related to a period of stability before the erosive processes from the historic cultivation take place.

The magnetic mineralogy referred by S_{-300} ratio is rather uniform for units 1–3 in all studied profiles. This is indicative of the dominance of magnetite grains as the main magnetic carriers for the sedimentary record of Katarraktes cave system, but further magnetic analysis is needed in order to assess the magnetic mineralogy of the site.

The above discussion concerning the behavior of the magnetic parameters, especially the magnetic susceptibility and the SIRM (which show the biggest variations) can be summarized in Fig. 6. A unified plot composing the results of the magnetic susceptibility and SIRM from the 3 profiles is presented in order to better distinguish the different units by means of magnetic properties. The position of the samples has been normalized within each unit using a linear correlation and all results have been plotted using different colors for each

profile respectively. The line represents the moving average of the obtained results excluding the points which corresponds to the fallen walls. This synthetic plot confirms the presence of high values in anthropogenic (or mixed) layers U_3 and U_1 respectively, while in U_2 values of k_{lf} and SIRM are systematic lower.

The stratigraphic and magnetic analysis of the archaeological sections at the Katarraktes cave system provides evidence that can be employed for the paleoenvironmental reconstruction of the site during the Middle – Late Holocene. The clayey sediments comprising U_{1b} and U_2 form naturally deposits accumulated uncomfortably above the earthen floor of Middle Holocene age (phase B), while the underlying anthropogenic strata (U_3). The stratigraphic position of these units following the morphology of the rockshelter's floor, as well as the erosional surfaces observed in the three profiles above the oldest archaeological floor (Fig. 4), suggest the occurrence of high-energy events (e.g. floods of Krousovitis River) that must have interrupted the human occupation in the site. Moreover, the two parts of a fallen earthen wall in Th7 profile recorded from archaeological data, as well as from the stratigraphic and magnetic analysis, further support the suggestion of the presence of catastrophic events in the site area. According to the archaeological datings these flood events should have been taken place at the time span between ~3120 cal yr BC and ~2720 cal yr BC. Evidence of possible flood events of Krousovitis River has also been reported from previous studies at the site (Pennos *et al.* 2008; Psomiadis *et al.* 2009).

The detailed analysis of the Katarraktes sequence reveals that U_{1b} consists of sediments deposited by fluvial processes. However this unit is only evident in Th7 profile since it is located at the deeper parts of the Katarraktes rockshelter compared to the other two profiles (Fig. 4). U_2, is apparent in all archaeological sections and is also composed of fluvial deposited sediments. The mineralogical analysis reinforces the above observation since the composition of the sediments corresponds to natural deposits. The presence of fine grained sediments and organic material across U_2, along with the small concentration of magnetic minerals demonstrate deposition under low energy conditions, most likely from slackwater during the floods of Krousovitis River. Studies from rockshelters sites around the Mediterranean have shown that these environments may form important slackwater sedimentation zones (Woodward & Goldberg 2001 and references therein). However, only few slackwater deposits in rockshelters and caves have been reported in Greece mainly from Voidomatis River basin (Lewin *et al.* 1991; Hamlin 2000; Woodward *et al.* 2001).

The detected flood events of the Krousovitis River must have acted as the key factor for the abandonment of the settlement in the study area between ~3120 cal yr BC and ~2720 cal yr BC. The timeframe of these events is in good agreement with paleoclimatic studies for the Katarraktes cave system, suggesting wet climatic conditions during this period (Psomiadis *et al.* 2009).

CONCLUSIONS

Stratigraphic analysis of three archaeological sections at the Katarraktes cave system combined with mineral magnetic analysis of sediments and archaeological data revealed the paleoenvironmental conditions under which the cave entrance phases accumulated. Both natural and anthropogenic sequences were observed, organized in three successive depositional units (U_1–U_3).

Fine-grained sediments lying uncomfortably above the earthen floor of Middle Holocene age and following the rockshelter's floor in combination with the absence of archaeological findings, suggests deposition by fluvial processes and in particularly from slackwater during the flood events of Krousovitis River. These slackwater deposits show rather small concentration of magnetic minerals reflected by low values of k_{lf} and SIRM that caused by increased organic sedimentation. Furthermore, the presence of ultra-fine superparamagnetic (SP) magnetite grains reflected by increased k_{fd} % values, also points to deposition under low energy conditions.

The flooding events of Krousovitis River took place between 3120–2720 cal yr BC and were possible the key factor for the abandonment of the settlement in the study area. The combined analysis followed in this study reveals the presence of two parts of a fallen wall that interrupt the naturally deposited sediments and point to a catastrophic event. Furthermore, additional magnetic measurements in the other archaeological section available in the site could provide more information in order to further constrain the detailed palaeoenvironmental signals of the cave entrance deposits of the site area.

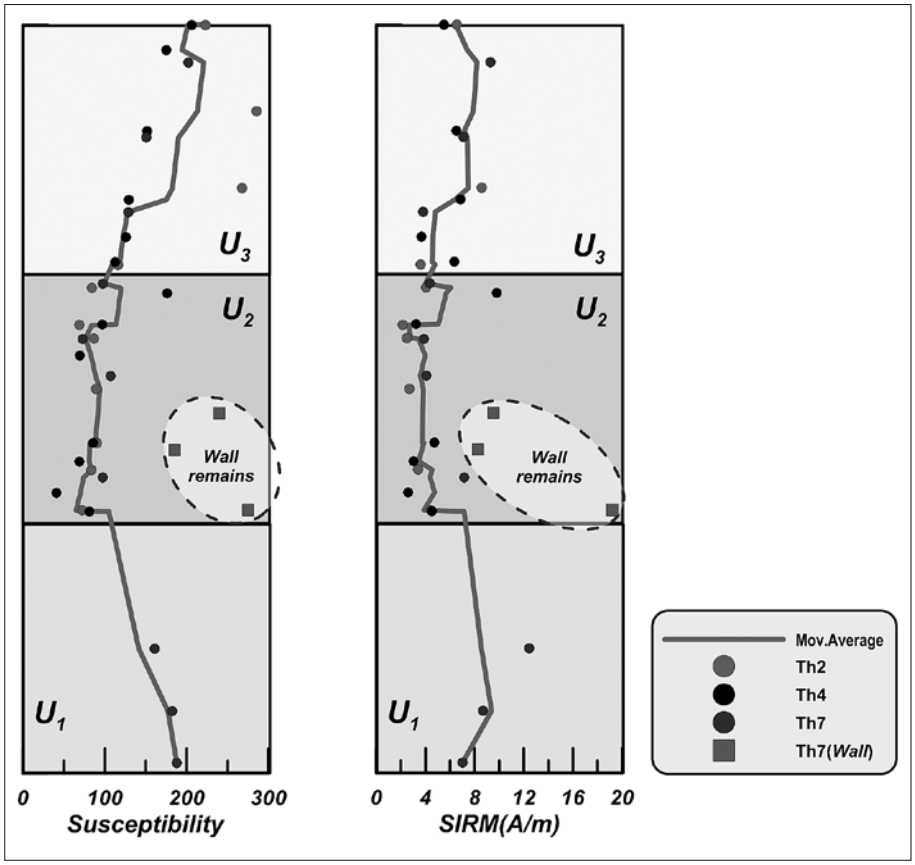

Fig. 6: Unified plot of magnetic susceptibility and SIRM for the three units (U_1–U_3). Line corresponds to the moving average of all values.

ACKNOWLEDGEMENTS

The authors would like to express their gratitude to the archaeologists Miteletsis M. and Syros A. and to geologist J. Vlastaridis of the Ephorate of Paleoanthropology and Speleology of the Northern Greece for their help during the sampling, as well as for providing their evaluation of the archaeological data. Special thanks to Prof. Reidar Lovlie and Prof. Stein Erik Lauritzen for their valuable conversations during the preparation of the manuscript. Dr. Kantiranis kindle performed the XRD analyses and is warmly thanked. The manuscript has been benefitted from the valuable comments of the reviewers Dr. Janez Turk and Dr. Nadja Zupan Hajna.

REFERENCES

Angelucci, D.E., 2003: Geoarchaeology and micromorphology of Abric de la Cativera (Catalonia, Spain).- Catena 54, 573–601.

Bailey, G.N., Adam, E., Panagopoulou, E., Perles, C. & K. Zachos, 1999: The Paleolithic archaeology of Greece and adjacent areas.- Proceedings of the ICOPAG Conference, British School at Athens, Athens, 1994.

Bar-Matthews, M., Ayalon, A., Kaufman, A. & G.J. Wasserburg, 1999: The Eastern Mediterranean paleoclimate as a reflection of regional events: Soreq cave, Israel.- Earth and Planetary Science Letters 166, 85–95.

Bar-Matthews, M. & A. Ayalon, 2005: Evidence from speleothem for abrupt climatic changes during the Holocene and their impact on human settlements in the Eastern Mediterranean region: Dating methods and stable isotope systematic.- Zeitschrift fur Geomorphologie, Supplement band 137, 45–59.

Chatzopoulou, K., Vasileiadou, A., Koliadimou, K., Tsoukala, E., Rabeder, G. & D. Nagel, 2001: Preliminary report on the Late Pleistocene small mammal fauna from Loutraki Bear-cave (Pella, Maced., Greece).- Cadernos Lab. Xeolóxico de Laxe, 26: 485–495, Coruña, Spain.

Collcutt, S.N., 1979: Analysis of Quaternary cave sediments.- World Archaeology 10, 290–301.

Courty, M.A. & J. Vallverdu, 2001: The Microstratigraphic Record of Abrupt Climate Changes in Cave Sediments of the Western Mediterranean.- Geoarchaeology: An International Journal 16, 467–500.

Dalan, R., 2008: A review of the role of magnetic susceptibility in archaeogeophysical studies in the USA: Recent developments and prospects.- Archaeological Prospection 15, 1–31.

Dearing, J.A., Dann, R., Hay, K., Lees, J., Loveland, P., Maher, B. & K. O'Grady, 1996: Frequency-dependent susceptibility measurements of environmental materials. -Geophysical Journal International 124, 228–240.

Ellwood, B.B., Petruso, K.M., Harrold, F.B. & M. Korkuti, 1996: Paleoclimate characterization and intra-site correlation using magnetic susceptibility measurements. and example from Konispol Cave, Albania.- J. Field Archaeol., 23, 263–271.

Ellwood, B.B., Harrold, F.B., Benoist, S.L., Straus, L.G., Morales, M.G., Petruso, K., Bicho, N.F., Zilhao, J. & N. Soler, 2001: Paleoclimate and Intersite Correlations from Late Pleistocene/Holocene Cave Sites: Results from Southern Europe.- Geoarchaeology: An International Journal, 16, 433–463.

Ellwood, B.B., Harrold, F.B., Benoist, S.L., Thacker, P., Otte, M., Bonjean, D., Long, G.J., Shahin, A.M., Hermann, R.P. & F. Grandjean, 2004: Magnetic susceptibility applied as an age-depth-climate relative dating technique using sediments from Scladina Cave, a Late Pleistocene cave site in Belgium.- Journal of Archaeological Science 31, 283–293.

Evans, M. & F. Heller, 2003: *Environmental Magnetism* – Principles and Applications of Enviromagnetics. Academic Press, pp. 293.

Frisia, S., Borsato, A., Mcdermott, F., Spiro, B., Fairchild, I., Longinelli, A., Selmo, E., Pedrotti, A., Dalmeri, G., Lanzinger, M. & K. van der Borg, 1998: Holocene climate fluctuations in the Alps as reconstructed from speleothems.- Preistoria Alpina 34, 111–118.

Gamble, C.S., 1986: *The Paleolithic settlement of Europe*. Cambridge University Press, Cambridge, pp. 471.

Hamlin, R.H.B., 2000: *Environmental change and catastrophic flooding in the Voidomatis and Aoos Basins, Northwest Greece.*- PhD Thesis, Leeds, University of Leeds, UK.

Karkanas, P., 1999: Lithostratigraphy and micromorphology of Theopetra cave deposits, Thessaly Greece: Some preliminary results.- In G.N. Bailey, E. Adam, E. Panagopoulou, C. Perle's & K. Zachos (Eds.), *The Palaeolithic archaeology of Greece and adjacent areas,* pp. 240–251, British School at Athens Studies 3., British School at Athens, London.

Karkanas, P., 2001: Site formation processes in Theopetra Cave: A record of climate change during the late Pleistocene and early Holocene in site formation processes in Theopetra Cave.- Geoarchaeology: An International Journal 16, 373–399.

King, J. & J.E.T. Channell, 1991: Sedimentary magnetism, environmental magnetism, and magnetostratigraphy.- In: *U.S. National Report to International Union Geodesy and Geophysics. Rev. Geophys. Suppl.,* 29, 358–370.

Lewin, J., Macklin, M.G. & J.C. Woodward, 1991: Late Quaternary fluvial sedimentation in the Voidomatis Basin, Epirus, northwest Greece.- Quaternary Research, 35, 103–115.

Papafilippou-Pennou, E., 2004: *Dynamic evolution and recent exogenic processes of Strymon river network in Serres graben (North Greece).*- PhD, Aristotle University of Thessaloniki, 212 pp. (in Greek with extended English abstract).

Pennos, Ch., Vaxevanopoulos, M., Syros, A., Miteletsis, M., Pechlivanidou, S. & I. Vlastaridis, 2008: Genesis and development of caves in Katarraktes region Sidirokastro, Macedonia, Greece. A geoarchaeological approach. – *5th Symposium of the Hellenic Society of Archaeometry,* 8–10 October, Thessaloniki, Greece. (in Greek)

Poulaki-Pantermali, E., Vaxevanopoulos, M., Koulidou, S. & A. Syros, 2006: Dam Katarraktes in Sidirokastro.- *Archaeological Work in Macedonia and Thrace, 18th Scientific Meeting,* Thessaloniki, Greece, 63–71. (in Greek)

Psilovikos, A., Vavliakis, E. & L. Sotiriadis, 1981: Granite core stones and tors in the Vrontou mountains.- Arbeit Institut Geographie 8, Salzbourg, 63–78.

Psomiadis, D., Dotsika, E., Zisi, N., Pennos, Ch., Pechlivanidou, S., Albanakis, K., Syros, A. & M. Vaxevanopoulos, 2009: Geoarchaeological study of Katarraktes cave system (Macedonia, Greece): isotopic evidence for environmental alterations.- Géomorphologie: relief, processus, environnement, 4, 229–240.

Seferiades, M., 1983 : Dikili Tash: introduction à la Préhistoire de la Macédoine orientale.- Bulletin de correspondance hellénique 107, 635–677.

Sherratt, A.G., 1986: The Pottery of Phases IV and V: The Early Bronze Age.- In: Renfrew C., Gimbutas M. & E.S. Elster (Eds.): *Excavations at Sitagroi. A Prehistoric Village in Northeastern Greece.* – Monumenta Archaeologica 13, University of California, Los Angeles, 429–476.

Šroubek, P., Diehl, J.F., Kadlec, J. & K. Valoch, 1998: Preliminary study on the mineral magnetic properties of sediments from the Kulna Cave.- Studia Geophysica et Geodaetica 3, 301–312.

Šroubek, P., Diehl, J.F., Kadlec, J. & K. Valoch, 2001: A Late Pleistocene paleoclimate record based on mineral magnetic properties of the entrance facies sediments of Kulna Cave, Czech Republic.- Geophys J. Int. 147, 247–262.

Šroubek, P., Diehl, J.F. & J. Kadlec, 2007: Historical climatic record from flood sediments deposited in the interior of Spirálka Cave, Czech Republic.- Palaeogeography, Palaeoclimatology, Palaeoecology 251, 547–562.

Stober, J.C. & R. Thompson, 1979: Magnetic remanence acquisition in Finnish lake sediments.- Geophysical Journal of the Royal Astronomical Society 57, 727–739.

Straus, L.G., Eriksen, B.V., Erlandson, J.M. & D.R. Yesner, 1996: *Humans at the end of the Ice Age: The archaeology of the Pleistocene-Holocene transition.*- Plenum Press, New York, 365 pp.

Straus, L.G., Morales, M.G., Farrand, W.R. & W.J. Hubbard, 2001: Sedimentological and stratigraphic observations in El Miron, a late quaternary cave site in the Cantabrian Cordillera, northern Spain.- Geoarchaeology: An International Journal 16, 603–630.

Syros A., Tsagkouli, C., Myteletsis, M. & I. Vlastaridis, 2008: Cave in Katarraktes-Fragma site in Sidirokastro.- *Archaeological Work in Macedonia and Thrace, 20th Scientific Meeting,* 12 March, Thessaloniki, Greece. (in Greek)

Syros, A. & M. Miteletsis, 2012: Cave in the site Katarraktes, Sidirokastro, Serres, Greece.- In *The Neolithic and Bronze age Balkans,* eds, in press.

Thompson, R. & F. Oldfield, 1986: *Environmental Magnetism.* Allen and Unwin, pp. 227, London.

Toškan, B. 2009: Small terrestrial mammals (soricomorpha, chiroptera, rodentia) from the early holocene layers of Mala Triglavca (SW Slovenia).- Acta carsologica, 38, 117–133.

Turk, J. & M. Turk, 2010: Paleotemperature record in late Pleistocene clastic sediments at Divje babe 1 cave (Slovenia).- Journal of Archaeological Science 37, 3269–3280.

Weymouth, J., 2003: *Hopeton Geophysical Survey: The 2003 Season.* Report submitted to the Midwest Archeological Center, National Park Service: Lincoln, NE.

Woodward, J.C. & P. Goldberg, 2001: The Sedimentary Records in Mediterranean Rockshelters and Caves: Archives of Environmental Change.- Geoarchaeology: An International Journal 16, 327–354.

Woodward, J.C., Hamlin, R.H.B., Macklin, M.G., Karkanas, P. & E. Kotjabopoulou, 2001: Quantitative sourcing of slackwater deposits at Boila rockshelter: A record of lateglacial flooding and paleolithic settlement in the Pindus Mountains, Northwest Greece.- Geoarchaeology: An International Journal 16, 501–536.

Zupan Hajna N., Mihevc A., Pruner P. & P. Bosák 2010: Palaeomagnetic research on karst sediments in Slovenia.- International Journal of Speleology, 39, 2: 47–60. Bologna.

COBISS: 1.01

KARST SOILS: DEPENDENCE OF CO_2 CONCENTRATIONS ON PORE DIMENSION

ODVISNOST KONCENTRACIJE CO_2 OD VELIKOSTI POR V KRAŠKIH PRSTEH

Martin BLECHA[1,2] & Jiří FAIMON[1]

Abstract UDC 631.41:551.435.8(437.32)

Martin Blecha & Jiří Faimon: Karst soils: Dependence of CO_2 concentrations on pore dimension

CO_2 concentrations were studied in the selected soils of the Moravian Karst, Czech Republic. The direct measurement in the air of drill-holes has indicated that the concentrations depend inversely on a pore dimension. The simplified relation between the drill-hole diameter and CO_2 concentration, $c^0_{CO2}=\frac{c_{CO2}-bD}{1+aD}$, was proposed, where c^0_{CO2} is the CO_2 concentration extrapolated to the zero drill-hole diameter in ppmv, c_{CO2} is directly measured CO_2 concentration in ppmv, and D is drill-hole diameter in cm. a and b are parameters in cm^{-1} and ppmv cm^{-1}, respectively. For the karst soils formed at grass field and deciduous forest, the values of a and b parameters were determined as –0.146±0.012 (standard error) cm^{-1} and 262.0±56.3 ppmv cm^{-1}, respectively. The dependence between c_{CO2} and D was less obvious for the heavy clay soils of coniferous forest. To understand the dependence better, a conceptual model was created taking into account the concentration gradients and mass fluxes.

Keywords: CO_2 concentration, drill-hole diameter, karst soil, model.

Izvleček UDK 631.41:551.435.8(437.32)

Martin Blecha & Jiří Faimon: Odvisnost koncentracije CO_2 od velikosti por v kraških prsteh

Raziskovali smo koncentracijo CO_2 v izbranih prsteh na Moravskem krasu v Češki republiki. Neposredne meritve v vrtinah so pokazale, da odvisnost koncentracije CO_2 od premera vrtin zadovoljivo opiše enačba $c^0_{CO2}=\frac{c_{CO2}-bD}{1+aD}$, kjer je D [cm] premer vrtine v cm, c_{CO2} je vrednost meritve, c^0_{CO2} [ppmv] je ekstrapolirana koncentracija CO_2 za D = 0, a [cm^{-1}] in b [ppmv/cm] pa sta regresijska parametra. Za prsti na kraških travnikih smo dobili vrednosti parametrov a = −0,146±0,012 cm^{-1} in b = 262,0±56,3 ppmv·$cm.^{-1}$. Odvisnost med c_{CO2} in D je manj značilna v glinenih prsteh iglastih gozdov. Merjene odvisnosti smo pojasnili z modelom, ki upošteva gradiente koncentracij in masne tokove.

Ključne besede: koncentracije CO_2, premer vrtin, kraška prst, modeliranje.

INTRODUCTION

Carbon dioxide is the key component in carbonate karst that affects (i) limestone dissolution (e.g. Stumm & Morgan 1996), (ii) calcite/aragonite speleothem growth (e.g. Dreybrodt 1988), or speleothem corrosion (Sarbu & Lascu 1997). Researchers believe that karst/cave CO_2 is derived from karst soils (e.g. Ford & Williams 2007). The soil CO_2 is produced by the respiration of (1) autotrophs and (2) heterotrophs (Kuzyakov & Larionova

[1] Department of Geological Sciences, Faculty of Science, Masaryk University, Kotlářská 2, 611 37 Brno, Czech Republic, e-mail: faimon@sci.muni.cz

[2] Research Institute for Soil and Water Conservation, Žabovřeská 250, 256 27 Praha 5 – Zbraslav, Czech Republic, e-mail: blecha.martin@vumop.cz

Received/Prejeto: 26.09.13

2005; Kuzyakov 2006). CO_2 production may depend on temperature/moisture, soil profile depth, organic matter content, total rainfall, photosynthesis/solar radiation, and various anthropogenic factors such as soil tillage, or artificial change in vegetation cover. The role of abiotic sources is also considered (e.g., Serrano-Ortiz et al. 2010). Soil CO_2 is generally an important part of the global carbon cycle (e.g., Schlesinger & Andrews 2000).

The CO_2 concentrations in karst soil air are typically measured in a range from 0.1 to 1.0 vol. % (Yoshimura *et al.* 2001; Li *et al.* 2002; Spötl *et al.* 2005; Kawai *et al.* 2006; Faimon & Ličbinská 2010; Sanchez-Cañete *et al.* 2011; Faimon *et al.* 2012a). Some indices, e.g., karst water chemistry, enhanced CO_2 levels in certain caves, limited total soil pore volumes, CO_2 fluxes into external atmosphere, etc., question the soil capability for filling cave volume up to given concentrations. This indicates some more productive CO_2 sources participating on karst CO_2. The idea of an "underground CO_2" was already proposed by Atkinson (1977). For the karst environment, an epikarstic source is sometimes hypothesized (Fairchild *et al.* 2000; Spötl *et al.* 2005; Faimon *et al.* 2012a; Cuesva *et al.* 2011, Peyraube *et al.* 2012, 2013). The hypothesis is supported by evident discrepancy between (1) CO_2 concentrations directly measured in karst soils and (2) CO_2 concentrations reconstructed from dripwater hydrogeochemistry (see, Faimon *et al.* 2012b). Recently, Benavente *et al.* (2010) confirmed the existence of the enhanced CO_2 concentrations deeply in subsoil by an in-situ measurement. Even thought we agree with the idea of the epikarstic source, we have primarily concentrated on karst soils and its efficiency to fill enlarged pores by CO_2. The purpose of this study is to demonstrate how the diameter of drill-hole in soil profile can influence CO_2 concentrations.

METHODS

RESEARCH LOCATION

The study was performed in the Moravian Karst, the largest karst area in the Bohemian Massif (Czech Republic). It represents a belt of Middle and Upper Devonian limestones, 3–6 km wide and 25 km long (corresponding to 94 km^2 area). Typical soils consist of Rendzic Lep-

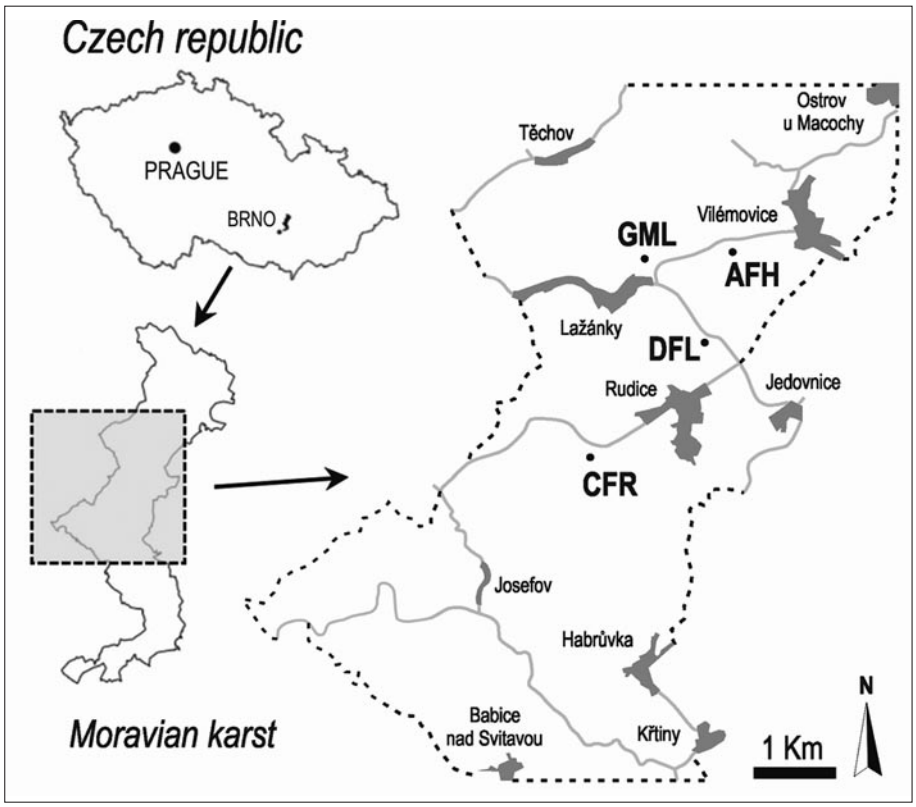

Fig. 1: Research location with monitoring sites.

Tab. 1: The soils and sampling sites.

Site	*coordinates*	*envir.*	*vegetation cover*	*pedogenic substrate*	*soil type*	*b. dens. g/cm3*	*por.*	*org. mat. wt. %*	*abbrevn.*
Harbechy Plateau	49°21´34´´N 16°43´49´´E	agricult. field	after harvest (wheat)	loam loesses	Haplic Luvisol	1.049	0.60	5.40	AFH
Lažánky I	49°21´24´´N 16°42´55´´E	meadow	grassy	devonian limestone	Rendzic Leptosols	0.702	0.72	13.22	GML
Lažánky II	49°20´47´´N 16°43´50´´E	forest	deciduous	loam loesses	Haplic Luvisol	0.880	0.65	8.88	DFL
Rudice	49°19´53´´N 16°42´34´´E	forest	coniferous	loam loesses	Stagnosols	1.086	0.57	8.51	CFR

envir. – environment; b. dens. – bulk density; por. – porosity; org. mat. – organic matter

tosols, Haplic Luvisols, and Albeluvisols. The research sites were located at the meadow and deciduous forests at Lažánky (Blansko), the agricultural field near the sinkhole Společňák at Vilémovice (Harbechy Plateau), and the coniferous forest at Rudice, see Fig. 1. The details on these sites/soils are illustrated in Tab. 1.

MONITORING

At every research location, shallow holes, 25 cm deep, and 7.0, 5.0, 2.7, and 2.0 cm in diameter were manually drilled into soils by using hand augers. These drill-holes were arranged into a line as follows: The 7-cm-hole was in the middle and further holes with decreasing diameters were on both sides. The drill-hole spacing was 20 cm each from other. The walls of drill-holes were reinforced by a plastic net. The top of the drill-hole was sealed by a plastic cap.

The CO_2 levels, temperature, and relative humidity in drill-hole air were repeatedly measured throughout two periods. The 1st period lasted from August 27 until September 13, 2012. The second began on May 5 and ended on May 17, 2013. The results were recorded between 3–6 P.M. The hand-held sensor FYA600–CO2H (Ahlborn, Germany) (±50 ppmv +2% of the values in the range < 5000 ppmv; ±100 ppmv +3% of the values in the range of 5000–10000 ppmv) working on principle of two-channel infrared absorption spectrometer (NDIR technology) was used to measure the CO_2 concentration. Since the sensor is cylindrical, 18 mm in diameter, it was placed directly into the drill-hole air at a depth of about of 11–12 cm. The sensor FHA646E1 (Ahlborn, Germany) was used to measure the temperature and relatively humidity (±0.4 °C in the range from –20 to 0 °C and ±0.1 °C in the range from 0 to +70 °C, and ±2% RH in the range from 0 to 100% RH at 25 °C). The sensors were plugged into the drill-hole by a rubber selvage to prevent CO_2 from escaping. The data were recorded after the stabilization of measured value. All the data were gathered by the data logger ALMEMO 2590 4S (Ahlborn, Germany).

RESULTS

The temperature of the external atmosphere varied between 15 and 25 °C except for September 13, 2012, being dropped to 11°C. In all the drill-holes, the temperature ranged from 9 to 19 °C and developed in conformity with the external atmosphere. The relative humidity of the air in the holes ranged from 92 to 100%. The CO_2 concentrations varied based on both time and drill-hole diameter. The CFR site was the only location where the CO_2 concentrations did not show any trend (Fig. 2). The enhanced concentrations of CO_2 (between 2382 and 7716 ppmv) were systematically measured in the drill-holes with the smallest diameter. In contrast, the lowest concentrations were found in the drill-holes with the biggest diameter (between 568 and 3192 ppmv). Absolute minimum in concentrations (568 ppmv) was observed in the 7-cm drill-hole at the AFH site on September 13, 2012. The highest maximum of carbon dioxide concentration, 7716 ppmv, was measured in the 2-cm drill-holes at the DFL site on May 9, 2013.

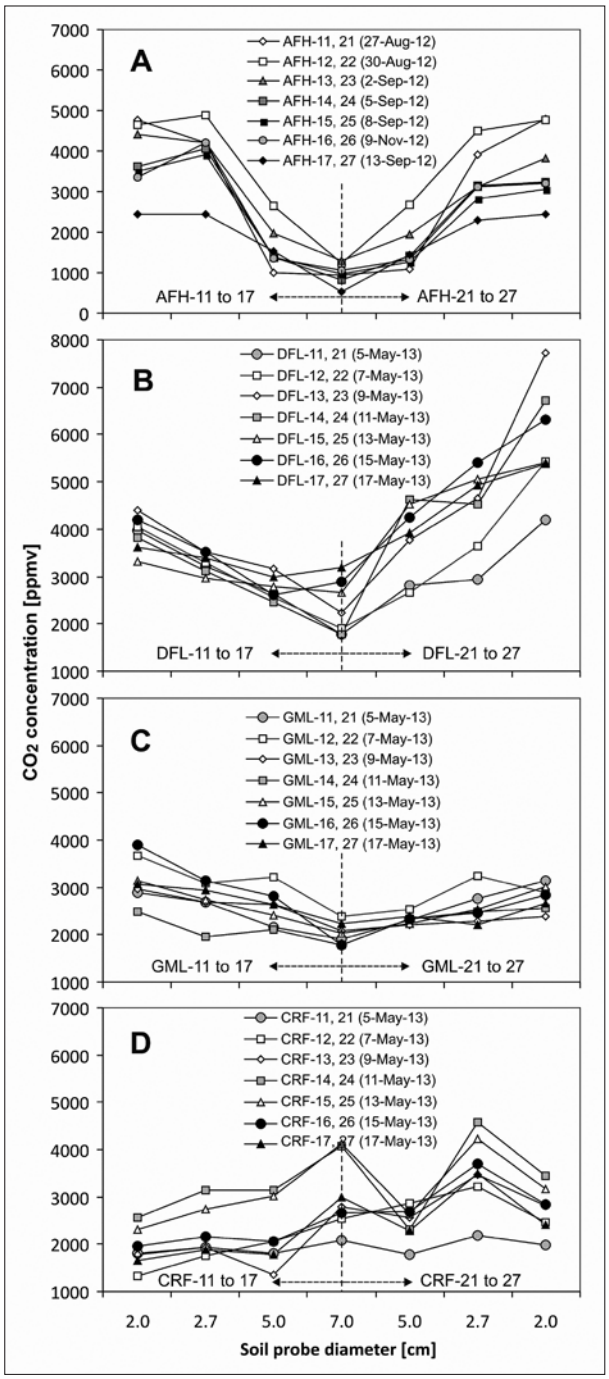

Fig. 2: CO_2 concentrations measured in the soil drill-holes of various diameters at the sites AFH (A), DFL(B), GML(C), and CRF (D). The drill-holes were 25 cm deep. The distance between the individual holes was 20 cm.

DATA ANALYSIS

CO_2 CONCENTRATIONS VS. DRILL-HOLE DIAMETER

The results of the correlation analysis of the variables, drill-hole diameter and measured CO_2 concentrations, are shown in Tab. 2. The strong negative correlations predominate for the AFH site (the correlations that are significant at $\alpha = 0.05$ appear in nine cases; the correlations significant at $\alpha = 0.10$ appear in additional four cases). The negative correlation for the DFL and GML sites are only slightly less convincing (at each site, the correlations significant at $\alpha = 0.05$ are visible in seven cases; the correlations significant at $\alpha = 0.10$ appear in additional three cases). In contrast, the correlations for the CRF site seemed to be inconclusive. They are paradoxically positive: the correlation significant at $\alpha = 0.05$ appear in two cases; the correlations significant at $\alpha = 0.10$ appear in one case).

TEMPERATURE EFFECT

The correlations between the logarithm of CO_2 concentration and reciprocal temperature in Kelvins were tested, based on the assumption that CO_2 concentrations correspond with CO_2 production and that the production obeys the Arrhenius equation. However, both the variables, $\ln(c_{CO2})$ and 1/T, correlate only sporadically, which is demonstrated in Tab. 3. Two negative correlations significant at $\alpha = 0.05$ were found for the AFH and GML sites. Only one significant negative correlation was found for the DFL soil. Paradoxically, just positive correlations predominate in case of the CFR site.

REGRESSION ANALYSIS

The data on CO_2 concentrations and diameters were regressed by the equation

$$c_{CO2} = s\,D + c^0_{(CO2),} \quad (1)$$

where c_{CO2} is the measured CO_2 concentration, s is the slope of dependence, D is the diameter [cm] and $c^0_{(CO2)}$ is the CO_2 concentration extrapolated to a zero D. The discovered linear dependence parameters (eq. 1) are shown in Tab. 4. For all the parameters, standard error and p-values are given. The dependence slope s ranged between –910.7 and –49.7 ppmv cm^{-1} for all the AFH, GML, and DFL sites; the higher the s value, the stronger the dependence of CO_2 concentration on the diameter D. The significance of the s-parameter is consistent with the results of the correlation analysis. The y-intercept, $c^0_{(CO2)}$, ranged from 2466 to 8395 ppmv for all of the AFH, GML, and DFL sites and changed with the slope s. All these $c^0_{(CO2)}$ parameters are significant at $\alpha = 0.05$. For the CRF sites, the s-parameters are paradoxically positive with high uncertainty in most cases. The significant values for CRF-12 and CRF-15 are the

Tab. 2: Pearson's correlations between soil c_{CO2} and drill-hole diameter.

AFH-11	AFH-12	AFH-13	AFH-14	AFH-15	AFH-16	AFH-17
–0.94	**–0.98**	**–0.98**	*–0.95*	*–0.94*	*–0.90*	**–0.99**
AFH-21	AFH-22	AFH-23	AFH-24	AFH-25	AFH-26	AFH-27
–0.94	**–1.00**	**–0.98**	**–0.98**	**–0.97**	**–0.96**	**–1.00**
DFL-11	DFL-12	DFL-13	DFL-14	DFL-15	DFL-16	DFL-17
–0.98	**–0.98**	**–0.95**	**–0.98**	*–0.90*	–0.83	–0.76
DFL-21	DFL-22	DFL-23	DFL-24	DFL-25	DFL-26	DFL-27
–0.90	*–0.92*	–0.90	–0.90	**–0.96**	**–0.99**	**–1.00**
GML-11	GML-12	GML-13	GML-14	GML-15	GML-16	GML-17
–0.99	–0.87	*–0.93*	–0.75	**–0.97**	**–0.96**	**–0.99**
GML-21	GML-22	GML-23	GML-24	GML-25	GML-26	GML-27
–0.98	–0.85	**–0.98**	*–0.95*	*–0.92*	**–0.95**	–0.55
CFR-11	CFR-12	CFR-13	CFR-14	CFR-15	CFR-16	CFR-17
0.64	**0.97**	0.55	*0.91*	**0.96**	0.82	0.85
CFR-21	CFR-22	CFR-23	CFR-24	CFR-25	CFR-26	CFR-27
–0.19	–0.26	–0.48	–0.12	0.14	–0.56	–0.01

The correlations highligted are significant at α = 0.05
The correlation by italic are significant at α = 0.10

only exception. The $c^0_{(CO2)}$ parameters are more significant.

The slopes $s = dc_{CO2}/dD$ follow the equation

$$\frac{dc_{CO2}}{dD} = a\, c^0_{CO2} + b, \qquad (2)$$

where *a, b* are the parameters and the other symbols have their standard meaning.

The parameters were found through regression analysis. They are listed in Tab. 5 by the monitoring sites.

For the individual sites, *a*-parameter varied between –0.13 and –0.16 cm^{-1}, and *b*-parameter ranged from 88 to 422 ppmv cm^{-1}. For the total combined data of all the sites, $a = -0.178$ cm^{-1} and $b = 421.2$ ppmv cm^{-1} (see Fig. 3). For the meadow and deciduous forest soils without the CFR soil, $a = -0.158$ cm^{-1} and $b = 310.6$ ppmv cm^{-1}.

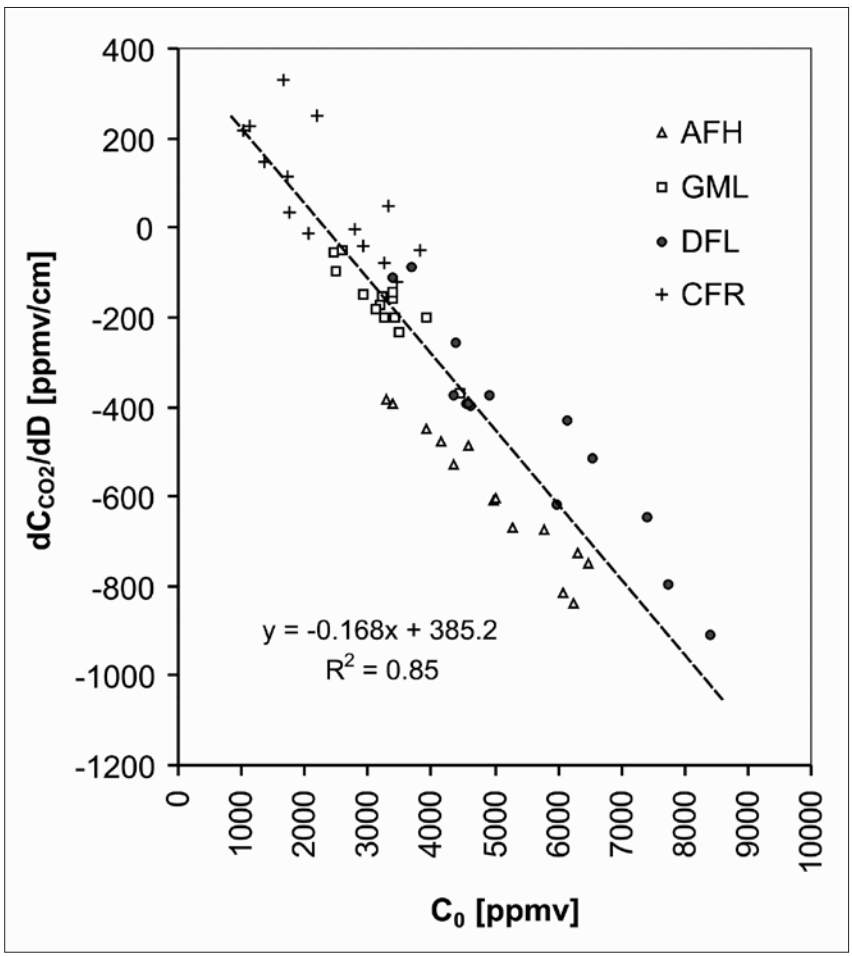

Fig. 3: Relation between the slopes and zero diameter concentrations.

Tab. 4: The regression parameters of the dependence $c_{CO2} = s\ D + c_{0(CO2)}$.

		s-parameter			*$c_{(CO2)}$ parameter*			*whole model*	
site	*date*	*s*	*std. err.* [a]	*p*	*$c_{0(CO2)}$*	*std. err.*	*p*	*R^2*	*p*
AFH-11[b]	27-Aug-12	*–840.1*	218.5	0.061	**6229.9**	1008.8	0.025	0.88	0.061
AFH-12	30-Aug-12	**–747.2**	101.5	0.018	**6470.8**	468.7	0.005	**0.96**	**0.018**
AFH-13	2-Sep-12	**–674.2**	98.3	0.021	**5793.6**	453.8	0.006	**0.96**	**0.021**
AFH-14	5-Sep-12	*–669.5*	161.6	0.054	**5266.6**	746.0	0.019	0.90	0.054
AFH-15	8-Sep-12	*–609.3*	159.1	0.062	**4987.9**	734.6	0.021	0.88	0.062
AFH-16	9-Nov-12	–602.7	209.7	0.103	**5008.7**	968.3	0.035	0.81	0.103
AFH-17	13-Sep-12	**–394.6**	45.3	0.013	**3386.3**	209.2	0.004	**0.97**	**0.013**
AFH-21	27-Aug-12	*–815.3*	201.0	0.056	**6090.3**	928.1	0.022	0.89	0.056
AFH-22	30-Aug-12	**–724.1**	32.5	0.002	**6311.3**	150.1	0.001	**1.00**	**0.002**
AFH-23	2-Sep-12	**–489.0**	66.4	0.018	**4581.7**	306.7	0.004	**0.96**	**0.018**
AFH-24	5-Sep-12	**–528.5**	75.0	0.020	**4360.4**	346.2	0.006	**0.96**	**0.020**
AFH-25	8-Sep-12	**–449.8**	82.5	0.032	**3910.0**	381.0	0.009	**0.94**	**0.032**
AFH-26	9-Nov-12	**–478.6**	99.5	0.041	**4169.1**	459.3	0.012	**0.92**	**0.041**
AFH-27	13-Sep-12	**–383.1**	24.5	0.004	**3276.4**	113.0	0.001	**0.99**	**0.004**
GML11	5-May-13	**–199.0**	21.0	0.011	**3246.0**	96.9	0.001	**0.98**	**0.011**
GML12	7-May-13	–202.0	81.3	0.131	**3931.9**	375.6	0.009	0.76	0.131
GML13	9-May-13	*–152.2*	41.8	0.068	**3230.3**	193.1	0.004	0.87	0.068
GML14	11-May-13	–98.0	60.4	0.246	**2493.4**	278.7	0.012	0.57	0.246
GML15	13-May-13	**–200.1**	35.8	0.031	**3418.6**	165.5	0.002	0.94	**0.031**
GML16	15-May-13	**–367.8**	75.4	0.040	**4448.4**	348.0	0.006	**0.92**	**0.040**
GML17	17-May-13	**–159.1**	12.3	0.006	**3381.4**	56.9	0.000	**0.99**	**0.006**
GML21	5-May-13	**–232.5**	30.6	0.017	**3503.1**	141.3	0.002	**0.97**	**0.017**
GML22	7-May-13	–145.3	63.7	0.150	**3373.5**	294.2	0.008	0.72	0.150
GML23	9-May-13	**–54.7**	7.5	0.018	**2466.0**	34.4	0.000	**0.96**	**0.018**
GML24	11-May-13	*–148.3*	35.2	0.052	**2907.7**	162.6	0.003	0.90	0.052
GML25	13-May-13	*–174.5*	51.3	0.077	**3188.2**	236.7	0.005	0.85	0.077
GML26	15-May-13	**–180.1**	40.6	0.047	**3113.2**	187.6	0.004	**0.91**	**0.047**
GML27	17-May-13	–49.7	53.2	0.449	**2586.8**	245.6	0.009	0.30	0.449
DFL-11	5-May-13	**–394.3**	61.9	0.024	**4545.0**	285.8	0.004	**0.95**	**0.024**
DFL-12	7-May-13	**–397.1**	62.8	0.024	**4613.1**	290.1	0.004	**0.95**	**0.024**
DFL-13	9-May-13	**–374.2**	85.2	0.048	**4900.4**	393.2	0.006	**0.91**	**0.048**
DFL-14	11-May-13	**–374.1**	57.1	0.022	**4360.8**	263.5	0.004	**0.96**	**0.022**
DFL-15	13-May-13	*–112.2*	37.9	0.098	**3402.1**	175.0	0.003	0.81	0.098
DFL-16	15-May-13	–257.2	121.1	0.168	**4377.1**	559.0	0.016	0.69	0.168
DFL-17	17-May-13	–89.2	54.6	0.244	**3672.9**	252.2	0.005	0.57	0.244
DFL-21	5-May-13	*–392.9*	134.3	0.100	**4572.4**	620.2	0.018	0.81	0.100
DFL-22	7-May-13	*–617.9*	183.1	0.078	**5992.1**	845.6	0.019	0.85	0.078
DFL-23	9-May-13	*–910.7*	312.4	0.100	**8394.6**	1442.5	0.028	0.81	0.100
DFL-24	11-May-13	–796.7	276.0	0.102	**7737.3**	1274.4	0.026	0.81	0.102
DFL-25	13-May-13	**–512.7**	112.4	0.045	**6552.3**	519.0	0.006	**0.91**	**0.045**
DFL-26	15-May-13	**–646.0**	56.1	0.007	**7406.7**	259.2	0.001	**0.99**	**0.007**
DFL-27	17-May-13	**–429.1**	25.4	0.003	**6144.4**	117.3	0.000	**0.99**	**0.003**
CRF-11	5-May-13	36.0	30.2	0.356	**1757.4**	139.7	0.006	0.41	0.356
CRF-12	7-May-13	**216.3**	35.1	0.025	**1018.1**	162.0	0.024	**0.95**	**0.025**
CRF-13	9-May-13	144.5	153.8	0.447	1359.6	710.3	0.196	0.31	0.447
CRF-14	11-May-13	*250.4*	79.9	0.089	**2195.1**	369.1	0.027	0.83	0.089
CRF-15	13-May-13	**328.3**	69.6	0.042	**1675.5**	321.6	0.035	**0.92**	**0.042**
CRF-16	15-May-13	112.9	56.4	0.183	**1736.6**	260.2	0.022	0.67	0.183
CRF-17	17-May-13	228.6	102.3	0.155	1125.2	472.3	0.140	0.71	0.155
CRF-21	5-May-13	–14.1	52.6	0.814	**2063.1**	242.8	0.014	0.03	0.814
CRF-22	7-May-13	–39.5	104.8	0.743	**2937.6**	484.0	0.026	0.07	0.743
CRF-23	9-May-13	–80.7	105.3	0.524	**3240.0**	486.3	0.022	0.23	0.524
CRF-24	11-May-13	–52.2	301.5	0.878	3826.5	1392.1	0.111	0.01	0.878
CRF-25	13-May-13	48.8	235.9	0.855	*3332.3*	1089.4	0.092	0.02	0.855
CRF-26	15-May-13	–118.8	124.2	0.440	**3464.8**	573.5	0.026	0.31	0.440
CRF-27	17-May-13	–3.1	174.0	0.987	*2806.8*	803.6	0.073	0.00	0.987

(a) standard error

(b) the first number means direction form central drill-hole; the second number corresponds to date

The highlighted parameters are statistically significant at $\alpha = 0.05$

The parameters by italic are significant at $\alpha = 0.10$

Tab. 5: The model a, b parameters.

	parameters						*whole model*	
	a	***std. err.*** [(a)]	***p***	***b***	***std. err.***	***p***	R^2	***p***
AFH	**–0.134**	0.011	0.000	66.7	55.1	0.250	**0.93**	**0.000**
GML	**–0.133**	0.017	0.000	**262.9**	55.2	0.000	**0.84**	**0.000**
DFL	**–0.140**	0.014	0.000	**317.8**	80.0	0.002	**0.89**	**0.000**
CRF	**–0.114**	0.028	0.001	**341.4**	69.3	0.000	**0.58**	**0.001**
as w CRF[(b)]	**–0.146**	0.012	0.001	**262.0**	56.3	0.000	**0.80**	**0.000**
AS[(c)]	**–0.168**	0.010	0.000	**385.2**	42.3	0.000	**0.85**	**0.000**

The highlighted parameters are statistically significant at α = 0.05
(a) standard error
(b) all soils without CRF
(c) all soil

MATHEMATICAL MODEL

Inserting the differences $\Delta c_{CO2} = (c_{CO2} - c^0_{CO2})$ for the differentials dc_{CO2} and $\Delta D = D$ for dD, and consecutive rewriting transform the eqn. (2) into

$$c^0_{CO2} = \frac{c_{CO2} - bD}{1 + aD}. \quad (3)$$

From a mathematical point of view, the expression (Eq. 3) is defined if $D \neq -\frac{1}{a}$. Because the diameter D must be positive, it should lie between the intervals $\frac{c_{CO2}}{b} \leq D < -\frac{1}{a}$ and $\frac{c_{CO2}}{b} \geq D > -\frac{1}{a}$.

DISCUSSION

The measured CO_2 concentrations agree with the values given by other researchers studying the karst soils. Under using the same monitoring methods, Faimon and Ličbinská (2010) and Faimon *et al.* (2012a) found the CO_2 concentration of about 2000–3000 ppmv in the Moravian Karst (Czech republic) for similar soils and 5-cm drill-hole diameters at 20 °C (May). Other researchers used methods based on the sampling of soil the atmosphere and their subsequent analysis in-situ or in the laboratory. Such concentrations vary from 500 to 9000 ppmv based on local conditions (Spötl *et al.* 2005; Kawai *et al.* 2006; Yoshimura *et al.* 2001; Li *et al.* 2002; Sanchez-Cañete *et al.* 2011).

Variations of CO_2 concentrations in individual drill-hole during monitoring periods are most likely controlled by external conditions. The effect of the light intensity on photosynthesis and, consecutively, on the respiration of autotrophs seems to be the most significant (Kuzyakov & Larionova 2005; Kuzyakov 2006). The temperature seems to have a rather small effect, as indicated by the weak correlations in Tab. 3. The impact of an external wind on total CO_2 efflux may be also important (Pérez-Priego *et al.* 2013). All the external influences have been eliminated in the mathematical model, Eq. (3).

The *a, b* parameters of the model somewhat differ among various soil samples (see Tab. 5). As the soil porosity (controlling CO_2 efflux) seems to be similar in all the soils (Tab. 1), CO_2 production may have a dominant effect. However, it is worth mentioning that the reached CO_2 concentrations do not follow the organic matter content in the soils (compare Tab. 1 and Fig. 2).

The analysis of the mathematical model (Eq. 3) showed that the difference between corrected and measured concentrations, $\Delta c = c^0_{CO_2} - c_{CO_2}$, increases with the value of *a*-parameter, whereas *b*-parameter decreases this effect. As it follows from Fig. 4, the *a*-parameter gives the slope and *b*-parameter gives the intercept of the dependence $c^0_{CO_2} = f(c_{CO_2})$. When compared the measured and corrected concentrations, the measured CO_2 concentrations in 2-cm drill-holes are affected by the systematical negative errors ranging from 22 to 31%. This error increases up to 575% in case of 7-cm drill-hole. Therefore, concentrations directly measured in drill-holes generally require correction, e.g., based on our mathematical model.

The conceptual model of the mechanism of attaining CO_2 concentration in soil drill-hole was derived in order to understand better the pore dimension effect (Fig. 5). The CO_2 production, along with the CO_2 efflux-

es from bulk soil into (1) the external atmosphere and (2) drill-hole free air, create the concentration gradients in both vertical and horizontal directions. In these directions, gaseous CO_2 migrates by diffusion under the different CO_2 diffusion coefficients in (1) bulk soil and (2) free air of the drill-hole. The vertical gradients in the soils should exceed the vertical gradient in the free air of the drill-hole. Therefore, the horizontal gradients between soils and air in the drill-hole/pore have diminished upwards and may turn their sign near the surface. This leads to CO_2 escaping horizontally through the drill-hole walls into the atmosphere. Because the diffusional flux depends on the diffusional area, CO_2 loss increases with the higher drill-hole diameters.

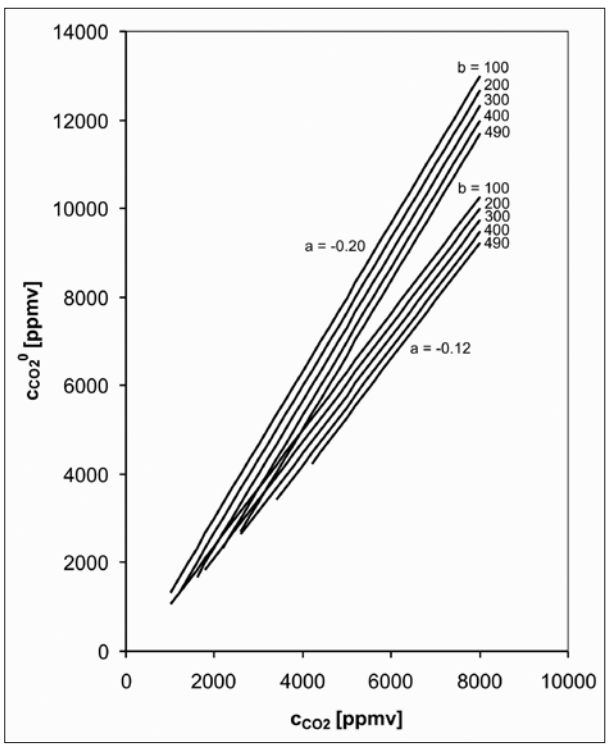

Fig. 4: Nomogram of the function $c_{CO2}^{\ 0} = f(c_{CO2})$ for diameter D = 2 cm and different a, b parameters. See text for details.

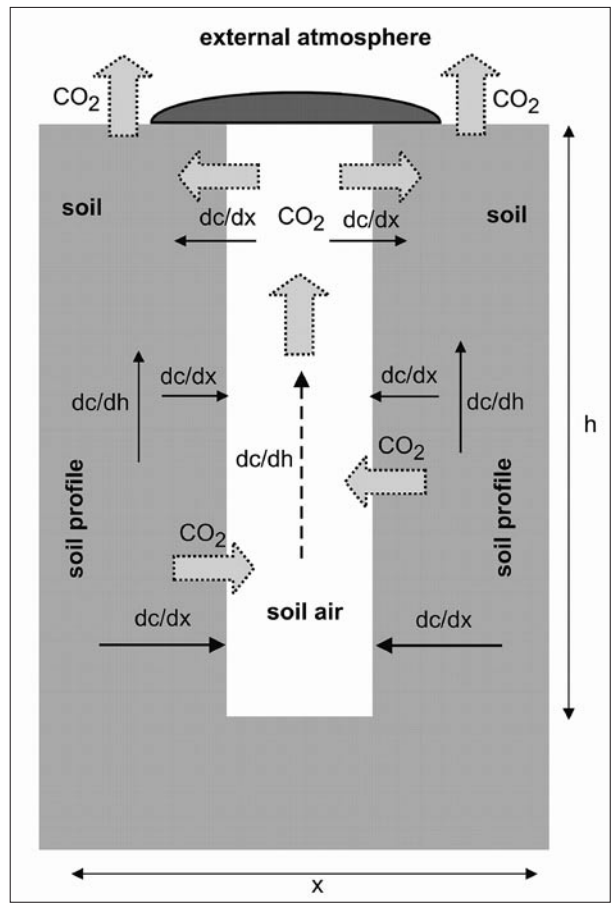

Fig. 5: Conceptual model of CO_2 concentration gradients and fluxes in soil profile.

As the conceptual model shows, CO_2 production, concentration gradients, and diffusional fluxes are fundamental for reaching steady state CO_2 concentrations in the given soil pore space. The input flux is responsible for the soil capacity to attain given concentration. However, soil permeability affects the output fluxes, which is important for establishing steady states. Because the soil capacity is limited for to preserving primordial concentrations in enlarged soil pores, it seems to be insufficient to reach the concentrations generally measured or deduced for the vadose zone (e.g., cave). Thus, these results re-open the hypothesis about an additional source of karst/cave CO_2 lying deeper in the epikarst.

CONCLUSIONS

Soil CO_2 was studied in the Moravian Karst (Czech Republic). It was proved that the CO_2 concentrations in common karst soils (developed at field, meadow, and deciduous forest) depend negatively on drill-hole diameter and, thus, on the dimension of pores in the soil profile. In contrast, this dependence was just un-

convincing in case of the loamy soils of deciduous forest.

The work generally indicated a low capability of shallow karst soils to fill bigger pores in soil profile by CO_2. This re-opens the question how such limited source could be sufficient to fill up more voluminous and well-vented caves, as it is generally believed. The work supports the idea of a deeper-laying epikarstic source of gaseous CO_2 that is involved in the basic karst processes.

The results represent a preliminary study that maps the former problems. Further studies are necessary to explain better both the sources and behavior of karst CO_2. From a technical point of view, this work simply shows a systematical negative error in determination of soil CO_2 concentrations by a direct measuring in drill-holes and offers the possibility of calibration. The findings of this research may be of interest to karsologists, speleologists, and environmentalists.

ACKNOWLEDGEMENTS

The work was conducted under the institutional support of research by Masaryk University. The authors thank two reviewers who wish to remain anonymous for their valuable comments that helped to improve this report.

REFERENCES

Atkinson, T., 1977: Carbon dioxide in the atmosphere of the unsaturated zone: An important control of groundwater hardness in limestones.- Journal of Hydrogeology, 35, 111–123.

Benavente, J., Vadillo, I., Carrasco, F., Soler, A., Lián, C. & F. Moral, 2010: Air carbon dioxide contents in the vadose zone of a Mediterranean karst.- Vadose Zone Journal, 9, 126–136.

Cuezva S., Fernandez-Cortes A., Benavente D., Serrano-Ortiz P., Kowalski A.S. & S. Sanchez-Moral, 2011: Short-term CO_2(g) exchange between a shallow karstic cavity and the external atmosphere during summer: Role of the surface soil layer.- Atmospheric Environment, 45, 1418–1427.

Dreybrodt, W., 1999: Chemical kinetics, speleothem growth and climate.- Boreas, 28, 347–356.

Faimon, J. & M. Ličbinská, 2010: Carbon dioxide in the soils and adjacent caves of the Moravian Karst.- Acta Carsologica, 39, 3, 463–475.

Faimon, J., Ličbinská, M. & P. Zajíček, 2012a: Relationship between carbon dioxide in Balcarka Cave and adjacent soils in the Moravian Karst region of the Czech Republic.- International Journal of Speleology, 41, 17–28.

Faimon, J., Ličbinská, M., Zajíček, P. & O. Šráček, 2012b: Partial pressures of CO_2 in epikarstic zone deduced from hydrogeochemistry of permanent drips, the Moravian Karst, Czech Republic.- Acta Carsologica, 41, 1, 47–57.

Fairchild, I.J., Borsato, A., Tooth, A.F., Frisia, S., Hawkesworth, C. J., Huang, Y., McDermott, F. & B. Spiro, 2000: Controls on trace element (Sr–Mg) compositions of carbonate cave waters: implications for speleothem climatic records.- Chemical Geology, 166, 255–269.

Ford, D. & P. Williams, 2007: *Karst hydrogeology and geomorphology.*- John Wiley & Sons, pp. 562, Chichester.

Kawai, T., Kano, A., Matsuoka, J. & T. Ihara, 2006: Seasonal variation in water chemistry and depositional processes in a tufa-bearing stream in SW Japan, based on 5-years of monthly observations.- Chemical Geology, 232, 33–53.

Kuzyakov, Y., 2006: Sources of CO_2 efflux from soil and review of partitioning methods.- Soil Biology & Biochemistry, 38, 425–448.

Kuzyakov, Y. & A.A. Larionova, 2005: Root and rhizomicrobial respiration: A review of approaches to estimate respiration by autotrophic and heterotrophic organisms in soil.- Journal of Plant Nutrition and Soil Science, 168, 503–520.

Li, T., Wang, S. & L. Zheng, 2002: Comparative study on CO_2 sources in soil developed on carbonate rock and non-carbonate rock in Central Guizhou.- Science in China (series D), 45, 8, 673–679.

Pérez-Priego O., Serrano-Ortiz P., Sánchez-Cañete E.P., Domingo F. & A.S. Kowalski, 2013: Isolating the effect of subterranean ventilation on CO_2 emissions from drylands to the atmosphere. Agricultural and Forest Meteorology, 180, 194–202.

Peyraube N., Lastennet R. & A. Denis (2012): Geochemical evolution of groundwater in the unsaturated zone of a karstic massif, using the P_{CO2}–SIc relationship.- Journal of Hydrology, 430–431, 13–24.

Peyraube N., Lastennet R., Denis A. & P. Malaurent (2013): Estimation of epikarst air P_{CO2} using measurements of water δ13CTDIC, cave air P_{CO2} and $\delta^{13}C_{CO2}$.- Geochimica et Cosmochimica Acta, 118, 1–17.

Sanchez-Cañete, E.P., Serrano-Ortiz, P., Kowalski, A.S., Oyonarte, C. & F. Domingo, 2011: Subterranean CO_2 ventilation and its role in the net ecosystem carbon balance of a karstic shrubland.- Geophysical Research Letters, 38, L09802.

Sarbu, S.M. & C. Lascu, 1997: Condesation corrosion in Movile cave, Romania.- Journal of Cave and Karst Studies, 59, 99–102.

Schlesinger, W.H. & J.A. Andrews, 2000: Soil respiration and the global carbon cycle.- Biogeochemistry, 48, 7–20.

Serrano-Ortiz P., Roland M., Sanchez-Moral S., Janssens I.A., Domingo F., Goddéris Y. & A.S. Kowalski, 2010: Hidden, abiotic CO_2 flows and gaseous reservoirs in the terrestrial carbon cycle: Review and perspectives. Agricultural and Forest Meteorology, 150, 321–329.

Spötl, Ch., Fairchild, I.J. & A.F. Tooth, 2005: Cave air control on dripwater geochemistry, Obir Caves (Austria): Implications for speleothem deposition in dynamically ventilated caves.- Geochimica et Cosmochimica Acta, 69, 2451–2468.

Stumm, W. & J.J. Morgan, 1996: *Aquatic chemistry: Chemical Equilibria and Rates in Natural Waters.*- Wiley-Interscience; 3rd edition, pp. 1022, New York.

Yoshimura, K., Nakao, S., Noto, M., Inokura, Y., Urata, M., Chen, P. & P.W. Lin, 2001: Geochemical and stable isotope studies on natural water in the Taroko Gorge karst area, Taiwan – chemical weathering of carbonate rocks by deep source CO_2 and sulfuric acid.- Chemical Geology, 177, 415–430.

COBISS: 1.01

HYDROCHEMICAL RESPONSE OF CAVE DRIP WATER TO SNOWMELT WATER, A CASE STUDY FROM VELIKA PASICA CAVE, CENTRAL SLOVENIA

SPREMEMBE HIDROKEMIJSKIH LASTNOSTI PRENIKLE VODE V JAMI KOT POSLEDICA DOTOKA SNEŽNICE: PRIMER JAME VELIKA PASICA, OSREDNJA SLOVENIJA

Wei LIU[1] & Anton BRANCELJ[2]

Abstract UDC 556.114:551.44(497.4)

Wei Liu & Anton Brancelj: Hydrochemical response of cave drip water to snowmelt water, a case study from Velika Pasica Cave, Central Slovenia

A more accurate interpretation of data is required in order to understand the processes of hydrological movement and hydrochemical variation of epikarst water flow. A drip, VP1, from the Velika Pasica Cave (Central Slovenia) was studied during a period which occurred at the end of a long wet, cold winter. The sources for the percolation water in the cave most probably were rain water and snowmelt water, as inferred from the surface hydrological conditions. The discharge was monitored during the study period in one hour intervals. Each hour a water sample from the drip was taken for measurements of electric conductivity and major ions concentrations. Due to the specific climatic condition within the shallow cave, the amount of discharge was the dominant driving force in the hydrochemical variation. The effect of CO_2 corrosion and prior calcite precipitation (PCP) was weakened with this condition; the high correlation between Mg^{2+}, Ca^{2+} and micro-variation in the Mg/Ca ratio indicated the weakened PCP. The low concentration of ions did not respond strongly with the recharge event. On the contrary, the drip water temperature preformed as a good water percolation tracer.

Key words: cave drip water, dilution, epikarst, hydrochemistry, snowmelt water.

Izvleček UDK 556.114:551.44(497.4)

Wei Liu & Anton Brancelj: Spremembe hidrokemijskih lastnosti prenikle vode v jami kot posledica dotoka snežnice: primer jame Velika Pasica, osrednja Slovenija

Za razumevanje procesov pretakanja in kemijskih sprememb v prenikajoči vodi v epikraški coni je potrebno bolj natančno zajemanje in interpretacija podatkov. Ob koncu dolge in hladne zime z obilnimi padavinam je bil v ta namen podrobneje analiziran curek, VP1, v jami Velika Pasica (osrednja Slovenija). Najverjetnejša vira prenikle vode v jami sta bila padavinska voda in snežnica, kot je razvidno iz podatkov iz površinskih opazovanj. Pretok curka je bil v času podrobnejših analiz spremljan v enournih intervalih. Vsako uro je bil odvzet tudi vzorec vode za meritve električne prevodnosti ter koncentracij glavnih ionov. Zaradi specifičnih klimatskih pogojev v plitvi kaški jami je bil glavni vzrok za kemijske spremembe pretok prenikle vode. Vplivi korozije zaradi koncentracije CO_2 in zaradi predhodnega izločanja kalcita (PCP) so bili v tem primeru zmanjšani; visoka korelacija med Mg^{2+} in Ca^{2+} ter le majhne spremembe v razmerju Mg/Ca so nakazovale oslabljen vpliv PCP. Nizka vsebnost ionov ni sledila povsem intenzivnosti padavin. V nasprotju s tem pa je temperatura prenikle vode delovala kot dobro sledilo le-te.

Ključne besede: epikras, hidrokemija, prenikajoča voda, razredčevanje, snežnica.

INTRODUCTION

Higher resolution and accurate data are necessary in order to understand the dynamics of groundwater hydrochemistry (McDonald *et al.* 2007; Yang *et al.* 2012). Most previous works have relied on relative long inter-

[1] Wei Liu, Department of Freshwater and Terrestrial Ecosystem Research, National Institute of Biology, Večna pot 111, SI-1000, Ljubljana, Slovenia; phone: +38670344830; E-mail: allen.wei.liu@nib.si

[2] Anton Brancelj, Department of Freshwater and Terrestrial Ecosystem Research, National Institute of Biology, Večna pot 111, SI-1000, Ljubljana, Slovenia; University of Nova Gorica, Vipavska cesta 13, SI-5000 Nova Gorica, Slovenia.

Received/Prejeto: 10.07.2013

vals (Backer *et al.* 1997; Fairchild *et al.* 2006) resulting in some important discoveries, but some details may have been overlooked. As the development of high accuracy technology for cave drip water monitoring has been applied to speleological hydrological studies (Fernandez-Cortes *et al.* 2008; Sheffer *et al.* 2011; Jex *et al.* 2012), increasingly details on micro-scales were discovered. Many caves have been monitored in order to interpret and define water flow variations in the vadose zone (Smart & Friederich 1987; Baldini *et al.* 2006; Kogovšek & Petrič 2012), which can elucidate details of hydrochemical processes within the caves (Vokal *et al*. 1999; Backer *et al.* 2000; Tooth & Fairchild 2003; Kogovšek 2011). Additionally, the hydro-chemists endeavoured to interpret the mineral variations of cave drip water spatially and temporally in detail (Baldini *et al.* 2006). Most research on cave drip water has focused on identifying criteria from the rain infiltration events (Kogovšek 2007). Kogovšek (2010) discussed the flood wave formed by snowmelt water in the vadose zone in the Postojnska jama. However, the fine time interval studies on hydrochemical response to snowmelt water in the epikarst are still rare.

The seasonal aridity and humidity, coldness and warmness significantly affect the chemical composition of karst water (Liu *et al.* 2007; Yang *et al.* 2012). Baker *et al.* (2000) found that the Mg/Ca ratio was indicative for relatively dry weather. Furthermore, Fairchild *et al.* (2006) found the Mg/Ca ratio was related to low-flow percolating conditions but it was a non-linear relationship. Zhang *et al.* (2010) stated that, under dry conditions, CO_2 controlled the hydrochemistry of karst water. However, the processes in wet, cold conditions with continuous recharge have not been studied in detail yet.

Numerous mechanisms are driving drip-water hydrochemistry under varying discharge conditions, therefore, single proxies as a means of variability control should be considered. Our objective in this paper is to present the hydrochemical variation of cave drip water after a long, cold, wet winter (with nil, or little biointerference) at a small scale, conducted in the shallow (i.e. epikarstic) Velika Pasica Cave. Under this specific climatic condition, a high-frequency sampling regime for hydrochemical characteristics for drip water was carried out inside the cave, in an attempt to provide a supplementary understanding of epikarst hydrochemical processes. The hypothesis we proposed is that major qualitative changes, in terms of physical and chemical characteristics in rain & melt water properties, occur in the thin epikarst zone.

STUDY SITE DESCRIPTION

The study site, Velika Pasica Cave (45°55'14''N, 14°29'41''E), is near the village Gornji Ig, 20 km south of Ljubljana (Slovenia). Entrance into the cave is at the elevation of 662 m a.s.l. (Fig.1, I). The cave formed in the thin bedded Norian-Retian dolomite of the Upper Triassic age with the strata of bedrock dipping north at 10–15° (Pleničar 1970). Approximately three hundred metres to the southwest, there is a 765 m hill, which slopes towards to the cave with an inclination of approximately 30°. There is no surface water around the cave, with the exception of a small ephemeral spring (Fig. 1, I) (Brancelj 2002).

The cave is positioned close to the top of the karstic plateau covered with a thin layer of soil, varying from 0–20 cm in depth. The thickness of the cave ceiling is 10–12 m at maximum, and only 2–5 m at minimum. The cave is a 126 m long horizontal gallery rich in flowstone decorations (Fig. 1, II). The only known entrance is located at the bottom of a 10 m deep circular depression with a diameter of 15 m (Brancelj 2002).

Resulting from the position and structure of the cave, all water within the cave is exclusively percolating water, entering the cave as permanent or temporary drips from the ceiling or temporary flows, after heavy rain or intensive snow melt, from the side of the galleries. Four permanent drips, designated as VP1, VP2, VP3, and VP4, are present in the cave (Fig. 1, II). Due to the restriction of the sampling devices, only drip VP1 was monitored for the critical hydrochemical period analysis. At site VP1, the ceiling depth is approximately 8 m. According to the monitoring results, VP1 was the most rapid responding drip with a wide discharge rate from 61 ml/min to 1350 ml/min during the period covered by this case study.

The climate of the Ljubljana area has continental characteristics with warm summers and moderately cold winters. Snow is common from December to February; on average there are 48 days with snow cover recorded each winter season (http://www.arso.gov.si/).

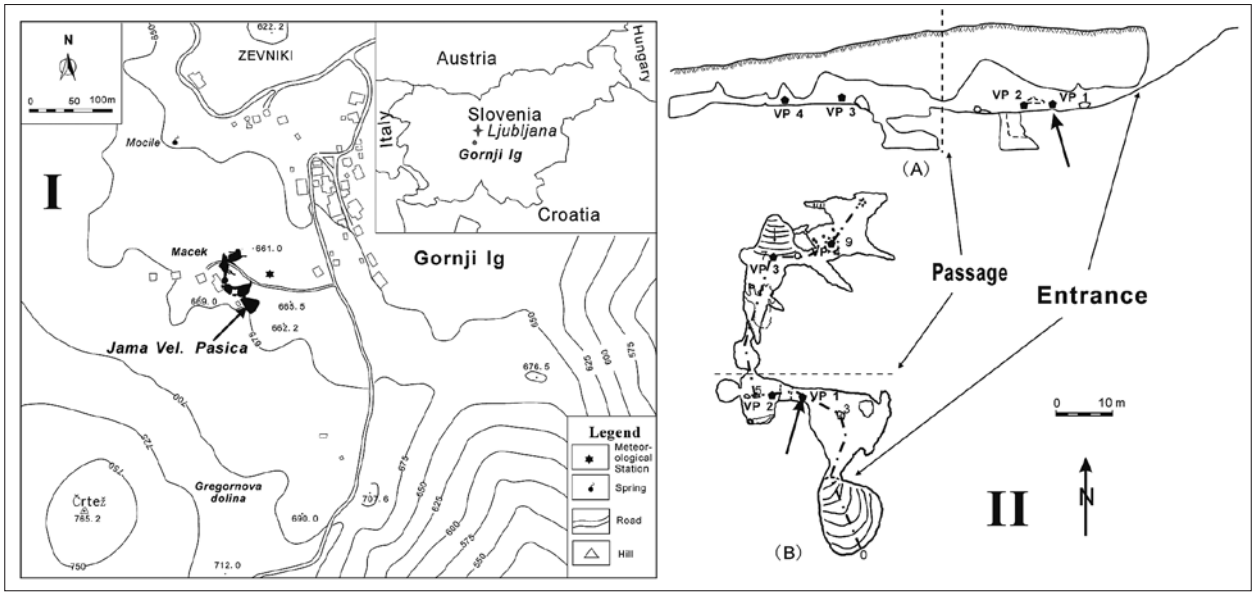

*Fig. 1: I (Left): Location of the Velika Pasica Cave (Slovenia). The black figure: the study cave; *: the outside meteorological station; Δ: the hill Črtež, the highest point of the region; : the spring Močilec, the only surface discharge of the region. II (Right): Cross-section (A) and ground plan (B) of the Velika Pasica Cave (Slovenia). VP1 – VP4: permanent dripping points. The arrowhead points the drip VP1 which is analysed in detail in this article.*

MATERIAL AND METHODS

The samples were collected from 18th to 22nd of March, 2013, coinciding with the end of the long cold, wet winter with some remnant snow melt (Fig. 2).

The discharge of drip VP1 was monitored in one hour intervals by a rain gauge (RG1-UM-3, Delta-T Device Company) with accuracy and resolution of ±0.2 mm, connected to a data-logger (DL2e, Delta-T Device Company). A plastic screen (2 m × 2 m) was placed in order to collect dripping water and direct it into the rain gauge funnel. A probe (ST1-05, Delta-T Device Company) (resistivity type; range of measurement of –25 to +100 °C; digital resolution of 0.1 °C) for water temperature was inserted in the lower part of the rain gauge, which also registered readings in one hour intervals. In order to determine the correlation and dissimilarity of temperature between the water at the epikarst discharge point and the drip water near the cave floor, two probes were placed at different places for two weeks, in October 2012. Results showed only a minor difference in water temperature between them.

An automatic water sampler was constructed for sampling in order to monitor the hydrochemical parameters of the drip water, collected as a water sample in a 60 ml PVC bottle each hour. Every 24 h, samples were transported to the laboratory. Electrical conductivity (EC) and the pH of the samples were measured immediately after transportation to the laboratory by a Multi 340i instrument with accuracy ±0.01 and a MultiCal pH-540 meter with accuracy ±0.01 (WTW Company). Based on the variations of EC, the most typical samples were chosen for ion analysis by ion chromatography (761Compact IC, Methrom) and they included K^+, Na^+, Ca^{2+}, Mg^{2+}, SO_4^{2-}, Cl^- and NO_3^- ions. Selected samples were stored at 5 °C in a refrigerator and analysed within 24 hours after collection. Other specific calculations, e.g. CO_2 partial pressure (pCO_2) and saturation index of calcite (SIc) were conducted by a speciation programme PHREEQC (Appelo & Postma 2005).

A meteorological station was set on the surface near the entrance to the cave in order to record air temperature and precipitation with another data-logger (DL2e, Delta-T Device Company) (Fig. 1, I). The time settings of the outside sensors were tuned with those inside the cave. However, the local meteorological station could not measure the snow depth, thus daily snow depth values were used from a nearby meteorological station – Pokojišče, which is a part of the state meteorological network, located 8.3 km west of the Velika Pasica Cave, at the elevation of 737 m a.s.l (http://www.arso.gov.si).

RESULTS

The meteorological data on daily precipitation and snow cover thickness from the Pokojišče station were available from the beginning of January till the beginning of April, 2013 (Fig. 2). In total, from January 1st to the March 31st, 2013, 595.5 mm of rain fell over 56 days, and 329 cm of snow in 35 days. In total, there were 63 days with snow cover on the ground. According to the location and the altitude of the Pokojišče station, the data supplied could be supplemented with information from a local meteorological station for the detailed study period from 18th March to 22nd March, as presented in this article (Fig. 3).

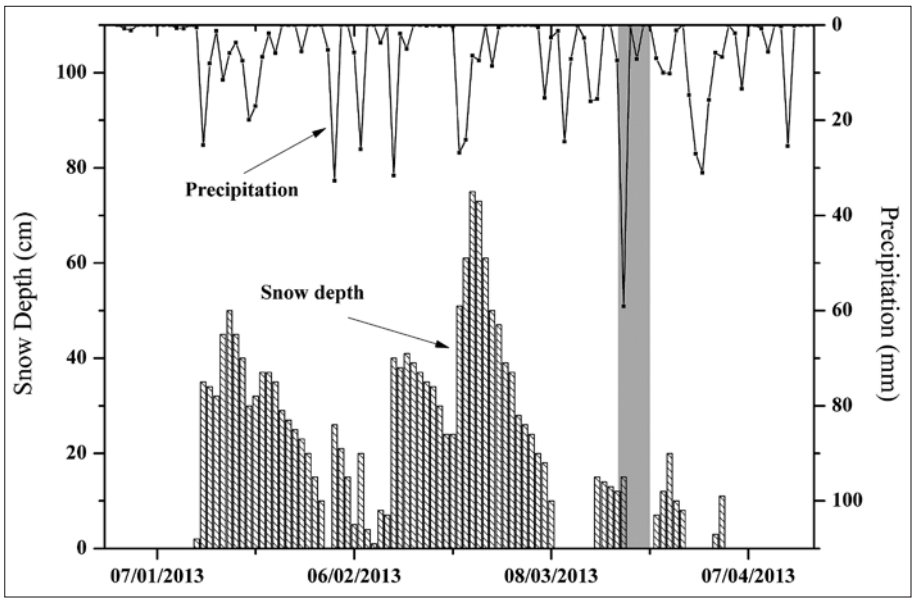

Fig. 2: The daily precipitation and daily snow depth at the Pokojišče meteorological station (SW of Ljubljana, Slovenia) from the beginning of January to the beginning of April, 2013; the grey area is the studied period discussed in this article, detailed in Fig. 3.

There were two rain events during the study period: one was on March 18th–19th , with 41.4 mm rain falling in 20 hours, and the other one was less intensive, from March 20th–21st, with 7.2 mm of rain in 14 hours (data from a local meteorological station). The surface temperature maintained the regular daily oscillations with the exception of March 19th when heavy rainfall occurred (Fig.3). Meanwhile, the rate of snow melt followed the surface temperature variation, but the rain water accelerated it significantly, as indicated by the increase of drip water discharge. Consequently, the snow melt was controlled by two impacts: the regular daily oscillations of temperature and rain fall, which resulted in two intensive percolation events. The first occurred following an intensive rain event, with rapid and significant response in the drip discharge. The drip started to respond in one hour after the rain event commence, and it rose to its peak at 1250 ml/min in three hours. The second resulted from a slight rainfall, with a lower, sluggish discharge. It took eight hours for the drip to rise to its peak at 800 ml/min. The warmth of the day temperature melted the snow simultaneously and the rainfall accelerated it significantly to cause the high discharge (Fig. 3).

Consequently, the drip discharge affected the hydrochemical features. The electrical conductivity (EC) represents the concentration of dissolved ions (Tab. 1), showed a reverse variation with the discharge (Fig. 3), but the EC varied sensitively following the discharge, which was also indicated by the high relationship (r = −0.915,

Tab. 1: The mean value and variations in chemical composition of the drip water in the Velika Pasica Cave (Slovenia) in a period 18th to 22nd March, 2013 (n = 19). EC (electrical conductivity); pCO_2 (partial pressure of CO_2); SIc (saturation index of calcite); Mg/Ca (molar ratio between Mg^{2+} and Ca^{2+}).

Statistic	EC µS/cm (25°C)	pH	T (°C)	Cl^- (mg/l)	NO_3^- (mg/l)	SO_4^{2-} (mg/l)	Na^+ (mg/l)	K^+ (mg/l)	Ca^{2+} (mg/l)	Mg^{2+} (mg/l)	HCO_3^- (mg/l)	pCO_2 (log10)	SIc	Mg/Ca
Mean	282.53	8.3	7.07	0.15	0.31	1.21	0.50	0.21	45.92	20.60	244.34	−3.00	0.60	0.75
C.V.	0.10	0.01	0.02	0.16	0.22	0.12	0.30	0.26	0.10	0.12	0.11	0.01	0.20	0.03
Max	318	8.3	7.25	0.21	0.47	1.50	0.85	0.35	51.81	24.39	281.84	−2.94	0.76	0.78
Min	215	8.2	6.80	0.11	0.22	0.93	0.36	0.14	35.27	14.81	182.78	−3.07	0.33	0.70

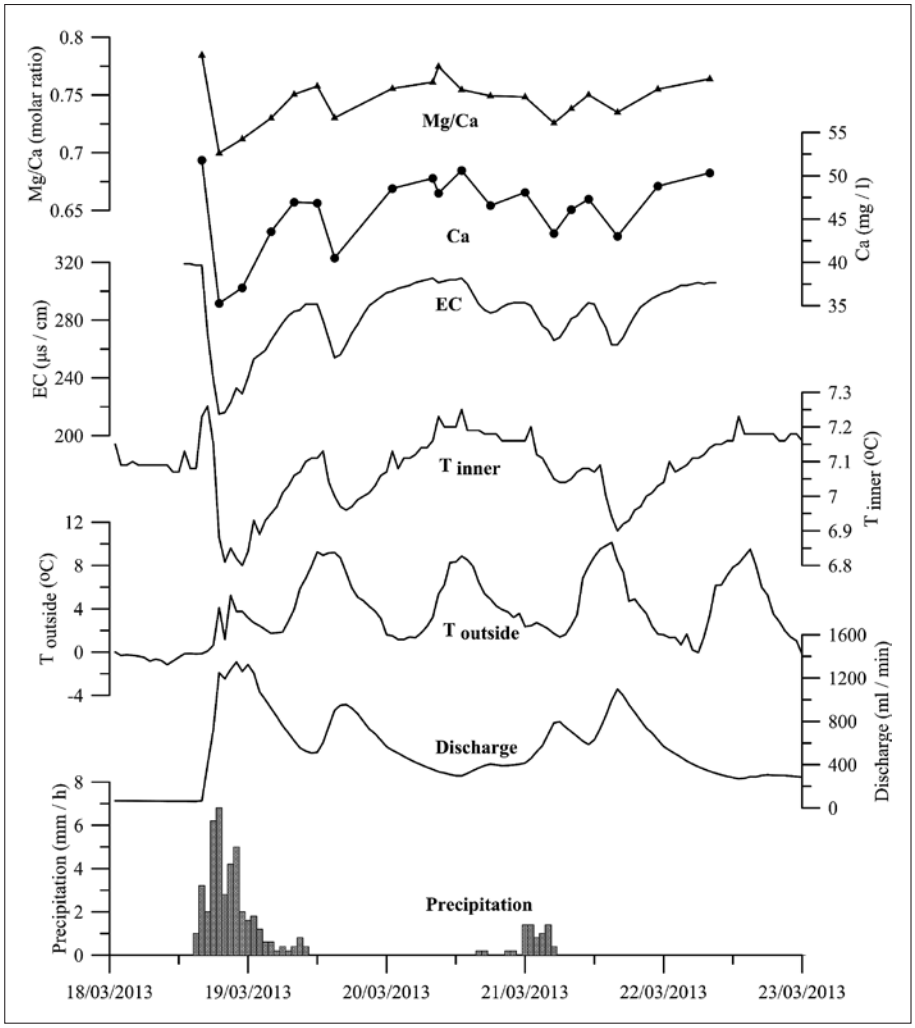

Fig. 3: The hourly variation of the precipitation, the discharge from drip VP1, the surface temperature (T outside), the temperature of drip water (T inner), electric conductivity (EC), Ca^{2+} concentration and Mg/Ca ration of the drip water during the period 18th to 22nd March, 2013.

Tab. 2: The Spearman correlation coefficients of the main hydrological and hydrochemical parameters of the cave drip water: the drip water temperature (T: °C); discharge of drip water (Q: ml/min); electric conductivity (EC: µm/cm); the ions, Cl^-, NO_3^-, SO_4^{2-}, Na^+, K^+, Ca^{2+}, Mg^{2+} and HCO_3^- (mg/l), CO_2 partial pressure (pCO_2) (log10) and Mg/Ca (m molar ratio) (n = 19).

	T	Q	EC	Cl	NO_3	SO_4	Na	K	Ca	Mg	HCO_3	pCO_2
Q	–0.976**											
EC	0.857**	–0.915**										
Cl	–0.317	0.310	–0.290									
NO_3	–0.250	0.251	–0.171	0.667**								
SO_4	0.740**	–0.799**	0.885**	0.066	0.132							
Na	–0.147	0.066	0.063	0.536*	0.575**	0.208						
K	0.502*	–0.466*	0.392	–0.548*	–0.597**	0.123	–0.276					
Ca	0.801**	–0.874**	0.972**	–0.349	–0.240	0.828**	0.047	0.418				
Mg	0.823**	–0.907**	0.981**	–0.327	–0.221	0.862**	0.055	0.366	0.981**			
HCO_3	0.805**	–0.888**	0.979**	–0.332	–0.240	0.844**	0.085	0.417	0.993**	0.991**		
pCO_2	0.193	–0.214	0.365	0.036	0.227	0.466*	0.419	0.240	0.393	0.368	0.393	
Mg/Ca	0.762**	–0.845**	0.901**	–0.120	–0.095	0.908**	0.035	0.182	0.856**	0.908**	0.885**	0.244

**. Correlation is significant at the 0.05 level (2-tailed).*

***. Correlation is significant at the 0.01 level (2-tailed).*

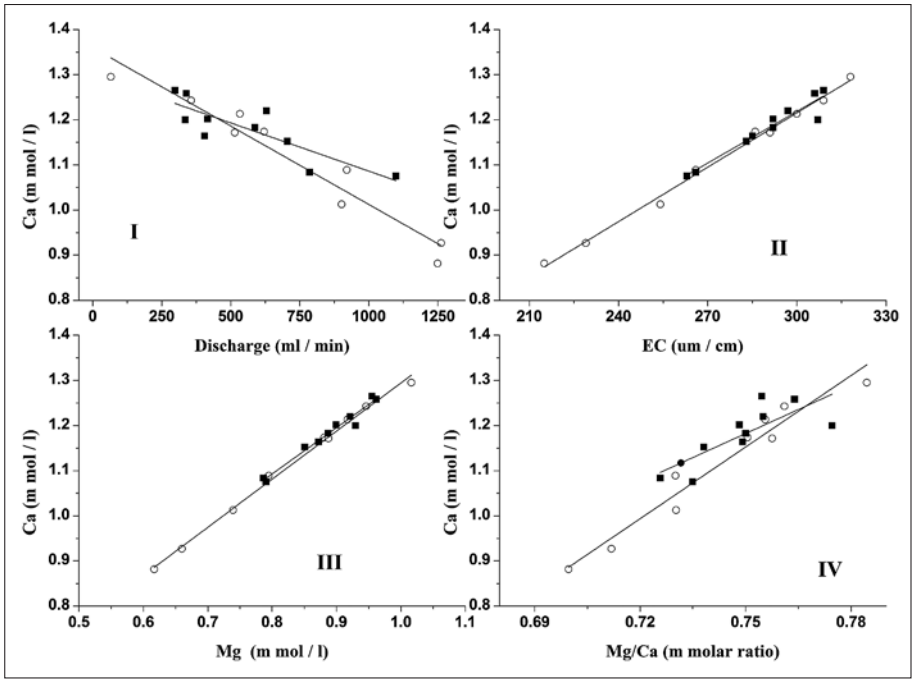

Fig. 4: Cross plots for the main hydrochemical and hydrological parameters of the drip water from the Velika Pasica Cave (Slovenia): (I) Ca^{2+} ions concentration vs. discharge of drip water; (II) Ca^{2+} ions concentration vs. electrical conductivity (EC); (III) Ca^{2+} ions concentration vs. Mg^{2+} ions concentration); (IV) Ca^{2+} ions concentration vs. Mg/Ca m molar ratio. The samples were divided into two groups according to two flood events: white circles represented the first flood event and the solid squares represented the second flood event.

$p \leqslant 0.01$, two-tailed) (Tab. 2). The dominant ion species at drip site VP1 were Ca^{2+}, Mg^{2+} and bicarbonate HCO_3^- (Tab. 1). All indicated relatively low variability, with the coefficient of variation (CV) = 10%, 12% and 11%, respectively, compared with the minor ions, such as Na^+ with CV = 30%, K^+ with CV = 26%. The main components, Ca^{2+} and Mg^{2+} and the Mg/Ca molar ratio, followed the EC variation pattern closely and they varied according to the discharge variation (Fig. 3). Following the previous high correlation, the variation in Mg^{2+} and HCO_3^- did not present in Fig. 3. The Mg/Ca molar ratio was relatively stable with a mean molar value of 0.75 and with CV = 3% (Tab. 1). Stable ratio between both ions was indicated with a significant correlation between them ($r = 0.981$, $p \leqslant 0.01$, two-tailed) (Tab. 2). It was also valid for Ca^{2+} *vs*. Mg/Ca ratio ($r = 0.856$, $p \leqslant 0.01$ two-tailed).

Regarding the minor ions: K^+, Na^+, SO_4^{2-}, Cl^- and NO_3^-, their concentrations were low but their CVs were higher than in the dominant ions (Tab. 1). Meanwhile they had low correlation coefficient with the discharge and the dominant ions (Tab. 2). As to pCO_2, it maintained stability at around $\log(pCO_2) = -3.00$, with CV = 1% (Tab. 1), but it was insignificant in relationship with other parameters, such as, Ca^{2+} ($r = 0.393$) (Tab. 2). The drip water temperature preformed as a special indicator for the drip discharge, correlated closely with the discharge rate ($r = -0.976$, $p \leqslant 0.01$, two-tailed). While its variation range during observed period was quite narrow, with CV = 2%.

In order to present the different response to the two flood events, samples were divided into two groups (Fig. 4). The variations of the main hydrochemical and hydrological parameters of the drip water presented similar and strong correlation between each other during this two events, e.g. in Fig. 4, II, the fitting lines of the two events between Ca^{2+} and EC overlapped. However, variation ranges for the parameters of the first flood event were larger than those of the second flood, which indicated that the higher discharge caused a lower ion concentration and the slow flow higher concentration. The higher discharge values of the first flood corresponded to the lower Ca^{2+}, EC, Mg^{2+} and Mg/Ca values (Fig. 4).

DISCUSSION

High heterogeneous and complex structure and void topology, epikarst reflects the large parameter for variability and uncertainty in the complicated hydraulic, mechanical, thermal, and chemical processes (Fairchild & Baker 2012). A study of a small discharge point from the epikarst could provide the details of local variation. Test site Sinji Vrh, a shallow artificial tunnel, located at in the western part of Slovenia was used to study the water

flow and solute transport in the unsaturated zone (Trček 2005). In this study, the Velika Pasica Cave, a small cave, located in the thick dolomitized epikarst zone, preformed as a natural discharge point for epikarst hydrochemical and hydrological research.

In order to further simplify the impact factors on the epikarst processes, the study period was chosen at the end of a long, cold and wet winter. During this time, there were two most probably sources for water replenishment to the drip water: snowmelt water and rain water. The day time warmth melted the surface snow cover, and the rainfall accelerated the melting. Thereafter, both converged and percolated down together, thus the two floods in the drip water discharge represented the superposition of these two signals. Additionally, when the rainfall ceased, the drip water discharge mainly represented the snow melt combined with the epikarst storage.

In order to achieve a better understanding of various karst processes, variations in the concentration of ions should be studied with other hydrochemical parameters (McDonald *et al.* 2007). During the specific study period, the low temperature and high humidity, accompanying the Mediterranean wet winter, weakened evaporation at the site. Meanwhile, due to this environmental condition, the respiration of the bio-activities from plant roots and soil microbes was weakened, as indicated by the CO_2 partial pressure in the drip water (pCO_2) with low value (mean = −3.00) and low variation (CV = 1%) (Tab. 1), although the CO_2 was the main driving force for the dissolution and precipitation of carbonate (Atkin *et al.* 2000; Liu *et al.* 2007), and the pCO_2 is generally higher in summer (Atkin *et al.* 2000). Liu *et al.* (2007) presented the yearly cyclical variation of those parameters which were higher in summer and lower in winter. Additionally, the entrance was the only detected outlet for the Velika Pasica Cave, thus the CO_2 exchanging from ventilation was insignificant here, which differs from situations in other caves (Tooth *et al.* 2003; Spötl *et al.* 2005).

The water percolated into the cave preformed a primary driving force for most variations recorded during the winter in the cave, in particular, for the cave water hydrochemical composition (Fig. 2). EC was an indicator of the amount of ions in solution. According to the ion analysis, Ca^{2+}, Mg^{2+} and HCO_3^- were the dominant ions in drip water. The variation of EC was highly negatively related to the discharge as well as the dominant ions (Fig. 3, Tab. 2). EC normally deceased after rainfall, and showed inverse variation with the discharge. While the strong correlation between the EC and discharge indicated that the intensity of the floods mainly controlled the hydrochemical variation by the mixing fresh infiltrated water (rain and snow) with stored water in vadose zone (i.e. the water stored in epikarst), which was differed from the summer time situation (Liu *et al.* 2007), as other factors also have significant impact during that season. Due to the dual-medium systems within epikarst (Akinson *et al.* 1977; Liedl *et al.* 2003), which are characteristic for the widespread fracture-net storage system and the well-developed fracture-net rapid discharge system (conduits), the intensive recharge could be discharged rapidly as considerably diluted drip water (Baldini *et al.* 2006; Fairchild & Baker 2012). The two different intensive flood events described here clearly indicated that the degree of dilution or mixing relied on the amount of recharge and the higher discharge correlates with the lower ion concentration (Fig. 4). When the fast flow cased, the stored water was dominate in the discharge, which corresponded with the increase of EC and the dominant ions concentration.

Baker *et al.* (2000) discussed that water /soil and water/ rock contact times, variable degrees of dilution and the prior calcite precipitation (PCP) in the vadose zone also controlled the calcium dissolution processes, as well as the replenishment from multiple reservoirs (McDonald *et al.* 2007). However, in this case study, Ca^{2+} and Mg^{2+} have a similar variation to the Mg/Ca ratio (Figs. 3 & 4), indicated by the high correlation coefficients (Tab. 2), which is not exactly similar in comparison with other caves (Baldini *et al.* 2006; Fairchild *et al.* 2006). Within recent years, the ratio of Mg/Ca in cave drip waters has acted as a good indicator of the climatic condition (Huang *et al.* 2001). The ratio in the Velika Pasica Cave was quite stable at 0.75, almost as a constant (with CV = 3%), which indicated that the parent rock was not pure dolomite and both ions were not precipitated after they dissolved, such as the PCP. In the discussion above, the low pCO_2 resulted in the low carbonate dissolution and the wet weather continued to replenish the stored water with the fresh infiltrated water (rain and snow). Thus, the resident time of stored water might not be long enough to accumulate a high Ca^{2+} concentration for PCP at the drip VP1 in a simple recharge system.

Apart of Ca^{2+} and Mg^{2+} ions, other dissolved ions also played important role in the studies on mixing processes of drip water in the unsaturated zone above the cave (Huang *et al.* 2001; Tooth & Fairchild 2003; Fairchild *et al.* 2006). However, excepting SO_4^{2-}, most of these ions had low concentrations (Tab. 1) and low correlation with the discharge (Tab. 2), which means they were not significantly affected by the percolation events. Origin of the rather high concentration of SO_4^{2-} ions might be from the dissolution of gypsum ($CaSO_4$) in the parent rock.

The temperature of the drip water presented high correlation and consistency with the discharge (Tab. 2), which also indicated the short resident time of the water. Therefore, the temperature of the drip water could act as an efficient tracer for the epikarst flow under such conditions (Anderson 2005).

CONCLUSION

In order to interpret geochemical processes during the snow melt period in the epikarst, high-frequency sample collection and chemical monitoring on cave drip water was carried out at Velika Pasica Cave (Central Slovenia). This study reveals that the major qualitative transformation between rain and dripping water in a sense of chemical and physical properties happened in a thin epikarst layer, which extends few meters in depth. The study period occurred at the end of a long, cold, wet winter. The main replenishment for the cave drip water was rain fall and snowmelt water. Under this special condition, some conclusions could be presented as: 1) After a long cold and wet period, the water percolated into the cave was performed a primary driving force for water hydrochemical variations in the cave during the winter, which performed as the dilution effect or mixing of the fresh and stored water in vadose zone; 2) The effect of CO_2 corrosion and PCP was weakened during this condition; 3) The main ion composition (Mg^{2+} and Ca^{2+}) presented high correlation with Mg/Ca ratio and the drip water discharge, indicated the weakened PCP; 4) The variation of low concentration ions had lower correlation with the discharge, as they did not strongly respond with the recharge event. On the contrary, the drip water temperature preformed as a good tracer on short term (within few hours).

The research revealed more detailed and accurate results from the high-frequency monitoring over a specific period, which confirmed and deepened the previous work on cave drip water. However, long-term monitoring should be continued for interpretation of the seasonal hydrochemical variation and climate change.

ACKNOWLEDGEMENTS

Authors would like to extend thanks to colleagues from the National Institute of Biology who contributed to field work, in collecting data and maintaining instruments. This research was founded by the Slovenian Research Agency (ARRS) within the program P1-0255 (Structure, function and communications in ecosystems) and within the Program for Young Researchers (Contract no. 1000-11-310196). We also extend our thanks to Professor Julia Ellis Burnet for linguistic corrections and two anonymous reviewers for their valuable comments and corrections on a previous version of the text.

REFERENCES

Anderson, M. P., 2005: Heat as a ground water tracer.- Ground water, 43, 6, 951–968.

Appelo, C.A.J. & D. Postma, 2005: *Geochemistry, Groundwater and Pollution.*- Balkema Publishers, pp.649, Leiden, The Netherlands.

Atkin, O.K., Edwards, E.J. & B.R. Loverys, 2000: Response of root respiration to changes in temperature and its relevance to global warming.- New Phytologist, 147, 141–154.

Atkinson, T.C., 1977: Diffuse flow and conduit flow in limestone terrain in the Mendip Hills, Somerset (Great Britain).- Journal of Hydrology, 35, 93-110.

Baker, A., Barnes, W.L. & P.L. Smart, 1997: Variations in the discharge and organic matter of stalagmite drip waters in Lower Cave, Bristol.- Hydrological Processes, 11, 1541–1555.

Baker, A. & Genty, D. & I.J. Fairchild, 2000: Hydrological characterization of stalagmite drip waters at Grotte de Villars, Dordogne, by the analysis of inorganic species and luminescent organic matter.- Hydrology and Earth System Sciences, 4, 3, 439–449.

Baldini, J.U.L., McDermott, F. & I.J. Fairchild, 2006: Spatial variability in cave drip water hydrochemistry: implications for stalagmite paleoclimate records.- Chemical Geology, 235, 3–4, 390–404.

Brancelj, A., 2002: Microdistribution and high diversity of Copepoda (Crustacea) in a small cave in central Slovenia.- Hydrobiology, 477, 59–72.

Fairchild, I.J., Tuckwell, G.W., Baker, A. & A. F. Tooth, 2006: Modelling of drip water hydrology and hydrochemistry in a weakly karstified aquifer (Bath, UK): implications for climate change studies.- Journal of Hydrology, 321, 1–4, 213–231.

Fairchild, I.J. & A. Baker, 2012: *Speleothem science: from process to past environments.*- Willey Blackwell, pp. 432, Oxford.

Fernandez-Cortes, A., Calaforra, J.M. & F. Snchez-Martos, 2008: Hydrogeochemical processes as environmental indicators in drip water: Study of the Cueva del Agua (Southern Spain).- International Journal of Speleology, 37, 1, 41–52.

Huang, Y., Fairchild, I.J., Borsato, A., Frisia, S., Cassidy, N.J., McDermott. F. & C.J. Hawkesworth, 2001: Seasonal variations in Sr, Mg and P in modern speleothems (Grotta di Ernesto, Italy).- Chemical Geology, 175, 3–4, 429–448.

Jex, C.N., Mariethoz, G., Baker, A., Graham, P., Andersen, M.S., Acworth, I., Edwards, N. & C. Azcurra, 2012: Spatially dense drip hydrological monitoring and infiltration behaviour at the Wellington Caves, South East Australia.- International Journal of Speleology, 41, 2, 283–296.

Kogovšek, J., 2007: Rainwater percolation dynamics assessment through the vadose karst zone on the basis of discharge measurements.- Acta Carsologica, 36, 2, 245–254.

Kogovšek, J., 2010: *Characteristics of percolation through the karst vadose zone.* -ZRC Publishing, pp.168, Ljubljana.

Kogovšek, J., 2011: Impact of chlorides, nitrates, sulfates and phosphates on increased limestone dissolution in the karst vadose zone (Postojna Cave, Slovenia).- Acta Carsologica, 40, 2, 319–327.

Kogovšek J. & M. Petrič, 2012: Characterization of the vadose flow and its influence on the functioning of karst springs: Case study of the karst system near Postojna, Slovenia.- Acta carsologica, 41, 1, 101–113.

Liedl, R., Sauter, M., Huckinghaus, D., Clemens, T. & G. Teutsch, 2003: Simulation of the development of karst aquifers using a coupled continuum pipe flow model.- Water Resources Research, 39, 3, 1057–1062.

Liu, Z.H., Li,Q., Sun, H.L. & J.L. Wang, 2007: Seasonal, diurnal and storm-scale hydrochemical variations of typical epikarst springs in subtropical karst areas of SW China: soil CO_2 and dilution effects.- Journal of Hydrology, 337, 1–2, 207–223.

McDonald, J., Drysdale,R., Hill,D., Chisari, R. & H. Wong, 2007: The hydrochemical response of cave drip waters to sub-annual and inter annual climate variability, Wombeyan Caves, SE Australia.- Chemical geology, 244, 605–623.

Pleničar, M., 1970: Tolmač k Osnovni geološki karti SFRJ, List Postojna. Zvezni geološki zavod Beograd. (= Basic geological survey; section Postojna), 62.

Sheffer N.A., Cohen, M., Morin, E., Grodek, T., Gimburg, A., Magal, E., Gvirtzman, H., Nied, M., Isele, D. & A. Frumkin, 2011: Integrated cave drip monitoring for epikarst recharge estimation in a dry Mediterranean area, Sif Cave, Israel.- Hydrological Processes, 25, 2837–2845.

Smart P.L. & H. Friederich, 1987: Water movement and storage in the unsaturated zone of a maturely karstified carbonate aquifer, Mendip Hills, England.- In: *Proceedings of environmental problems in karst terranes and their solutions conference,* 28th–30th, October 1986, Bowling Green, Kentucky. 57–87, KY, USA.

Spötl, C., Fairchild, I.J. & A. F. Tooth, 2005: Cave air control on drip water geochemistry, Obir Caves (Austria): Implications for speleothem deposition in dynamically ventilated caves.- Geochimica et Cosmochimica Acta, 69, 10, 2451–2468.

Tooth, A.F. & I.J. Fairchild, 2003: Soil and karst hydrological controls on the chemical evolution of speleothem-forming drip waters, Crag Cave, southwest Ireland. -Journal of Hydrology, 273, 1–4, 51–68.

Trček, B., 2005: The use of natural tracers in the study of the unsaturated zone of a karst aquifer.- Geologija, 48, 1, 141–152.

Vokal, B., Obelič, B., Genty, D. & I. Kobal, 1999: Chemistry measurements of dripping water in Postojna Cave.- Acta Carsologica, 28, 1, 305–320.

Yang, R., Liu Z.H., Cheng, Z.C. & M. Zhao, 2012: Response of epikarst hydrochemical changes to soil CO_2 and weather conditions at Chenqi, Puding, SW China.- Journal of Hydrology, 468–469, 151–158.

Zhang, C., Yan, J., Pei, J.G. & Y.J. Jiang, 2010: Hydrochemical variations of epikarst springs in vertical climate zones: a case study in Jinfo Mountain National Nature Reserve of China.- Environmental Earth Sciences, 63, 2, 375–381. Doi: 10.1007/s12665–010–0708–y.

COBISS: 1.01

GEOTHERMAL POTENTIAL AND SUSTAINABLE USE OF KARST GROUNDWATER IN URBAN AREAS–BELGRADE, CAPITAL OF SERBIA CASE STUDY

GEOTERMALNI POTENCIAL IN TRAJNOSTNA RABA KRAŠKE PODTALNICE NA URBANIH OBMOČJIH – PRIMER BEOGRADA, GLAVNEGA MESTA SRBIJE

Dejan MILENIC[1] & Ana VRANJES[1]

Abstract **UDC** 662.997:551.444(497.11Beograd)

Dejan Milenic & Ana Vranjes: Geothermal potential and sustainable use of karst groundwater in urban areas–Belgrade, capital of Serbia case study

The increase in energy demand due to urban expansion and migration to urban areas has a negative impact on the environment and the city budget. Development plans of cities are more frequently based on the implementation of energy efficiency measures, which among other things include the use of renewable energy sources. In the area of Belgrade, research was conducted aimed at assessing the geothermal potentiality of the field and defining the possibility of groundwater exploitation. The research has been directed to groundwater formed in karst aquifers. Geothermal field evaluation was preceded by the formation of geological and hydrogeological bases, then, the development of a conceptual model of karst distribution in the city area and the systematization of data measured in the observation well network. The potentiality assessment is followed by defining of the conditions and possibilities of the exploitation of karst water as a form of geothermal energy in heat pump systems. In the exploitation of karst water in the city, it is significant to establish mechanisms of sustainable management, especially in terms of protection of resources. In recent years, there has been recorded a constant increase in the number of heating and cooling systems of buildings using groundwater as an energy source in the territory of Belgrade. Potential causes of the negative impact of exploitation of karst water are the overexploitation of resources, creating of the effect of "thermal feedback" as a result of incompetent disposition, namely restoring of groundwater to the aquifer.

Keywords: geothermal energy, karst aquifer, urban area, sustainable utilisation.

Izvleček UDK 662.997:551.444(497.11Beograd)

Dejan Milenic & Ana Vranjes: Geotermalni potencial in trajnostna raba kraške podtalnice na urbanih območjih – primer Beograda, glavnega mesta Srbije

Večanje potreb po energiji zaradi širitev urbanih okolij in migracij v mesta ima negativen vpliv na okolje in mestne proračune. Razvojni načrti mest bolj pogosto temeljijo na uvajanju ukrepov za varčevanje z energijo, ki med drugim vključujejo tudi rabo obnovljivih virov energije. Na območju mesta Beograda je bila izvedena raziskava z namenom izdelave ocene geotermalnega potenciala območja in možnosti izrabe podzemne vode. Usmerjena je bila v proučevanje podzemne kraške vode. Pred izdelavo ocene geotermalnega polja so bile narejene geološke in hidrogeološke podlage, nato postavljen konceptualni model razporeditve krasa v mestu in urejena baza podatkov merjenih v mreži opazovalnih vodnjakov. Oceni potenciala je sledila določitev pogojev in možnosti izrabe kraške vode kot oblike geotermalne energije v sistemu toplotnih črpalk. Pri izrabi kraške vode v mestu je pomembno vzpostaviti mehanizme trajnostnega upravljanja, še posebej v smislu varovanja virov. V zadnjih letih je bilo na območju mesta Beograda zabeleženo stalno naraščanje števila sistemov ogrevanja in hlajenja stavb z uporabo podzemne vode kot vira energije. Možna vzroka negativnih vplivov izrabe kraške vode sta prekomerno izkoriščanje virov in ustvarjanje „povratnega toplotnega učinka“ zaradi neprimernega načina vračanja podzemne vode v vodonosnik.

Ključne besede: geotermalna energija, kraški vodonosnik, urbano območje, trajnostna raba.

[1] University of Belgrade, Faculty of Mining and Geology, Department of Hydrogeology, Djusina 7, 11000 Belgrade, Serbia, e-mail: dejan.milenic@rgf.bg.ac.rs, vranjes_ana@yahoo.ie

Received/Prejeto: 25.02.2014

SCOPE OF THE WORK AND SIGNIFICANCE OF RESEARCHING OF KARST AQUIFERS IN URBAN AREAS

The expansion of urban surfaces and population growth in already existing urban areas is a distinctive phenomenon of the society management in the 21st century. According to statistical estimates, more than a half of the world's population lives in cities, while in some countries even 90% of the population lives in urban areas (Marsalek *et al.* 2007). Intensive urbanization and disappearance of "free" green space on the account of asphalt and concrete, results in changing of conditions and the quality of the environment on one side, and on the other, in an increase in energy demand, since buildings are one of the largest consumers of energy. To meet energy needs (heating, air conditioning, interior lighting) buildings "consume" about 40% of the world energy , 16% of fresh water and 25% of timber, whereby 70% of the total emission of sulphur dioxide and 50% of total carbon dioxide emission is produced (Santamouris 2007).

According to the condition of the housing stock and the annual energy consumption for residential heating, Belgrade falls into the category of energy-inefficient cities. The largest number of flats (70% of the existing housing stock) in the territory of Belgrade was built in the period before the year 1980, i.e. before the year 1987, when the first actual regulations on thermal protection of buildings were introduced. The annual energy consumption for heating of flats ranges from 150 to 250 kWh/m^2, depending on the age and condition of the property (Cukovic Ignjatovic 2009).

Urban areas represent a unique system, which operates completely by the activity of anthropogenic factors, having a direct impact on the environment, inevitably, causing changes that are manifested in the form of micro-climatic changes. The impact of urbanization on groundwater resources, as one of environmental elements, is reflected in the change of groundwater recharge and exploitation conditions. The impact is indirect and affects water balance elements (precipitation, evaporation, run off).

On the other hand, in urban areas, groundwater suffers from multiple exposure to the risk of contamination, which is manifested in the form of chemical contamination or as "thermal feedback" pollution (the change of groundwater temperature in the aquifer under the impact of anthropogenic factors, which occurs due to uncontrolled "artificial" aquifer recharge).

The aforementioned urbanization impact on groundwater increases if the groundwater beneath the city is formed in karst aquifers. Open karst structures are directly exposed to anthropogenic impacts, thus accidents such as damages to the sewage system, the hot water

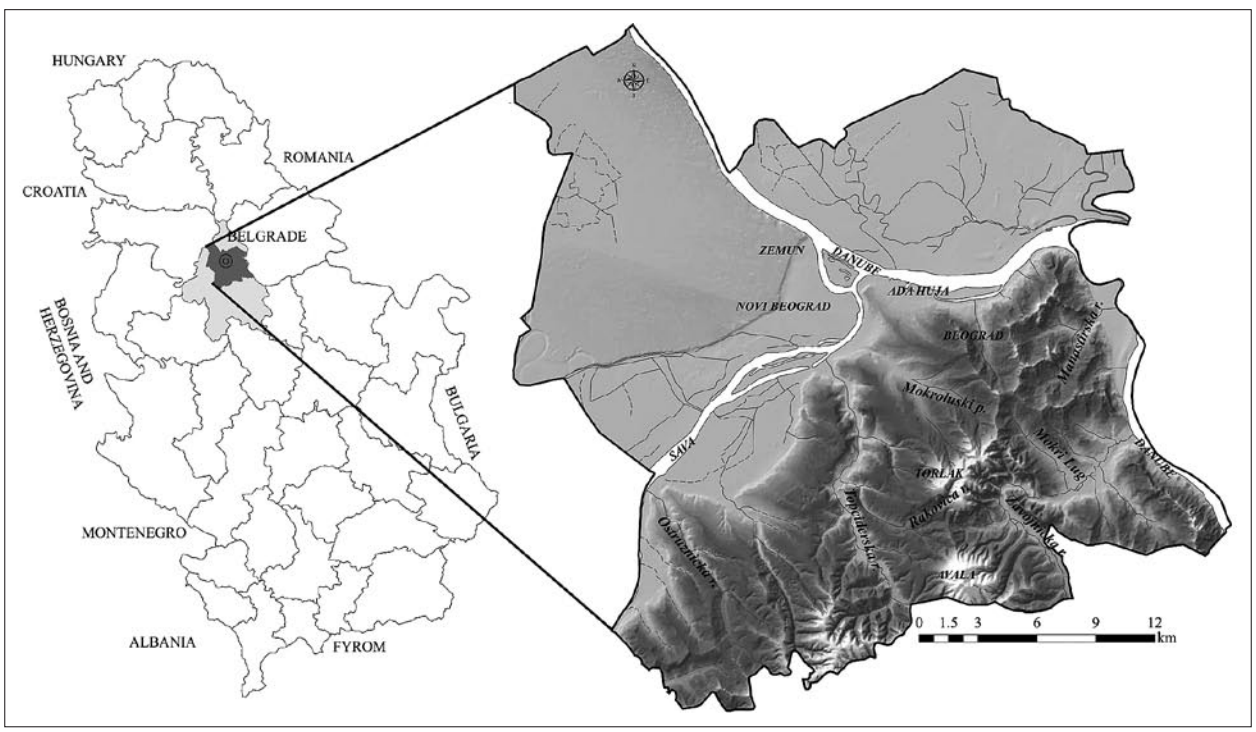

Fig. 1: Geographical position of Belgrade urban city area.

network, the rain collector, the road and other asphalt surface drainage waters, a number of industrial plants, uncontrolled development of wells and groundwater return into the aquifer and inadequate storage of hazardous materials (petroleum and petroleum products, paints, varnishes ...) may adversely affect the karst water.

The significance of the research of karst aquifers in urban areas, in addition to the aspect of protection in recent years, is aimed at the exploitation of karst water as the geothermal resource for heating and cooling of buildings. Nowadays, due to the increasing energy needs strategic plans of town development are based on the use of renewable energy sources, and the evaluation of the geothermal potentiality of the terrain becomes part of planning documents in the development of detailed urban plans.

The city core of Belgrade is largely formed in karst parts of the terrain. For the purpose of assessing the geothermal potentiality of karst groundwater, defining the impact of urbanization on the karst aquifer, along with considering the conditions, opportunities and effect of karst water exploitation in the city of Belgrade area, there were analyzed:

General characteristics
- Climate characteristics with an urbanization impact analysis
- Hydrographic features with an urbanization impact analysis
- Geomorphologic features with an urbanization impact analysis
- Geological setting of the terrain
- Demographics with an analysis of urban population trends
- State in building with an analysis of the housing stock energy efficiency
- Thermal energy supply with an analysis of the existing capacity of remote heating

Geothermal characteristics
- Hydrogeological characteristics
- Karst distribution in the city of Belgrade area
- Karst aquifer features (conditions of recharge and discharge)
- Quantitative and qualitative characteristics of karst water
- Geothermal indicators in the city area

Results of the conducted research are presented for the urban city area (Fig. 1). The urban city area covers a surface of about 770 km^2. In the entire territory of the city, there are approximately 1.650,000 inhabitants, of whom about 80% lives in the urban city area. Statistical data imply the growing tendency of urban population, namely 52% of the population moved to the territory of the city.

GENERAL CHARACTERISTICS OF BELGRADE TERRITORY

CLIMATE CHARACTERISTICS OF BELGRADE URBAN CITY AREA

The climate of Belgrade urban city area is considerably different from that of the surrounding area, which is primarily conditioned by the anthropogenic impact (urbanization of large areas), as well as by the impact of two factors, the radiation balance and water balance, which can be said to be characterized by local specificities (Unkasevic 1994). Different radiation balance is the consequence of the weaker reflection of solar radiation due to the existence of "street canyons". Differences in water balance are owing to minor sinking of precipitation in the soil as the soil is covered, whereby the runoff is increased and soil moisture reduced. The difference also arises in evaporation due to reduced soil moisture. The consequence of these differences results in stronger heating of the city area. Differences are also highly expressed in some other elements such as wind, fog and smog. The impacts of topography (vertical gradient), the base (rivers, land, vegetation) the city structure (urban "heat island") lay down local climatic specificities of Belgrade. Values of basic climatic elements in the territory of Belgrade are presented in Tab.1.

Tab. 1: Mean annual values of climatic elements in Belgrade urban city area.

Climatic parameter	***Precipitation***	***Temperature***	***Relative air humidity***	***Atmospheric pressure***	***Potential evapotranspiration***
Unit	mm/yr	°C	%	mbar (hPa)	mm/yr
Value	680	12	69	1001	649

HYDROGRAPHIC CHARACTERISTICS OF BELGRADE URBAN CITY AREA

The hydrographic network of Belgrade area via the Sava and Danube catchment area belongs to the Black Sea basin. The average flow of the Danube in Belgrade is 5260 m^3/s, and of the Sava 1650 m^3/s. Lowland parts of the terrain north of the Sava and Danube rivers are characterized by a developed network of reclamation canals, with a total length of about 1000 m, while natural streams are poorly developed. South of the Sava and Danube rivers, parts of "Belgrade hills" are characterized by a number of permanent and temporary streams. In this part of the field, there is a centrifugal type of the drainage network. Right tributaries of the Sava are the Ostruznicka Reka River, the Topciderska Reka River and the Mokroluski Potok stream, which is mostly piped. In the urban city core, the hydrographic network is altered under the influence of urbanization; rivers and streams are cased and carried into the sewage system. The left tributary of the Danube is the Tisa River, while the larger tributaries on the right bank are the Manastirska Reka River and the Zavojnicka Reka River (Fig. 1).

GEOMOPHOLOGICAL CHARACTERISTICS OF BELGRADE URBAN CITY AREA

Belgrade surroundings comprise two different natural units: the Pannonian plain in the north, and Sumadia, south of the Sava and Danube rivers (Fig. 1). The most prominent shape of the Sumadia hill relief, regarding the urban city area, is Avala hill (511 m), while Ada Huja Eyot with 70.15 m is the lowest elevation. The largest part of the Belgrade city core is located on a hilly, gently rolling relief. Eolian, karst and marine processes, among geomorphological processes, played a significant role, in shaping of the hilly terrain relief parts. The most interesting forms of the karst process are the Tasmajdan cave and the Tasmajdan cliff in the city center.

Parts of the terrain north of the Sava and Danube rivers are characterized by a typical lowland type of a terrain. Absolute elevations of this part of the field range from about 69 m to about 76 m. In this part of the field, there are numerous ponds and marshes whose existence was caused by fluctuations in the level of the Danube River. The fluvial process played the most significant role in shaping of the lowland part of the field while shapes of proluvial and eolian processes (loess plateaus) are also visible.

GEOLOGICAL AND HYDROGEOLOGICAL CHARACTERISTICS OF BELGRADE URBAN CITY AREA

The oldest rocks in the city belong to the Paleozoic, and are found in farthest southwest of the territory. Beginning with the Paleozoic, rocks of Mesozoic and Cenozoic ages alternate, where hiatus can be perceived in sedimentation. Rocks of Jurassic age are the oldest member of the Mesozoic era in the urban city area. During the Upper Jurassic the differentiation of the seabed was made and a deep depression formed, which led to the creation of ophiolite, a diabase-chert formation, flysch, reef limestone. The complete development of the Cretaceous period may be traced in the city area. Flysch sediments both of Lower Cretaceous, and Upper Cretaceous ages are the most common members of the Belgrade area.

From the hydrogeological point of view, a significant member of the Cretaceous is a facies of reef and sub-reef limestones of Urgonian development. The Urgonian limestone facies is considerably distributed in the city center and its wider surroundings. Cretaceous sediments being in the Urgonian limestone facies are the floor to Tertiary sediments in the urban territory of Belgrade. The roof of Urgonian limestone is represented by limestones of Tortonian and Sarmatian age and Quaternary sediments. The thickness of the Urgonian limestone is unknown, since drill holes and wells did not enter the bed of Urgonian sediments.

During the Tertiary a limestone facies of Tortonian and Sarmatian ages was formed, which from the hydrogeological aspect also played a significant role in the formation of groundwater. The limestone facies of Tortonian age at the surface of the terrain was stated in central parts of the city, while in the wider city environment, a facies was discovered by drilling, thus its distribution is not clearly defined. Tortonian limestones in the central parts of the city lie in the Cretaceous bed, while being covered by a younger layer, most frequently by Pannonian clay and marl and loess deposits, and in some parts of the city Sarmatian sediments as well. The rugged reef paleorelief is the consequence of the absence of the Sarmatian over the Tortonian.

Sarmatian sediments have extensive distribution in the territory of the city of Belgrade being identified over the entire space. The Sarmatian sediments are represented by marl and marly limestone and limestone. It has been found, by test drilling, that the total thickness of the Sarmatian deposits is about 35 m (Knezevic & Sumar 1994). The Sarmatian limestones gradually wedge out towards the confluence of the Sava into the Danube, as their thickness increases towards the central parts of the city. The development of Sarmatian limestone was found on the left bank of the Sava by drilling below gravel-sand layers at different depths from 20 m to 40 m. Limestone of Sarmatian age was also found on the right bank of the Sava by test drilling.

In addition to limestone sediments of the Tortonian and Sarmatian, sandy-gravelly Quaternary sediments

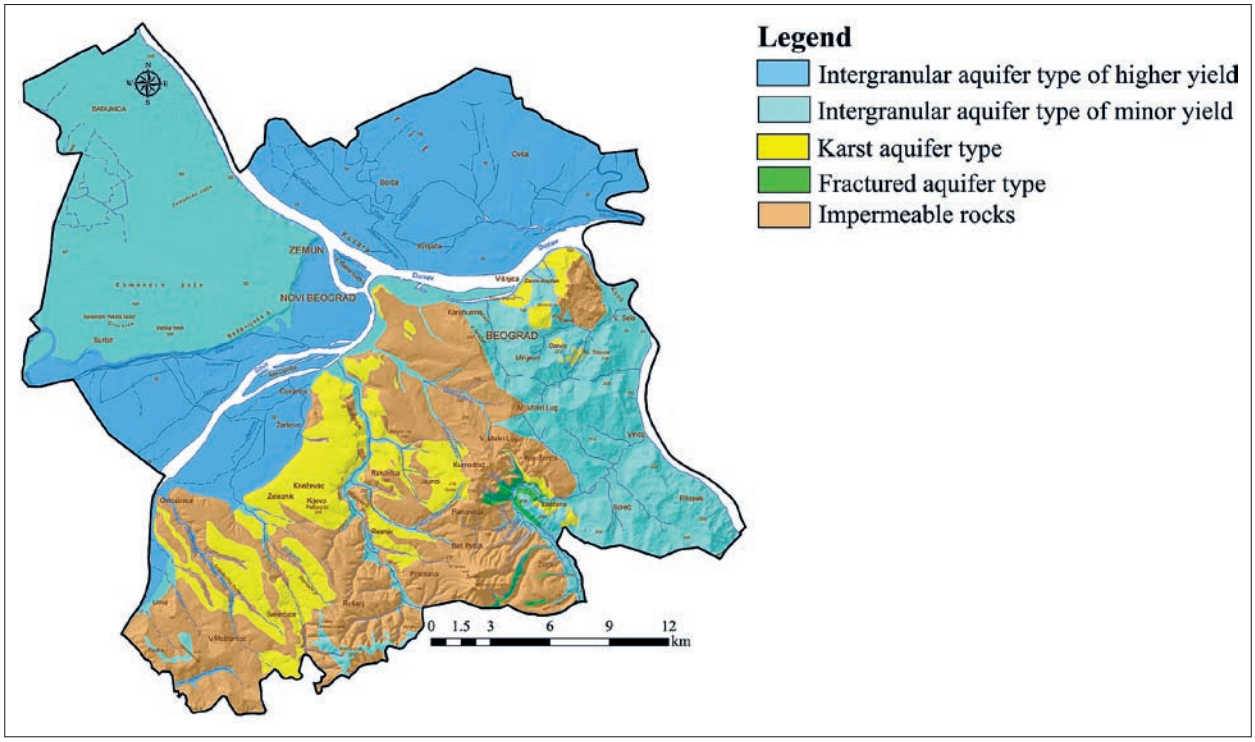

Fig. 2: Hydrogeological map of Belgrade urban city area.

play an important role in the formation of ground water resources. During the Quaternary at least twenty climate cycles have been recorded. During colder periods of the Quaternary Belgrade belonged to a periglacial area where loess deposits were accumulated. All parts of the Quaternary period, as well as all genetic types (except glacial) are represented in the vicinity of Belgrade.

Based on the structural type of porosity, in the urban city area, there were singled out:

- intergranular aquifer type of higher yield within sandy-gravel sediments
- intergranular aquifer type of minor yield within a sand facies of Sarmatian age
- karst aquifer within limestone of Cretaceous and Tortonian-Sarmatian age
- fractured aquifer within the serpentinite of Jurassic age
- impermeable parts of the terrain within the flysch sediments and clayey-sandy sediments of the Pannonian

A hydrogeological map of Belgrade urban city area is shown in Fig. 2.

GEOTHERMAL CHARACTERISTICS AND NEW HYDROGEOLOGICAL ZONING OF BELGRADE

Each hydrogeological phenomenon or facility with the groundwater temperature higher than the mean annual air temperature, whose value for Belgrade is 12 °C, points to a potential source of geothermal (hydrogeothermal) energy. The increased temperatures of groundwater in relation to the reference air temperature are the result of geological-tectonic structure and the hydrogeological conditions in the field, as well as anthropogenic activities.

NEW HYDROGEOLOGICAL ZONING OF BELGRADE

The new hydrogeological zoning largely relies on the existing one, and is based on the analysis of the data of hydrogeological explorations carried out in the last thirty years. The results of recent studies have confirmed the existing hydrogeological knowledge, but also pointed to the potential of so far unexplored parts of the terrain from the aspect of the tapping and exploitation of groundwater resources. The latest research, has primarily contributed

Tab. 2: Yield and temperatures of groundwater measured in wells / piezometers within karst aquifer in city area.

Well/Piezometer mark	*Well/Piezometer depth (m)*	*Well/Piezometer yield (l/s)*	*Groundwater temperature (°C)*
Well depth up to do 100 m			
B–1	54.0	/	**17**
BS–1	61.0	9.0	**22**
PdUS–5	79.0	/	**15.0**
PdUS–1	80.0	/	**15.0**
CGL–1	80.0	1.0	**17**
PdUS–4	82.0	/	**16.0**
B–1	83.0	2.0	**16**
B–4 BIP	87.00	9.0	
B–2 BIP	94.00	12.0	**16**
IBS–1/11	97.0	2.0	**17**
Well depth 100–300 m			
B–1 BIP	100.0	14.0	**16.5**
BBB–1	100.0	10.0	**15**
B–1/2000	100.0	10.0	**16**
IEBS–1/12	100.0	6.0	**16**
IB–1	100.0	5.0	**16**
IBS–1/11	100.0	2.0	**15**
BM–1	101.0	2.0	**17**
BS–2	103.0	4.50	**21**
OB–1	162.0	2.0	**21**
IB–2	150.0	10.0	**17**
IEBV–1/08	106.0	3.0	**21**
IB–1	120.0	7.0	**17**
PdUS–3	130.0	/	**15.0**
IEBBD–1	141.0	4.0	**20**
IB–1	142.0	2.0	**16**
B–3 BIP	144.50	4.0	**15.5**
IB–1	152.0	1.0	**17**
Well depth 300–500 m			
BS–3	321	15.0	
Well depth over 500 m			
VL–1	800	0.3 flowing of well	**25**

to the perception of hydrogeological structure of deeper parts of the terrain and consideration of geometry of some types of aquifers. Newer geological explorations, carried out in the central parts of the city and in the vicinity of the mouth of the Sava river into the Danube, helped a great deal. In addition to the latest results of hydrogeological and geological explorations, the new zoning is carried out due to the territorial development of the city of Belgrade.

Hydrogeological zoning is made for the whole city of Belgrade territory, and there are singled out altogether ten areas with the corresponding sub-areas. The geological structure factor played the main role in singling out certain areas, then the hydrogeological structure factor while some areas were singled out according to the geomorphologic conditions in the field. The hydrogeological areas are singled out primarily for more complete and more systematic consideration of the hydrogeological characteristics of the study area, which is distinguished by its pronounced complexity. By creating the hydrogeological zoning, there were formed bases for the evaluation of geothermal potentiality of the terrain.

GEOTHERMAL CHARACTERISTICS OF THE CITY OF BELGRADE TERRITORY

The average values of heat flow for the city of Belgrade territory range from about 100 mW/m^2 to 120 mW/m^2, while the average value for the continental part of Europe is about 60 mW/m^2 (according to Cemark & Rybach 1979 as cited by Milivojevic 1989). Values of the geother-

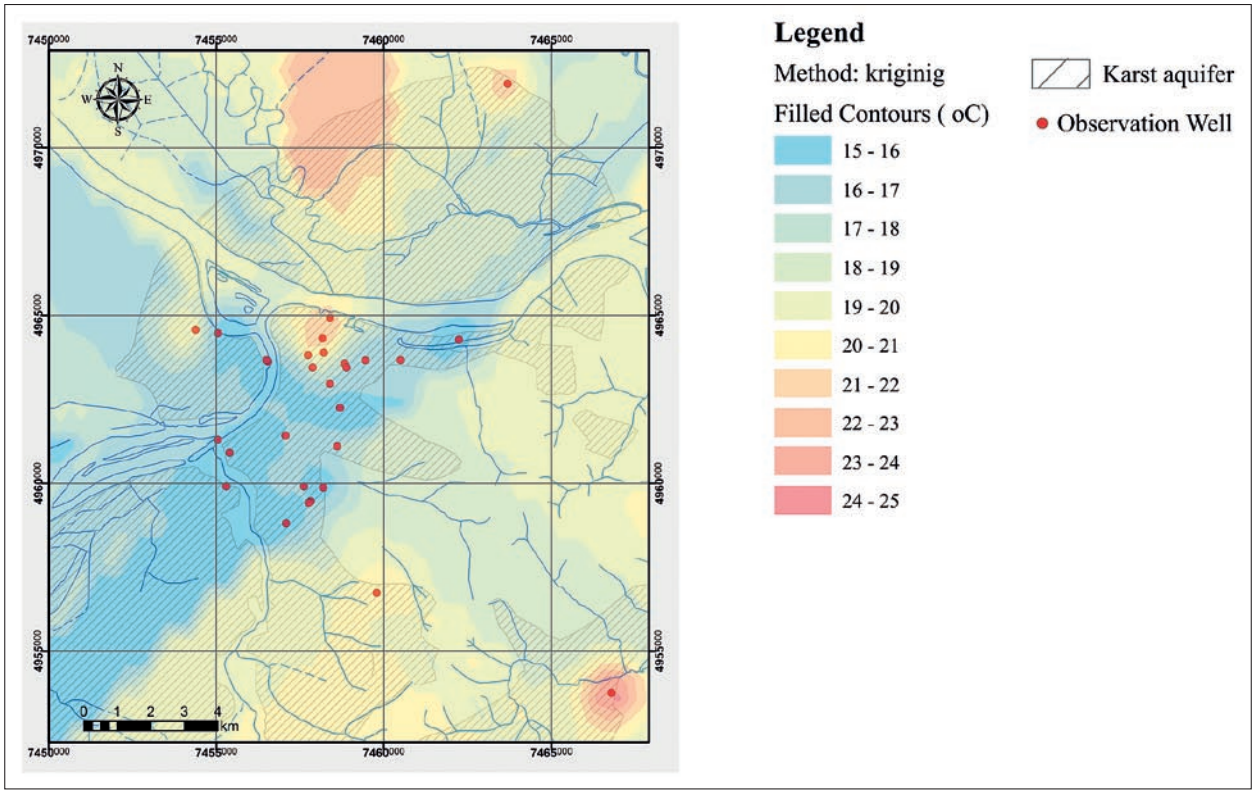

Fig. 3: Isotherms in urban city area.

mal degree throughout the city of Belgrade territory are higher in relation to the average increase in temperature in the continental parts of the Earth. The value of the geothermal degree in the central parts of the city is 10 m/°C (Milivojevic 1982), while the largest anomalies were registered in the area of Avala hill (south-eastern parts farthest of the urban city area). East of Avala, in the valley of the Zavojnicka River, groundwater is formed within the karst aquifer, in a closed hydrogeological structure. The groundwater temperature measured at wells in the Zavojnicka River ranged from 19 °C to 25 °C (Fig. 5b). The increased temperatures are explained by the absence of circulation till the test holes are made within the karst aquifer. (Milivojevic 1982).

It is observed by analyzing hydrogeological phenomena and facilities in the territory of Belgrade through the survey of hydrogeological zones, that the groundwater temperature ranges from 11 °C to 30 °C. Groundwater temperatures monitored at the spring range from 10 °C to 15 °C. The warmest occurrence of the groundwater is related to the karst aquifer in the central parts of the city core. While drilling, temperature on well BS–1 (100 m) in Skadarlija was 34 °C (Dokmanovic 1997). During the exploitation of the aquifer the temperature dropped to 22–24 °C (the BS-1 well location is shown in Fig. 5b). Within the urban city area, the highest drilling depth is 800 m (the well VL–1). The measured temperature of rocks at the well ort is 43 °C, and the groundwater temperature on the surface of the terrain is 25 °C. The hole is drilled in Sarmatian limestone (the location of the well is shown in Fig. 5b).

In Fig. 3 there are shown isotherms of the urban city core area designed on the basis of the groundwater temperatures measured at the wells and piezometers (Tab. 2).

KARST AQUIFER OF BELGRADE, DISTRIBUTION AND BASIC CHARACTERISTICS

The karst aquifer in the territory of Belgrade is formed within the limestone of Urgonian age as well as within the limestone of Tortonian and Sarmatian ages. Open karst surfaces occupy about 10% of the territory of the

urban city area, being mainly the Tortonian-Sarmatian limestones. Although there are some differences in mechanical properties of rocks of Tortonian and Sarmatian ages (Tortonian limestone is sturdy, cracked to a lesser extent than the limestone of Sarmatian age and in colour they resemble the Urgonian limestone, while the Sarmatian limestone is cavernous, of white-yellow colour) the karst aquifer is observed as a part of the "package" of Tortonian and Sarmatian limestones, i.e. the stratigraphic division has not been conducted. In order to assess the geothermal potentiality of the terrain and to define the conditions and possibilities of exploitation of the karst groundwater, a conceptual model of the assumed limestone distribution in the urban city area has been developed, and the conditions of the karst aquifer recharge and drainage as well as the basic chemical properties of the karst waters perceived. The model of the limestone distribution is made on the basis of karst surface development and on the basis of data obtained by the exploratory drilling.

DISTRIBUTION OF KARST AQUIFER

Limestone of Cretaceous age (K_1^{4-5}). In the urban territory of Belgrade, limestone of Cretaceous age is found on the left and right sides of the Topcider River (Fig. 5a).The limestone extends discontinuously, which is probably the consequence of sedimentation, namely the appearances of paleorelief. Drilling in parts of the city center over the Urgon limestone of Tortonian and Sarmatian ages was found. The thickness of the limestone of Urgon age is not known, since drill holes and wells did not enter the bed of Urgon sediments.

Limestone of Tortonian-Sarmatian age(M_2^2–M_3^1). The development of Tortonian limestone can be traced along the Sava slope (right bank), from flowing of the Mokri Lug Stream into the Sava to the Kalemegdan area. Limestone is also noted in the left side of the Sava, along the left bank of the confluence. Tortonian limestone lies in the Cretaceous bed in the central part of the city. It emerges partly to the surface, affecting the steep relief of the urban areas, and, partly, it is overlain by younger layers (Sarmatian limestone). Moving away from the city center, smaller isolated outcrops are found at both sides of the Rakovica Stream (west side of the Torlak hill). Likewise, less isolated parties of limestone have been discovered in the valley of the Mokri Lug Stream. Outcrops of limestone are found in the village of Lestane in eastern part of the city area. The development of Tortonian and Sarmatian limestones on the left and right banks of the Sava immediately before its confluence with the Danube is shown in the profile B-B (Fig. 4).

MODEL OF KARST AQUIFER DISTRIBUTION IN BELGRADE AREA

A model of limestone distribution in the urban area of Belgrade was developed based on surface development of limestone and data obtained by test drilling.

BASIC CHARACTERISTICS OF KARST AQUIFER

Conditions of aquifer recharge and discharge

The dominant way of karst aquifer recharge is by rainfall infiltration. Factors that generally affect the recharge of aquifers in urban areas are:

- covering of the field by asphalt and concrete surfaces

asphalt and concrete surfaces reduce the possibility of rainfall infiltration while surface runoff is increased

- losses in water system network

losses in water system network participate in recharge of aquifers (the pipeline route passes through central parts of the city, from the Makis area on the Sava to the Tasmajdan area and is mostly laid in limestone). Losses in the network of 20% are equivalent to 300 mm of a rain annual height (Marsalek *et al.* 2007)

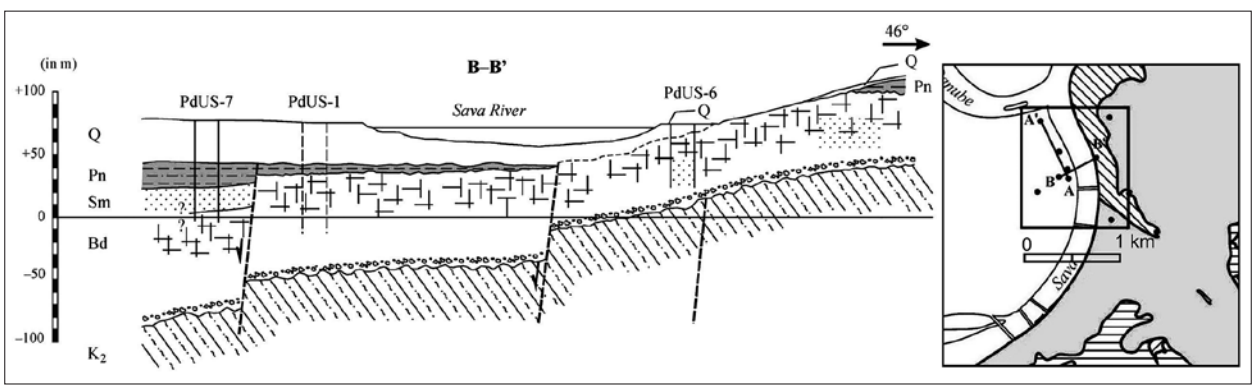

Fig. 4: Geological cross section of field near confluence of Sava and Danube (Rundic et al. 2011).

Legend: K_2 – Upper Cretaceous; Bd – Badenian limestone and sand; Sm – Sarmatian sand, marl and limestone; Pn – Pannonian marl and silty marl; Q – Loess and other soft deposits

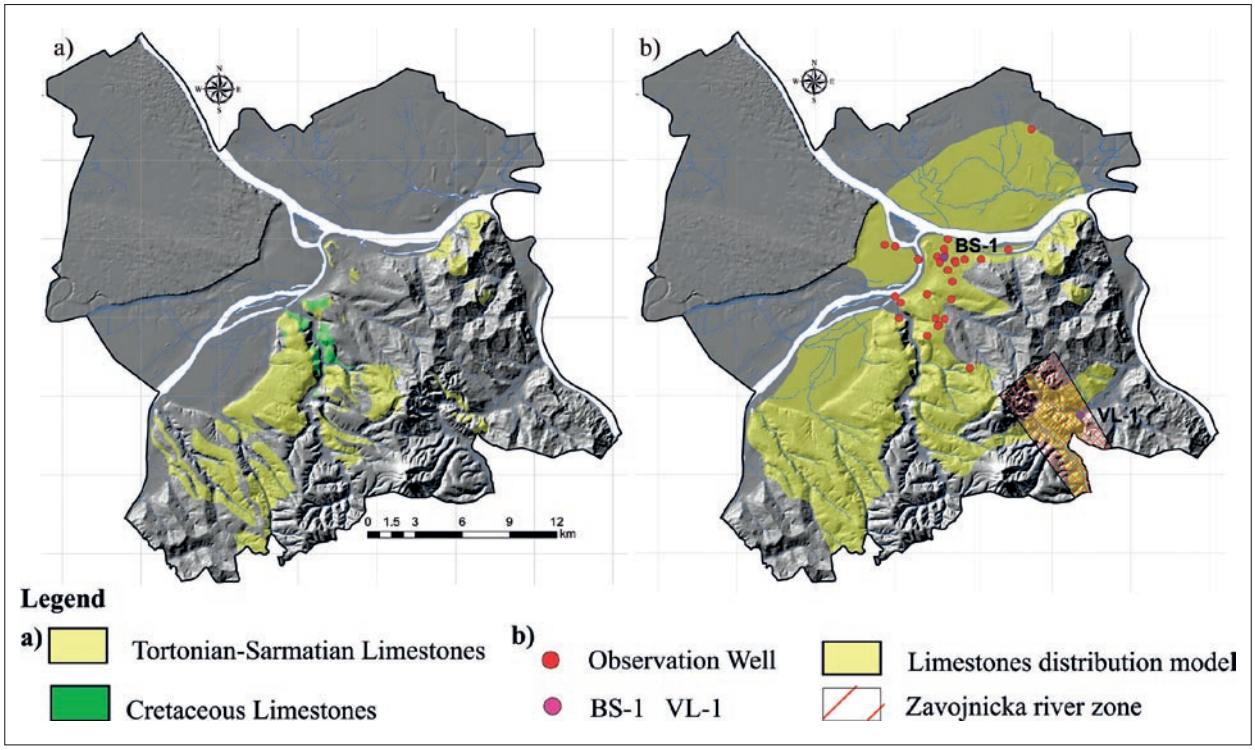

Fig. 5: a) Surface development of limestone. b) Conceptual model of assumed distribution of karst aquifer in Belgrade area (Vranjes 2012).

- annual precipitation amount

in urban areas there is 5–10% more precipititation on yearly basis than in rural areas, and in the course of a single shower there is 30% more precipitation in the city than in its rural areas. (Marsalek *et al.* 2007)

Karst waters are characterized by a stable temperature and chemical regime. The reason for this is depth to the groundwater level, which is over 15 m (deep aquifer water levels, which can reach depths up to 60 m, are typical of Urgon age limestone) and slower water exchange.

The dominant form of karst aquifer discharge is by production wells. Groundwater temperatures and well yield within the karst aquifer are shown in Tab. 2.

GEOTHERMAL POTENTIAL OF KARST WATER IN BELGRADE AREA

Up to now the use of karst water resources has been quite limited. The sources of water supply for the city of Belgrade were formed in alluvial deposits of the Sava, and the only purpose of the karst water was for the production of beer and soft drinks. Nowadays, the industrial production of beer and soft drinks is significantly reduced, half of the plant is closed, and the organized exploitation of the karst water almost does not exist.

With the development of heat pump technology new possibilities for the use of groundwater resources are opened. Heat pumps are devices that provide heat exchange, namely they subtract heat from one medium to add it to another one and vice versa. The working principle of a heat pump is based on the following: the fluid from which heat is substracted is led to the evaporating side of the device, while the fluid to which the heat is delivered is led to the condenser of the device.

Energy potential of groundwater resources and its applicability in heat pump systems are defined by three factors: groundwater yield, groundwater temperature and chemism of groundwater. Thermal power source of groundwater is directly dependent on the amounts, the specific heat of water and temperature reductions that can be achieved in a heat pump, thus the temperature of resources does not exceed the freezing point.

Dependence is expressed by the following equation

$$E = C_p \times Q \times \Delta T \quad (1)$$

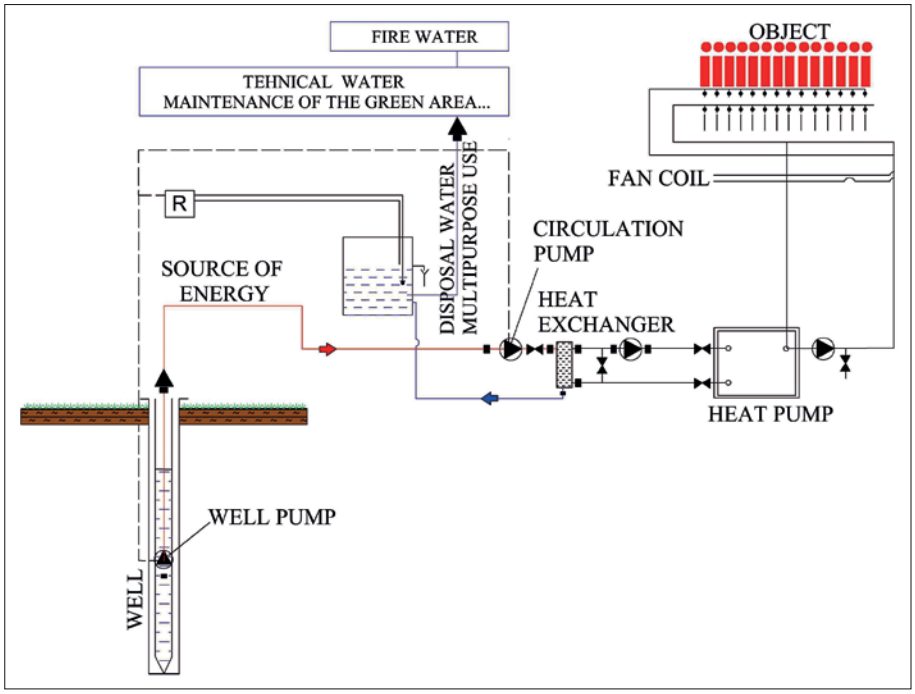

Fig. 6: Schematic view of multi-purpose utilisation of groundwater.

E – available nominal power (kW)

C_p – specific heat of water (constant, 4.2 KJ/kg/°C)

Q – yield of wells (kg/s, the same as l/s)

ΔT – temperature reduction which can be achieved in a heat pump (up to 5 °C)

The calculation of available thermal power of karst water in the urban city area was made based on the results of hydrogeological research. The mean temperature of karst water (17 °C) obtained by years of observation of a network of wells and piezometers (Tab. 2) was used in calculation. Volumes of groundwater included in the calculation of thermal power were defined on the basis of the conceptual model of assumed karst distribution, karst aquifer geometry, effective porosity-estimated value of effective porosity of limestone is at 1% minimum. (Kresic 1997)

According to equation (1) thermal power of karst water in the city area is 47 MW, which is about 2% of the total installed capacity of district heating in the city area, that is 15% of the installed capacity of a heating plant which supplies the central city core parts.

During the exploitation of groundwater for the needs of heating/cooling, it is significant to act in accordance with the principles of optimization and maximum energy efficiency. The increase in the efficiency of the system is achieved by multi-purpose utilisation of groundwater. The scheme of multi-purpose utilisation of groundwater is shown in Fig. 6. Chemism of groundwater affects the sustainability of the designed heating/cooling system significantly, beginning with the exploitation of resources, its application, to the disposition of resources. In developing of a well, the adverse impact of chemistry of groundwater is seen through the occurrences of corrosion or encrustations, which results in the reduction of exploitation, that is absorption capability of the well. The following components: the pH value, the content of iron and manganese, the content of calcium ions, then carbonate, bicarbonate, chloride, gases, water hardness, and mineralization affect the selection of materials, thermo-technical equipment, heat exchangers and heat pumps.

In Belgrade, hydrogeothermal energy is mostly used for heating/cooling of residential buildings. In recent years, the policy of geothermal energy use in public buildings such as educational institutions (schools) and institutions of social care (kindergartens) has been successfully implemented. The scheme of thermotechnical facilities installed in a building where mentally disordered people reside is presented in Fig. 7.

The building is located in the central part of the city. Its surface is 2500 m^2. Three reversible heat pumps water-water, with the heating capacities of $Q_{gr.}$ = 40.3/60.5 kW, electric power of $P_{el.hl.}/P_{el.gr.}$ = 8/13.4 kW, the coefficient of efficiency COP = 4.52, and the ratio of energy efficiency EER = 5.04 have been installed in the building. Each heat pump has its heat exchanger, rated at 47 kW capacity. The heat exchanger type is: LPM-LSL1 – 40, the primary fluid in the heat exchanger is 16 °C/8 °C, and the secondary 4 °C/ 8 °C.

For the purpose of providing resources a production well was developed. The well was developed in Sarmatian limestone. The depth of the well is 100 m, the

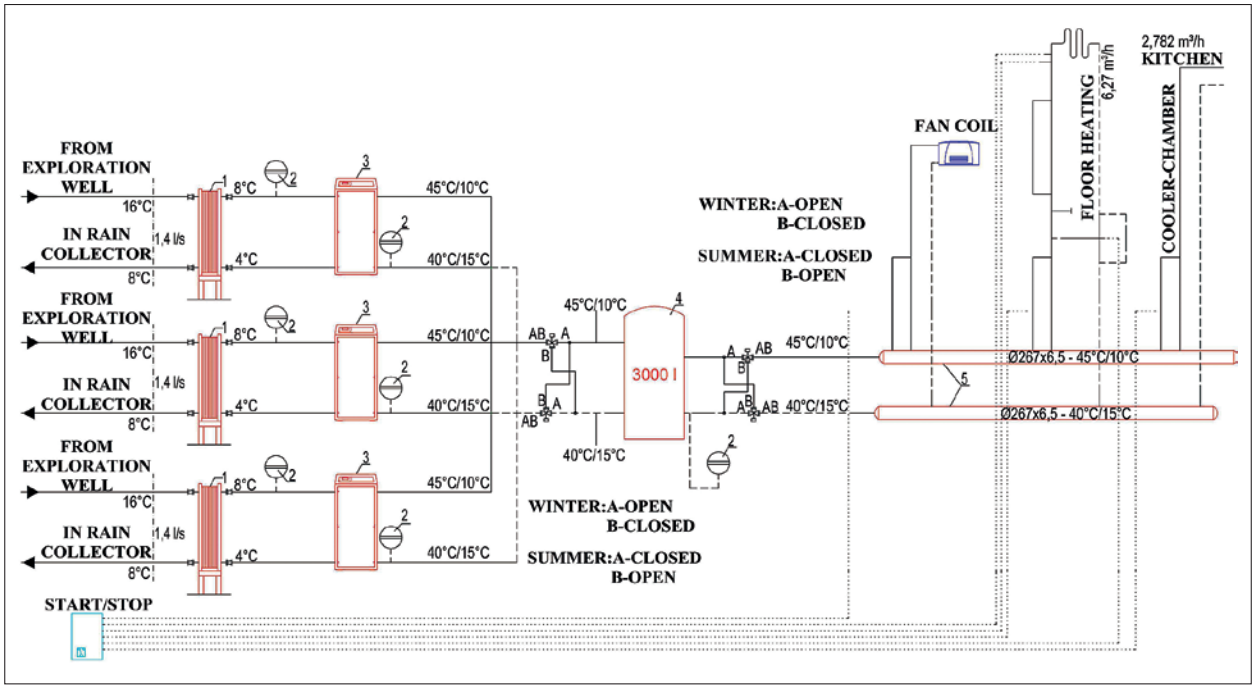

Fig. 7: Scheme of thermotechnical installations of building in central part of city (modified from Slavica 2012). 1-Heat Exchanger; 2-Closed membran expansion tank; 3-Heat pump; 4-Buffer hot water; 5-Splitter/Collector.

yield 6 l/s, and the groundwater temperature is 16 °C. The well is equipped with a well pump with the capacity of 5.5 l/s for the lift height of H = 60 m. The power of the pump motor is 7. 5 kW.

Groundwater with the temperature of 16 °C flows from a well to a heat exchanger, where the heat is exchanged. The temperature of well water drops to 8 °C and then the water runs to the rain collector.

PROBLEMS OF SUSTAINABLE UTILISATION OF GEOTHERMAL RESOURCES IN URBAN AREAS

The exploitation of geothermal resources in the concept of air conditioning of facilities should be conducted in a manner that does not threaten groundwater reserves, in terms of quantity and quality. Likewise, the disposition or disposal of "energy utilized" groundwater should be conducted in a manner that does not threaten surface and ground waters in terms of quantity and quality. Generally, there are three ways of dispositioning the groundwater: letting it flow into open recipients (rivers, canals), letting it flow into closed recipients (rain collectors, sewage system), bringing it back to the aquifer (infiltration, injection well). In urban areas two most common ways of the groundwater disposal are letting it flow into rain collectors or injection of the groundwater into the aquifer via injection wells.

The increase in the share of geothermal energy in the total energy balance of the city carries the potential risk of endangering resources and causing offensive state of karst water. A negative effect on the groundwater may be due to:

Exploitation of resources beyond legally prescribed conditions. The failure to comply with legal procedures in the research stage and then in the stage of groundwater exploitation implies the lack of compulsory design and accompanying technical documentation. Project solutions and conditions of groundwater exploitation developed by experts are provided by project documentation, whereby conditions for sustainable use and monitoring of groundwater are achieved.

Uncontrolled exploitation of resources, most frequently by unqualified persons. Practice has shown that with an increasing number of facilities using geothermal energy in the Belgrade area, the number of unqualified persons responsible for protecting resources has also increased, thus problems both in the phase of the drilling of wells in the karst environment, as well as in the exploitation

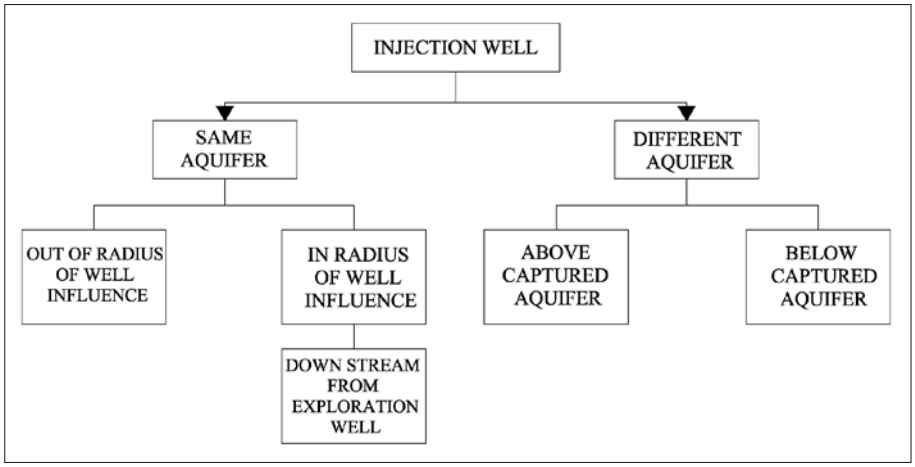

Fig. 8: Flowchart of different solutions for injection well.

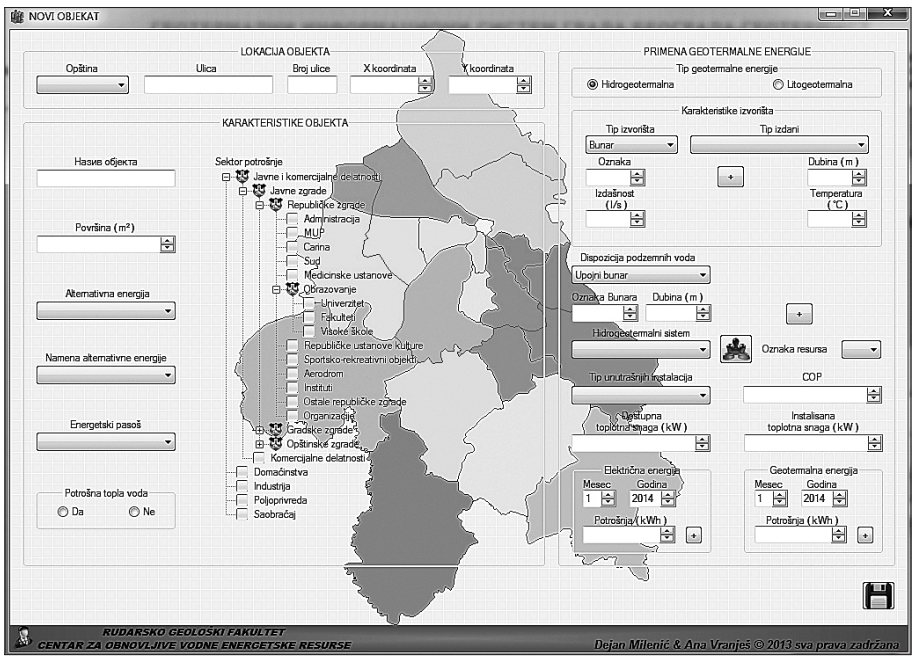

Fig. 9: Appearance of the main window of geothermal information database Geothermist.

phase arise. Unsuccessful drilling of a well poses a risk to groundwater contamination. During exploitation, due to neglecting of legally prescribed research procedures on a well (pumping tests and conducting of chemical analysis, as well as monitoring changes in temperature and groundwater levels) overexploration of wells, changes in water chemistry, and therefore the failure of the entire system, occur.

Uncontrolled disposal of groundwater after running through heat pump system. Disposal of "energy utilized" karst water in the urban environment is a complex engineering requirement, with regard to that natural temperature conditions are altered as a result of a "poorly" designed system of restoring resources to the aquifer. Restricted availability of free surfaces (land occupancy by constructed facilities) is a limitation occurring in urban areas in designing of injection wells. In Fig. 8, there is shown the flowchart of variant solutions for groundwater disposal to the aquifer via the injection well.

With the aim of preventing the aforementioned negative consequences, the Geothermal Information Database (Milenic & Vranjes 2013), called *Geothermist* was built up for the area of Belgrade. The basic aim of establishing of an information database is the systematization and categorization of geothermal research data, in order to activate mechanisms for sustainable management of geothermal resource utilisation in the city. In Fig. 9, there is shown the layout of the main window for data entry.

CONCLUSION

The assessment of the geothermal potentiality of the terrain from the point of view of energy evaluation and possibilities of the exploitation of karst water resources was carried out in the area of Belgrade. In the research process, an analysis of geological setting of the field was carried out, and hydrogeological characteristics of the field, as well as geothermal indicators in the city area perceived. Based on the results of the analysis, a conceptual model of the assumed distribution of the karst aquifer was developed. The interpretation of data related to the yield of wells, the temperature and quality of the groundwater was made. The data were classified and used to make maps of isotherms for the city area. After completing all necessary bases, the calculations of thermal power of karst water followed. From the relation between the mean value of groundwater temperature, and the amount and the specific heat of the water it has been calculated that the thermal power from karst groundwater in the urban city area is 47 MW.

Recently there has been an increase in the number of buildings in the city area that use karst water as an energy source for heating/cooling. While designing such systems of climatisation, it is important to follow the principle of optimization and the principle of maximum energy efficiency, and it can be reached by multi-purpose use of the groundwater. In low-temperature climatisation systems, karst groundwater, after it goes through the heat exchanger, and depending on the buliding's needs, may be used for the maintenance of the green area surrounding the building or for the sake of fire protection. And if the quality is good enough, it may be used for the building's water supply and welness and spa purposes.

The problem of sustainable utilization of geothermal resources in urban areas is related to the exploitation conditions and the disposition of the "energy" utilized groundwater. Restrictions in the use and disposition of groundwater in urban areas are related to the degree up to which the field is constructed. Two most common ways of the groundwater disposal in urban areas are letting it flow into a closed recipient (rain collector) or constructing injection wells. The calculation of the optimum distance between the two wells is the greatest challenge in forming the doublets. An inadequately designed injection well, regarding its position in relation to the exploitation well, can lead to the change of primary conditions of the system functioning, in form of hydraulic feedback and thermal feedback. The sustainability of such systems is only possible with proper management mechanisms. Uncontrolled exploitation of karst resources in terms of the overexploitation of resources, or the system development without the design documentation, endangers the resource from the aspects of both amount and quality.

REFERENCES

Cermak, V. & L. Rybach (eds.), 1979: *Terrestrial Heat Flow in Europe*, Springer Verlag, pp. 328, Berlin.

Cukovic Ignjatovic, N., 2009: *Problems of Front Cover Treatment in Contemporay Approach to Building Alteration*, Master's thesis, University of Belgrade, Faculty of Architecture.

Dokmanovic, P., 1997: *Hydrogeological Characteristics of Tertiary Basins in Serbia south of Sava and Danube*, PhD thesis, University of Belgrade, Faculty of Mining and Geology.

Knezevic, S. & M. Sumar, 1994: Contribution to Geology Knowledge of City of Belgrade.-Annales géologiques de la péninsule Balkanique, 58, 2, 73–81.

Kresic, N., 1997: *Hydrogeology and groundwater modeling,* CRC, pp. 363, Florida.

Marsalek, J., Jienez-Cisneros, B., Karamouz, M., Malmquist, P.A., Goldenfum, J. & B. Chocat, 2007: *Urban Water Cycle Processes and Interactions*, Urban Water Series–UNESCO-IHP, pp. 131, Paris.

Milenic, D. & A. Vranjes, 2013: Geothermist, Geothermal information database of Belgrade city area, Licensed software, University of Belgrade, Faculty of Mining and Geology, Belgrade

Milivojevic, M., 1982: *Paleohydrogeothermal Occurrences of Avala*, University of Belgrade, Faculty of Minig and Geology, pp. 203, Belgrade.

Milivojevic, M., 1989: *Evaluation of Geothermal Resources of Territory of Serbia without Autonomous Provinces*, PhD thesis, Univesity of Belgrade, Faculty of Minig and Geology, Belgrade.

Rundic, Lj., Ganic, M., Knezevic, S. & A. Soliman, 2011: Upper Miocene Pannonian sediments from Belgrade (Serbia): new evidence and paleoenvironmental considerations.- Geologica Carpathica, 62, 3, 267–278.

Santamouris, M., 2007: Energy in Buildings and Citizenship, *Proceedings of 38 International congress on heating, cooling and air conditioning*, 5th–7th December 2007, Belgrade, 13–26, Belgrade.

Slavica, V., 2012: *Main Design of thermotechnical instalation, Institution for the casual and temporary residence "Predah" with the necessary facilities, Shakespeare street, Belgrade*, project reports, Institute of Transportation, CIP.

Unkasevic, M., 1994: *Climate of Belgrade*, Scientific book, Belgrade.

Vranjes, A., 2012: *Hydrogeothermal resources of the Belgrade city area*, PhD thesis, University of Belgrade, Faculty of Mining and Geology, pp. 617.

COBISS: 1.01

AN ADVECTION–DILUTION MODEL TO ESTIMATE CONDUIT GEOMETRY AND FLOW

OCENA GEOMETRIJE IN TOKA V KRAŠKIH PREVODNIKIH Z ADVEKCIJSKO RAZREDČITVENIM MODELOM

Guangquan LI[1]* & Hong LIU[1]

Abstract UDC 556.3:551.44

Guangquan Li & Hong Liu: An advection–dilution model to estimate conduit geometry and flow

As conduit water carries pollutants introduced from a point recharge downgradient, a contaminant-free seepage from the surrounding limestone is added into the conduit water and actively dilutes the pollutants. In this study, the transport with advection and this active dilution but no dispersion, is solved using the method of characteristics. The complete solution considering initial condition, boundary condition, and production is presented. Scale analysis reveals that the model is applicable when injection of pollutants at sinkholes persists long enough but unsuitable for analysis of dye tracing experiments. An approach combining the model with dye tracing experiment is used to quickly estimate the geometry and flow of a major conduit from Ames Sink to Wakulla Spring, Northwest Florida.

Key words: karst conduit, dilution, method of characteristics, breakthrough curve.

Izvleček UDK 556.3:551.44

Guangquan Li & Hong Liu: Ocena geometrije in toka v kraških prevodnikih z advekcijsko razredčitvenim modelom

V članku predstavimo model advekcijskega prenosa točkovno injiciranega sledila skozi kraški prevodnik, ob upoštevanju razredčenja zaradi dotoka sveže vode iz okoliškega masiva. Disperzije ne upoštevamo. Diferencialno enačbo z robnimi in začetnimi pogoji, rešimo analitično z metodo metodo karakteristik. Analiza velikostnih redov pokaže, da je model uporaben pri dolgotrajnem vnosu sledila, manj primeren pa pri analizi sledilnih poskusov. V članku prikažemo uporabo modela v kombinaciji s sledilnim poskusom pri oceni geometrije in pretoka v kraškem prevodniku med ponorom Ames in izvirom Wakulla na severovzhodnem delu Floride.

Ključne besede: kraški prevodnik, razredčenje, metoda karakteristik, prebojna krivulja.

INTRODUCTION

A karst aquifer is featured with interconnected solution caves or conduits which provide preferential pathways for groundwater flow and contaminant migration (Shuster & White 1971; Kiraly 1998). Transport of contaminants in karst aquifers is driven by a fast turbulent flow in cavernous conduits as well as a very slow laminar flow in the limestone matrix (including small pores, fissures and fractures). These dual flows are the most distinct feature of karst aquifers, and thus contaminant migration in the aquifers has two completely different time scales. Contaminants entering the aquifers from sinkholes with point recharges flush through the conduits after days to weeks, while pollutants seeping downward with non-point recharges via the surface reside in the aquifers for tens of years (Even *et al.* 1986).

[1] International Joint Research Center for Karstology, Yunnan University, 5 Xueyun Rd., Kunming, Yunnan 650223, China, e-mail: guangquanli74@gmail.com (Guangquan LI), hongliu@ynu.edu.cn (Hong LIU)

Received/Prejeto: 18.04.2013

During a storm event, the head in a conduit may exceed the head in the matrix, such that water and contaminants are emplaced from the conduit into the matrix, which later get released back into the conduit when the pressure difference between the conduit and the matrix becomes reversed. That scenario has been discussed by Field (1993) and Li *et al.* (2008). In this paper, we shall only discuss an ordinary hydrogeologic condition in which contaminant-free water is driven from the matrix into a conduit and actively dilutes pollutants introduced from a sinkhole or doline. Water seeping from the matrix into conduits is typically slow and pollutant-free, as the potential contaminants have enough time to experience adsorption by rock minerals as well as decomposition by bacteria. In contrast, pollutants entering from sinkholes, dolines, swallow holes, grikes, etc. have much less time and available surface area for such physical adsorption or biochemical reactions (Field & Pinsky 2000), and can therefore contaminate the aquifer to a large extent in a short period.

Decrease of contaminant concentration in a conduit is caused by three primary mechanisms: a passive decrease induced by hydrodynamic dispersion in the conduit (Taylor 1954), a passive retention/release between mobile– and immobile–water regions, and an active dilution by the matrix seepage. There is significant prior work regarding transport in a karst conduit. An advection–dispersion equation with a supplemental equation accounting for retention in immobile–water regions has been developed by Toride *et al.* (1993) to describe transport in soils and was first introduced by Field & Pinsky (2000) to transport in a single conduit. The model is called 2RNE (two–region non–equilibrium). The weakness of that model includes –1) it requires specifying fitting parameters such as an exchange coefficient between mobile– and immobile–water regions; 2) water exchange between the conduit and the surrounding matrix is not considered such that conduit flow was assumed to have a constant velocity. Despite these disadvantages, the 2RNE is widely used for analysis of transport in karst conduits, because retention/release was well modeled and it can successfully reproduce the often–observed strong skewness in spring breakthrough curves, e.g., Field & Li (2011). Birk *et al.* (2006) used a hybrid method (with MODFLOW and the Darcy–Weisbach equation to simulate matrix seepage and conduit flow, respectively) to model the discharge response and the breakthrough curve at a spring. In that scenario, water entering the sinkhole is solute-free, while water released from the matrix is rich in Calcium. Using the method of characteristics, Li (2009) derived an analytical solution for the case where the seepage flow from the matrix carries solutes into a conduit, being diluted by a solute-free sinkhole flow. Li & Loper (2011) developed a new model in which advection, dilution and dispersion were included, sought an approximate analytical solution for the initial–value problem, and successfully simulated a dye tracing experiment performed by Davies *et al.* (2004) between Ames Sink and Indian Spring, Northwest Florida. Later, Li (2011) used transform of variables to obtain the solution for the initial-value problem as well as the solution for the boundary-value problem of that model. In this paper, we are interested with a simple transport model that can be used to quickly estimate geometry and flow of a conduit.

In our conceptual model, contaminant enters a conduit with the sinkhole recharge, is diluted by the uncontaminated seepage released from the surrounding limestone, and eventually is transported to a spring. (Dissolved minerals and decomposed organic matters from the matrix into the conduit will be considered afterward in this paper). We firstly construct the mathematical model and present its solution by intentionally neglecting conduit dispersion. Secondly, an approach is used to estimate the geometry and flow of a major conduit in the Woodville Karst Plain, Northwest Florida. Thirdly, the role of conduit dispersion is analyzed and a sufficient condition for applying the advection-dilution model is offered.

ADVECTION–DILUTION IN A CONDUIT

THE GOVERNING EQUATION

The essential features of the advection–dilution in a conduit may be described using a relatively simple one–dimensional equation. Ignoring longitudinal dispersion and assuming zero production (i.e., no contaminant enters the conduit from the matrix), solute mass conservation requires:

$$\frac{\partial C}{\partial t} + \frac{\partial}{\partial z}[W(z)C] = 0, \tag{1}$$

where C [M/L^3] is the solute concentration in the conduit (averaged over the cross–sectional area), W [L/T] is the speed of conduit water averaged over the conduit cross-section, z [L] is the distance downstream from the

sinkhole, and t [T] is time. Assuming a circular conduit with constant radius a [L] and a constant specific flux q [L/T] of water entering the conduit from the matrix, the velocity of conduit flow is increased in the downstream direction according to water mass conservation, i.e.,

$$W(z) = W_0 + \frac{z}{\tau}, \tag{2}$$

where W_0 is the averaged speed at the sinkhole ($z = 0$) and

$$\tau = \frac{a}{2q}. \tag{3}$$

The conduit domain is $0 \le z \le Z$, where Z is the downstream location of the spring. Equation differs from the traditional advection–dispersion equation in that it neglects dispersion but incorporates the specific water flux q, which causes active dilution. The linear increase of velocity with downstream position z is due to the addition of matrix water uniformly (assumed) into the conduit. Equation (2) does not contradict the Darcy-Weisbach equation. Combining Equation (2) with the Darcy–Weisbach equation would yield a non–linear pressure distribution along the conduit that is possible. If the seepage flux q is set to zero, the flow velocity along the conduit would be a constant and the pressure would degenerate into a linear distribution.

Equation (1) is a first–order partial differential equation, the solution of which requires specifying an initial condition in the conduit, i.e.,

$$C(z,0) = C_I(z), \text{ for } z \ge 0, \tag{4}$$

and a boundary condition at the conduit entrance, i.e.,

$$C(0,t) = C_B(t), \text{ for } t \ge 0. \tag{5}$$

ANALYTICAL SOLUTION USING METHOD OF CHARACTERISTICS

Substituting Equation (2) into (1) yields a first–order wave equation with the characteristic equation (Strauss 1992) being

$$\frac{dz}{z + W_0\tau} = \frac{dt}{\tau} = -\frac{dC}{C}. \tag{6}$$

The characteristic curves, plotted in Fig. 1, are obtained by integrating the first two terms of Equation (6) and expressed as

$$z + W_0\tau = W_0\tau e^{(t-\eta)/\tau}, \tag{7}$$

where η is a constant of integration that represents the intersection of the curves at the t axis. From the Lagrangian viewpoint, the characteristic is the displacement–time curve for fluid particle, and thus according to (7), $\left.\frac{dz}{dt}\right|_{z=0} = W_0$, which is correct because fluid particle at the conduit entrance has the speed W_0.

The characteristics fill the first quadrant of the z–t plane as η varies from $-\infty$ to ∞. The characteristic for $\eta = 0$ passes through the points (0, 0) and (Z, T) where

$$T = \tau \ln\left(\frac{Z}{W_0\tau} + 1\right) \tag{8}$$

is the travel time for fluid particle to reach the spring from the sinkhole. This characteristic divides the first quadrant of the z–t plane into two domains. Characteristics in domain B, having $\eta < 0$, intersect the line $z = 0$, $t > 0$ and solutions in this domain satisfy the boundary condition, while characteristics in domain I, having $\eta < 0$, intersect the line $z > 0$, $t = 0$ and solutions in this

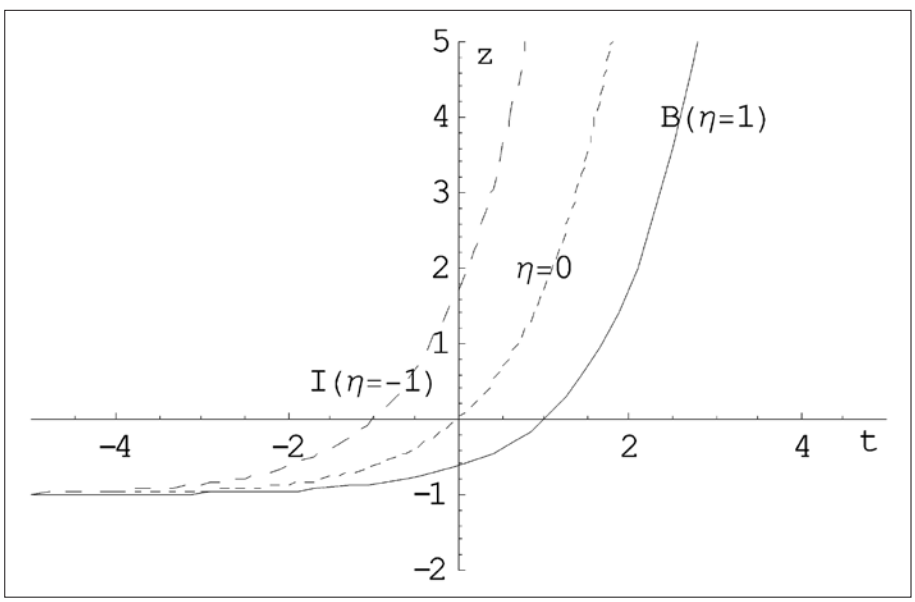

Fig. 1: Characteristic curves, $z + W_0\tau = W_0\tau e^{(t-\eta)/\tau}$. As η changes, the curves fill the first quadrant of the plane. I and B denote the domains determined by the initial condition and the boundary condition, respectively.

domain satisfy the initial condition. The characteristics have positive slope, so that as time goes on, progressively more solute concentration in the conduit is determined by the solution having characteristics in domain B.

The two families of solutions applicable in the two domains are easily obtained from Equation (6). Integrating the second and third terms of Equation (6) yields a family of solutions satisfying the initial condition, while the second family of solutions is obtained by integrating the first and third terms of that equation and satisfying the boundary condition. The combined solution is expressed as (see Appendix A for detailed derivation):

$$C(z,t)=C_I((z+W_0\tau)e^{-t/\tau}-W_0\tau)e^{-t/\tau}, \text{ in domain I.} \quad (9a)$$

$$C(z,t)=C_B\left(t-\tau\ln\left(\frac{z}{W_0\tau}+1\right)\right)\frac{W_0\tau}{W_0\tau+z}, \text{ in domain B.} \quad (9b)$$

For $t < T$, the solute concentration at the spring ($z = Z$) is determined by the initial condition, while for $t > T$, the concentration is determined by the boundary condition.

It is interesting to explore the physical meaning of Equation (9). Similar to Equation (8), the travel time for fluid particle to reach the downstream location z from the conduit entrance is $\tau\ln\left(\frac{z}{W_0\tau}+1\right)$. Therefore, $C_B\left(t-\tau\ln\left(\frac{z}{W_0\tau}+1\right)\right)$ in Equation (9b) represents the solute concentration of the sinkhole flow at time $t-\tau\ln\left(\frac{z}{W_0\tau}+1\right)$.

For Equation (9a), supposing the fluid particle reaching z at time t starts from downstream location z^*, the traveling time from z^* to z will be $\tau\ln\left(\frac{z+W_0\tau}{z^*+W_0\tau}\right)$. This time is equal to t, from which we get $z^* = (z + W_0\tau)e^{-t/\tau}-W_0\tau$ that appears in Equation (9a). This is the starting position of fluid particle in the conduit that will reach z at time t. To facilitate understanding the exponential term in Equation (9a), we need to rewrite the formula for z^* into $\frac{z^*+W_0\tau}{z+W_0\tau}=e^{-t/\tau}$. Using Equation (2), this equation can be further rewritten as $\frac{W(z^*)}{W(z)}=e^{-t/\tau}$, the left side of which represents exactly the ratio of the contaminated water at z^* diluted by the side seepage from z^* through z.

The solution presented in Equation (9) assumes that water entering the conduit from the matrix contains no solute. The case where the matrix water contains solute is a production-value problem, which has been analytically solved by Li (2009). The general problem in which solute can preexist in the conduit (the initial-value problem), can enter the conduit from the sinkhole (the boundary-value problem), and can release from the matrix into the conduit (the production-value problem), is a superposition of these three problems, because the governing equation is linear with respect to concentration. The complete solution is listed in Appendix B.

EXAMPLES

This section contains two simple solutions illustrating the behavior of the breakthrough curves generated at the spring ($z = Z$) from two classes of initial and boundary conditions.

STEP INITIAL CONDITION AND ZERO BOUNDARY CONDITION

In this case, the initial concentration of solute in the conduit is assumed to be a step function, i.e.,

$$C_I(z)=\begin{cases}0 & 0\le z<z_1\\ C_0 & z_1\le z<z_2,\\ 0 & z_2\le z<Z\end{cases} \quad (10)$$

and water entering the conduit at the sinkhole contains no solute: $C_B(t) = 0$. Equation (10) is an idealization of contaminant hotspot. Substituting Equation (10) into (9) and evaluating the result at the spring yields

$$C(Z,t)=\begin{cases}0 & 0\le t<t_2\\ C_0e^{-t/\tau} & t_2\le t<t_1,\\ 0 & t_1<t\end{cases} \quad (11)$$

where

$$t_i=\tau\ln\left(\frac{Z+W_0\tau}{z_i+W_0\tau}\right), \quad (12)$$

for i = 1, 2. This breakthrough curve is plotted in Fig. 2. Water containing solute that is initially at $z = z_2$ arrives at the spring first and is relatively undiluted, while water that travels farther experiences greater dilution, so that the concentration at the spring decays with time. Since longitudinal dispersion has been ignored, there is no spreading in the breakthrough curve.

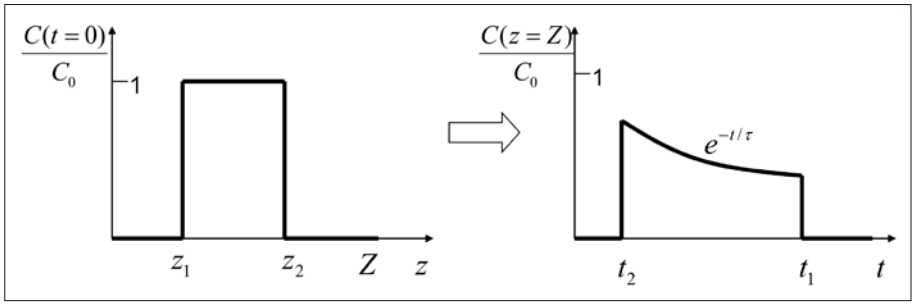

Fig. 2: Spring breakthrough curve generated by solute hotspot preexisting in a conduit (no solute enters from the sinkhole).

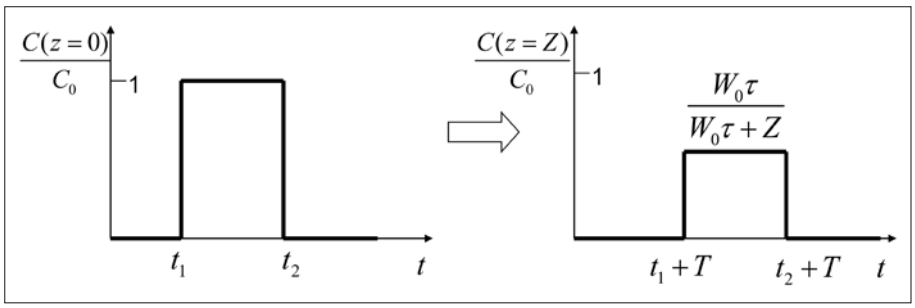

Fig. 3: Spring breakthrough curve generated by a rectangular pulse of solute introduced from the sinkhole (the conduit is initially solute-free).

ZERO INITIAL CONDITION AND STEP BOUNDARY CONDITION

In this case, the conduit initially contains no solute, i.e., $C_I(z) = 0$, and a pulse of solute enters the conduit at the sinkhole uniformly over a prescribed interval of time:

$$C_B(t)=\begin{cases}0 & 0\le t<t_1\\ C_0 & t_1\le t<t_2.\\ 0 & t_2\le t\end{cases} \tag{13}$$

Substituting Equation (13) into (9) yields

$$C(t,Z)=\begin{cases}0 & t\le T<+t_2\\ C_0\dfrac{W_0\tau}{Z+W_0\tau} & T+t_1\le t<T+t_2,\\ 0 & T+t_2\le t\end{cases} \tag{14}$$

where T is given by (8). As can be seen in Fig. 3, this breakthrough curve is the result of a simple binary mixing between conduit water and matrix water. **In contrast** to the first example, the solute concentration at the spring is constant.

APPLICATION AND LIMITATION

This section focuses on the extraction of information regarding geometry and flow of a conduit from analysis of the breakthrough curve, employing the solution developed above.

Referring to the solution in Equation (14) and to Fig. 3, the peak concentration of solute at the spring, C_P, relative to that entering at the sinkhole is given by

$$\frac{W_0\tau}{Z+W_0\tau}=\frac{C_p}{C_0}=\frac{Q_0}{Q_S}, \tag{15}$$

where Q_0 and Q_S are the water fluxes at the sinkhole and the spring, respectively.

Substituting Equation (15) into (8), it follows that

$$\tau=\frac{T}{\ln(Q_S/Q_0)}. \tag{16}$$

Substituting Equation (16) into (3) gives

$$q=\frac{a}{2T}\ln\left(\frac{Q_S}{Q_0}\right), \tag{17}$$

which can be used to estimate the specific seepage from the matrix into the conduit. On a related note, it is necessary to know the travel time T. Noting $W_0=\frac{Q_0}{\pi a^2}$, Equations (15) and (16) may be combined to estimate the conduit length:

$$Z=\frac{(Q_S-Q_0)\,T}{\pi a^2\ln(Q_S/Q_0)}. \tag{18}$$

There are two ways to get the ratio C_p/C_0, or Q_0/Q_S. The first is to chemically measure the peak concentration of a long-persisting tracer rich in surface water but

devoid in matrix water, while the second is to physically measure the water fluxes at the sinkhole and spring. The travel time T from sinkhole to spring can be measured by a dye tracing experiment. Thus these two quantities can be entered into the model to calculate the seepage flux and the conduit length via Equations (17) and (18), respectively. This approach does not require dealing with dispersion.

A REAL WORLD EXAMPLE

The results given above can be applied to extract information about conduit geometry and flow. To demonstrate this, a dye tracing experiment conducted by Davies *et al.* (2004) in the Woodville Karst Plain, Northwest Florida, USA, is chosen. Conduits in this plain are phreatic, as the plain is very close to the coast of the Gulf of Mexico. In the dye tracing experiment, dye traveled from Ames Sink to Wakulla Spring, for a straight-line distance of 9.3 km after 528 hours (Davies *et al.* 2004). Allowing for an estimated tortuosity 1.3 (Li 2012), the actual traveling distance is approximately 12 km. The conduit radius ranges from 1 to 15 m and the spring discharge ranges from 5 to 20 m^3/s (Davies *et al.* 2004). The recharge to Ames Sink is estimated to be 0.01 m^3/s (Kincaid 2004). Thus the conduit radius and matrix seepage are calculated through Equations (17) and (18); see Tab. 1.

Essentially, this approach to estimate the parameters of a conduit inputs the time of the peak concentration on the breakthrough curve from dye tracing experiment into our advection-dilution model. (The peak amplitude on the breakthrough curve from dye tracing experiment can never be used into our model, for conduit dispersion invariably decreases it significantly). This approach is based upon the fact that the time of the peak concentration is not sensitive to dispersion; see Fig. 2, Li & Loper (2011).

*Tab. 1: Parameters of geometry and flow of the major conduit from Ames Sink to Wakulla Spring, Northwest Florida. Numbers with * present calculated values.*

Parameter	Value		Units
	Uniform conduit	Two segments	
Conduit length, Z	12	12	km
Travel time, T	528	528	hour
Spring discharge, Q_S	10	10	m^3/s
Water flux at sinkhole, Q_0	0.01	0.01	m^3/s
Conduit radius, a	8.54*	7.54*, 10.8*	m
Specific water flux across wall, q	0.0155*	0.0145*	mm/s

To test validation of the uniform-conduit assumption, we now divide the conduit into two segments with different radius. Assume the radius radio between the upstream segment and the downstream segment, $k = 0.7$, we use the transport time in the whole conduit T, the total length of the conduit Z, the sinkhole recharge Q_0 and the spring discharge Q_S, to calculate the radius of the upstream segment and the velocity of the seepage from matrix into conduit (refer to Appendix C). The result is listed also in Tab. 1. With the radius ratio being 0.7, the cross-sectional area of the downstream segment is double that of the upstream segment. Though the cross-section varies significantly, the resulting seepage velocity only changes a little. Therefore, the seepage velocity is not sensitive to the variation of conduit cross-section and the uniform-radius model is reliable.

THE ROLE OF DISPERSION

Releasing a tracer with a step function of time into a sinkhole, the spreading length can be estimated as $\Delta x=8\sqrt{D_c T}$ (see Figure 10.6.1, Bear 1972, p. 628), wherein D_c is dispersion in the conduit. Assuming $D_c \sim aW$ (i.e., conduit dispersivity is scale–variant and of the same order as conduit radius.) and inserting $T \sim Z/W$, it follows that $\Delta x=8\sqrt{aZ}$. Thus the spreading time in the breakthrough curve is $\Delta t=\Delta x/W=8\sqrt{aZ/W}$. This spreading can be neglected when and only when

$$\frac{\Delta t}{\tau_c}=\frac{8\sqrt{aZ}}{W\tau_c}=\frac{8\sqrt{aZ}}{L_p}\ll 1, \tag{19}$$

where τ_c is the duration of injection, and $L_p = W\tau_c$ is the length scale of the plume. Therefore, as the conduit length Z increases, dispersion shall not be ignorable. Only for release of a long solute pulse (large τ_c) at the sinkhole, or very small a or Z, conduit dispersion may be neglected.

The Peclet number is defined as $P_e=\frac{WZ}{D_c}\sim\frac{Z}{a}$, being widely used to quantify the ratio between advection and dispersion at a certain distance (Bear 1972). It is worth noting that a large Peclet number only states that dispersion may be neglected at that distance, but in no way necessarily assures that dispersion can be ignored in the transport process from the sinkhole to the spring. Taking dye tracing experiments as example, it is not recommended to neglect dispersion. Inequality (19) suggests how long the solute should last (or how short the domain should be) such that the above dispersion–free model can behave well.

Inequality (19) can be rewritten as

$$\frac{\Delta t}{\tau_c}=\frac{8Z}{L_p}\left(\frac{1}{\sqrt{P_e}}\right)\ll 1. \tag{20}$$

Supposing $L_p \leq Z$, it is evident that only at very large Peclet number (i.e., $P_e \geq 10000$), dispersion can be neglected with respect to advection. This value is far larger than any Peclet numbers ever observed for conduit flows in karstic aquifers. Therefore, it is concluded that our model is generally not applicable to transport in a real conduit. The only hope for application of this model is under an extreme condition that the duration of solute injection must be very long, or equivalently $L_p \gg Z$. As a reminder, the above condition is a very conservative (sufficient) one, because it is based upon a rectangular tracer pulse injected at sinkhole. In practice, a natural solute at sinkhole may have a much more gradual shape, rather than a sharp rectangle, which has been analyzed in Li *et al.* (2010).

DISCUSSION

Conduit flow in a karst aquifer is often a combination of water entering at a sinkhole or doline and water released from the surrounding limestone matrix. Contaminants can enter a conduit with the sinkhole recharge and will be diluted by the uncontaminated seepage from the matrix. This advection–dilution process has been solved analytically using the method of characteristics and the solution is presented in Equation (9). Without conduit dispersion, there is no spreading in the shape of spring breakthrough curves; see Fig. 2 and 3.

The issue whether dispersion can be neglected or not depends on whether it is evaluated locally or globally. The former refers to solute transporting over a length scale of the solute plume, while the latter refers to solute transporting over the conduit length. The latter is more rigorous than the former. Li *et al.* (2010) analyzed the former and got $\frac{a}{L_p} \ll 1$, as a sufficient and necessary condition for neglecting dispersion locally. That inequality can be rewritten as $\frac{Z}{L_p}\left(\frac{1}{P_e}\right) \ll 1$, being more accurate than the traditional condition, $\frac{1}{P_e} \ll 1$. In this paper we are further concerned with the global ignorability of dispersion (a stricter condition), and inequality (19) is offered as a sufficient criteria for assessment of the applicability of the model in this paper.

Numerical simulation often suffers from a notorious problem that it cannot accurately simulate the transport of contaminant plume near the sharp edge of the plume. This is because when the Peclet number is large, dispersion is small with respect to advection, such that undesired numerical dispersion will become dominant to decrease the accuracy of numerical solutions, even causing unphysical numerical oscillations. In that case, very fine grids would have to be adopted to guarantee a small cell Reynolds number (Thomas 1995) such that a realistic solution can be obtained. Sun (1989) has drawn a similar conclusion that when dispersion is very small, it is better to adopt particle–tracking method (ignoring dispersion) to simulate transport.

CONCLUSIONS

In this paper, an analytical solution to dilution of a conservative contaminant in a conduit due to water infiltrating from the surrounding limestone (referred to as seepage) is presented. The main assumptions involved in the model include –1) there is negligible dispersive transport in the conduit; 2) the conduit radius is uniform along the conduit; and 3) the seepage rate across the wall is uniform along the conduit. The first assumption limits the applicability of the model (e.g., unsuitable for dye tracing experiments in which dye is injected instantaneously so that τ_c is too small to satisfy inequality (19)). Nevertheless, the model may be applicable to the case that contaminant is naturally introduced into a conduit by long-duration rainstorm events. The second assumption has been tested to be valid. The effect brought by the third assumption is unclear and may be a good topic for future study.

The solutions presented by Li & Loper (2011) and Li (2011) considered advection, dilution and dispersion, but were approximate solutions. This paper presents the exact solution to a transport model only considering advection and dilution. Therefore, this model may be used as a benchmark. Scale analysis shows that for a rectangular injection at a sinkhole, inequality (19) provides a sufficient condition for neglecting conduit dispersion. Nonetheless, this inequality is conservative

(too restricting) and is not necessary for application of the model to a natural/gradual injection.

The model in this paper is useful mainly in two aspects. 1) The solution provides a useful benchmark to check numerical solutions. That is, numerical solutions of transport in a conduit at the limit of small dispersion (large Peclet number) should converge to the analytical solution expressed by Equation (9). 2) The model can be applied to field study with dye tracer test. As demonstrated, if travel time from sinkhole to spring is measured by a dye tracing experiment and the conduit length, sinkhole recharge and spring discharge are estimated beforehand, then they can be inputted into the model to quickly extract the average conduit radius and seepage velocity, without any needs to deal with dispersion. In the future, we will investigate how the variation of specific seepage affects transport in conduits.

ACKNOWLEDGEMENTS

This research was supported by the National Science Foundation of China under grant 41162008 and grant 41371040. The authors are deeply grateful to an anonymous reviewer and Editor-in-Chief Franci Gabrovšek for their insightful comments and constructive suggestions.

REFERENCES

Bear, J., 1972: Dynamics of Fluids in Porous Medium. New York, Dover, 764 pp.

Birk, S., Liedl, R. & M. Sauter, 2006: Karst spring responses examined by process–based modeling.- Ground Water, 44(6), 832–836, doi: 10.1111/j.1745-6584.2006.00175.x.

Davies, G., Kincaid, T., Hazlett, T., Loper, D., DeHan, R. & C. McKinlay, 2004: Why do quantitative groundwater tracing? Lessons and examples from the Woodville Karst Plain of North Florida. GSA 2004 Denver Annual Meeting, 18, November 7–10, Paper No. 49–22.

Even, H., Magaritz, M. & R. Gerson, 1986: Timing the transport of water through the upper vadose zone in a karstic system above a cave in Israel.- Earth Surface Processes and Landforms, 11, 181–191.

Field, M., 1993: Karst hydrology and chemical contamination.- Journal of Environmental Systems, 22(1), 1–26.

Field, M. & G. Li, 2011: Inversion for the input history of a dye tracing experiment.- Journal of Cave and Karst Studies, 73(1), 16–20, doi: 10.4311/jcks2010es0143.

Field, M. & P. Pinsky, 2000: A two–region nonequilibrium model for solute transport in solution conduits in karstic aquifers.- Journal of Contaminant Hydrology, 44(3–4), 329–351.

Kincaid, T., 2004: Ames Sink Tracer Test. http://www.globalunderwaterexplorers.org/content/ames-sink-tracer-test (accessed November 1, 2012).

Kiraly, L., 1998: Modeling karst aquifers by the combined discrete channel and continuum approach.- Bulletin du. Centre d'Hydrogeologie, 16, 77–98.

Li, G., 2009: Analytical solution of advective mixing in a conduit.- Ground Water, 47(5), 714–722, doi: 10.1111/j.1745-6584.2009.00575.x.

Li, G., 2011: Spatially varying dispersion to model breakthrough curves.- Ground Water, 49(4), 584–592, doi: 10.1111/j.1745–6584.2010.00777.x.

Li, G., 2012: Calculation of karst conduit flow using dye tracing experiments.- Transport in Porous Media, 95(3), 551–562, doi: 10.1007/s11242-012-0061-6.

Li, G., Loper, D. & R. Kung, 2008: Contaminant sequestration in karstic aquifers: Experiments and quantification.- Water Resources Research, 44, W02429, doi:10.1029/2006WR005797.

Li, G. & D. Loper, 2011: Transport, dilution, and dispersion of contaminant in a leaky karst conduit.- Transport in Porous Media, 88(1), 31–43, doi:10.1007/s11242-011-9721-1.

Li, G., Shang, Y. & J. Gao, 2010: Scale analysis of the significance of dispersion in mixing–transport in conduits.- Journal of Cave and Karst Studies, 72(3), 150–155, doi: 10.4311/jcks2009es0106.

Shuster, E. & W. White, 1971: Seasonal fluctuations in the chemistry of limestone springs: A possible means for characterizing carbonate aquifers.- Journal of Hydrology, 14, 93–128.

Strauss, W., 1992: Partial Differential Equations: An Introduction. New York, John Wiley & Sons, 425 pp.

Sun, N., 1989: Mathematical Modeling of Groundwater Pollution. Beijing, The Geological Press of China, 361 pp (in Chinese).

Taylor, G., 1954: The dispersion of matter in turbulent flow through a pipe.- Proceedings of the Royal Society (London) A, 223, 446–468, doi:10.1098/rspa.1954.0130.

Thomas, J., 1995: Numerical Partial Differential Equations. New York, Springer, 436 pp.

Toride, N., Leij, F. & M. van Genuchten, 1993: A comprehensive set of analytical solutions for nonequilibrium solute transport with first–order decay and zero–order production.- Water Resources Research, 29(7), 2167–2182.

APPENDIX A

This appendix contains a detailed derivation of solution (9). From the second and third terms of Equation (6), along the characteristic (refer to Fig. 1) we have

$$\frac{dC(z,t)}{C} = \frac{-dt}{\tau}. \tag{A1}$$

Integrating the two sides of Equation (A1) and using initial condition (4), we get

$$C(z,t)=C(W_0\tau e^{(t-\eta)/\tau}-W_0\tau,t)=C_I(W_0\tau e^{-\eta/\tau}-W_0\tau)e^{-t/\tau}. \tag{A2}$$

Inserting Equation (7) into (A2), it follows that

$$C(z,t)=C_I((z+W_0\tau)e^{-t/\tau}-W_0\tau)e^{-t/\tau}. \tag{A3}$$

Please note that the initial condition requires (see Fig. 1)

$$\eta = t-\tau\ln(\frac{z}{W_0\tau}+1)<0 \tag{A4}$$

On the other hand, from the first and third terms of Equation (6), along the characteristic we have

$$\frac{dC(z,t)}{C} = \frac{-dz}{W_0\tau+z}. \tag{A5}$$

Integrating the two sides of Equation (A5) and using boundary condition (5) yield

$$C(z,t) = C(z,\eta+\tau\ln(\frac{z}{W_0\tau}+1))=C_B(\eta)\frac{W_0\tau}{W_0\tau+z}. \tag{A6}$$

Inserting Equation (7) into (A6), it follows that

$$C(z,t) = C_B(t-\tau\ln(\frac{z}{W_0\tau}+1))\frac{W_0\tau}{W_0\tau+z}. \tag{A7}$$

The boundary condition requires (see Fig. 1)

$$\eta>0. \tag{A8}$$

Equations (A3), (A4), (A7) and (A8) can be summarized as follows:

$$C(z,t)=\begin{cases} C_I((z+W_0\tau)e^{-t/\tau}-W_0\tau)e^{-t/\tau}, \text{ in domain I} \\ C_B\left(t-\tau\ln\left(\frac{z}{W_0\tau}+1\right)\right)\frac{W_0\tau}{W_0\tau+z}, \text{ in domain B} \end{cases}. \tag{A9}$$

APPENDIX B

This appendix presents a generalization of solution (9) to the case that water entering the conduit from the matrix contains solute (a production-value problem). The solution for this case has been presented by Li (2009). Since the mathematical problem is linear with respect to concentration, that solution can be superposed on solution (9); the complete solution is

$$C(z,t)=\begin{cases} C_I((z+W_0\tau)e^{-t/\tau}-W_0\tau)e^{-t/\tau}+\dfrac{C_M}{\tau}\displaystyle\int_0^t e^{(\varsigma-t)/\tau}j(z_d(\varsigma),\varsigma)d\varsigma \ \text{ in domain I.} \\ C_B\left(t-\tau\ln\left(\dfrac{z}{W_0\tau}+1\right)\right)\dfrac{W_0\tau}{W_0\tau+z}+\dfrac{C_M}{\tau}\displaystyle\int_\eta^t e^{(\varsigma-t)/\tau}j(z_d(\varsigma),\varsigma)d\varsigma \ \text{ in domain B.} \end{cases}, \tag{B1}$$

where C_M is the solute concentration in the matrix, $j(z, t)$ is the dimensionless specific flux of solute at the conduit wall, η is defined in Equation (7) and Z_D is defined by

$$z_d(\varsigma)=(z+W_0\tau)e^{(\varsigma-t)/\tau}-W_0\tau. \tag{B2}$$

APPENDIX C

This appendix seeks how to calculate the radius and seepage velocity of a conduit consisting of two segments with different radius. First we suppose the conjunction is at the middle of the conduit and the radius ratio between the upstream segment and the downstream segment is k. The conduit discharge at the conjunction is denoted as Q_M. Water mass conservation yields

$$Q_M-Q_0=\pi a_1 Zq, \tag{C1}$$

$$Q_S-Q_M=\pi a_2 Zq. \tag{C2}$$

Dividing (C1) by (C2) yields

$$Q_M=\frac{Q_0+kQ_S}{1+k}. \tag{C3}$$

Now we apply Equation (18) to the upstream segment and the downstream segment, which yields

$$\frac{(Q_M-Q_0)T_1}{\pi a_1^2\ln(Q_M/Q_0)}=\frac{Z}{2}, \tag{C4}$$

$$\frac{Q_S-Q_M(T-T_1)}{\pi a_2^2\ln(Q_S/Q_M)}=\frac{Z}{2}, \tag{C5}$$

where T_1 is the transport time within the upstream segment. Diving (C4) by (C5) yields

$$T_1\ln\left(\frac{Q_S}{Q_M}\right)=k(T-T_1)\ln\left(\frac{Q_M}{Q_0}\right). \tag{C6}$$

Substituting (C3) into the above equation and solving for T_1 yields

$$T_1=\frac{kT\ln\left[\dfrac{Q_0+kQ_S}{(1+k)Q_0}\right]}{\ln\left[\dfrac{(1+k)Q_S}{Q_0+kQ_S}\right]+k\ln\left[\dfrac{Q_0+kQ_S}{(1+k)Q_0}\right]}. \tag{C7}$$

With T_1 known, we substitute (C3) into (C4) to solve for the radius of the upstream segment.

$$\pi a_1^2 = \frac{2k(Q_S - Q_0)}{(1+k)Z \ln\left[\frac{Q_0 + kQ_S}{(1+k)Q_0}\right]} T_1. \tag{C8}$$

With a_1 known, substituting (C3) into (C1) yields the seepage velocity

$$q = \frac{k(Q_S - Q_0)}{\pi(1+k)Za_1}. \tag{C9}$$

In summary, (C7), (C8), and (C9) can yield the transport time within the upstream segment, the radius of the upstream segment, and the velocity of seepage from matrix into conduit.

COBISS: 1.01

STRUCTURAL CONTROL ON DEVELOPMENT OF KARST LANDSCAPE IN THE SALENTO PENINSULA (APULIA, SE ITALY)

STRUKTURNI VPLIV RAZVOJA KRAŠKEGA POVRŠJA NA POLOTOKU SALENTO (APULIJA, JV ITALIJA)

Mari Pepe[1] & Mario Parise[2]

Abstract UDC 551.435.8(450.75)

Mari Pepe & Mario Parise: Structural control on development of karst landscape in the Salento Peninsula (Apulia, SE Italy)

Apulia region (SE Italy) is particularly prone to karst processes, due to the extensive presence of carbonate rocks. Karst marks the whole region, and represents the main landscape features, with a variety of landforms ranging from large-size dolines, to poljes, and fluvial-karstic valleys; given the configuration of Apulia, a great role in the presence of widespread karst features is also played by coastal landforms. The Salento peninsula, in southern Apulia, is characterized by very low relief and cropping out of different types of carbonate rocks, ranging in age from Cretaceous to Quaternary. Recognition of karst features in this setting, and the likely implications for geohazards, is quite difficult, because of the subtleness of the features, and the facility for man to cancel or modify them. Nevertheless, the presence of dolines is definitely a typical aspect of the area, which also implies some consequences in terms of risk to the built-up environment. This work focuses on the area of Barbarano del Capo, where two cover-collapse dolines are well known in the geological literature as *Vora Grande* and *Vora Piccola*. Despite the fact that morphometrical and stratigraphical features have already been investigated, few informations are available about the hydro-geomorphological and structural settings of the area. This article presents the results of morphological and structural analyses, aimed to understand the role of tectonics in the development of karst features, and their evolution.

Keywords: sinkholes, karst, tectonics, morphometry, karst landforms, Salento peninsula, Apulia.

Izvleček UDK 551.435.8(450.75)

Mari Pepe & Mario Parise: Strukturni vpliv razvoja kraškega površja na polotoku Salento (Apulija, JV Italija)

Za pokrajino Apulijo (JV Italija) so značilni kraški procesi, zaradi velike razširjenosti karbonatnih kamnin. Kras označuje celotno pokrajino in predstavlja glavne površinske oblike, od velikih vrtač, do polj in fluvialnih kraških dolin. Glede na položaj Apulije imajo pomembno vlogo v prisotnosti razširjenih kraških oblik tudi obalne površinske oblike. Polotok Salento v južni Apuliji kaže značilnosti nizkega reliefa z izdanki različnih karbonatnih kamnin krednih do kvartarnih starosti. Določanje kraških oblik ter povezava z naravnimi nesrečami je težka zaradi razširjenosti oblik in zmožnosti človeka, da preoblikuje površje. Kljub temu je prisotnost vrtač zelo značilna za to pokrajino. Hkrati pa to lahko povzroča nekatere neugodne posledice pri gradnjah na tem terenu. Ta študija je usmerjena na območje Barbarano del Capo, kjer se nahajata dve pokriti udorni vrtači, v geološki literaturi dobro znani kot *Vora Grande* in *Vora Piccola*. Kljub temu, da so bile morfometrične in stratigrafske oblike že raziskane, pa je malo dostopnega o hidro-geomorfoloških in strukturnih podatkih. Članek predstavlja rezultate morfoloških in strukturnih analiz, da bi razumeli vlogo tektonike v razvoju kraških oblik.

Ključne besede: vrtače, kras, tektonika, morfometrija, kraške površinske oblike, polotok Salento, Apulija.

[1] Basin Authority of Apulia, Valenzano, Italy, e-mail: mari.pepe81@gmail.com
[2] CNR-IRPI, Bari, Italy, e-mail:m.parise@ba.cnr.itpi.it

Received/Prejeto: 23.09.2013

INTRODUCTION

Karst processes are the main geomorphic agents in Apulia region (SE Italy), due to the extensive presence of carbonate rocks, ranging from the Jurassic to the Quaternary ages. Karst landforms are widespread all over the region, and often designated with different terms. As a matter of fact, due to historical reasons the local language developed distinct and variable linguistic roots in different parts of the region. Thus, even the terms used to indicate the natural landscape greatly change throughout Apulia. This is, for instance, the case of dolines, one of the most common features in the Apulian landscape: a high variety of dolines has been documented, with different genesis, morphology and size, governed by the local characteristics of carbonate rock masses and hydrology. Dolines are designated with very different terms, such as *pulo*, *gurgo*, *grave*, *àviso*, and *vora,* depending on the local dialects (see Parise *et al.* 2003).

The Salento peninsula, hosting the southernmost carbonate block of the region, is entirely modeled by karst processes, and particularly susceptible to dolines, due to favourable stratigraphic conditions: among the other types, many examples of cover-collapse dolines (*sensu* Waltham *et al.* 2005) can be numbered, promoted by the presence of Tertiary and Quaternary clastic carbonates over the Cretaceous limestone bedrock (e.g. Delle Rose *et al.* 2004, 2007; Parise 2008a; Festa *et al.* 2012).

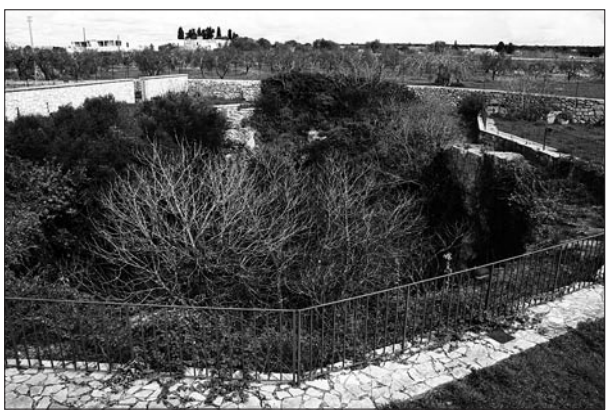

Fig.1: Overall view of Vora Grande (Photo: M. Parise).

Seawater along the Salento coastlines enhances hyperkarst processes, that are at the origin of the wide presence of coastal dolines (Delle Rose & Parise 2002, 2005; Delle Rose *et al.* 2004; Parise 2008a; Bruno *et al.* 2008a, b; Del Prete *et al.* 2010; Margiotta *et al.* 2012). In particular, the interplay between coastal doline activity and sea wave erosion produces on the Ionian side of Salento peculiar shoreline morphologies, locally designated as *spunnulate* (*e.g.* Bruno *et al.* 2008a and references therein; Basso *et al.* 2013). In addition to dolines produced by natural karst processes, many cases of anthropogenic sinkholes have been registered in Salento, ascribed to intense underground quarrying (*e.g.* Delle Rose *et al.* 2007; Parise 2008a, 2010a; De Pascalis *et al.* 2010; Lollino & Parise 2010; Parise & Lollino 2011; Lollino *et al.* 2013).

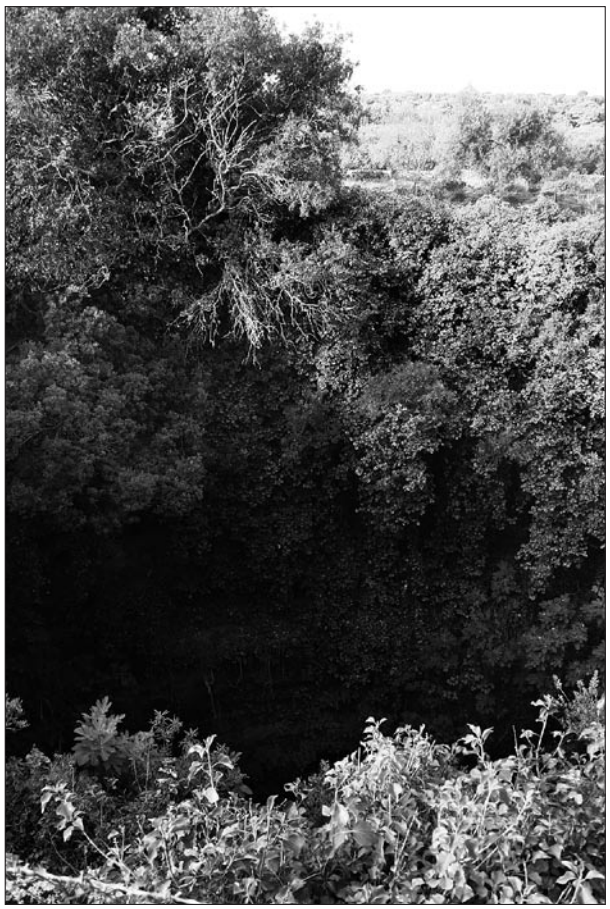

Fig. 2: Vora Piccola (Photo: M. Parise).

Together with dolines, other depression-like landscapes are extremely important in terms of land management in the karst of Apulia: these can cover limited areas, often hosting temporary lakes or marshlands (Lopez *et al.* 2009; Parise 2009), or affect larger territories as poljes (Parise 2006). Since these depressions represent the low-altitude lands, they are often flooded in the aftermath of heavy rainstorms, a situation which results in continuous heavy economic losses in Salento, and the rest of Apulia as well (Parise 2003; Andriani & Walsh

2009; Cotecchia & Scuro 2010). The effects of the floods are often exacerbated by land mismanagement actions, typically carried out without having a proper knowledge of the karst landforms and their hydrological functioning (Calò & Parise 2006; Parise & Gunn 2007; De Waele *et al.* 2011). Closure and clogging of swallow holes, and extensive covering of karst with asphalt roads and the expansion of urbanized areas obstruct the natural drainage of runoff during and after heavy rainstorms, enhancing the consequent losses to society.

Starting from the above considerations, this work examines the main landforms of the karst landscape in a sample area of Salento, namely Barbarano del Capo, where two cover-collapse dolines are well known in the geological literature as *Vora Grande* (Fig. 1) and *Vora Piccola* (Fig. 2), for their respective sizes. Both dolines, few hundreds of meters apart, are included in the Regional Register of Caves, managed by the Apulian Speleological Federation (Giuliani 2000) and were carefully described for the first time by a local scholar, Cosimo De Giorgi, at the end of the XIX century (De Giorgi 1896). Further morphological descriptions have been provided by Beccarisi *et al.* (2003), Delle Rose *et al.* (2004) and Parise (2008a). All these authors agree that both dolines formed through collapse of the cavern vaults, enhanced by local litho- stratigraphical changes in the Plio-Pleistocene calcarenites. At present, they still show instability conditions, as testified by the recent fall at the eastern margin of *Vora Grande* (February 2011).

The two *Vore* are also interesting examples of the interaction between man and development of dolines: remains of quarry activity at the margin of one of the doline might represent evidence of a likely (even though so far not proved) anthropogenic trigger. The abundance of quarries in this site is due to the common employment of calcarenites for buildings in the past. Ancient human activities in this site are also testified by carriage tracks of Roman age (Sammarco & Parise 2008).

The abundance and variety of karst landforms, involving various kinds of carbonate rocks, with different textures and cementation degree, makes this area suitable for geological evaluations on development of the karst landscape. In particular, this work estimates the possible connection between the shape of morphokarst elements and the spatial distribution of mechanical discontinuities in the rock masses, as already tried in several karst areas worldwide, including the Classical Karst (*i.e.*, Šebela 1998; Cucchi *et al.* 2001; Šebela *et al.* 2005, and references therein). Quantitative methods have been employed for both the morphometry of karst landforms and the structural analysis.

METHODS

Given the main aim of the work (that is, to look for, and discuss, any likely relationships between the main features of karst landforms and the geological structures), to perform the morphometric analysis of dolines in the study area, a detailed hydro-geomorphological map has been realized, based upon field surveys and interpretation of multi-temporal aerial photographs, covering the time span from 1955 to 2001. Recognized elements have been drawn up in a digital format using as base the topographic map at 1:5.000 scale provided by Apulia Region, and Geographic Information System (GIS) tools have been employed to manage the spatial data. In particular, a hierarchical distinction among the recognized morphokarst elements has been outlined, based on visibility, extension and depth. The term *doline* refers in our work to topographically depressed areas of generally limited extent, showing a marked altitude drop. These latter are often enclosed in wider, flatter *depressions*, with boundaries more difficult to be outlined, and that show a less appreciable difference in altitude with respect to surrounding areas. Thus, dolines and depressions will be the two categories of karst features mostly dealt with in the following analyses and descriptions. In addition, the main scarps bordering the *Serre* ridges, and the few ephemeral streams arising from these slopes, have also been outlined.

Cartographical data have been then employed for the morphometric analysis, carried out separately on the two categories of dolines and depressions. The following parameters, considered as the most representative for a morphometric description of the considered karst landforms (*e.g.* Williams 1971; Drake & Ford 1972; Mills & Starnes 1983), have been adopted: i) Total number; ii) Minimum and maximum area; iii) Density (total number / total area); iv) Total area; v) Percentage of involved areas; vi) Ratio between major axis (a) and minor axis (b) (*elongation ratio*, *e.g.* Bruno *et al.* 2008a).

Finally, the structural analysis has been undertaken. Dip-directions of faults and joints have been measured and statistically analyzed at the available outcrops of the carbonate rock masses (the Cretaceous limestone

bedrock and the Pleistocene calcarenites). Spatial distribution of measurement stations provides a quite uniform outline of structural data across the study area. A total number of 15 measurement stations have been selected, 8 of which are located along the *Serre* ridges (*Serre di Montesardo* to the north-east and *Serre Falitte* to the south-west), whilst the remaining 7 along the intervening structural lowlands. At each station, a minimum number of 40 measurements has been assumed as the threshold of statistical significance. Results have been then analyzed and plotted on rose diagrams and cumulative curves, in order to detect the likely connections between structural data and morphometric parameters.

GEOLOGICAL AND GEOMORPHOLOGICAL SETTING

The Apulia region represents the outcropping sector of the south-Apennines foreland, connected to the westward subduction of the Adria Plate underneath the Apennine Chain (Mostardini & Merlini 1986; Casero *et al.* 1988; Doglioni 1991), since Late Oligocene to Early Pleistocene (Boccaletti *et al.* 1990). Regionally the Apulian

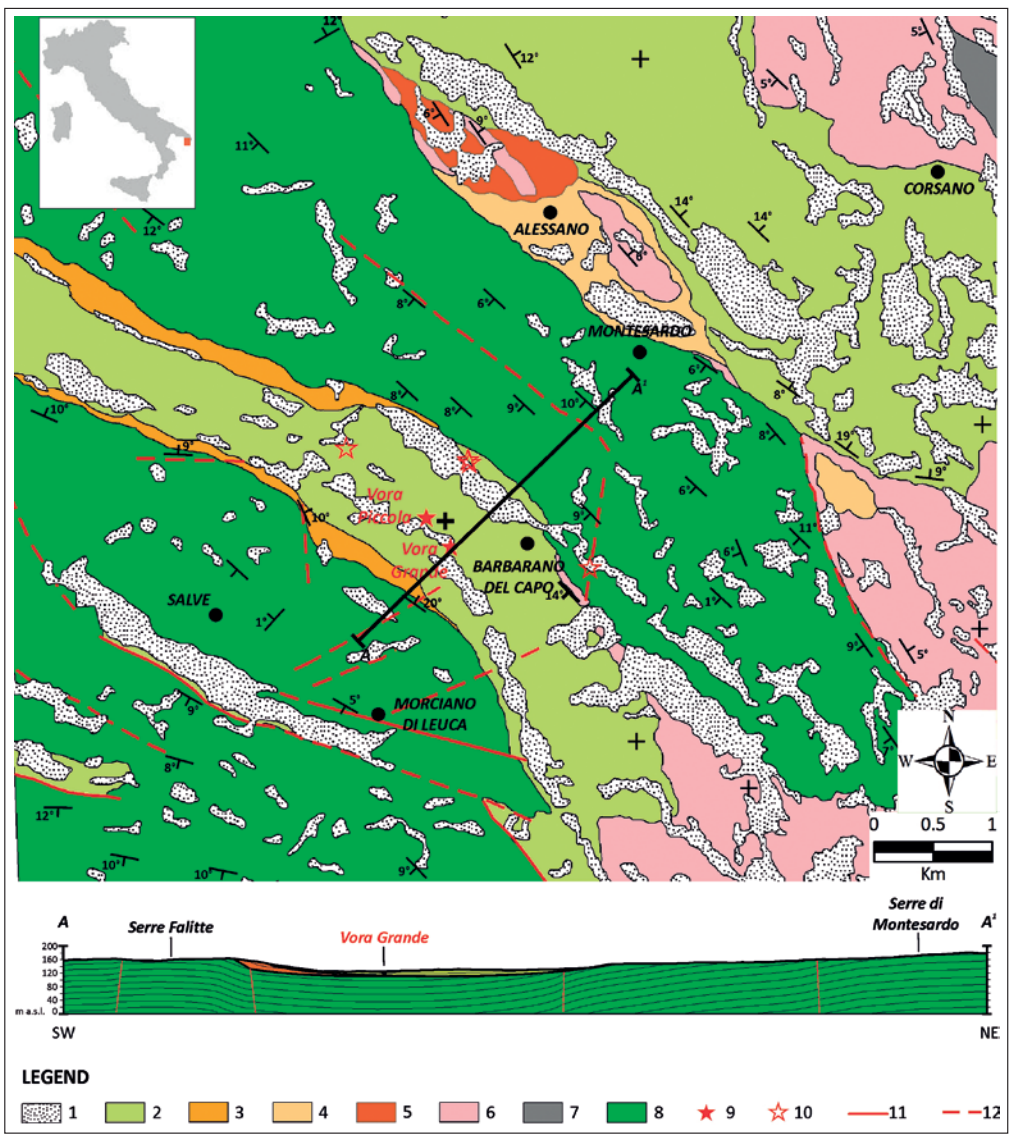

Fig. 3: Sketch map and cross-section of the study area (modified after Ricchetti and Ciaranfi, 2009 – sheet 536 Ugento of the New Geological Map of Italy, 1:50.000 scale).

Legend:

1. Eluvial-colluvial deposits (Middle Pleistocene – Holocene);
2. Miggiano Synthem (Middle Pleistocene);
3. Gravina Calcarenites Fm. (Lower Pleistocene);
4. Uggiano La Chiesa Fm. (Middle-Upper Pliocene);
5. Trubi (Lower Pliocene);
6. Andrano Calcarenites Fm. (Upper Miocene);
7. Castro Limestone Fm. (Upper Oligocene);
8. Altamura Limestone Fm. (Upper Cretaceous);
9. Active sinkhole;
10. Filled sinkhole;
11. Fault;
12. Uncertain fault.

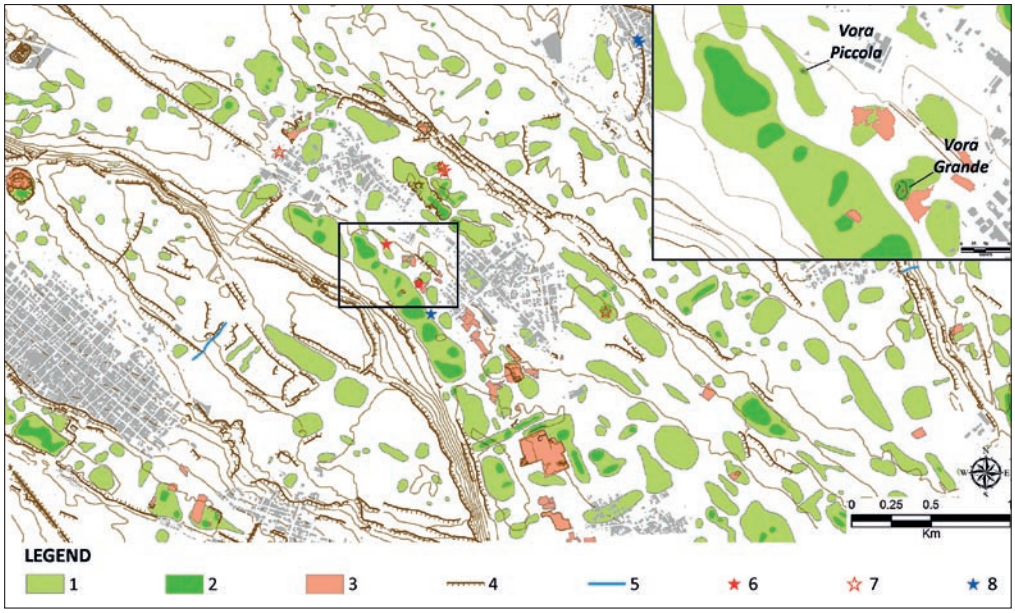

Fig. 4: Hydro-geomorphological map of the study area, with detail of the two Vore (inset in the upper right corner).

Legend:
1. Depression;
2. Doline;
3. Quarry;
4. Scarp;
5. Stream;
6. Active sinkhole;
7. Filled sinkhole;
8. Artificial cave.

Foreland corresponds to a wide WNW-ESE trending antiform (Ricchetti 1980; Royden *et al.* 1987), due to buckling of the subducting slab. The exposed sector of the antiform is segmented by large deformation zones in three main blocks, represented from north to south by the Gargano, the Murge and the Salento highlands (Ricchetti *et al.* 1988; Funiciello *et al.* 1991; Gambini & Tozzi 1996). This latter represents the less uplifted block and performs the lowest topographic relief.

The strong development of karst-landscape in most of Apulia is definitely ascribable to the preponderance of carbonate rocks, originated in different palaeo-geographical settings. From bottom to top, the overall carbonate sedimentary succession is composed of Jurassic-Cretaceous limestones and dolostones of a passive margin (the so-called *Murge Limestones Group*), from 3 to 5 km thick, unconformably overlain by Palaeogene to Neogene calcarenites and calcirudites of foreland to foredeep settings, unevenly preserved only in the Gargano highland and the Salento Peninsula, finally capped by Quaternary terraced marine calcarenites.

Accordingly, many carbonate units are exposed in the study area, ranging from Cretaceous to Quaternary ages, with lateral and vertical changes in both facies and mechanical properties (Fig. 3). Following the new Geological Map of Italy (1:50.000 scale), the oldest unit at the outcrop is represented by Upper Cretaceous limestones of inner-shelf (*Altamura Limestone* Fm.), unconformably overlain by Upper Miocene to Lower Pleistocene calcarenites and calcirudites of intertidal to neritic environments (*Andrano Calcarenites*, *Trubi*, *Uggiano-La Chiesa* and *Gravina Calcarenites* Fms.), finally capped by Middle Pleistocene terraced marine calcarenites of intertidal setting (*Miggiano* Synthem). The *Altamura Limestone* Fm., representing the Cretaceous bedrock, is exposed along narrow, NW-SE-trending ridges (the so-called *Serre Salentine*), whilst the overlying deposits are preserved in the intervening structural lowlands with the lowest stratigraphic units only exhumed along the footslopes of the *Serre* margins. The two *Vore* are hosted within the *Miggiano* Synthem, made up of medium to coarse macro-fossiliferous calcarenites and calcirudites, with diffuse bioturbation, referable to an intertidal environment (Ricchetti & Ciaranfi 2009 – sheet 536 "Ugento" of the Geological Map of Italy, at the 1:50.000 scale).

The hydro-geomorphological map (Fig. 4) shows that the morphological pattern of the study area mainly follows the regional structures. Karst landscape is dominated by dolines and depressions, while fluvio-karst valleys appear to be limited to the fault scarps bounding the *Serre Salentine*. The major axes of both dolines and depressions present NW-SE and NE-SW main trends. Along the structural lowlands intervening between the Serre ridges, the depressions are typically wider and more markedly elongated in a NW-SE direction. *Vora Grande* and *Vora Piccola* are located on the same NW-SE-elongated plain, bounded by the ridges of *Falitte Serre* to the south-west, and of *Montesardo Serre* to the north-east. From these two lateral ridges to the intervening plain, elevation drops about 20–30 m: this altitude gap is sufficient to produce a variety of landforms, as in other inland sectors of Salento (Palmentola 1987; Parise 2008b).

COVER-COLLAPSE DOLINES IN BARBARANO DEL CAPO: VORA GRANDE AND VORA PICCOLA

Vora Grande and *Vora Piccola* are located at the eastern periphery of Barbarano del Capo, few hundreds of meters from the Sanctuary of Madonna del Belvedere in Leuca Piccola, which hosts an interesting underground crypt dug into the local calcarenites, a remarkable example of the ability to realize man-made underground cavities in the area (Sammarco & Parise 2008).

Vora Grande (PU 114 in the Register of Natural Caves of Apulia), actually fenced-in all along, is situated southeast of *Vora Piccola* (PU 115), in turn located few tens of meters far from the country road to the Sanctuary. The two *Vore* respectively reach 35 m and 25 m of depth. In plan view, *Vora Grande* shows an elliptical shape, with a NS-oriented, 30 m-long major axis. Elongation changes in depth, following a NW-SE orientation (Beccarisi *et al.* 2003). *Vora Piccola*, instead, shows a less-pronounced elliptical shape in plan view, with a 15 m-long major axis, oriented in NW-SE direction. These two sites still show instability conditions, as an effect of the geomechanical degradation of rock masses and the vertical to over-hanging walls: a big volume of rock recently (February 2011) fell from the southeastern margin of *Vora Grande*, due to intense rainfalls and likely favored by discharge of runoff water that is channeled into the doline by means of pipes (Pepe and Parise 2011; Fig. 5).

Fig. 5: Recent fall at the eastern margin of Vora Grande in February 2011 (Photo: M. Parise).

Both *Vore* affect the Middle Pleistocene deposits of the *Miggiano* Synthem. The detailed litho-stratigraphic description of the sedimentary succession exposed along their walls is provided by Bossio *et al.* (1987, 1998). From bottom to top, the sedimentary succession consists of: yellowish calcarenites and calcirudites, arranged in dm-thick beds, exposed below 20 m of depth; yellowish carbonate-rich sands, about 15–15.5 m thick, with more lithified layers in the uppermost 4–5 meters; well-lithified calcarenites, about 4.5–5 m thick. Selective erosion highlights diagenetic changes in the upper part of the succession. Furthermore, thin karst conduits and intrastratal caves are cut by the walls of the *Vore*. Therefore, combined karst and mechanical erosion has promoted the genesis of rock ledges overlooking inside the caves. These ledges are locally accessible by artificial ways, dug into the calcarenites. Wide detrital cones lay at the bottom of the *Vore*, clogging any possible exploration of the underground cave systems.

Assuming a basal karst level about 10–20 m below the current bottom of the *Vore*, Beccarisi *et al.* (2003) have worked out an evolutionary model of the two dolines, starting with the genesis of a proto-cave, following with its widening under chemical and mechanical processes, and with the upward migration of the vaults by collapse of the cavern roofs. These processes were probably enhanced by the involvement of more erodible sandy layers. This rapid evolution easily brought to reach the calcarenite layers on top, without any need for further chemical processes (*e.g.* condensation) aiding carbonate solution, and not properly testified by morphological evidences (Dunne 1990; Parise 2008a). The final collapse of the remaining cap, resulting in doline opening, was probably promoted by the presence of mechanical discontinuities in the calcarenite layers above the underground voids.

The exact definition of the absolute time of opening of the doline is still a challenge. A clue is noticeable along the margins of *Vora Piccola*, where traces of quarries are cut by the walls of the sinkhole. This element provides information about relative timing, suggesting that quarries were prior to doline opening (Delle Rose *et al*. 2004; Parise 2008a). It is not excluded that quarry activity may have triggered the collapse, but this should require stronger evidences.

Apart from *Vora Grande* and *Vora Piccola*, the analysis of multi-year air-photos has revealed the presence in the study area of at least four more collapse dolines, filled after the '70s and now part of the inhabited area. A strong drop in floor is still recognizable at these places (Fig. 6). Despite the number of samples it is insufficient for any statistical statement, anyway some general features of these collapse dolines can be outlined. In plan view, they mainly show sub-circular shapes, with diameters in the order of few tens of meters. When slight elongation occurs, the major axes follow NNW-SSE trends. As regards position, all collapse dolines are lo-

cated in the plain intervening between the *Serre Falitte* and the *Serre di Montesardo*, nearby the lowermost topographical sectors of wider *depressions*. However, not all collapse dolines involve Middle Pleistocene calcarenites of the *Miggiano* Synthem: one of them, in fact, is hosted within the Cretaceous limestones of the *Altamura Limestone* Fm (Fig. 3), with no sedimentary cover involved, unless eroded. In this case, the vicinity of the *Serre di Montesardo* fault scarp (Fig. 4) may be liable for a belt of mechanical weakness, where karst processes have been enhanced.

Fig. 6: Evidence of an ancient sinkhole, today partly filled and included in the anthropogenic setting (Photo: M. Pepe).

Apart from the aforementioned collapse dolines, a number of solution dolines have also been detected, scattered along the main morpho-structural plains. At first glance, these landforms seem to be randomly shaped. A more careful insight reveals that smaller dolines mainly perform circular shapes; larger dolines tend to elliptical, or anyway elongated, shapes. As observed by Bruno *et al.* (2008a) in other karst areas of Apulia region, this feature can be ascribed to coalescence of neighbouring dolines, where elongation is controlled by alignment of incipient dolines. However, elongation of dolines not always coincides with that of the depressions where they are included (Fig. 4).

RESULTS

MORPHOMETRIC ANALYSIS

The morphometric analysis of the karst landforms performs different values of all parameters, whether considering dolines or depressions (Tab. 1). The total number of depressions is 274, corresponding to a density of 11.87 in the total area of study (20 km^2). As concerns dolines, the density value drops to 8.10, with 86 features identified. In terms of total extent, the considered landforms diverge one order of magnitude: the total surface coverage of depressions is 2.93 km^2, against the 0.25 km^2 of dolines. Accordingly, in terms of percentage, depressions represent 14.63% of the total area, and dolines only 1.26%. Depressions and dolines show also different values of the mean major axis / minor axis ratio (a/b), indicating a higher elongation in the former. The parameter elongation is defined as the ratio of the equivalent circular diameter to the major axis length (Schumm 1956). It indicates that the most elongated among depressions concentrate in the range 80–100° of the azimuth values, while dolines are elongated in the range of 0–20° (Fig. 7).

Taking into account the azimuth values of the major axes of both the categories of landforms, the outcomes reveal that dolines and depressions show similar orientations, both following Apenninic trends. In particular, the maximum peak for dolines (25%) is at 100–120°, whilst for depressions (30%) it is at 120–140° (Fig. 8). Being

Tab. 1: General morphometric features of dolines and depressions in the study area.

Area of survey	***20 km^2***	
	DEPRESSIONS	DOLINES
Number of elements	274	86
Minimum area	0.00027769 km^2	0.00019109 km^2
Maximum area	0.16924151 km^2	0.02274375 km^2
Density	11.87 Depressions/km^2	8.10 Dolines/km^2
Total area	2.93 km^2	0.25 km^2
Percentage	14.63%	1.26 %
Major axis (a) / minor axis (b) ratio	2.17	1.88

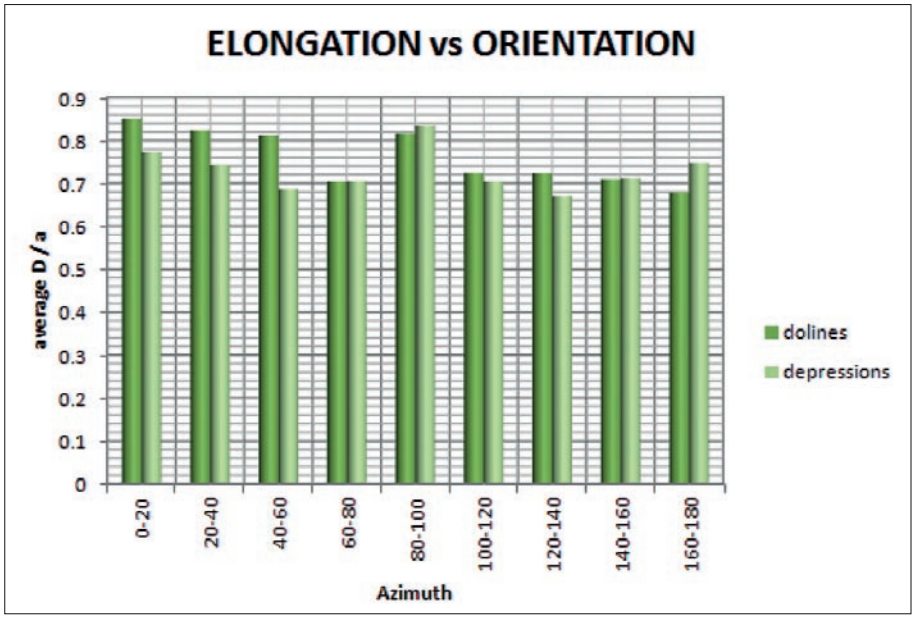

Fig. 7: Histogram showing elongation values for dolines and depressions, depending on the azimuth values (D = diameter of equivalent circle).

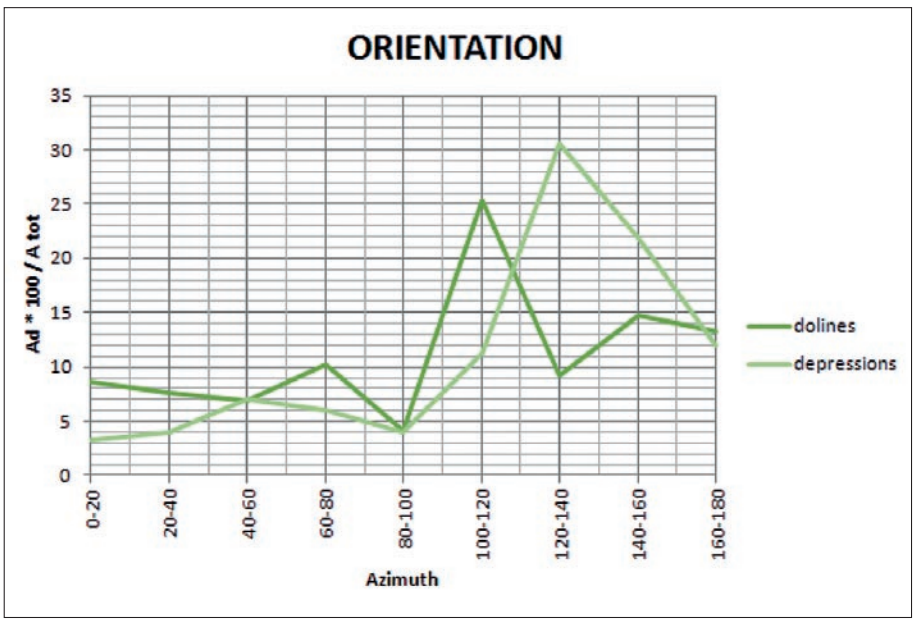

Fig. 8: Cumulative curves of major axes orientations, respectively for dolines and for depressions (A_d = area of individual doline or depression; A_{tot} = total area of dolines or of depressions).

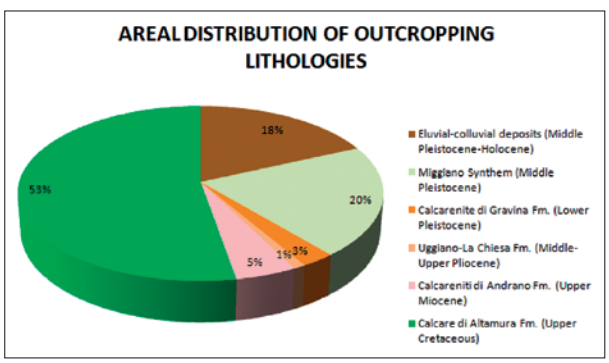

Fig. 9: Areal distribution of outcropping lithologies.

the study area geologically characterized by a high variety of carbonate rocks at the outcrop (Fig. 9), a further analysis of the morphometric data seems necessary, as a function of lithologies. In this analysis, the Holocene eluvial-colluvial deposits have not been taken into account. Computation of the areal percentages of dolines and depressions, depending on the lithologies involved (Fig. 10), has highlighted that the most karstified unit is the youngest one, the *Miggiano* Synthem, with 23% of its area involved in depressions. The Andrano Calcarenites follow very close (22% areal coverage for depressions) whilst significantly low is the area affected by depression for Uggiano la Chiesa Fm. Minor differences can be

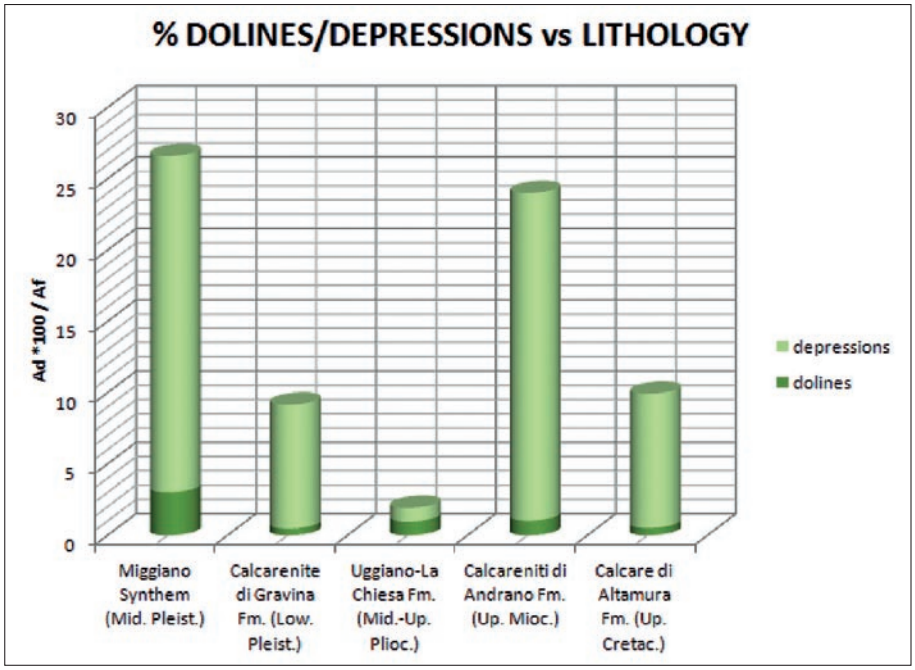

Fig. 10: Areal percentages of dolines and depressions, as a function of lithologies (A_d = area of individual doline or depression; A_f = area of individual lithology).

Tab. 2: Summary of prevailing major axes orientations of karst landforms according to the different lithologies.

LITHOLOGICAL UNITS	AZIMUTH VALUES (°)	
	Dolines	Depressions
Miggiano Synthem	100–120	120–160
Gravina Calcarenites Fm.	120–140	140–160
Uggiano-La Chiesa Fm.	–	60–80
Andrano Calcarenites Fm.	160–180	120–140
Altamura Limestone Fm.	140–160	120–140

observed among the various lithologies when analyzing dolines: in this case, all the rock types show similar values, with the maximum again for the Miggiano Synthem (3% areal coverage).

Finally, cumulative curves of the azimuth values of the major axes highlight a net preponderance of Apenninic trends, in both dolines and depressions sets for all the lithologies, with the only exception of the Uggiano-La Chiesa Fm., that shows a trend about ENE-WSW (Fig. 11). Nevertheless, the data seem more concentrated for the samples of depressions, whilst the doline azimuth

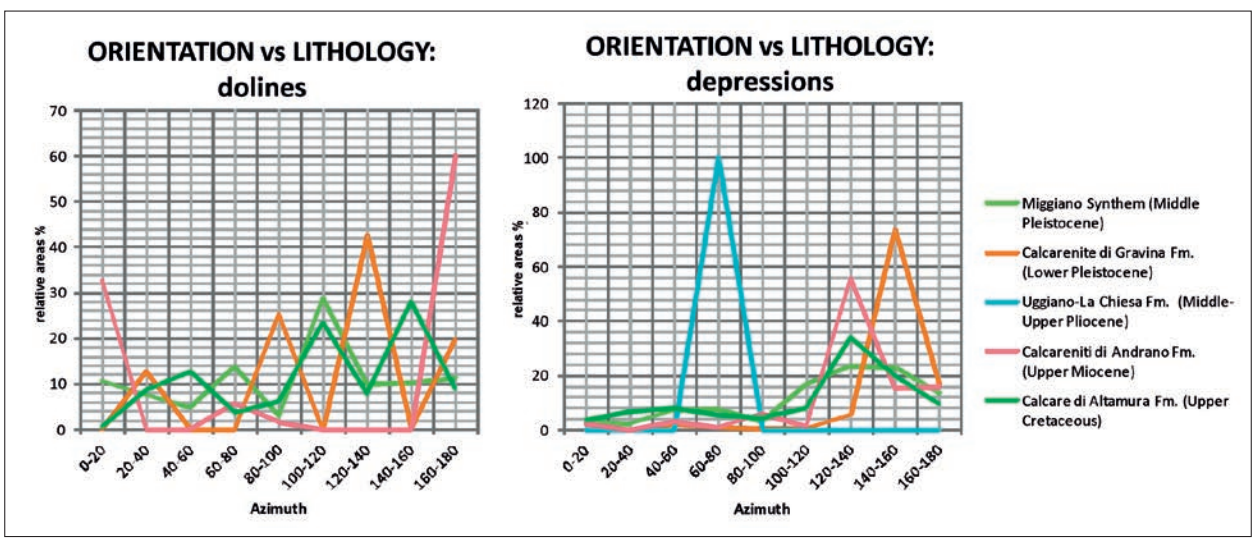

Fig. 11: Azimuth values of major axes of dolines and depressions, as a function of lithology. Relative areas refer to the total area of dolines in individual lithological unit.

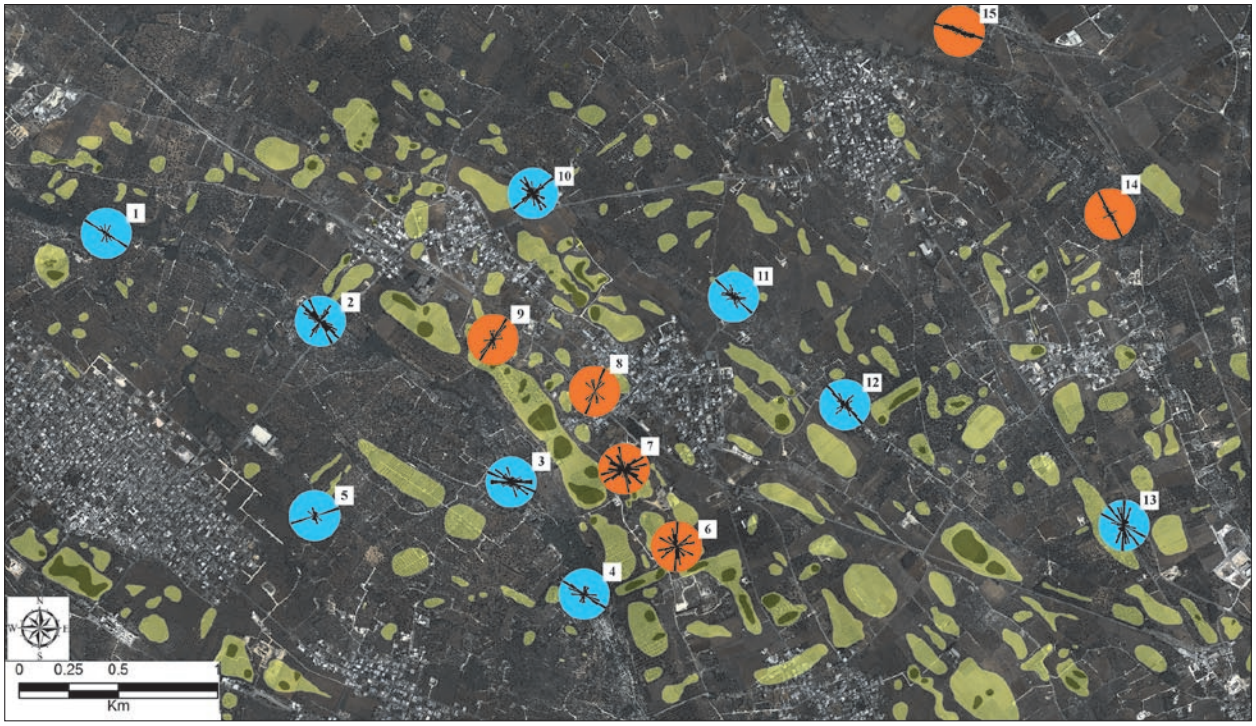

Fig. 12: Results of the structural measurements on the Cretaceous limestones (blue rose diagrams) and on the Miocene-Pleistocene calcarenites (orange rose diagrams). The forms in light and dark green are, respectively, depressions and dolines, as represented in the hydro-geomorphological map in fig. 4.

values appear to be more scattered, even though the peaks are still within the main Apenninic trend (Fig. 11, Tab. 2).

TECTONIC AND/OR STRATIGRAPHIC CONTROL IN DEVELOPMENT OF KARST

The structural setting of the study area, and more in general that of the whole Salento Peninsula, is characterized by gentle bending and high-angle, mainly normal faults, strongly affecting the regional-scale morphology.

The most important fault systems are represented by normal, NW-SE and NNW-SSE-trending faults (Apenninic faults), affecting the Cretaceous and Eocene-Miocene units. These fault systems, showing evidences of strike-slip movement (Tozzi 1993; Gambini & Tozzi 1996), dissect the wide Salento horst into uplifted and lowered blocks, resulting in alternating morpho-structural ridges (the Serre Salentine ridges) and elongated depressions. Apenninic faults are also responsible for

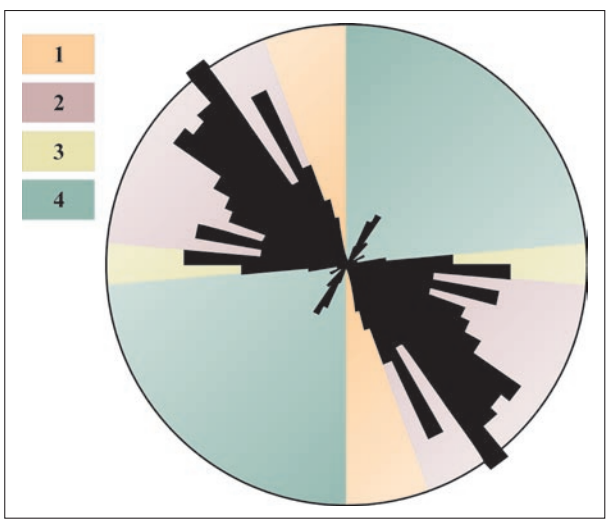

Fig. 13: Trends of regional faults in the Southern Murge and the Salento Peninsula (after Tozzi 1993). Legend: 1. NNW-SSE trending faults (sub-vertical, strike-slip and dip-slip normal faults, best represented by the morpho-tectonic scarps bordering the Serre highlands in the Salento area), connected with the post-orogenic extension in the Apulian foreland (Miocene-post Pliocene); 2. NW-SE trending faults (dip-slip normal and sub-vertical faults, best developed in the Murge highland, producing a horst-and-graben setting), connected with the post-orogenic extension in the Apulian foreland (Miocene); 3. E-W trending faults (sub-vertical, dip-slip normal faults), characterizing the boundary between the Murge highland and the Salento area (Eocene-Oligocene); 4. NE-SW trending faults (sub-vertical, dip-slip normal faults; Plio- Pleistocene).

the main slopes bordering both the Adriatic and the Ionian sides of the peninsula (*e.g.* Neboit 1975; Baldassarre *et al.* 1978; Delle Rose & Parise 2003); some authors, instead, interpreted the Adriatic slopes as the original edge of the Mesozoic carbonate platform (Bosellini *et al.* 1999). Both NW-SE and NNW-SSE-trending fault systems first activated in Eocene-Oligocene, together with open to gentle folds (Festa *et al.* 2012), at the onset of Apennines orogenesis. However, Apenninic faults show evidences of reactivation in Pliocene and Pleistocene times (e.g. Tozzi 1993; Pieri *et al.* 1997; Delle Rose 2001; Festa *et al.* 2012), possibly related to the post-orogenic extension in the Apulian foreland (Tozzi 1993). A secondary fault system is represented by normal, NE-SW-trending faults (anti-Apenninic faults), which become preponderant just in local reliefs of the peninsula, such as near Otranto town (Tozzi 1993). Recent meso-structural analyses by Di Bucci *et al.* (2009) ascribe both Apenninic and Anti-Apenninic faults to middle and late Pleistocene extensional tectonics. Finally, normal, EW-trending faults mark the boundary between the Murge and the Salento highlands, producing a series of slopes, best represented by the *Soglia Messapica line*, and progressively loosing significance far from this belt.

Structural data obtained by field measurements in the 15 selected stations (Fig. 12) indicate some slight differences depending on lithologies (Fig. 12). In the Cretaceous limestones exposed along the *Serre Salentine* ridges, joints often perform preferential orientations. In particular, in six measurement stations out of nine (stations 1, 2, 3, 4, 11 and 12 in Fig. 12) a net preponderance of Apenninic faults, striking N100 to N160 has been observed. In two stations (stations 5 and 10 in Fig. 12) Anti-Apenninic faults prevail, while no preferential orientation characterizes the joints at station 13 (Fig. 12). In the Miocene to Pleistocene calcarenites, instead, strong lateral changes are observed, with joints orientations following either Apenninic (stations 14 and 15 in Fig. 12) or anti-Apenninic (stations 8 and 9 in Fig. 12) trends, or none of them (stations 6 and 7 in Fig. 12).

The collected structural data show a good agreement between the local joint distribution and the regional tectonic lineations (Fig. 13). The comparison between the cumulative curves of the major axes for the analyzed karst features shows that the maximum peak for both depressions and dolines is for the Apenninic elongation. Furthermore, relative peaks observed in cumulative curves of dolines and of depressions perform a good fit.

DISCUSSION AND CONCLUSION

Identification and mapping of karst landforms in the Barbarano del Capo area allowed to sketch the main morphokarst features of this sector of Salento Peninsula, and to connect them to the general geological- structural setting. The morphometric analysis carried out separately on dolines and depressions highlights that density values, total areas and mean major axis / minor axis ratio and elongation are higher for depressions.

Furthermore, the evident preponderance of Apennines orientation of major axes, irrespective of age and mechanical properties of lithologies involved, suggests a primary control of post-orogenic structures on karst development. This represents an important outcome, which highlights the possibility that some of the karst landforms observed in the more recent deposits might be the surficial effect of relict and/or buried similar landforms in the underlying carbonate bedrock. In terms of consequences for the evaluation of geological hazards in karst (i.e., opening of sinkholes; Parise, 2010b) this has to be taken into the due account.

The structural analysis carried out on local joints, and the comparison with regional lineaments, allowed to present some considerations on the geological-tectonic control on karst landforms: despite the fact that major axes of karst depressions generally follow the main structures, some differences can be pointed out between the main parameters of dolines and depressions, which are mostly a function of the affected lithologies.

The main tectonic lineaments of the Salento peninsula have been the object of several specific studies (Bossio *et al.* 1987; Ciaranfi *et al.* 1988; Tozzi 1993), but still little is known about their control over development of karst landforms (Gil *et al.* 2013). The interest of this topic, which has also significant hydrogeological implications, should require additional data, covering the whole Salento Peninsula. The integration of the geomorphological karst data with those deriving from direct surveys and analysis in caves (Iurilli *et al.* 2009) should be in particular appropriate, in order to achieve a deeper knowledge of the water circulation pattern.

REFERENCES

Andriani, G.F. & N. Walsh, 2009: An example of the effects of anthropogenic changes on natural environments in the Apulian karst (southern Italy).- Environmental Geology, 58, 313–325.

Baldassarre, G., Boenzi, F., Ciaranfi, N., D'Alessandro, A., Dazzaro L., Iannone, A., Laviano, A., Loiacono, F., Maggiore, M., Pennetta, L., Pieri P., Rapisardi, L., Ricchetti, G., Sardella, A. & N. Walsh, 1978: Dati preliminari sulla neotettonica dei fogli 148 (Vasto), 154 (Larino), 188 (Gravina di Puglia), 201 (Matera), 202 (Taranto) e 203 (Brindisi).- Pubbl. N. 155 del C.N.R., Progetto Finalizzato Geodinamica, 35–67.

Basso, A., Bruno, E., Parise, M. & M. Pepe, 2013: Morphometric analysis of sinkholes in a karst coastal area of southern Apulia (Italy).- Environmental Earth Sciences, 70, 6, 2545–2559.

Beccarisi, L., Cacciatore, G., Chiriacò, L., Delle Rose, M., Giuri, F., Marras, V., Quarta, G., Resta, F. & P. Solombrino, 2003: Le Vore di Barbarano: note descrittive e speleogenesi.- Thalassia Salentina, 26, 145–154.

Boccaletti, M., Ciaranfi, N., Cosentino, D., Deiana, G., Gelati, R., Lentini, F., Massari, F., Moratti, G., Pescatore, T., Ricci Lucchi, F. & L. Tortorici 1990: Palinspastic restoration and paleogeographic reconstruction of the peri-Tyrrhenian area during the Neogene.- Palaeogeogr., Palaeoclimat., Palaeoecol., 77, 41–50.

Bosellini, A., Bosellini, F.R., Colalongo, L., Parente, M., Russo, A. & A. Vescogni, 1999: Stratigraphic architecture of the Salento coast from Capo D'Otranto to S. Maria di Leuca (Apulia, Southern Italy).- Rivista Italiana di Paleontologia e Stratigrafia, 105, 3, 397–416.

Bossio, A., Mazzei, R., Monteforti, B. & G. Salvatorini, 1987: Studi sul Neogene e Quaternario della Penisola Salentina: II. Evoluzione paleogeografica dell'area di Leuca nel contesto della dinamica mediterranea.- Quad. Ric. Centro Studi Geol. Ing., Lecce, 11, 31–47.

Bossio, A., Esu, D., Foresi, L.M., Girotti, O., Iannone, A., Luperto, E., Margiotta, S., Mazzei, R., Monteforti, B., Ricchetti, G. & G. Salvatorini, 1998: Formazione di Galatone, nuovo nome per un'unità litostratigrafia del Salento (Puglia, Italia meridionale).- Atti Soc. Toscana Sc. Nat., 105, 151–156.

Bruno, E., Calcaterra, D. & M. Parise, 2008a: Development and morphometry of sinkholes in coastal plains of Apulia, southern Italy. Preliminary sinkhole susceptibility assessment.- Engineering Geology, 99, 198–209.

Bruno, E., Calcaterra, D. & M. Parise, 2008b: Author's reply to discussion by I. Yilmaz on "Development and morphometry of sinkholes in coastal plains of Apulia, southern Italy. Preliminary sinkhole susceptibility assessment".- Engineering Geology, 101, 285–287.

Casero, P., Roure, F., Endignoux, L., Moretti, I., Müller C., Sage, L. & R. Vially, 1988: Neogene geodynamic evolution of the southern Apennines.- Mem. Soc. Geol. Ital., 41, 109–120.

Ciaranfi, N., Pieri, P. & G. Ricchetti, 1988: Note alla Carta geologica delle Murge e del Salento (Puglia centro-meridionale).- Mem. Soc. Geol. Ital., 41, I, 449–460.

Calò, F. & M. Parise, 2006: Evaluating the human disturbance to karst environments in southern Italy.- Acta Carsologica, 35, 2, 47–56.

Cotecchia, V. & M. Scuro, 2010: Portrait of a coastal karst aquifer: the city of Bari.- AQUA Mundi, 187–196.

Cucchi, F., Marinetti, E., Potleca, M. & L. Zini, 2001: Influence of geostructural conditions on the speleogenesis of the Trieste Karst (Italy).- Geologica Belgica, 4, 3–4, 241–250.

De Giorgi, C., 1896: Le vore di Barbarano.- L'Universo, 9, 129–131.

Delle Rose, M., 2001: Salento Miocene: a preliminary palaeoenvironmental reconstruction.- Thalassia Salentina, 25, 159–197.

Delle Rose, M. & M. Parise, 2002: Karst subsidence in south-central Apulia Italy.- International Journal of Speleology, 31 (1/4), 181–199.

Delle Rose, M. & M. Parise, 2003: Il condizionamento di fattori geologico-strutturali e idrogeologici nella speleogenesi di grotte costiere del Salento.- In: *Proc. XIX Nat. Congr. Spel., Bologna,* 27–31 August 2003, 27–36.

Delle Rose, M. & M. Parise, 2005: Speleogenesi e geomorfologia del sistema carsico delle Grotte della Poesia nell'ambito dell'evoluzione quaternaria della costa Adriatica Salentina.- Atti e Memorie Commissione Grotte "E. Boegan", 40, 153–173.

Delle Rose, M., Federico, A. & M. Parise, 2004: Sinkhole genesis and evolution in Apulia, and their interrelations with the anthropogenic environment.- Natural Hazards and Earth System Sciences, 4, 747–755.

Delle Rose, M., Parise, M. & G.F. Andriani: 2007: Evaluating the impact of quarrying on karst aquifers of Salento (southern Italy).- In: Parise, M. & J. Gunn (Eds.): *Natural and anthropogenic hazards in karst areas: Recognition, Analysis and Mitigation.* Geological Society, London, Special Publications 279, pp. 153–171.

Del Prete, S., Iovine, G., Parise, M. & A. Santo, 2010: Origin and distribution of different types of sinkholes in the plain areas of Southern Italy.- Geodinamica Acta, 23, 1/3, 113–127.

De Pascalis, A., De Pascalis, F. & M. Parise, 2010: Genesi ed evoluzione di un sinkhole connesso a cavità antropiche sotterranee nel distretto estrattivo di Cutrofiano (prov. Lecce, Puglia).- *Proc. 2° Workshop Int. "I sinkholes. Gli sprofondamenti catastrofici nell'ambiente naturale ed in quello antropizzato",* Roma, 3–4 dicembre 2009, 703–718.

De Waele, J., Gutierrez, F., Parise, M. & L. Plan, 2011: Geomorphology and natural hazards in karst areas: a review.- Geomorphology, 134, 1–2, 1–8.

Di Bucci, D., Coccia, S., Fracassi, U., Iurilli, V., Mastronuzzi, G., Palmentola, G., Sansò, P., Selleri, G. & G. Valensise, 2009: Late Quaternary deformation of the southern Adriatic foreland (southern Apulia) from mesostructural data: preliminary results.- Italian Journal of Geosciences, 128, 1, 33–46.

Doglioni, C., 1991: A proposal of kinematic modelling for W-dipping subductions – Possibile applications to the Tyrrenian-Apennines system.- Terra Nova, 3, 423–434.

Drake, J.J. & Ford, D.C., 1972: The analysis of growth patterns of two-generation populations: the example of karst sinkholes.- Can. Geogr., 16, 381–384.

Dunne, T., 1990: Hydrology, mechanics, and geomorphic implications of erosion by subsurface flow. – In: Higgins, C.G. & D.R. Coates, (Eds.): *Groundwater geomorphology.* Geological Society of America spec. paper 252, pp. 1-28.

Festa, V., Fiore, A., Parise, M. & A. Siniscalchi A., 2012: Sinkhole evolution in the Apulian karst of southern Italy: a case study, with some considerations on sinkhole hazards.- Journal of Cave and Karst Studies, 74, 2, 137–147.

Funiciello, R., Montone, P., Parotto, M., Salvini, F. & M. Tozzi, 1991: Geodynamic evolution of an intraorogenic foreland: the Apulia case history (Italy).- Boll. Soc. Geol. It., 110, 419–425.

Gambini, R. & M. Tozzi, 1996: Tertiary geodynamic evolution of the Southern Adria microplate.- Terra Nova, 8, 593–602.

Gil, H., Pepe, M., Soriano, M.A., Parise, M., Pocoví, A., Luzón, A., Pérez, A. & A. Basso, 2013: Sviluppo ed evoluzione di sprofondamenti in rocce solubili: un confronto tra il carso coperto del Bacino dell'Ebro (Spagna) e la Penisola Salentina (Italia).- Memorie Descrittive Carta Geologica d'Italia, 93, 253–276.

Giuliani, P., 2000: Elenco delle grotte pugliesi catastate al 31 ottobre 1999.- Itinerari Speleologici, 9, 5–41.

Iurilli, V., Cacciapaglia, G., Selleri, G., Palmentola, G. & G. Mastronuzzi, 2009: Karst morphogenesis and tectonics in south-eastern Murge (Apulia, Italy).- Geogr. Fis. Dinam. Quat., 32, 145–155.

Lollino, P. & M. Parise, 2010: Analisi numerica di processi di instabilità di cavità sotterranee e degli effetti indotti in superficie.- *Proc. 2nd Int. Workshop "I sinkholes. Gli sprofondamenti catastrofici nell'ambiente naturale ed in quello antropizzato",* Rome, 3–4 december 2009, 803–816.

Lollino, P., Martimucci, V. & M. Parise, 2013: Geological survey and numerical modeling of the potential failure mechanisms of underground caves. - Geosystem Engineering, 16, 1, 100–112.

Lopez, N., Spizzico, V. & M. Parise, 2009: Geomorphological, pedological, and hydrological characteristics of karst lakes at Conversano (Apulia, southern Italy) as a basis for environmental protection.- Environmental Geology, 58, 2, 327–337.

Margiotta, S., Negri, S., Parise, M. & R. Valloni, 2012: Mapping the susceptibility to sinkholes in coastal areas, based on stratigraphy, geomorphology and geophysics.- Natural Hazards, 62, 2, 657–676.

Mills, H.H. & D.D. Starnes, 1983: Sinkhole morphometry in a fluviokarst region: eastern Highland Rim, Tennessee, U.S.A.- Z. Geomorphol., 27, 39–54.

Mostardini, F. & S. Merlini, 1986: Appennino Centro Meridionale e Proposta di Modello Strutturale.- Mem. Soc. Geol. Ital., 35, 177–202.

Neboit, R., 1975: Plateaux et collines de Lucanie orientale et des Pouilles. Étude morphologique. Libr. Honore Champion, 715 pp, Paris.

Palmentola, G., 1987: Lineamenti geologici e morfologici del Salento leccese.- Quaderni Ricerche Centro Studi Geotecnica e di Ingegneria, 11, 7–30, Lecce.

Parise, M., 2003: Flood history in the karst environment of Castellana-Grotte (Apulia, southern Italy).- Natural Hazards and Earth System Sciences, 3, 6, 593–604.

Parise, M., 2006: Geomorphology of the Canale di Pirro karst polje (Apulia, Southern Italy).- Zeitschrift für Geomorphologie N.F. 147, 143–158.

Parise, M., 2008a: I sinkholes in Puglia.- In: Nisio S. (Ed.) I fenomeni naturali di sinkhole nelle aree di pianura italiane.- Memorie Descrittive della Carta Geologica d'Italia, 85, 309–334.

Parise, M., 2008b: Elementi di geomorfologia carsica della Puglia.- In: Parise M., Inguscio S. & Marangella A. (eds.), *Atti del 45° Corso CNSS-SSI di III livello di "Geomorfologia Carsica*. Grottaglie, 2–3 febbraio 2008, 93–118.

Parise, M., 2009: Lakes in the Apulian karst (Southern Italy): geology, karst morphology, and their role in the local history.- In: Miranda, F.R. & L.M. Bernard, (eds.) *Lake pollution research progress.* Nova Science Publishers, Inc., New York, pp. 63–80.

Parise, M., 2010a: The impacts of quarrying in the Apulian karst.- In: Carrasco F., La Moreaux J.W., Duran Valsero J.J. & Andreo B. (eds.), *Advances in research in karst media*. Springer, 441–447.

Parise, M., 2010b: Hazards in karst.- In: O. Bonacci (Ed.) *"Sustainability of the karst environment. Dinaric karst and other karst regions"*. IHP-UNESCO, Series on Groundwater no. 2, 155–162.

Parise, M. & J. Gunn (eds.), 2007: *Natural and anthropogenic hazards in karst areas: Recognition, Analysis and Mitigation.*- Geological Society, London, Special Publications, 279.

Parise, M. & P. Lollino, 2011: A preliminary analysis of failure mechanisms in karst and man-made underground caves in Southern Italy.- Geomorphology, 134, 1–2, 132–143.

Parise, M., Federico, A., Delle Rose, M. & M. Sammarco, 2003: Karst terminology in Apulia (southern Italy).- Acta Carsologica, 32, 2, 65–82.

Pepe, M. & M. Parise, 2011: Structural control in sinkhole development: the case study of Barbarano del Capo (Salento peninsula, Apulia region, South-East Italy).- Proc. 1st Int. Workshop "Methods and Technologies for Environmental Monitoring and Modelling: Landslides and Ground Water Dynamics", Potenza, 29 September – 3 October 2011, 153–157.

Pieri, P., Festa, V., Moretti, M. & M. Tropeano, 1997: Quaternary tectonic of the Murge area (Apulian foreland – Southern Italy).- Annali di Geofisica, 40, 5, 1395–1404.

Ricchetti, G., 1980: Contributo alla conoscenza strutturale della Fossa Bradanica e delle Murge.- Boll. Soc. Geol. It., 49, 4, 421–430.

Ricchetti, G. & N. Ciaranfi, 2009: Note illustrative della Carta Geologica d'Italia alla scala 1:50.000, foglio 536 "Ugento", 121 pp., Litografia Artistica Cartografica S.r.l., Firenze(website http://www.isprambiente.gov.it/Media/carg/note_illustrative/536_Ugento.pdf).

Ricchetti, G., Ciaranfi, N., Luperto Sinni, E., Mongelli, F. & P. Pieri, 1988: Geodynamics and sedimentary and tectonic evolution of the Apulian Foreland [in italian].- Mem. Soc. Geol. It., 41, 57–82.

Royden, L., Patacca, E. & P. Scandone, 1987: Segmentation and configuration of subducted lithosphere in Italy: an important control on thrust-belt and foredeep-basin evolution.- Geology, 15, 714–717.

Sammarco, M. & M. Parise, 2008: Cavità artificiali per uno studio di storia salentina: il caso dell'ipogeo di Leuca Piccola a Barbarano (Lecce).- Proc. XX Congr. Naz. Speleologia, Iglesias, Memorie dell'Istituto Italiano di Speleologia, s. II, 21, 546–550

Schumm, S., 1956: Evolution of drainage systems and slopes in badland at Perth Amboy, New Jersey.- Bulletin of Geological Society of America, 67, 597–646.

Šebela, S., 1998: Tectonic structure of Postojnska Jama cave system.- Založba ZRC 18, 112 pp., Ljubljana.

Šebela, S., Gosar, A., Košťák, B. & J. Stemberk, 2005: Active tectonic structures in the W part of Slovenia – Setting of micro-deformation monitoring net.- Acta Geodyn. Geomater., 2, 1, 45–57, Prague.

Tozzi, M., 1993: Assetto tettonico dell'Avampaese Apulo meridionale (Murge meridionali-Salento) sulla base dei dati strutturali.- Geologica Romana, 29, 95–111.

Waltham, T., Bell, F. & M. Culshaw, 2005: *Sinkholes and Subsidence: Karst and Cavernous Rocks in Engineering and Construction*.- Springer Praxis, Berlin.

Williams, P.W., 1971: Illustrating morphometric analysis of karst with examples from New Guinea.- Z. Geomorphol., 15, 40–61.

COBISS: 1.01

STRUCTURAL GEOLOGICAL CHARACTERISTICS OF KARST CAVES AND MAJOR STONE FOREST, YUNNAN, CHINA

STRUKTURNO GEOLOŠKE ZNAČILNOSTI KRAŠKIH JAM IN GLAVNEGA KAMNITEGA GOZDA, YUNNAN, KITAJSKA

Stanka ŠEBELA[1] & Hong LIU [2,3]

Abstract UDC 551.435.84:551.243(510)

Stanka Šebela & Liu Hong: Structural geological characteristics of karst caves and Major stone forest, Yunnan, China

Karst areas of Shilin County southeast of Kumning were studied to understand the role of geological structures in the formation of karst features as stone forest and selected caves. Detailed structural geological mapping of fissure orientations within selected caves and of the Major stone forest was accomplished and presented as rose diagrams. Regional geological structures were compared with statistical evaluation of structural geological elements obtained from field mapping. There is a good correlation between surface and underground fissure orientations and cave passage orientations with regionally important fault zones, including the Xiaojiang Fault (N-S direction) and Red River Fault (NW-SE direction). The most frequent cave passages orientation, in a nearly N-S direction, is associated with nearly E-W compression and nearly N-S extension from late Pliocene to mid-Pleistocene. A second tectonic stage from late-Pleistocene to the present, with the tectonic stress field mainly of NNW-SSE compression and NEE-SWW extension, is in accordance with the most frequent fissure orientations in Major stone forest with a direction of N20–30°W (11.4%).

Keywords: structural geology, rose diagrams, karst caves, Major stone forest, Yunnan, China.

Izvleček UDK 551.435.84:551.243(510)

Stanka Šebela & Hong Liu: Strukturno geološke značilnosti kraških jam in glavnega kamnitega gozda, Kitajska

Proučevali smo kraške terene v okrožju Shilin JV od Kumninga, da bi razumeli vlogo geoloških struktur pri oblikovanju kraških pojavov kot kamnitih gozdov in izbranih jam. Izvedli smo podrobno strukturno geološko kartiranje smeri razpok v izbranih kraških jamah ter v glavnem kamnitem gozdu, kar je predstavljeno z rozetami. Rezultate strukturnih geoloških elementov pridobljenih s terenskim kartiranjem smo primerjali z regionalnimi geološkimi strukturami. Obstaja dobra korelacija med površinskimi in podzemeljskimi smermi razpok ter med smerjo jamskih rovov in regionalno pomembnimi prelomnimi conami, to je s prelomom Xiaojiang (smer S-J) in s prelomom Red River (smer SZ-JV). Najpogostejša smer jamskih rovov v generalni smeri S-J je povezana s kompresijo v smeri skoraj V-Z ter z ekstenzijo v generalni smeri S-J iz obdobja zgornjega Pliocena do srednjega Pleistocena. Druga tektonska faza iz zgornjega Pleistocena do danes, z napetostjo tektonskega polja predvsem s kompresijo v smeri SSZ-JJV in ekstenzijo v smeri SVV-JZZ je v skladu z najpogostejšo smerjo razpok v glavnem kamnitem gozdu v smeri S20–30°Z (11,4%).

Ključne besede: strukturna geologija, rozete, kraške jame, glavni kamniti gozd, Yunnan, Kitajska.

INTRODUCTION

Exposed karst areas in China comprise about 9.3% of the territory. In Yunnan karst landscapes comprise 44% of the area. Stone forests (shilins in Chinese) are the most notable karst areas in Yunnan. The Major and Naigu stone forests are part of the South China Karst region inscribed in UNESCO World Heritage List since 2007. The South China Karst region encompasses over half a million square km, and represents one of the most spec-

[1] ZRC SAZU Karst Research Institute, Titov trg 2, 6230 Postojna, Slovenia, e-mail: sebela@zrc-sazu.si
[2] Yunnan Institute of Geography, Yunnan University, Xuefu rd. 20, CN-650223 Kunming, P.R.China, e-mail: hongliu@yni.edu.cn
[3] Yunnan International Karst Environmental Laboratory, Xueyun rd. 5, CN-650223 Kunming, P.R.China

Received/Prejeto: 25.01.2013

tacular examples of humid tropical to sub-tropical karst, a type of terrain formed mainly by dissolving rock that usually features fissures, sinkholes, underground streams and caves.

The Major stone forest was visited by an average of 1 million people per year by 1988 and by 2.05 million visitors in 2005. Karst areas are important for tourism as well as the economic development of the area (Knez *et al.* 2012a, b).

Recent investigations of Chinese karst geomorphology are numerous (Luo *et al.* 2003; Gu *et al.* 2002; He *et al.* 2001; Song & Liang 2001; Frančišković-Bilinski *et al.* 2003; Šebela *et al.* 2001; Šebela *et al.* 2004; Kogovšek 2010; Knez & Slabe 2010; Knez *et al.* 2010; Knez *et al.* 2011; Knez *et al.* 2012a, etc.).

Karst caves are also good places to study different climate conditions (Wang *et al.* 2001), as well as paleomagnetic and tectonic conditions in the last 100,000 to 500,000 years.

The principal aim of this study was to identify the significant structural geological elements that influence the formation and shaping of selected karst caves and shilins in Shilin County (Yunnan) and to identify possible connections between karst forms and active tectonic structures.

STRUCTURAL GEOLOGY OF THE STUDY AREA

The study area shows tectonic deformation due to the movement of the Asian continent caused by the thrust of the Indian collision. The great geological discontinuity that separates Cambodia, Laos and Vietnam from China results from Cenozoic strike-slip strain. This suggests that this narrow zone acted as a continental transform plate boundary in the Oligo-Miocene. Extrusion of Cambodia, Laos and Vietnam alone accounted for 10–25% of the total shortening of the Asian continent. The territory of Cambodia, Laos and Vietnam was extruded towards the SE as a result of the India-Asia collision (Leloupe *et al.* 1995).

The Tibetan Plateau is a region where modern tectonic movement is the most intensive. The collision between the Indian Plate and Eurasian Plate, the uplifting of the Tibetan Plateau, and its influence on the tectonic movement of eastern part of the Asia Continent represent an important influence on the region. The collision between the two plates leads to the sharp upheaval of the Tibetan Plateau and the obvious thickening of its underlying crust (Wang *et al.* 2003).

Crustal motion in the eastern Tibetan Plateau is caused by Indo-Asian collision (Gang & Mian 2010). Tectonic stress from the relative movement between the Indo-Australian and Eurasian plates causes a strong compressive stress in the NNE-SSW direction and the N-S crust shortening in the Tibetan plateau and its surroundings (Xu & Zhao 2010).

Present-day tectonic styles and rates cannot be extrapolated far into the past because the deformation of Asia started only with the onset of collision, prior to 50 Ma. Large-scale left-lateral shear followed by a reversal to right lateral occurred along the Ailao Shan-Red River zone in the mid-late Cenozoic (Leloupe *et al.* 1995).

The Red River Fault zone (Fig. 1) is the major geological discontinuity that separates South China from territory of Cambodia, Laos and Vietnam. Motion along the Red River Fault zone switched from left lateral in the Oligo-Miocene to right lateral in the Plio-Quaternary. Estimates have ranged from 200–250 km right lateral to more than 1500 km left lateral movement (Leloupe *et al.* 1995). The current dextral slip-rate is 2–10 mm/yr (Allen *et al.* 1984; Wang & Burchfield 2000). The present-day stress field is NNW-SSE shortening. The Ailao Shan-Red River shear zone is mostly strike-slip with transpression in the NW and transtension in the SE (Briais *et al.* 1993).

Tomography shows that there is an obvious lower velocity plume upwelling at 450-km depth at the western side of the Red River Fault. Studies provide seismic evidence for the subducting slab, which is located at around western side of the Red River Fault, and for subduction towards the northeast. Seismic evidence is presented for an upwelling mantle plume, the main cause of which is leading to subduction in West Yunnan (He 2011).

The Xianshui He Fault is an active left-lateral strike-slip fault in the southeastern Tibetan Plateau. It is a major strike-slip fault accommodating the east-southeast extrusion of the Tibetan lithosphere. Both geological and GPS measurements indicate 10–20 mm/year slip on the northwestern segments and 5–9 mm/year on the southeastern segments of the Xianshui He Fault. There were six $M \geq 6.9$ earthquake events between 1893 and 1981. However, no $M \geq 5$ events have occurred on the fault since 1981. Because of its high slip rates and frequent earthquakes, the Xianshui He Fault has been the focus of attention within the seismological community (Gang & Mian 2010).

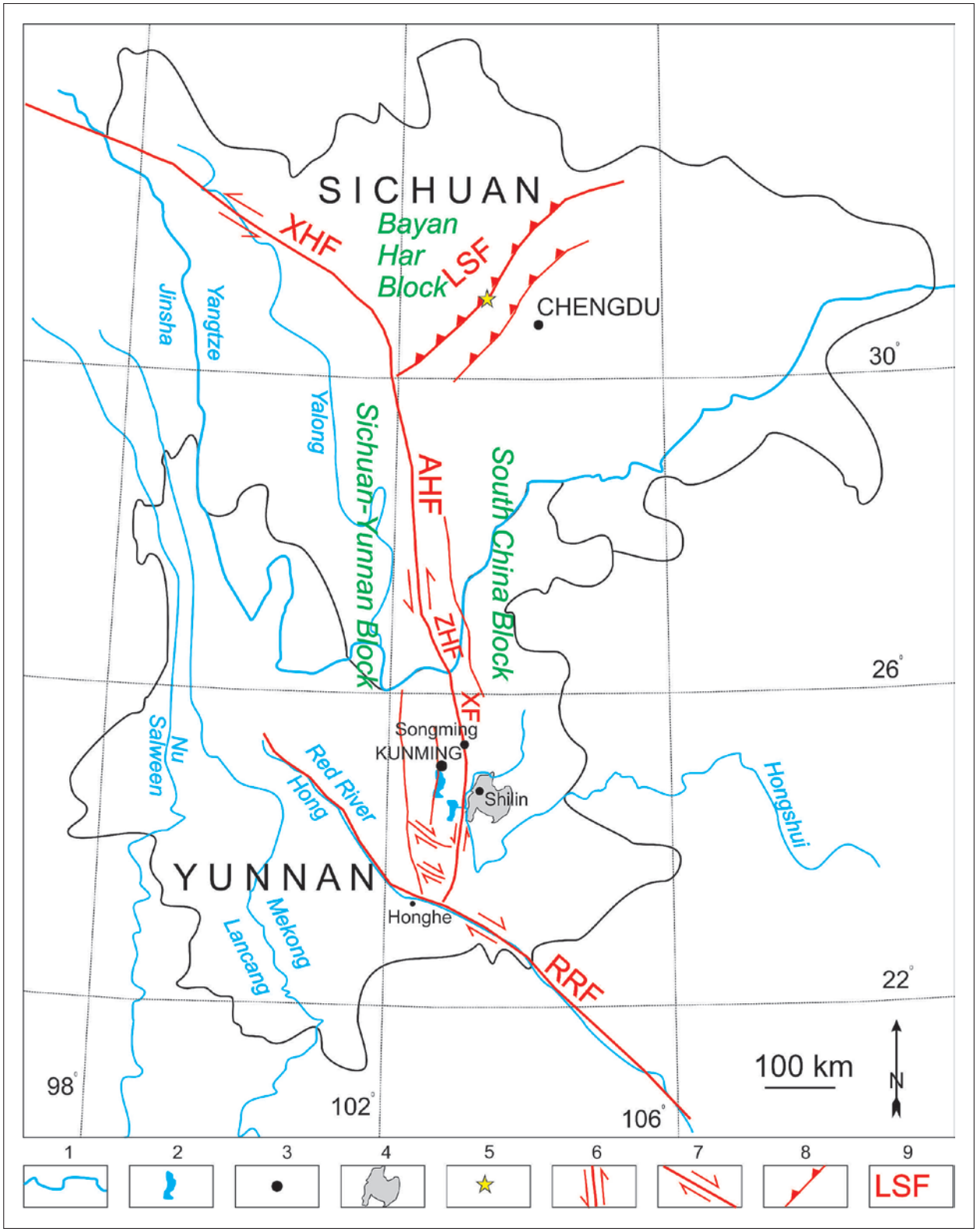

Fig. 1: Structural-geological position of Shilin County in Yunnan Province, south China. 1– river, 2– lake, 3– town, 4– Shilin county, 5– 2008 Wenchuan earthquake, 6– sinistral horizontal strike-slip fault, 7– dextral horizontal strike-slip fault, 8– thrust fault, 9– faults (LSF– Longmen Shan Fault, XHF– Xianshui He Fault, AHF– Anning He Fault, ZHF– Zemu He Fault, XF– Xiaojiang Fault, RRF– Red River Fault).

Major earthquakes along the Xianshui He Fault zone all occurred within the region with positive Coulomb failure stress change, except for Zhuwo earthquake in 1967. In other words, the occurrence of major earthquakes along the Xianshui He Fault zone influences the occurrence of subsequent earthquakes (Wang *et al.* 2008).

The Xianshui He-Xiaojiang Fault zone and the Longmenshan Fault zone divide this region into 3 tectonic blocks: the Sichuan-Yunnan Block, the Bayan Har Block and the South China Block. The Xianshui He-Xiaojiang fault is also one of the most active fault zones in Chinese mainland. Although present-day activity in the Longmenshan fault zone is weak, the seismogenic fault produced the *Ms* = 8.0 Wenchuan earthquake (Fig. 1) on 12 May 2008 (Wang *et al.* 2010). The arc-like Xianshui He-Xiaojiang Fault system extends for 1500 km within Qinghai, Sichuan and Yunnan province and ends at point north of the Red River Fault zone (He & Yasutaka 2007).

The Anning He-Zemu He-Xiaojiang Fault system, also called the Xiaojiang Fault system is the southward continuation of the Xianshui He Fault. Geological and GPS slip rates are 5–10 mm/year along the northern segments and 4 mm/year along the southern segments. More than ten $M > 6$ earthquakes have occurred along the Xiaojiang Fault system in the past 500 years; the largest one was the 1833 *M* 8.0 Songming earthquake on the central segment of the Xiaojiang Fault. After the 1850 *M* 7.5 Xichang earthquake, three *M* 6.5–6.8 earthquakes occurred on this fault system in 1909, 1952, and 1966 (Gang & Mian 2010). The average sinistral strike-slip rate on the Anning He Fault since the Late Pleistocene is about 3–7 mm/a (He & Yasutakyr 2007).

The Kunming basin is a new generation faulted basin, which is controled by active north-south trending faults. Stress fields in the region of Kunming had two major stages. In the first stage (from late-Pliocene to mid-Pleistocene) the tectonic stress field was characteristic of nearly E-W compression and nearly N-S extension. In the second stage (from late-Pleistocene to the present) the tectonic stress field has been mainly consistent with NNW-SSE compression and NEE-SWW extension (Yi *et al.* 2010).

The Kunming basin is the largest Quaternary-inherited downfaulted basin in the Yunnan-Guizhou plateau, where the strata deposited in Quaternary are characterized by large variations of thickness and complicated facies. The Quaternary tectonic activity of the Xiaojiang Fault zone is characterized by strong sinistral strike slip (Wang *et al.* 2009).

During the late Cenozoic, inhomogeneously distributed extension has been expressed by numerous Quaternary basins along the southern part of the Xianshui He-Xiaojiang Fault system (Fig. 1). Quaternary basins and lakes north of Dali and within the southern part of the Xiaojiang Fault zone are areas of local active extension (Wang & Burchfield 2000).

The Pliocene-Quaternary sedimentary fill in pull-apart basins associated with the left lateral Xianshui He-Xiaojiang Fault system indicates that this structure was initiated by at least 2–4 Ma ago (Wang *et al.* 1998).

Xianshui He-Xiaojiang Fault is left lateral structure. There is southwestward extrusion from eastern Tibetan Plateau and clockwise rotation around the Eastern Himalayan Syntaxis of the rhomboid-shaped Sichuan-Yunnan block, which is moving faster than the plateau. The Xiaojiang Fault zone has N-S strike and a total length of 400 km in Yunnan Province. The Xiaojiang Fault zone is exhibiting significant neotectonic activity. Since the end of Late Pleistocene the strike slip rate has been found to be about 6 mm/yr along the southern segment of the eastern branch of Xiaojiang Fault zone (Paradisopoulou *et al.* 2007).

The crustal structure shows remarkable contrasts between the two sides of the Xiaojiang Fault zone. The crust to the east of the Xiaojiang Fault zone presents characteristics of crustal structure in a stable platform, while the crust to the west is complicated with a lower velocity zone in middle of the upper crust. It is inferred that the Xiaojiang Fault zone has cut through the entire thickness of the crust (Wang *et al.* 2009).

Assuming that the slip rate of 15±2 mm/yr is constant throughout the entire history of the Xianshui He-Xiaojiang Fault system, 11±1.5 Ma is needed for the Xianshui He-Xiaojiang Fault system to attain the 160 km of total offset. This implies that left-slip faulting on the Xianshui He-Xiaojiang Fault system might have started at 11±1.5 Ma (He *et al.* 2006).

The Longmen Shan Fault zone is the boundary between the Tibetan Plateau and the rigid South China Block. The loading rate on the Longmen Shan Fault is lowered when the Xianshui He Fault experiences clusters of big earthquakes (Gang Luo & Mian Liu 2010).

Crustal motion in the western Sichuan area presents a clockwise rotation around the Eastern Himalayan Syntax. The crust moves southward in the interior of Sichuan-Yunnan Block, and moves southwestward in the southwest Yunnan region (Wang *et al.* 2010).

The focal mechanisms of the 1966 earthquakes on the N-S striking Xiaojiang Fault (Fig. 1) imply left-lateral slip along it. A normal component of slip on the roughly N-S faults south of Kunming has created several Quaternary half-grabens, some of them filled by lakes (Tapponier & Molnar 1977).

The 12 May 2008 Wenchuan earthquake ruptured about 300 km of the Longmen Shan Fault (Fig. 1) in the

eastern Tibetan Plateau. In spite of stress increase from the Wenchuan earthquake, the southeastern segments of the Xianshui He Fault stay in a stress shadow because of the stress release by six $M \geq 6.9$ events in this part of the Xianshui He Fault since 1893 (Gang & Mian 2010). The Great Wenchuan earthquake came as a surprise, because that part of the fault has low fault slip rates, which are less than 3 mm/year, one order of magnitude lower than slip rates on the Xianshui He Fault and other major faults in eastern Tibet (Gang & Mian 2010).

METHODOLOGY

Detailed structural geological mapping was accomplished in the studied area, including the area of Major Shilin (0.7 km²) and selected caves (Jibailongdong, Dieyundong, Zhiyundong, Baiyun cave, Guanyindong, Xinshidong, Niubizidong, Xifenlandong and Shimalogdong). Fissure orientations were analysed by RockWare softwear and presented by rose diagrams at 10 degree class intervals. Cave passage orientations were weighted according to speleological maps, analysed by RockWare softwear and presented by rose diagrams as well. Finally, the obtained results were compared with regional structural geological conditions and active tectonic situation regarding studied references.

RESULTS

MAJOR STONE FOREST

The Major stone forest (Figs. 2, 3 and 4) is one of the best known tourist sites in Yunnan. It is situated about 80 km southeast of Kunming (Fig. 1). Shilin is a type of pinnacle karst formed on a plateau of gently dipping limestone (Knez & Slabe 2002). Subsoil karren and stone forests are one of the most characteristic features of the karst surface in Yunnan. Carbonate rocks are in many places covered by thick sediments under which subsoil karren developed into stone forests (Knez & Slabe 2010).

Stone forest refers to a particular karst landscape, composed of a group of densely distributed limestone columns standing on an undulating karst plateau. The columns are usually 10 m high, with their upper part decorated with sharp karren. The formation of rocky columns is closely related to the subsoil dissolution by the CO_2-rich vadose water (Xie & Li 1995–1999).

The main strata in the Major stone forest area include carbonate rocks of the Qixia Formation and Maokou Formations of Lower Permian age. These units average 505 m thick and consist of shallow sea platform facies, massive dolomites, bioclastic limestones, calcarenites and calcilutites. Most of the carbonate rocks in the area are coarsely crystalline, which makes dissolution relatively easy (Chen *et al.* 1998). Basalts of the Late Permian age (Song & Liang 2009) and red mudstones, siltstones, sandstones and conglomerates of the Tertiary age, constitute the cover of karst terrain (Xie & Li 1995–1999).

The strata are part of a westward dipping (2–6°) monocline. Conjugate shear joints (NE-SW and NW-SE) are well developed and these fractures provided the main passageways for surface water and underground water in the pre-karst development stage. The distribution, density and orientation of the fractures controlled the depth, size and orientation of the karst topography.

The Shilin karst area covers 350 km². Around 70 caves (Fig. 2) have been explored from 1995–2000. They can be classified into three types. The first are fracture-like caves, formed by enlargement by water along fractures. The second types, horizontal caves, are mainly developed in the Fengcong (peak cluster) shallow depression landscape areas, adjacent to the Shilin landscapes. The third types, slope caves, are mainly distributed at Fengcong-depression karst areas or hillsides of lower mountains, where ground water table is around 100–150 m deep. Generally cave development in Shilin area has five characteristics. (1) Cave development is mainly concentrated in three elevation zones. (2) The development of caves is strongly controlled by the lithology of carbonate rocks. Most caves developed in Permian and Carboniferous carbonates. (3) Small (some 10 m long) and medium (some 100 m long) scale caves dominate. (4) Most caves have active water flow. (5) The orientation of cave passages is obviously controlled by structural orientation of fissures. There is a great difference between caves of the east and west part of the region. In west the orientation of caves is dominantly

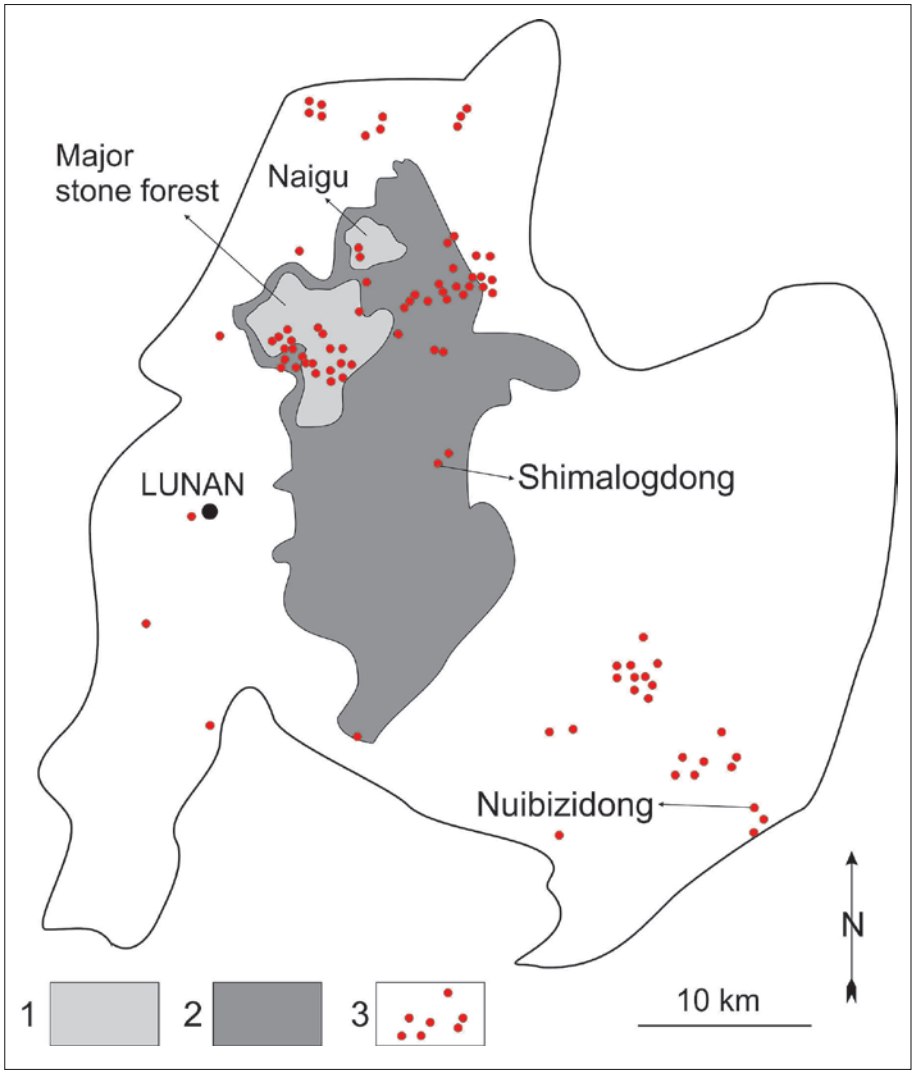

Fig. 2: Protected karst areas of Shilin County. 1 – 1st and 2nd class protected area (Major and Naigu stone forests), 2 – 3rd class protected area, 3 – karst caves (after Knez et al. 2011).

N-S or near N-S direction. But in the east the W-E or near W-E orientation predominates (Liu & Yan 2003). Song & Liang (2009) presented two evolution models of Shilin landscapes. In first model the shilin landscape on karst hilltops is guided by spacing of fractures, where soil and residuum are very thin. The second model represents shilin development in the basalt area that covers palaeokarst features. Karst development in limestone

Fig. 3. Major stone forest (Photo: S. Šebela).

Fig. 4. Major stone forest (Photo: S. Šebela).

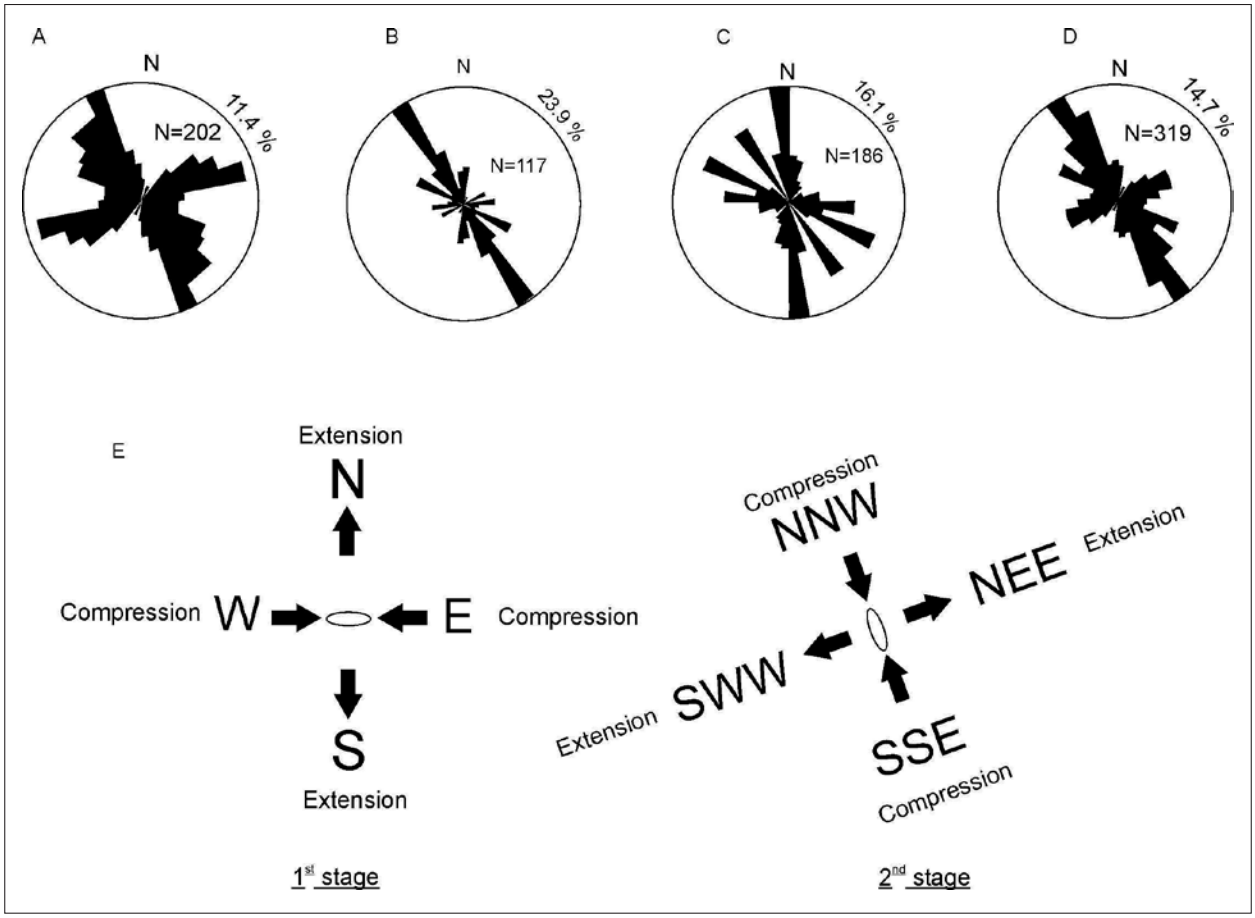

Fig. 5: Rose diagrams with 10° class intervals. A – Fissure orientations at the Major stone forest, B – Fissure orientation of cave passages (Jibailongdong, Dieyundong, Zhiyundong, Baiyun Cave), C – Passage orientations of caves (Jibailongdong, Dieyundong, Zhiyundong, Baiyun Cave, Guanyindong, Xinshidong, Niubizidong, Xifenlandong and Shimalogdong), D – Fissure orientations of the Major stone forest and caves (Jibailongdong, Dieyundong, Zhiyundong, Baiyun Cave), E – Quaternary tectonic stress field (1st stage – late Pliocene-mid Pleistocene; 2nd stage – late Pleistocene-present, after Yi et al. 2010).

under the basalt is stronger than in soil-covered limestone (Song & Liang 2009; Ginés *et al.* 2009).

The Major stone forest is situated at about 1750 m above sea level and Naigu stone forest at 1820 m above sea level (Fig. 2). Main geomorphological types are plateau hills, low mounts, depressions, basins, stone hillocks, stone forests, fields of "stone teeth", lakes and river valleys (Xie & Li 1995–1999).

The results of detailed structural geological field mapping of Major stone forest are presented as rose diagrams (Fig. 5, A). The prevailing fissure orientation at Shilin is N20–30°W and represents 11.4%. The second most frequent is the direction N70–80°E (11%). Generally there are two prevailing fissure orientations, the most represented NW–SE and the second-one NE–SW (almost close to E–W).

Limestone bedding-planes in Major stone forest are mostly subhorizontal or dip at a 5° angle. There are some gentle anticlines.

SELECTED KARST CAVES OF THE SHILIN COUNTY

In the vicinity of the Major stone forest, we studied nine karst caves (Jibailongdong, Dieyundong, Zhiyundong, Baiyun cave, Guanyindong, Xinshidong, Niubizidong, Xifenlandong and Shimalogdong, Fig. 6) and performed structural geological mapping of four caves (Jibailongdong, Dieyundong, Zhiyundong, Baiyun cave (Šebela *et al.* 2001; Šebela *et al.* 2004)). Karst caves are found below densely packed pinnacles. Rose diagrams of cave passage orientations are presented for 6.2 km of cave passages.

DIEYUNDONG

The northern cave entrance is situated at 1715 m above the sea. The cave is 280 m long (Fig. 6). At the SE part of the cave the bedding-planes dip at 5° towards south and the rock is mostly Permian thick-bedded limestone.

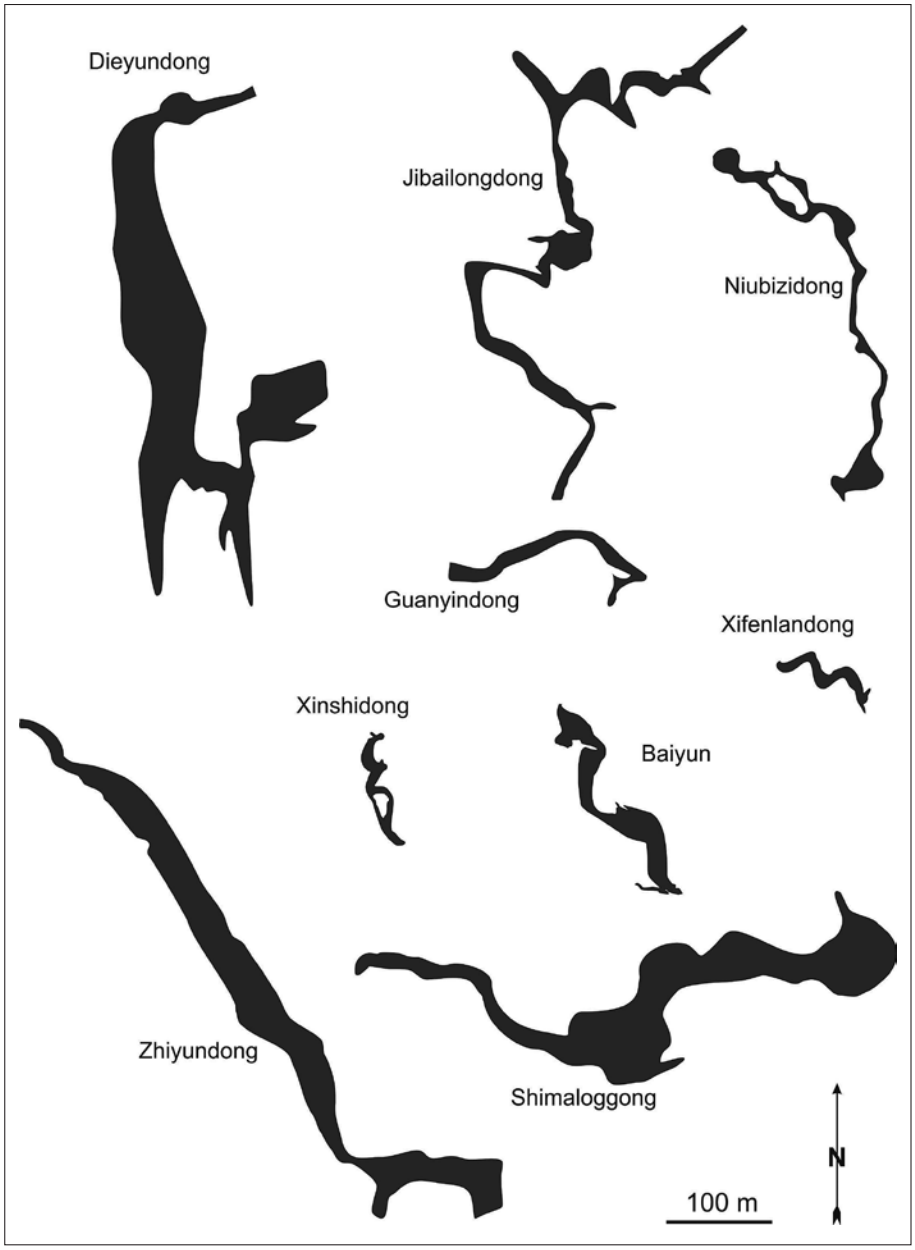

Fig. 6: Studied caves ground-plans (maps are not in the actual relative location with respect to one another).

The most frequent passage orientation is N0–10°W (48.7%), the second direction is N0–10°E (23%) and the third direction is N50–60°E (15%). Prevailing fissures are oriented N0–10°E (40.9%) and N0–10°W (35%). Passages and fissures are prevailingly oriented in the direction N–S (Šebela *et al.* 2004).

JIBAILONGDONG

The cave (1730 m above the sea) is 460 m long (Fig. 6). The passage is developed mostly in Permian thick bedded limestone. The dip angle of the bedding-planes is 0–5° mostly towards NW, and in southern part also towards SE. In the cave three main passage directions are observed: N0–10°W (21.9%), N50–60°W (17%) and N80–90°E (9%). The passage runs in the general directions of N–S and NW–SE. The most frequent fissure orientation measured in the cave is N60–70°W (35%), the second direction is N10–20°W (20%) and the third one is N30–40°W (15%). The prevailing fissure orientation is NW-SE (Šebela *et al.* 2004).

ZHIYUNDONG

The general passage orientation is NW–SE (Figs. 6 and 7). The cave is 360 m long and situated 1755 m above the sea. The predominant thick-bedded Permian limestone dips towards W and NW at 5°. Along the 172°/90°

joint at northern part of the cave a small (0.5 cm) dextral horizontal strike-slip movement was determined. Most fissures run in NW–SE direction. The most frequent orientation of the passage is N30–40°W (47.1%), in the second place are two directions N90–100°E (16%) and N60–70°W (16%). Most fissures in the cave are oriented N40–50°W (35.7%) and N50–60°W (28%) (Šebela *et al.* 2004).

Fig. 7: Zhiyundong entrance (Photo: S. Šebela).

GUANYINDONG

The cave is situated about 10 km NE from the Major stone forest. It is 240 m long and represents an active ponor cave (Fig. 6). The prevailing passage direction is N60–70°E (29.4%), the second direction is N40–50°W (24%) and the third N80–90°E (17%). There are two principal fissure orientations N–S and almost E–W. Permian limestones dip for 5–10° mostly towards SE.

BAIYUN CAVE

Baiyun Cave is situated inside the Naigu stone forest (Figs. 2, 6 and 8), which covers an area of 8 km^2 and is developed in the dolomite and limestone of the Permian Qixia formation. There are unique shapes like mushrooms, resulting from the differential dissolution of the different lithologies.

The cave is situated at an altitude of 1700 m. The general direction of the cave is NW–SE. The passage is up to 25 m wide and 380 m long. The prevailing fissure direction in the cave is N30–40°W (36.1%). The second prevailing direction is N20–30°W (23%). Regarding the tectonic situation, the Baiyun Cave is situated about 20 km east of the Xiaojiang fault system (Fig. 1), which runs in the general direction N–S. The cave has 36.6% of its passages in the direction N0–10°W, and in second place 27% in the direction N110–120°E.

The prevailing fissure direction and prevailing direction of cave passages of Baiyun Cave do not compare well (Šebela *et al.* 2004).

Fig. 8: Naigu stone forest (Photo: S. Šebela).

XINSHIDONG

The cave (Fig. 6) is situated at the SE corner of Naigu stone forest at 1785 m above the sea and has 175 m of passages developed in Permian limestones. At the northern entrance the beds dip for 5° towards NW. The prevailing passage orientation is N20–30°W (25%), the second is N20–30°E (21%) and the third is N10–20°E (18%). The cave walls have been covered by cave sediments and fissures are not well detected.

The rose diagram for combined fissure orientations for four caves (Jibailongdong, Dieyundong, Zhiyundong, Baiyun Cave) includes a population of 117 measurements (Fig. 5, B). The maximum percentage of 23.9% belongs to the N30–40°W direction, 13% has a N20–30°W direction and 11% belong to N60–70°W. The N-S direction (N0–10°W) represents 6% and direction N0–10°E is 7%. The standard deviation is 5.84% and confidence interval 13.67°.

DISCUSSION

These basic statistics, giving the most frequent directions of studied cave passages (Fig. 5, C) at the distribution intervals of 10°, indicates that most passages (16.1%) have developed in the direction of N0–10°W. The second most prevalent direction is N60–70°W (13%) and the third N30–40°W (12%). The interval of confidence is 27.12°, with a standard deviation of 4.29%. The results represent the most frequent directions for nine studied caves (Jibailongdong, Dieyundong, Zhiyundong, Baiyun Cave, Guanyindong, Xinshidong, Niubizidong, Xifenlandong and Shimalogdong; Fig. 6).

Field structural geological mapping showed that in some cases cave passages run along fractures. In this manner, we were able to follow a well-defined fracture in the ceiling of Zhiyundong running in a NW-SE direction. The fractures in the cave ceiling are mainly subvertical. The main passage in Dieyundong, running in the direction N0–10°W, corresponds to the direction of the ceiling fracture. Clear slickensides in studied karst caves are rare. The clearest one studied in this project is visible in Zhiyundong, where along the subvertical almost E–W oriented fissure (dip direction 172°) a small (0.5 cm) dextral horizontal strike-slip movement was determined.

To get the better general view of the fissure orientations in the studied area we united the data obtained from Major stone forest (Fig. 5, A) and from four structural-geologically mapped caves (Jibailongdong, Dieyundong, Zhiyundong, Baiyun Cave; Fig. 5, B). Combined data for 319 fissures are presented on Fig. 5, D. Combining fissure populations gives representative view of the fissure orientation on the karst areas in Shilin County (on the surface and in underground). The prevailing fissure orientation is NW–SE (N30–40°W = 14.7%, N20–30°W = 11.8%, N40–50°W = 9.5%), and the second orientation is NE-SW (N60–70°E = 7.5%, N70–80°E = 7.5%).

It is interesting that in the Major stone forest (Fig. 5, A) less than 4% of surface fractures lie in a N0–10°W direction whereas this is the most frequent (16.1%) direction of all studied cave passages (Fig. 5, C). Otherwise, the direction N30–40°W, which is the most frequent for united fissures data (14.7%; Fig. 5, D) represents 12% of cave passages orientation (Fig. 5, C).

The stress field in the region has had two major stages. From late Pliocene to mid-Pleistocene the tectonic stress field was characteristic of nearly E-W compression and nearly N–S extension (Yi *et al.* 2010). The most frequent cave passage orientation (Fig. 5, C) in the direction almost N–S has to be connected with this tectonic episode. In the second stage from late-Pleistocene to the present the tectonic stress field has mainly been characteristic of NNW–SSE compression and NEE–SWW extension. This second stage is in accordance with the most frequent fissure orientations in Major stone forest in the direction N20–30°W (11.4%), representing the orientations of the surface karren karst features. The formation of karst underground and surface features depends on regional tectonic deformations on Cenozoic extension of the studied area.

CONCLUSIONS

Detailed structural-geological mapping was carried out in Major stone forest and in 9 karst caves (Jibailongdong, Dieyundong, Zhiyundong, Baiyun Cave, Guanyindong, Xinshidong, Niubizidong, Xifenlandong and Shimalogdong, Fig. 6) in the Shilin County. Field measurements of fissures, bedding-planes, and cave passage orientations were accomplished (Fig. 5). In the studied caves the bedding-planes are mostly subhorizontal, and in most cases the caves are formed within massive or thickbedded Permian limestone or dolomitic limestone. The bedding-plane dip angle generally does not exceed 5°. Gentle folds, such as an anticline in the Jibailongdong, are present. It has been pointed by Sweeting (1995) that the structures in the limestones of the Major stone forest are open synclines and anticlines.

Statistical evaluation of the most frequent directions of passage orientation (Fig. 5, C) and fissure orientation in caves (Fig. 5, B) is illustrated by rose diagrams. The best comparison between passage and fissure orientation is the example of Dieyundong (Fig. 6), where the passage is significantly developed along N–S trending fissures and joints.

The data, including all nine studied caves (Fig. 5, C), show that most (16.1%) passages are oriented in the direction N0–10°W, being followed by the directions N60–70°W (13%) and N30–40°W (12%). The most frequently (23.9%) oriented fissures from four mapped caves are evaluated in a N30–40°W direction (Fig. 5, B), which is the third common orientation of nine studied cave passages.

The most prevailing cave passage orientation in N-S direction is parallel to closest Xiaojiang Fault, and the general direction NW–SE of the fissures orientation (underground and surface, Fig. 5, D) to southern more distant Red River Fault (Fig. 1). Both faults are active faults and development of karst features (stone forest and caves) is connected with active tectonics of central Yunnan.

Considering that the region around Kunming is still tectonically active (Wang & Burchfield 2000) and considering the age of cave sediments in the Baiyun Cave (112,300–117,900 years; Šebela *et al.* 2004) and several older periods of the cave development we can rank this cave and probably many others at least in the Upper Pleistocene (less than 780,000 years).

In the vicinity of the Major stone forest (Fig. 1), in a diameter of 30 km, all 9 karst studied caves are formed below shilin karst topography. Yu and Yang (1997) determined from absolute age analysis of related secondary carbonate accumulation that the earliest modern shilin had begun to evolve in the Naigu region, where the Baiyun Cave is situated, in the late Pliocene (about 2 Ma).

The most frequent cave passages orientation (Fig. 5, C) in the direction almost N–S is connected with nearly E-W compression and nearly N–S extension from late Pliocene to mid-Pleistocene (Yi *et al.* 2010). The second tectonic stage from late-Pleistocene to the present with tectonic stress field mainly of NNW–SSE compression and NEE–SWW extension is in accordance with the most frequent fissure orientations in Major stone forest in the direction N20–30°W (11.4%), representing the orientations of the surface karren karst features (Fig. 5, A).

ACKNOWLEDGEMENTS

We would like to thank the Yunnan Institute of Geography (Yunnan University), China's Ministry of Science and Technology, the Slovenian Research Agency, and the Administration of Shilin and the Shilin Research Foundation, who enabled the research work. Liu Hong, Chen Xiaoping, Zhang Fan and Huang Chuxing (Yunnan Institute of Geography, Kunming) provided cave maps. The study is part of the projects "Karst Research programme" (P6–0119) and IGCP-UNESCO Project 598 ("Environmental change and sustainability in karst systems"). We are grateful to Dr. David Culver for revision of the manuscript and to reviewers for constructive suggestions.

REFERENCES

Allen, C.R., Gillespie, A.R., Han, Y., Sieh, K.E., Zhang, B. & C. Zhu, 1984: Red River and associated faults, Yunnan Province, China: Quaternary geology, slip rates and seismic hazard.- Geol. Soc. Am. Bull., 95, 686–700.

Briais, A., Patriat, P. & P. Tapponier, 1993: Updated interpretation of magnetic anomalies and seafloor spreading stages in the South China Sea: implications for the Tertiary tectonics of SE Asia.- J. Geophys. Res., 98, 6299–6328.

Chen, X., Gabrovšek, F., Huang C., Jin Y., Knez, M., Kogovšek, J., Liu H., Petrič, M., Mihevc, A., Otoničar, B., Slabe, T., Shi M., Šebela, S., Wu W., Zhang S. & N. Zupan Hajna, 1998: *South China Karst I*.- Založba ZRC, Zbirka ZRC 19, pp. 247, Ljubljana.

Frančišković-Bilinski, S., Bilinski, H., Barišić, D. & N. Hrvatinčić, 2003: Analysis of Karst Tufa from Guangxi, China.- Acta Geologica Sinica (English edition), 77, 2, 267–275.

Gu, J., Zhang X. & H. Fang, 2002: Characteristics and genetic analysis of the deep-buried weathered-crust karst hydrocarbon reservoirs of the Lower Paleozoic Group in the Tarim Basin.- Acta Geologica Sinica (English edition), 76, 4, 494–502.

Gang, L. & L. Mian, 2010: Stress evolution and fault interactions before and after the 2008 Great Wenchuan earthquake.- Tectonophysics, 491, 127–140.

Ginés, A., Knez, M., Slabe, T. & W. Dreybrodt (eds), 2009: *Karst Rock Features, Karren sculpturing*.- Založba ZRC, Carsologica 9, pp. 561, Postojna-Ljubljana.

He, C., 2011: Seismic Evidence for Plume and Subducting Slab in West Yunnan, Southwestern China.- Acta Geologica Sinica (English edition), 85, 3, 629–636.

He, H.-L. & I. Yasutaka, 2007: Faulting on the Anninghe fault zone, Southwest China in Late Quaternary and its movement model.- Acta Seismologica Sinica, 20, 5, 571–583.

He, K., Liu C. & S. Wang, 2001: Karst collapse mechanism and criterion for its stability.- Acta Geologica Sinica (English Edition), 75, 3, 330–335.

He, H., Ran H. & I. Yasutaka, 2006: Uniform Strike-slip rate along the Xianshuihe-Xiaojiang Fault System and its implications for Active Tectonics in Southeastern Tibet.- Acta Geologica Sinica (English Edition), 80, 3, 376–386.

Knez, M. & T. Slabe, 2002: Lithologic and morphological properties and rock relief of the Lunan stone forests.- In: Gabrovšek, F. (ed.) *Evolution of Karst: from Prekarst to Cessation*. Založba ZRC, pp. 259–266, Ljubljana.

Knez, M. & T. Slabe, 2010: Karren of Mushroom Mountain (Junzi Shan) in the Eastern Yunnan Ridge, Yunnan, China: Karstological and Tourist Attraction.- Acta Geologica Sinica (English edition), 84, 2, 424–431.

Knez, M., Liu H. & T. Slabe, 2010: High Mountain Karren in Northwestern Yunnan, China.- Acta Carsologica, 39, 1, 103–106.

Knez, M., Liu H. & T. Slabe, (eds) 2011: *South China Karst II*.- Založba ZRC, Carsologica 12, pp. 237, Ljubljana-Postojna.

Knez, M., Kogovšek, J., Hong L., Mulec J., Petrič M., Ravbar, N. & T. Slabe, 2012a: Karstological study of new Kunming airport building area (Yunnan, China).- Environ Earth Sci, 67, 273–283.

Knez, M., Hong L. & T. Slabe, 2012b: Major stone forest, lithomorphogenesis and development of typical shilin (Yunnan, China).- Acta Carsologica 42, 2–3, 205–218.

Kogovšek, J., 2010: Characteristics of Underground Water Flow at Different Water Levels in Tianshengan Karst Area, Yunnan, China.- Acta Geologica Sinica (English Edition), 84, 1, 206–212.

Leloupe, P. H., Lacassin, R, Tapponier, P., Schärer, U., Zhong D., Liu X.n, Zhang L., Ji S. & T. T. Phan, 1995: The Ailao Shan-Red River shear zone (Yunnan, China), Tertiary transform boundary of Indochina.- Tectonophysics, 251, 3–84.

Liu, H. & Z. Yan, 2003: The characteristics of Cave development in shilin.- Chinese Electronic Periodical Services, 18, 6, 891–898.

Luo, G., Yan C., Li X., Jiang J. & J. Ma, 2003: Exploration of water resource and multiple model for water resource development in karst areas with the Preferred Plane Theory.- Acta Geologica Sinica (English Edition), 77, 1, 129–135.

Paradisopoulou, P.M., Garlaouni, C. G., Jin X., Papadimitriou E.E., Karakostas, V.G. & J. Yang, 2007: Application of the stress evolutionary model along the Xiaojiang fault zone in Yunnan Province.- Acta Geophysica, 55, 4, 577–593.

Song, L. & F. Liang, 2001: Distribution of CO_2 in soil air affected by vegetation in the Shilin National Park.- Acta Geologica Sinica (English Edition), 75, 3, 288–293.

Song, L. & F. Liang, 2009: Two important evolution models of Lunan Shilin karst.- In: Ginés, *et al.* (eds) *Karst Rock Features, Karren sculpturing*. Založba ZRC, Carsologica 9, pp. 453–459, Postojna-Ljubljana.

Sweeting, M. 1995: *Karst in China. Its Geomorphology and Environment*.- Springer Verlag, pp. 265, Berlin, Heidelberg, New York.

Šebela, S., Kogovšek, J., Slabe, T., Liu H. & P. Pruner, 2001: Baiyun cave in Naigu Shilin, Yunnan, China.- Acta Geologica Sinica (English Edition), 75, 3, 279–287.

Šebela, S., Slabe, T., Liu H. & P. Pruner, 2004: Speleogenesis of Selected Caves beneath the Lunan Shilin and Caves of Fenglin Karst in Qiubei, Yunnan.- Acta Geologica Sinica (English Edition), 78, 6, 1289–1298.

Tapponier, P. & P. Molnar, 1977: Active faulting and tectonics of China.- J. Geophys. Res., 82, 2905–2930.

Wang, E., Burchfield, B.C., Royden, L.H., Chen, L., Chen, J., Li W. & Z. Chen, 1998: The late Cenozoic Xianshuihe-Xiaojiang, Red River, and Dali fault systems of south-western Sichuan and central Yunnan, China.- Geological Society of America Special Paper, 327, 1–108.

Wang, E. & B.C. Burchfield, 2000: Late Cenozoic to Holocene deformation in southwestern Sichuan and adjacent Yunnan, China, and its role in formation of the southeastern part of the Tibetan Plateau.- Geol. Soc. Am. Bull., 112, 3, 413–423.

Wang, Y.J., Cheng, H., Edwards, R.L., An, Z.S., Wu, J.Y., Shen, C.-C. & J.A. Dorale, 2001: A High-Resolution Absolute-Dated Late Pleistocene Monsoon Record from Hulu Cave, China.- Science, 294, 2345–2348.

Wang, C., Lou H., Wang X., Qin J., Yang R. & J. Zhao, 2009: Crustal structure in Xiaojiang fault zone and its vicinity.- Earthq Sci, 22, 347–356. DOI: 10.1007/s11589-009-0347-0

Wang, H., Liu J., Shi Y.L., Zhang H. & G.M. Zhang, 2008: Dynamic simulation of interactions between major earthquakes on the Xianshuihe fault zone.- Science in China Series D: Earth Sciences, 51, 10, 1388–1400.

Wang, C., Wu J., Lou H., Zhou M. & Z. Bai, 2003: P-wave crustal velocity structure in western Sichuan and eastern Tibetan region.- Science in China Series D: Earth Sciences, 46, 254–265.

Wang, H., Liu J., Shen X.H., Liu M., Li Q.S., Shi Y.L. & G.M. Zhang, 2010: Influence of fault geometry and fault interaction on strain partitioning within western Sichuan and its adjacent region.- Science in China Series D: Earth Science, 53, 7, 1056–1070.

Zhang, P., Johnson, K.R., Chen Y., Chen F., Ingram, L., Zhang, X., Zhang C., Wang S., Pang F. & L. Long, 2004: Modern systematic and environmental significance of stable isotopic variations in Wanxiang Cave, Wudu, Gansu, China.- Chinese Science Bulletin, 49, 15, 1649–1652. DOI: 10.1360/03wd0382

Zhang, Y., Dong S. & N. Yang, 2009: Active Faulting Pattern, Present-day Tectonic Stress Field and Block Kinematics in the East Tibetan Plateau.- Acta Geologica Sinica (English Edition), 83, 4, 694–712.

Xu, J. & Z. Zhao, 2010: Normal Faulting Type Earthquake Activities in the Tibetan Plateau and Its Tectonic Implication.- Acta Geologica Sinica (English Edition), 84, 1, 135–144.

Xie, Y. & Y. Li, 1995–1999: Karst Geology, Geomorphology and Ecosystems of Shilin, Yunnan.- [Online] Available from: http://www.karst.edu.cn/guidebook/shilin.htm [Accessed 11st October 2012].

Yi, D., Zhen-Jie J. & X. Fu-Ren, 2010: The Quaternary Tectonic Stress Field of the Kunming Basin and its Surrounding Areas.- Earthquake Research in China, 24, 1, 70–81.

Yu, J. & B. Yang, 1997: Palaeo-environments during formation of Lunan Stone Forest.- In: Song, L., Waltham, T., Cao, N. & F. Wang, (eds.) *Stone Forest: A Treasure of Natural Heritage, Proceedings of International Symposium for Lunan Shilin to Apply for World Natural Heritage Status.* China Environmental Science Press, pp. 63–67. Bejing.

COBISS: 1.01

THE USE OF DAMAGED SPELEOTHEMS AND *IN SITU* FAULT DISPLACEMENT MONITORING TO CHARACTERISE ACTIVE TECTONIC STRUCTURES: AN EXAMPLE FROM ZÁPADNÍ CAVE, CZECH REPUBLIC

UPORABA DEFORMIRANIH SIG TER *IN SITU* MERJENJE PREMIKOV PRELOMOV ZA DOLOČITEV AKTIVNIH TEKTONSKIH STRUKTUR: PRIMER IZ JAME ZÁPADNÍ CAVE, ČEŠKA REPUBLIKA

Miloš BRIESTENSKÝ[1]*, Josef STEMBERK[1], Matt D. ROWBERRY[1]

Abstract UDC 551.242:551.435.84(437.3)

Miloš Briestenský, Josef Stemberk & Matt D. Rowberry: The use of damaged speleothems and in situ fault displacement monitoring to characterise active tectonic structures: an example from Západní Cave, Czech Republic

The EU-TecNet fault displacement monitoring network records three-dimensional displacements across specifically selected tectonic structures within the crystalline basement of central Europe. This paper presents a study of recent and active tectonics at Západní Cave in northern Bohemia (Czech Republic). It extends previous geological research by measuring speleothem damage in the cave and monitoring displacements across two fault structures situated within the Lusatian Thrust Zone. The speleothem damage reflects strike-slip displacement trends: the WSW-ENE striking fault is associated with dextral strike-slip displacement while the NNW-SSE striking fault is associated with sinistral strike-slip displacement. These measurements demonstrate that the compressive stress σ1 is located in the NW or SE quadrant while the tensile stress σ3 is oriented perpendicular to σ1, i.e. in the NE or SW quadrant. The *in situ* fault displacement monitoring has confirmed that movements along the WSW-ENE striking fault reflect dextral strike-slip while movements along the NNW-SSE striking fault reflect sinistral strike-slip. In addition, however, monitoring across the NNW-SSE striking fault has demonstrated relative vertical uplift of the eastern block and, therefore, this fault is characterised by oblique movement trends. The fault displacement monitoring has also shown notable periods of increased geodynamic activity, referred to as pressure pulses, in 2008, 2010–2011, and 2012. The fact that the measured speleothem damage and the results of fault displacement monitoring correspond closely confirms the notion that, at this site, the compressive stress σ1 persists in the NW or SE quadrant. The presented results offer an insight into the periodicity of pressure

Izvleček UDK 551.242:551.435.84(437.3)

Miloš Briestenský, Josef Stemberk & Matt D. Rowberry: Uporaba deformiranih sig ter in situ merjenje premikov prelomov za določitev aktivnih tektonskih struktur: primer iz jame Západní Cave, Češka Republika

EU-TecNet projektna mreža spremljanja premikov prelomov beleži tri dimenzionalne premike v izbranih tektonskih strukturah kristalinske osnove osrednje Evrope. Članek predstavlja študijo recentne in aktivne tektonike v jami Západní Cave na severu Češke Republike. Gre za razširitev predhodnih geoloških raziskav z merjenjem deformacij sige ter za merjenje premikov dveh prelomnih struktur znotraj Lusatian narivne cone. Deformacija sige kaže na zmične premike: prelom v smeri ZJZ-VSV je povezan z desnim horizontalnim zmikom, medtem ko je prelom v smeri SSZ-JJV povezan z levim horizontalnim zmikom. Premiki kažejo, da se kompresijska napetost σ1 nahaja v SZ ali JV kvadrantu, medtem ko je raztezna napetost σ3 usmerjena pravokotno na σ1, to je v SV ali JZ kvadrantu. *In situ* spremljanje tektonskih premikov je potrdilo, da premiki ob ZJZ-VSV usmerjenih prelomih kažejo desne zmike, medtem ko premiki ob SSZ-JJV usmerjenih prelomih odražajo leve zmike. Hkrati pa so meritve SSZ-JJV usmerjenih prelomov pokazale relativen vertikalni dvig vzhodnega bloka, kar kaže, da ima prelom poševne premike. Spremljanje premikov ob prelomih je pokazalo tudi izrazita obdobja povečane geodinamične aktivnosti, ki jih imenujemo napetostni pulzi v letih 2008, 2010–2011 in 2012. Značilnosti deformacije sige in rezultati o premikih preloma potrjujejo, da kompresijska napetost σ1na tej lokaciji ostaja v SZ ali JV kvadrantu. Rezultati predstavljajo pogled v obdobja napetostnih pulzov, kar kaže na potrebo po dolgotrajnem monitoring, da bi lahko bolje razumeli geodinamične procese ter hkrati pokazali , da je možno določiti premike, ki nastajajo ob posameznih prelomih na način, ki ga ni mogoče določiti z geodetskimi meritvami s pomočjo GNSS.

[1] Department of Engineering Geology, Institute of Rock Structure and Mechanics, Academy of Sciences of the Czech Republic, V Holešovičkách 41, 182 09 Prague 8, Czech Republic, e-mail: briestensky@irsm.cas.cz; stemberk@irsm.cas.cz; e-mail: rowberry@irsm.cas.cz

* Corresponding author

Received/Prejeto: 14.08.2013

pulses, demonstrate the need for protracted monitoring periods in order to better understanding geodynamic processes, and show that it is possible to characterise the displacements that occur across individual faults in a way that cannot be accomplished from geodetic measurements obtained by Global Navigation Satellite Systems.
Keywords: active tectonics, speleothem damage, fault displacement, stress field, Lusatian Thrust Zone, Západní Cave.

Ključne besede: Aktivna tektonika, deformacija sige, premiki ob prelomu, napetostno polje, Lusatian narivna cona, jama Západní Cave.

INTRODUCTION

The EU-TecNet fault monitoring network has been recording three-dimensional displacements across specifically selected tectonic structures within the shallow crust for more than a decade (Stemberk *et al*. 2003; Briestenský *et al*. 2007; Košťák *et al*. 2011). The network was established to characterise the displacements that occur across individual faults as these cannot be resolved from geodetic measurements obtained by Global Navigation Satellite Systems (GNSS). It currently records displacements across more than one hundred tectonic structures within the crystalline basement of central Europe (EU-TecNet 2013). This intracratonic region is particularly suitable for the study of microdisplacements because the highly fractured crystalline basement is not associated with significant seismic activity (Stemberk *et al*. 2010).

The relative three-dimensional displacements are measured using specially designed optical-mechanical crack gauges (Košťák & Popp 1966; Košťák 1969). These are permanently installed in caves or other underground spaces because such settings are able to preserve a three-dimensional record of deformation unaffected by subsequent erosion and they are largely shielded from climatic effects such as diurnal or seasonal massif dilations (Briestenský *et al*. 2010, 2011a, b). The data are recorded across the monitoring network once a month due to the fact that the readings have to be taken manually (Klimeš *et al*. 2012). The network has, nonetheless, demonstrated that underlying tectonic processes are initiated as a result of the widespread redistribution of stress and strain within the crust (Košťák *et al*. 2007; Stemberk *et al*. 2010; Košťák *et al*. 2011, Briestenský *et al*. 2014).

This paper presents a study of recent and active tectonics at Západní Cave in northern Bohemia (Czech Republic). It extends previous geological research by measuring speleothem damage in the cave and monitoring displacements across two fault structures located within the Lusatian Thrust Zone. The overall objectives of the paper are to: (i) provide a geological and geomorphological overview of Ještěd Ridge; (ii) provide a detailed geological description of Západní Cave; (iii) present the measurements of speleothem damage in the cave; and (iv) present the results of the displacement monitoring across two faults in the cave. The measurements of speleothem damage and the results of fault displacement monitoring have been used to compute the recent regional stress field.

METHODS

A number of previous studies have shown that damaged speleothems may be indicative of active tectonics (e.g. Kashima 1993; Gilli 2005; Becker *et al*. 2012; Camelbeeck *et al*. 2012). In certain situations within cave systems it is clear that damaged speleothems are associated with fault outcrops (Šebela 2008). At Západní Cave the idea that tectonic activity was responsible for the significant number of fresh speleothem breaks was suggested by their association with the main faults although it was, of course, important to consider other possible mechanisms that may lead to such damage such as freezing, gravitational movements, or sediment infill volume changes. The most appropriate places in which to study the speleothems were selected, in so far as is possible, usually in the cave ceiling (Briestenský *et al*. 2011a). At each location the amount of displacement was recorded along with the displacement vector.

The *in situ* fault displacements were recorded using two permanently installed optical-mechanical crack gauges. Their ability to record data in three-dimensions is critical as the movement between fault planes is frequently characterised by slip (Košťák 2006). These mea-

sure relative displacement and angular rotation using the moiré phenomenon of optical interference (Oster & Nishijima 1963). The moiré patterns appear when two identical overlapping periodic structures undergo a small relative displacement causing the development of a series of characteristic macroscopic interference fringes whose arrangement and periodicity does not necessarily resemble that of the overlapping structures (Marti *et al*. 2013). Its configuration, however, is deterministic and the observed patterns reflect the amount and direction of relative movement (Marti *et al*. 2013). The gauge itself comprises two pairs of two identical overlapping glass plates referred to as the combined indicator (Košťák 1991). The plates are each etched with one spiral grid and two rectangular grids, one horizontal and one vertical (Klimeš *et al*. 2012).

The moiré interference of two regular Archimedes spirals is represented by a family of hyperbolas with a common principal axis that follows the direction of the displacement. The family comprises a variable number of macroscopic fringes proportional to the amount of relative displacement. Therefore, if the orientation of the principal axis and the number of fringes is known, through a simple trigonometric transformation the amount of relative displacement can be calculated (Košťák 1991). The moiré interference of two identical overlapping sets of parallel lines is represented by a family of oblique parallel lines which slope according to the direction of the rotation. The family comprises a variable number of macroscopic fringes whose period is proportional to the amount of relative rotation α (Košťák 1991). It is possible to record relative displacements in three co-ordinates (*x*, *y*, *z*) with a precision of better than ±0.007 mm and horizontal and vertical rotations (*gxy* and *gxz*) with a precision of better than ± 0.00016 rad.

THE GEOLOGY AND GEOMORPHOLOGY OF JEŠTĚD RIDGE

The studied cave is situated within the broad geomorphological unit of the Ještěd-Kozákov Ridge and, more specifically, within the subunit of Ještěd Ridge (Demek 1987). The Ještěd-Kozákov Ridge has a length of almost 60 km and a width that does not exceed 15 km and comprises part of the Western Sudetes. It runs from the northwestern hills of Pískový vrch (547 m asl) and Ostrý vrch (514 m asl) to the southeastern hill of Kozákov (744 m asl). The ridge is intersected by the deep valleys of the Mohelka and Jizera Rivers. The highest, and best-known, point along the ridge is the summit of Ještěd (1012 m asl) which overlooks the city of Liberec and which hosts a spectacular hyperboloid television tower. The Ještěd Ridge is a wedge-shaped horst trending NW-SE. It is composed of strongly folded, mainly during the Variscan Orogeny (Chlupáč 1964), slightly to epizonally metamorphosed rocks dating from the late Proterozoic and Paleozoic, which were uplifted during Saxonian movements (Kozdrój *et al*. 2001). The northeastern part of the horst is separated from the Železný Brod Crystalline Complex, the Variscan granitoids of the Krkonoše Pluton, and the Cambrian-Ordovician Jizera orthogneiss by the NW-SE trending Machnín Fault. The southwestern part of the horst borders the platform sediments of the Bohemian Cretaceous Basin and Mnichovo Hradiště Basin that forms part of South Krkonoše Piedmont Basin. This contact is represented by a wider fault zone, called the Lusatian Thrust. This thrust represents the most significant fault zone in the northern part of the Bohemian Massif while it also comprises part of an important feature that crosses much of central Europe (Malkovský 1979). It strikes from Dresden in Germany to Turnov in the Czech Republic with a length more than 110 km (Malkovský 1977). Its thrust plane dips to the NNE by 15–75° (Pošmourný 1967; Kurka & Bělohradský 1979; Coubal *et al*. 1999). The present position of the crystalline block and platform sediments, which is divided by the Lusatian Thrust (Fig. 1), has resulted from several generations of movement (Coubal 1989). The most recent morphostructural development of Ještěd Ridge began in the Pliocene, with intense activity in the Pleistocene, which is considered to be ongoing (Kopecký 1970). It has been proposed that, since that time, the amplitude of vertical movement has ranged from around 500 m to 700 m (Vyskočil & Kopecký 1974) to perhaps more than 1000 m (Malkovský 1979). The entire course of the fault is covered by Quaternary sediments and it does not have a morphological expression (Coubal *et al*. 1999). There are also a number of faults running parallel to the Lusatian Thrust and these separate the Ještěd Crystalline Unit into partial blocks (Fig. 1). The Ještěd Ridge karstic area has developed in WSW-ENE trending strips of metamorphosed Devonian limestones (Chlupáč 1998), most of which have tectonised limits (Kachlík 2002).

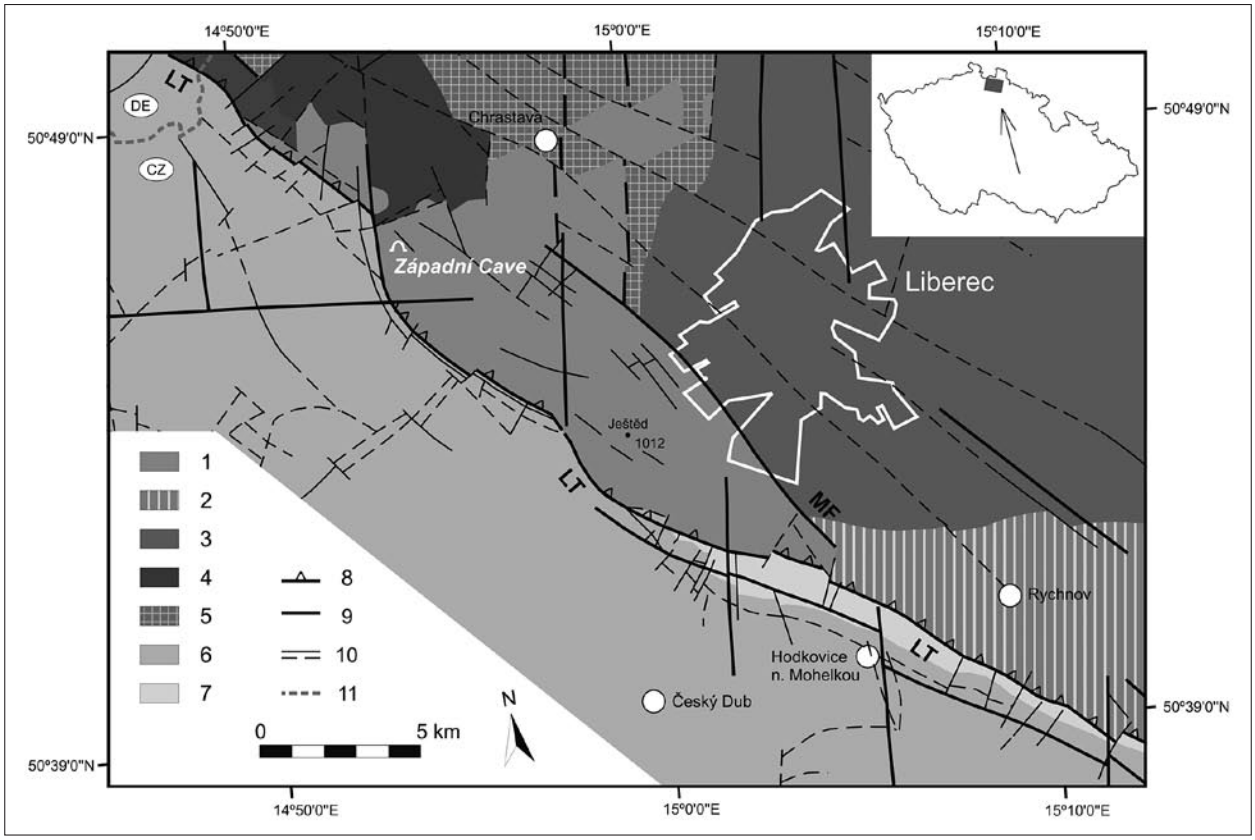

Fig. 1: The geological units and fault systems in the vicinity of Západní Cave (modified after Chaloupský et al. 1989; Kozdrój et al. 2001). Krkonoše-Jizera Crystalline Unit – 1: Ještěd Crystalline Unit; 2: Železný Brod Crystalline Unit; 3: Krkonoše Granites; 4: Lusatian Granodiorite Massif; 5: Jizera Metamorphic Complex; 6: Bohemian Cretaceous Basin. South Krkonoše Piedmont Basin – 7: Mnichovo Hradiště Basin. 8: thrust; 9: main faults; 10: secondary faults (either certain, assumed, or concealed under a sedimentary cover); 11: state boundary. LT: Lusatian Thrust; MF: Machnín Fault.

THE GEOLOGY AND GEOMORPHOLOGY OF ZÁPADNÍ CAVE

The cave is located within a small body of crystalline limestones in the Ještěd Crystalline Complex approximately 15 km west of Liberec, close to the village of Jítrava, in northern Bohemia (Fig. 1). This complex forms part of the western sector of the larger Krkonoše-Jizera Crystalline Unit (Chaloupský *et al.* 1989). It is the largest cave found within the karstic part of Ještěd Ridge and its entrance is situated in an old limestone quarry on western slope of Vápenný Hill (790 m asl). The quarry represents one of the most important stratigraphic and paleontological localities in the Czech part of the West Sudetes due to its well documented Devonian fauna (Koliha 1929). The beds here form an asymmetrical, almost isoclinal brachyanticline, which is reversed to the SE. The core of the structure consists of black pyrite-bearing phyllitic shales of Lower Fammenian age, overlain by an approximately 20 m-thick bed of crystalline limestones. These limestones were slightly metamorphosed during the Variscan Orogeny. The superincumbent bed is represented by a thick complex of green and grey schists, greywacke, and conglomerate from the Lower Carboniferous (Chlupáč 1964; Budil *et al.* 1999). The cave has developed along two faults: 80°→150° (dip→dip direction) and 70°→062° (Bosák & Horušický 1978). The NNW-SSE striking fault has the same orientation as the nearby Lusatian Fault (Fig. 1). In total the length of the cave passages attains approximately 280 m while the denivelation is 25 m (Hromas *et al.* 2009). It is divided into two parts: Staré jeskyně Cave, discovered in 1958, and Nové jeskyně Cave, discovered in 1962. Staré jeskyně Cave consists of high, predominately narrow, passages that have developed along fractures. Its main corridor has a length of

40 m and a width of between 0.5–1 m. Nové jeskyně Cave comprises a larger hall that narrows progressively away from the entrance and is occasionally flooded. It hosts an unusual range of cave decorations such as transparent stalactites and excentriques while the cave walls are draped by flowstone. The clastic sedimentary fills consist of loams with gravels and cobbles (Bosák & Horušický 1978).

RESULTS

SPELEOTHEM DAMAGE MEASURED ALONG THE TWO MAIN FAULTS

During our research, which focused on mapping the structural and morphological features of the cave, it was noted that speleothems precipitated along fractures were commonly damaged by fresh cracks and breaks. The damage is clearly associated with both of the aforementioned faults. In those places where the speleothems had not broken completely it could be seen that the displacements were characterised by strike-slip movements (Fig. 2). Moreover, in places where the speleothems were accessible, the displacements could be measured using a slide gauge (Fig. 3). The measured speleothem damage, characterised by strike-slip movements, showed dextral strike-slip displacements ranging from 1.24 mm to 3.40 mm along the WSW-ENE striking fault and sinistral strike-slip displacements ranging from 4.10 to 5.60 mm along the NNW-SSE striking fault. On the basis of the results of this survey, the recent local stress field orientation was determined (Jurková & Briestenský 2008). The observed senses of displacement demonstrates that compressive stress σ_1 is located in the NW or SE quadrant while the tensile stress σ_3 is oriented perpendicular to σ_1, i.e. in the NE or SW quadrant (Fig. 2).

IN SITU FAULT DISPLACEMENT MONITORING

In 2007, due to the presence of the damaged speleothems and the location of the cave within the Lusatian Thrust

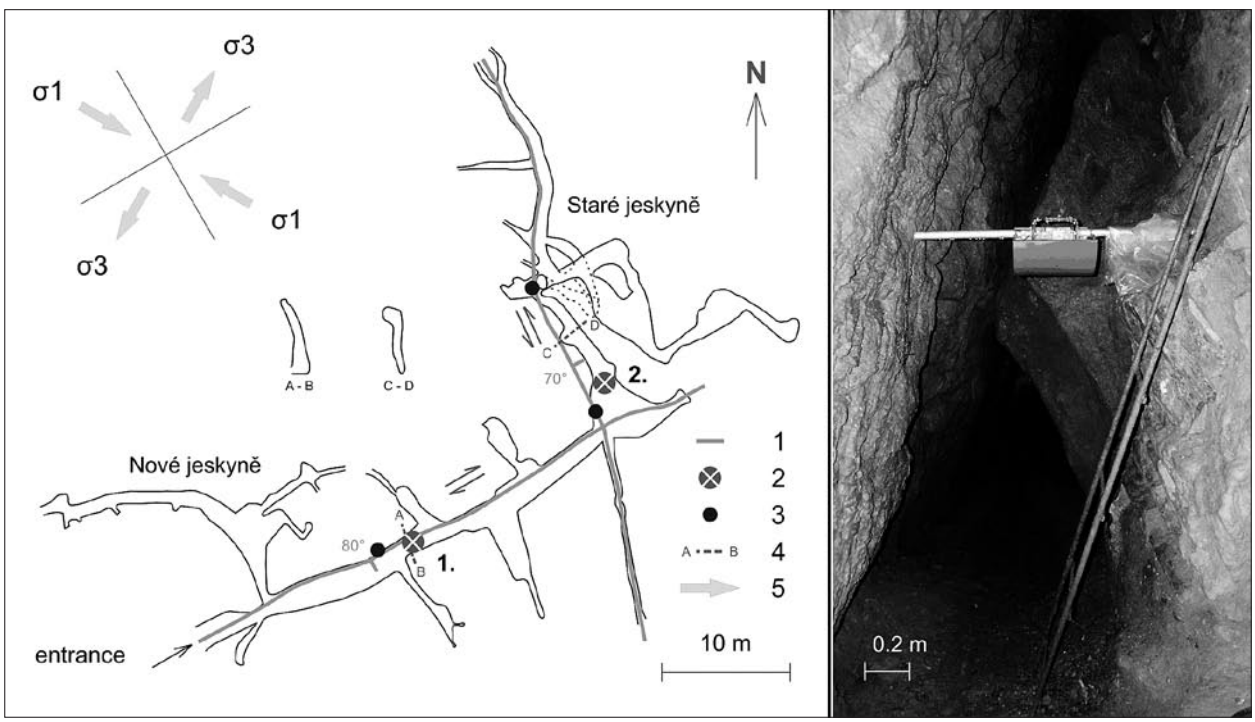

Fig. 2: A sketch of Západní Cave showing the position of damaged speleothems and the location of the two permanently installed optical-mechanical crack gauges (modified after Skřivánek & Hromas 1961). 1: significant faults with recorded displacement directions indicated by arrows: 2: sites in which the fault displacements are recorded using optical-mechanical crack gauges; 3: sites in which the damaged speleothems have been measured using a slide gauge; 4: space profiles; 5: computed stress directions according to speleothem deformation and fault displacements recorded in the cave. The photograph on the right shows the location of gauge N1 across the WSW-ENE striking fault, taken from the NE (Photo: T. Nýdl).

Zone, the authors decided to install two optical-mechanical crack gauges in order to record direct *in situ* fault displacements. The location of the instruments is shown in Fig. 2. In accordance with the monitoring interval at many of the sites within EU-TecNet fault displacement monitoring network the data have been recorded once a month since May 2007. The results of fault displacement monitoring show significant fault trends at both of the monitored sites. The WSW-ENE striking fault records a long-term dextral strike-slip trend of 0.25 mm over a period of 4.5 years (Site N1, Fig. 2 & Fig. 4) while the NNW-SSE striking fault records long-term uplift of the eastern block of 0.5 mm over a period of 5.5 years together with a silent sinistral trend of 0.05 mm over a period of 4.5 years (Site N2, Fig. 2 & Fig. 4).

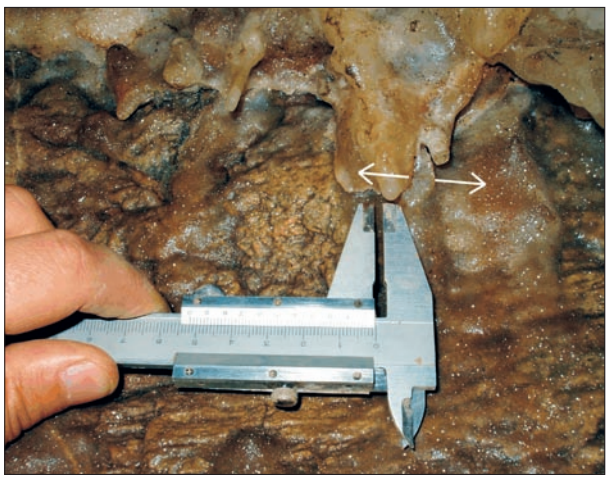

Fig. 3: An example of the speleothem damage measured along the main corridor of the cave. The arrows on the photograph indicate the direction of displacement (Photo: M. Briestenský).

The vertical trend that characterises the NNW-SSE striking fault (70°→062°) demonstrates recent activity on, and the persisting thrusting of, the Lusatian Fault. The fact that the measured speleothem damage and the results of fault displacement monitoring correspond closely confirms the notion that, at this site, the compressive stress σ1 persists in the NW or SE quadrant. This regional stress field is consistent with other studies, such as those conducted in western Bohemia, in which a compressive stress orientation of σ_1 in the NW quadrant was also recognised (e.g. Grünthal & Stromeyer 1992; Wirth *et al.* 2000). It also supports the notion that, "farther from the Alpine chain, a more consistent direction of compression has dominated first NW-SE, then NNW-SSE" (Bergerat 1987). Therefore, the two methods used in this study deliver similar results, and these are consistent with other models of the regional stress field in central Europe. Although many studies have noted an association between damaged speleothems and active tectonics, until recently comparatively few had been able

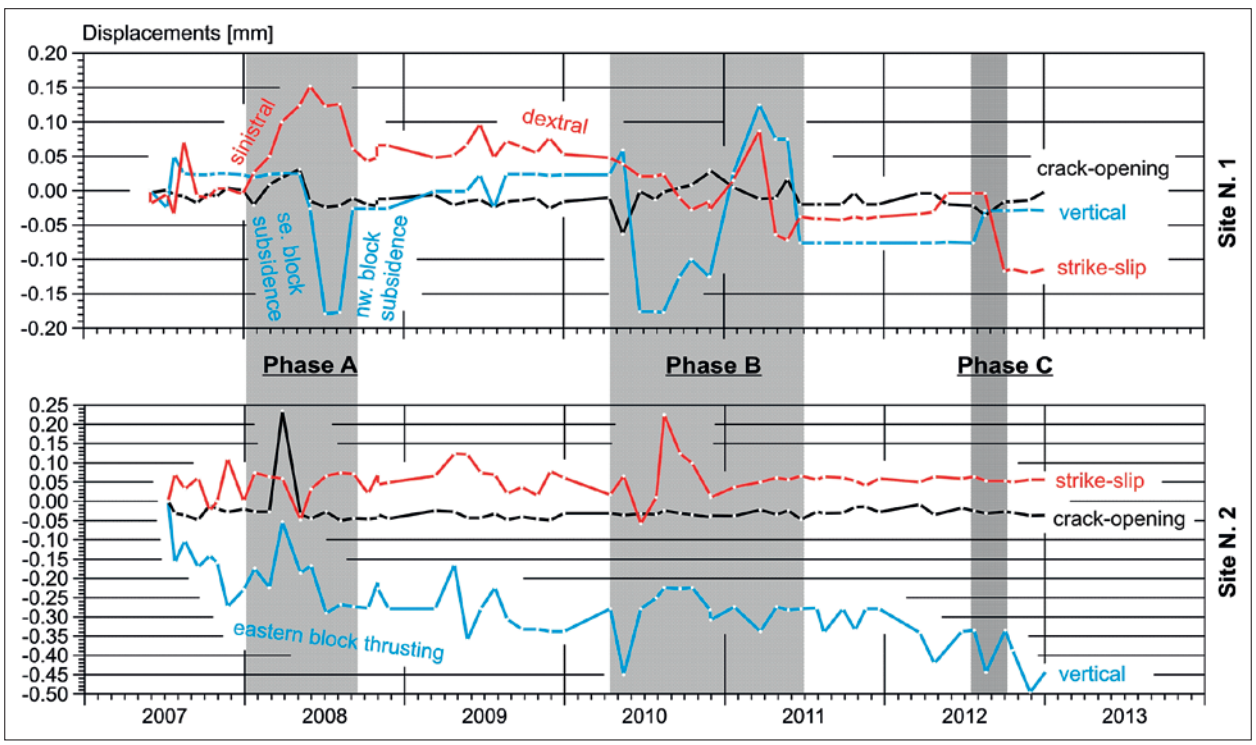

Fig. 4: Fig. 4: The results of in situ fault displacement monitoring obtained using permanently installed optical-mechanical crack gauges located across two faults within Západní Cave. Also marked are the notable pressure pulses recorded in 2008, 2010–2011, and 2012.

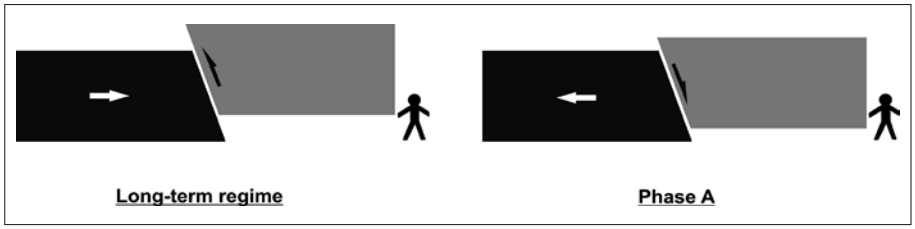

Fig. 5: Schematic models of the displacements recorded across the NNW-SSE striking fault in Západní Cave. Left: the overall results of the long-term monitoring from 2007–2012. Right: the results obtained during the notable pressure pulse in 2008.

to directly relate speleothem damage to direct measurements of fault displacement (Briestenský *et al*. 2011a; Camelbeeck *et al*. 2012).

The fault displacement monitoring also shows notable periods of increased geodynamic activity, referred to as pressure pulses, in 2008, 2010–2011, and 2012. These pressure pulses simultaneously interfere with the long-term displacement trends at both sites. Three pulses have been registered since monitoring began in 2007 (Fig. 4 A, B, C). The most susceptible instrument appears to be N1 as, at this locality, the pressure pulses seem to last for longer periods and induce larger displacement amplitudes. The long-term trend is one of progressive compression as shown by the eastward horizontal shift of the western block and uplift of the eastern block (Fig. 4 & Fig. 5 (left)). However, during "Phase A" there is significant fault relaxation, as shown by the westwards horizontal shift of the western block horizontal and subsidence of the eastern block (Fig. 4 & Fig. 5 (right)).

These three pressure pulses are considered to reflect periods in which there are significant modifications to the stress field. It is clear that the pressure pulses are coeval and, therefore, the displacements cannot be associated with local seismic tremors, neither as co-seismic nor post-seismic processes. This corroborates the previous proposition that the pressure pulses reflect the "slow process of stress/strain transformation that leads to fault displacement and possibly earthquakes" (Stemberk *et al*. 2010). These pulses may occur prior to earthquake activity, often preceding it by several months. Košťák *et al*. (2011) noted that neither the sources nor the periodicity of the pressure pulses is known. This study offers the first real insight into the latter and demonstrates the value of long-term monitoring in relation to better understanding geodynamic processes.

CONCLUSIONS

The measured speleothem damage and the results of the *in situ* fault displacement monitoring within Západní Cave provide evidence for recent and ongoing tectonic movements across two fault structures within the Lusatian Thrust Zone. The measured speleothem damage, characterised by strike-slip movements, shows dextral strike-slip displacements ranging from 1.24 to 3.40 mm along the WSW-ENE striking fault and sinistral strike-slip displacements ranging from 4.10 to 5.60 mm along the NNW-SSE striking fault. The compressive stress σ_1 is located in the NW or SE quadrant while the tensile stress σ_3 is oriented perpendicular to σ_1, i.e. in the NE or SW quadrant. The results of fault displacement monitoring show a long-term dextral strike-slip trend of 0.25 mm over a period of 4.5 years along the WSW-ENE trending fault while the NNW-SSE trending fault presents evidence for uplift of the eastern block (0.5 mm over a period of 5.5 years) together with a silent sinistral trend (0.05 mm over a period of 4.5 years). It is not possible to extrapolate these measurements in order to provide further information about either the origin or development of the cave system due to the fact that displacement trends are known to both oscillate over protracted periods and accelerate during periods of increased geodynamic activity. For example, there are notable periods of increased geodynamic activity in 2008, 2010–2011, and 2012. The fact that the measured speleothem damage and the results of fault displacement monitoring correspond closely confirms the notion that, at this site, the compressive stress σ1 persists in the NW or SE quadrant. The presented results demonstrate that it is possible to characterise the displacements that occurs across individual faults in a way that cannot be accomplished from geodetic measurements obtained by Global Navigation Satellite Systems.

ACKNOWLEDGEMENTS

The authors wish to acknowledge the financial support provided by the Czech Ministry of Education, Youth, and Sports (COST OC 625.10), the Czech Science Foundation (GA205/05/2770, GA205/06/1828 & GA205/09/2024), and the Grant Agency of the Academy of Sciences of the Czech Republic (IAA300120801). The study was conducted within the framework of the research plan for the Institute of Rock Structure and Mechanics ASCR (A VOZ30460519) and CzechGeo/EPOS (Project No. LM2010008).

REFERENCES

Becker, A., Häuselmann, P., Eikenberg, J. & E. Gilli, 2012: Active tectonics and earthquake destructions in caves of northern and central Switzerland.- International Journal of Speleology, 41, 1, 35–49.

Bergerat, F., 1987: Stress fields in the European platform at the time of Africa-Eurasia collision.- Tectonics, 6, 2, 99–132.

Bosák, P. & R. Horušický, 1978: Současný stav výzkumů krasových jevů Ještědského hřbetu [The current state of research into karst phenomena along Ještěd Ridge].- Československý kras, 29, 47–52.

Briestenský, M., Košťák, B., Stemberk, J., Petro, L., Vozár, J. & L. Fojtíková, 2010: Active tectonic fault microdisplacement analyses: a comparison of results from surface and underground monitoring in western Slovakia.- Acta Geodynamica et Geomaterialia, 7, 4, 387–397.

Briestenský, M., Stemberk, J., Michalík, J., Bella, P. & M.D. Rowberry, 2011a: The use of a karstic cave system in a study of active tectonics: fault movements recorded at Driny Cave, Malé Karpaty Mts (Slovakia).- Journal of Cave and Karst Studies, 73, 2, 114–123.

Briestenský, M., Stemberk, J. & Ľ. Petro, 2007: Displacements registered around the March 13th 2006 Vrbové earthquake M = 3.2 (Western Carpathians).- Geologica Carpathica, 58, 5, 487–493.

Briestenský, M., Thinová, L., Stemberk, J. & M.D. Rowberry, 2011b: The use of caves as observatories for recent geodynamic activity and radon gas concentrations in the Western Carpathians and Bohemian Massif.- Radiation Protection Dosimetry, 145, 2–3, 166–172.

Briestenský, M., Thinová, L., Praksová, R., Stemberk, J., Rowberry, M.D. & Z. Knejflová, 2014: Radon, carbon dioxide, and fault displacements in central Europe related to the Tōhoku Earthquake.- Radiation Protection Dosimetry, doi: 10.1093/rpd/ncu090.

Budil, P., Štěpánek, P., Adamovič, J., Coubal, M., Chlupáč, I., Opletal, M. & J. Valečka, 1999: Examples of important geological localities in the Sudetes (Czech Republic).- Polish Geological Institute Special Papers, 2, 27–32.

Camelbeeck, T., Ruymbeke, M., Quinif, Y., Vandycke, S, Kerchove, E. & Z. Ping, 2012: Observation and interpretation of fault activity in the Rochefort cave (Belgium).- Tectonophysics, 581, 48–61.

Chaloupský, J. *et al.* 1989: *Geologie Krkonoš a Jizerských hor* [Geology of the Krkonoše and Jizerské Mts].- Academia, pp. 288, Prague.

Chlupáč, I., 1964: Nový nález fauny ve slabě metamorfovaném paleozoiku Ještědského pohoří [New faunal finds in the low-grade metamorphic Paleozoic mountains of Ještěd].- Časopis pro mineralogii a geologii, 9, 1, 27–35.

Chlupáč, I., 1998: Poznámky k rozšíření devonu a stavbě metamorfovaného paleozoika v jižní a střední části Ještědského pohoří [Notes on the Devonian distribution and structure of metamorphosed Paleozoic rocks in southern and central parts of the Ještěd Mts].- Zprávy o geologických výzkumech v roce 1997, 19–22.

Coubal, M., 1989: *Projevy saxonské tektogeneze v centrální části České křídové pánve* [The manifestation of Saxonian tectonics in the central part of the Bohemian Cretaceous Basin].- Manuscript, Archive of Czech Geological Institute, pp. 236, Prague.

Coubal, M., Čech, S., Málek, J. & V. Prouza, 1999: *Lužický zlom.- Závěrečná zpráva grantového projektu GAČR č. 205/96/1754* [Lusatian Fault – final report of grant project GAČR No. 205/96/1754].- Manuscript, Archive of Czech Geological Institute, Prague.

Demek, J., 1987: *Zeměpisný lexikon ČSR, hory a nížiny* [Geographical lexicon of ČSR, mountains and lowlands].- Academia, pp. 584, Prague.

EU-TecNet, 2013: The EU-TecNet monitoring network TM-71.- [Online] Available from: http://www.irsm.cas.cz/ext/tecnet/index.php [last accessed: 22 November 2013].

Gilli, E., 2005: Review on the use of natural cave speleothems as palaeoseismic or neotectonics indicators.- Comptes Rendus Geosciences, 337, 13, 1208–1215.

Grünthal, G. & D. Stromeyer, 1992: The recent crustal stress field in central Europe – trajectories and finite-element modeling.- Journal of Geophysical Research, 97, B8, 11.805–11.820.

Hromas, J. *et al.* 2009: Jeskyně [Caves].- In: Mackovčin, P. & M., Sedláček (eds.): *Chráněná území ČR* [Preserved areas of the Czech Republic].- Agentura ochrany přírody a krajiny ČR, pp. 608, Prague.

Jurková, N. & M. Briestenský, 2008: Recent movements along tectonic failures in Západní Cave (Ještěd Ridge, Northern Bohemia).- Slovenský kras, 46/25.

Kachlík, V., 2002: *Geologická mapa 1:10 000, list 03–13–20 Kryštofovo údolí* [Geological map 1:10 000, Sheet No 03–13–20 Kryštofovo údolí].- Manuscript, Archive of Czech Geological Institute, Prague.

Kashima, N., 1993: Fracture of speleothems in Hoshino-no-ana Cave, Minami-Daito Island, Okinawa Prefecture, Southwest Japan.- Journal of the Speleological Society of Japan, 18, 33–41.

Klimeš, J., Rowberry, M.D., Blahůt, J., Briestenský, M., Hartvich, F., Košťák, B., Rybář, J., Stemberk, J. & P. Štěpančíková, 2012: The monitoring of slow moving landslides and assessment of stabilisation measures using an optical-mechanical crack gauge.- Landslides, 9, 3, 407–415.

Koliha, J., 1929: *Svrchní devon v pohoří Ještědském* [Upper Devonian in Ještěd Mountains].- Věstník Státního geologického Ústavu, 5, 268–292.

Kopecký, A., 1970: Neotektonický vývoj severních a severovýchodních Čech [Neotectonic development of northern and northeastern Bohemia].- Věstník Ústředního ústavu geologického, 45, 339–346.

Košťák, B., 1969: A new device for in situ movement detection and measurement.- Experimental Mechanics, 9, 8, 374–379.

Košťák, B., 1991: Combined indicator using moiré technique.- In: Sorum G. (ed.) *Field Measurements in Geomechanics, Proceedings of the 3rd International Symposium on Field Measurements in Geomechanics*, 9th–11th September 1991, Oslo. Balkema, 53–60, Rotterdam.

Košťák, B., 2006: Deformation effects in rock massifs and their long-term monitoring.- Quarterly Journal of Engineering Geology and Hydrogeology, 39, 249–258.

Košťák, B., Cacoń, S., Dobrev, N.D., Avramova-Tacheva, E., Fecker, E., Kopecký, J., Petro, Ľ., Schweizer, R. & A.A. Nikonov, 2007: Observations of tectonic microdisplacements in Europe in relation to the Iran 1997 and Turkey 1999 earthquakes.- Izvestiya Physics of the Solid Earth, 43, 6, 503–516.

Košťák, B., Mrlina, J., Stemberk, J. & B. Chán, 2011: Tectonic movements monitored in the Bohemian Massif.- Journal of Geodynamics, 52, 1, 34–44.

Košťák, B. & K. Popp, 1966: Moiré strain gauges.- Strain, 2, 2, 1–12.

Kozdrój, W., Krentz, O. & M. Opletal, 2001: *Comments on the geological map Lausitz-Jizera-Krkonoše (without Cenozoic sediments) 1: 100 000. Mit Geologische Karte und Legende*.- Sächsisches Landesamt für Umwelt, Landwirtschaft und Geologie, pp. 64, Freiberg.

Kurka, J. & V. Bělohradský, 1979: Průběh a charakter lužického zlomu mezi obcemi Světlá pod Ještědem a Zdislava [The course and character of the Lusatian Fault between the villages of Světlá pod Ještědem and Zdislava].- Acta Musei Bohemiae Borealis, Scientiae Naturales, 11, 185–196.

Malkovský, M., 1977: *Důležité zlomy platformního pokryvu severní části Českého masívu* [Significant faults in the platform cover of the northern Bohemian Massif].- Výzkumné práce Ústředního Ústavu Geologického, pp 30, Prague.

Malkovský, M., 1979: *Tektogeneze platformního pokryvu Českého masívu* [Tectonogenetic platform cover of the Bohemian Massif].- Ústřední ústav geologický, pp. 176, Prague.

Marti, X., Rowberry, M.D. & J. Blahůt, 2013: A MATLAB® code for counting the moiré interference fringes recorded by the optical-mechanical crack gauge TM-71.- Computers & Geosciences, 52, 164–167.

Oster, G. & Y. Nishijima, 1963: Moiré patterns.- Scientific American, 208, 5, 54–63.

Pošmourný, K., 1967: Geologicko-petrografické poměry krystalinika západní části Ještědského hřbetu [Geological and petrographical situation of the crystalline complex in the western part of Ještěd Ridge].- Acta Musei Bohemiae Borealis, Scientiae Naturales, 3, 15–25.

Šebela, S., 2008: Broken speleothems as indicators of tectonic movements.- Acta Carsologica, 37, 52–62.

Skřivánek, F. & J. Hromas, 1961: *Plán Západní jeskyně* [Map of Západní Cave].- Archiv Základní Organizace České Speleologické Společnosti 4–01, Liberec.

Stemberk, J., Košťák, B. & S. Cacoń, 2010: A tectonic pressure pulse and increased geodynamic activity recorded from the long-term monitoring of faults in Europe.- Tectonophysics, 487, 1–12.

Stemberk, J., Košťák, B. & V. Vilímek, 2003: 3D monitoring of active tectonic structures.- Journal of Geodynamics, 36, 1–2, 103–112.

Vyskočil, P. & A. Kopecký, 1974: *Neotectonics and recent crustal movements in the Bohemian Massif*.- Výzkumný ústav geodetický, topografický a kartografický (VÚGTK), pp. 179, Prague.

Wirth, W., Plenefisch, T., Klinge, K., Stammler, K. & D. Seidl, 2000: Focal mechanisms and stress field in the region Vogtland/Western Bohemia.- Studia Geophysica et Geodaetica, 44, 2, 126–141.

COBISS: 1.01

ILLUSTRATING THE SUPERPOSITION OF SIGNALS RECORDED BY THE GROTTA GIGANTE PENDULUMS WITH MUSICAL ANALOGUES

GLASBENA ANALOGIJA SUPERPOZICIJE SIGNALOV NIHAJNIH NAKLONOMETROV IZ JAME GROTTA GIGANTE (VELIKA JAMA V BRIŠČIKIH) Z GLASNEBO ANALOGIJO

Carla BRAITENBERG[1] & Ildikoʻ NAGY[1]

Abstract UDC 551.442(450.361)

Carla Braitenberg & Ildikoʻ Nagy: Illustrating the superposition of signals recorded by the Grotta Gigante pendulums with musical analogues

The Grotta Gigante houses a geodetic station since 1959, which has the goal to observe deformation of the cave. The instrumentation consists of two ultra-broad-band pendulum type tiltmeters, and two medium-to-longperiod tiltmeters, next to thermometer and pressure gauge. The exceptionally long and continuous time-series of the tiltmeters allows us to demonstrate the existence of several astonishing phenomena that cause the cave to change continuously in shape, also if only to a small amount and which can be recorded with sophisticated instruments, as the ones installed. The movements due to the different causes sum up to produce the complete observed signal, and our goal is to separate and identify the different phenomena. To illustrate the work we do in identifying the different agents, the analogy holds to a musician listening to a symphony- concert and identifying the melody of the first violin, flute, triangle, the violoncello and the double bass, and then identifying the corresponding musicians and instruments on stage. As the music has high and low tones, the deformation of the cave is composed of slow and fast movements, continuous movements, or abrupt, sudden events, that repeat very rarely. Here we show the observation sequence of tilt for the time interval 1966–2012, and discuss the deformation due to the following causes: temperature, underground water-level, sea level of the Adriatic sea, position of sun and moon and vibration of the Earth due some of the greatest mega-earthquakes ever recorded. To illustrate the analogues to music we use to explain the association of different frequency ranges to different causes of deformation signal to the general public of the cave. The results show an excellent example of scientifically sound and important instrumentation installed in a show-cave visited regularly by the public.

Keywords: Grotta Gigante (Northeastern Italy), horizontal pendulums, Earth music, Popular Geology, Ground water-movement.

Izvleček UDK 551.442(450.361)

Carla Braitenberg & Ildikoʻ Nagy: Glasbena analogija superpozicije signalov nihajnih naklonometrov iz jame Grotta Gigante (Velika jama v Briščikih) z glasnebo analogijo

V Veliki jami v Briščikih je že od leta 1959 geodetska postaja, ki je namenjena meritvam deformacij jame. Inštrument sestavljajo dva nihajna naklonomera z izjemno široko pasovno širino in dva naklonomera v območju srednjih in dolgih nihajnih časov. Izjemno dolga zvezna časovna vrsta meritev nosi zapis dogodkov, ki spreminjajo obliko jame. Čeprav gre za zelo majhne premike, občutljivi instrumenti to zaznajo. Premiki jame ustvarjajo signale, ki jih poskušamo ločiti in pripisati različnim vzrokom. To delo lahko primerjamo s poslušanjem koncerta, kjer različne zvoke pripisujemo različnim instrumentom in glasbenikom. Kot ima glasba visoke in nizke tone, so lahko tudi premiki počasni, hitri, zvezni, nenadni, pogosti ali redki. V članku obravnavamo časovno vrsto iz obdobja 1996–2012 in opisujemo deformacije zaradi sprememb temperature, nivoja podzemne vode, nivoja Jadranskega morja, položaja sonce in lune in nekaj najmočnejših do sedaj zabeleženih potresov. Različna frekvenčna območja signalov pripadajo različnim vzrokom, kar obiskovalcem jame ponazorimo z glasbeno analogijo. Opisana raziskava je lep primer izvajanja in predstavitve znanstvenih raziskav v turistični jami.

Ključne besede: Grotta Gigante (Velika jama v Briščikih), severovzhodna Italija, vodoravna nihala, glasba Zemlje, poljudna geologija, tok podzemne vode.

[1] Department of Mathematics and Geosciences, University of Trieste, via Weiss 1, 34100 Trieste, e-mail: berg@units.it

Received/Prejeto: 05.07.2013

INTRODUCTION

The horizontal pendulums situated in the largest cave of the Italian Karst, in the Grotta Gigante, are very sophisticated instruments able to capture very small movements of the cave, as they detect cave rotation and horizontal cave shearing (Marussi 1960; Braitenberg 1999a; Braitenberg & Zadro 1999). Moreover they are sensitive to transient mass changes that induce changes in the inclination of the plumb line. The particular setup of these instruments is unique, as they are suspended from the top of the cave, making the cave the instrument casing. The Grotta Gigante station belongs to the world wide tiltmeter stations that have the scope to measure tilt either for the purpose of risk estimations in volcanic or seismic environments, or for the scientific purpose of better understanding the earth deformations (e.g. Zadro & Braitenberg 1999). Due to the different dynamic forces and atmospheric agents the superficial layers of the earth's crust deform continuously, a phenomenon that can be detected by surface measurements like the classical repeated leveling (e.g. Spampinato *et al.* 2013), satellite geodetic observations as GPS and Interferometric techniques like InSAR (Interferometric Synthetic Aperture Radar) and underground observations with tiltmeters and extensometers.

Due to their exceptional dimensions, made possible by the spectacular size of the cave (112 m height), the Grotta Gigante pendulums are extremely stable with a background noise which is several orders of magnitude less than traditional instruments of smaller size. This fact allows to detect extremely weak signals, that otherwise are masked by the noise. The different measurements made for observing deformation are illustrated in Fig. 1: two fixed GPS stations give us the horizontal and vertical movement of the benchmark in a global reference frame, the difference between the two GPS stations gives us either tilting if we take the difference between the two vertical movement rates, or horizontal extension rates, if we take the difference between the horizontal movement rates (Pinato Gabrieli *et al.* 2006). The horizontal extension can be observed also with a strainmeter installed underground, that consists in a device measuring the distance changes between two fixed points in a well or cave. The tilting underground is observed with a horizontal pendulum, or with water tube tiltmeters, bubble tiltmeters, or vertical pendulums (for a review on the instrumentation see Zadro & Braitenberg 1999).

A product of year-long study of the observations, is the identification of the many signals that compose the observed time variation of tilt (Braitenberg *et al.* 2001). We find different causes that make the earth deform, and which are captured by the pendulums. Our station being located in a touristic cave, we are confronted frequently with the problem of making our knowledge of the signals understandable to the general public and giving explanations of what the pendulums are observing. A typical feature of the observed deformation is, that the different causes that generate deformations, also have different characteristic periods, so we are able to separate them by filtering procedures. This concept is difficult to understand for many people and they cannot

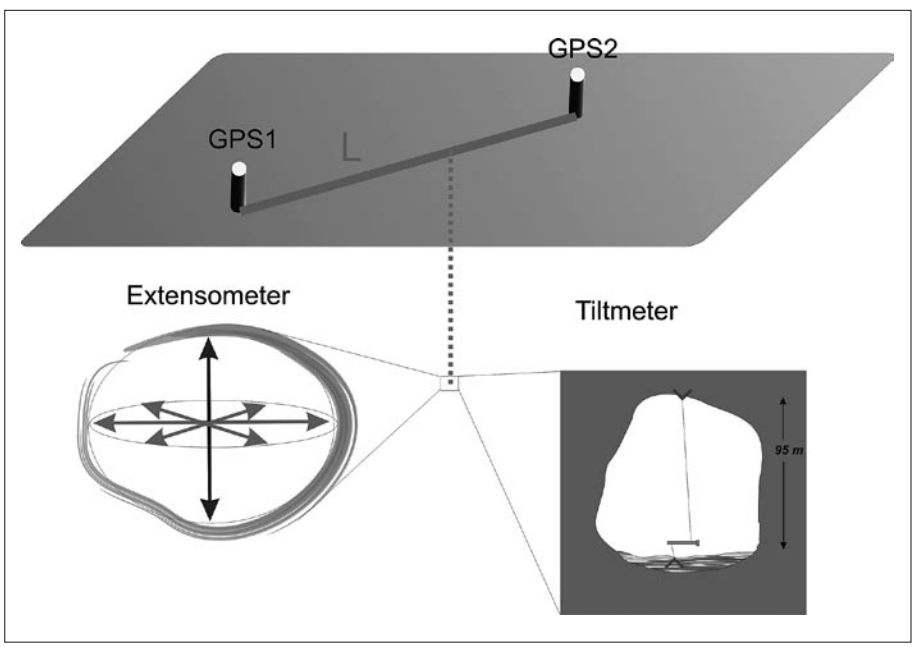

Fig. 1: Deformation measurement on and under the Earth surface. Cartoon illustrating the differential GPS measurements (tilt and extension), the extensometer and tilt measurements in caves.

imagine what we are talking about. The first obstacle in explaining the signals is the concept of superposition of signals at different frequencies, or equivalently different periods and their association to cause and effect. Here we show an easily accessible way of explanation, which uses analogies to the world of classical written music and which was possible due to the cooperation of an internationally known composer, Olga Neuwirth, and Peter Plessas from a specialized sound-studio, the IEM – Institute of Electronic Music and Acoustics, Graz. Here we publish an excerpt of the data record of the Sumatra-Andaman Island earthquake of 2004, transformed into a piece of music. It is Olga Neuwirth's composition "Kloing!" for computer-controlled piano, pianist and video. In this piece, the computer-controlled piano player reproduces a score deducted from the seismic data by the composer, while a human performer "competes" against the automatic piano in a spectacular duel. The full composition includes a video where simultaneously pictures are screened, showing famous pianists, the geodetic observation station in Trieste and a 1905 Welte-Mignon piano (http://www.festival-automne.com/olga-neuwirth-show1498.html).

DESCRIPTION OF INSTRUMENTS IN GROTTA GIGANTE

The ultra broad band horizontal geodetic pendulums of the Grotta Gigante are designed to measure the Earth crustal movement over a large range of periodicities, from quasi static changes, typical of secular tectonic movements to rapid seismic deformations. It measures the variation of the direction of two earth-fixed reference points with respect to the plumb line (vertical) (Zadro & Braitenberg 1999; Braitenberg 2011). The Fig. 2 shows two phenomena picked up by the pendulums, the rotation or shear of the cave through which the upper mounting of the pendulum is shifted horizontally relatively to the lower mounting (Fig. 2a), and the change in direction of the plumb line due to mass changes (Fig. 2b).

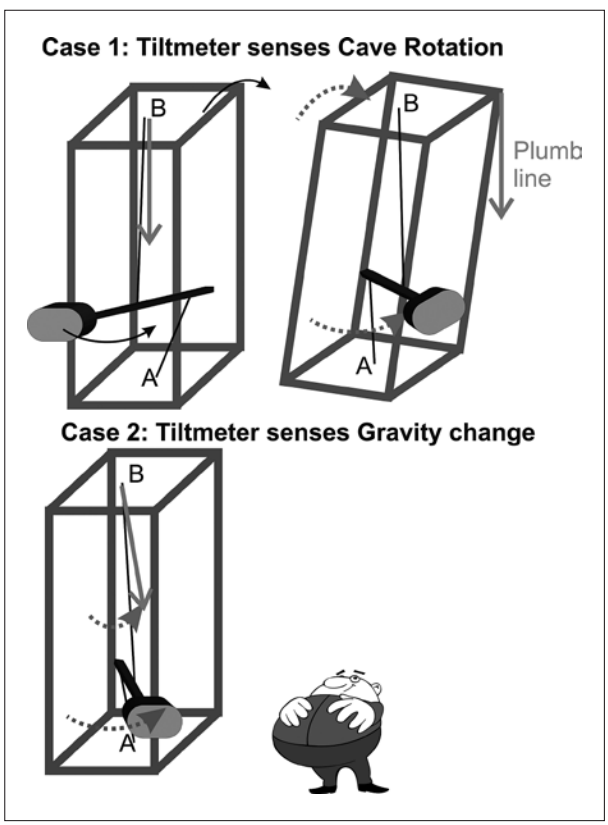

Fig. 2: Two aspects of the sensitivity of a tiltmeter. Case 1: Response of the tiltmeter to rotation or shear of the cave. Case 2: Response of the cave to the angular change of the plumb line.

The essential elements of the horizontal pendulums are shown in Fig. 3. Fig. 3a shows the suspension of the pendulum in the cave. The mechanical parts and the acquisition system are shown in Fig. 3b. The digital acquisition system (Braitenberg *et al.* 2004; 2006) consisting of a laser beam and a position device built by the colleagues Dr. Giovanni Romeo and Dr. Quintilio Taccetti from the Istituto Nazionale di Geofisica e Vulcanologia (INGV). It replaced the analog acquisition on photographic paper.

The vertical pendulum is made of a mass suspended by a rod or wire which can oscillate in the vertical plane about a horizontal axis. The horizontal pendulum is made of a mass attached to a rod which can oscillate in a subhorizontal plane about a near to vertical axis. This axis makes a small angle φ with respect to the vertical axis (Fig. 3b). Compared to the vertical pendulum of equal dimensions, the horizontal pendulum has an increased oscillation period. Supposing the upper fixed point of the near to vertical axis is shifted with respect to the lower fixed point along the Meridian, so that the line connecting the two fixed points makes an angle φ with the vertical, then the rod has its equilibrium position in the Meridian plane. If the direction of the vertical changes due to a mass change or the axis changes due to a deformation of the cave towards east by a small angle α, the rod will rotate towards east by the angle α/sin φ. Having two pendulums mounted at 90° to each other,

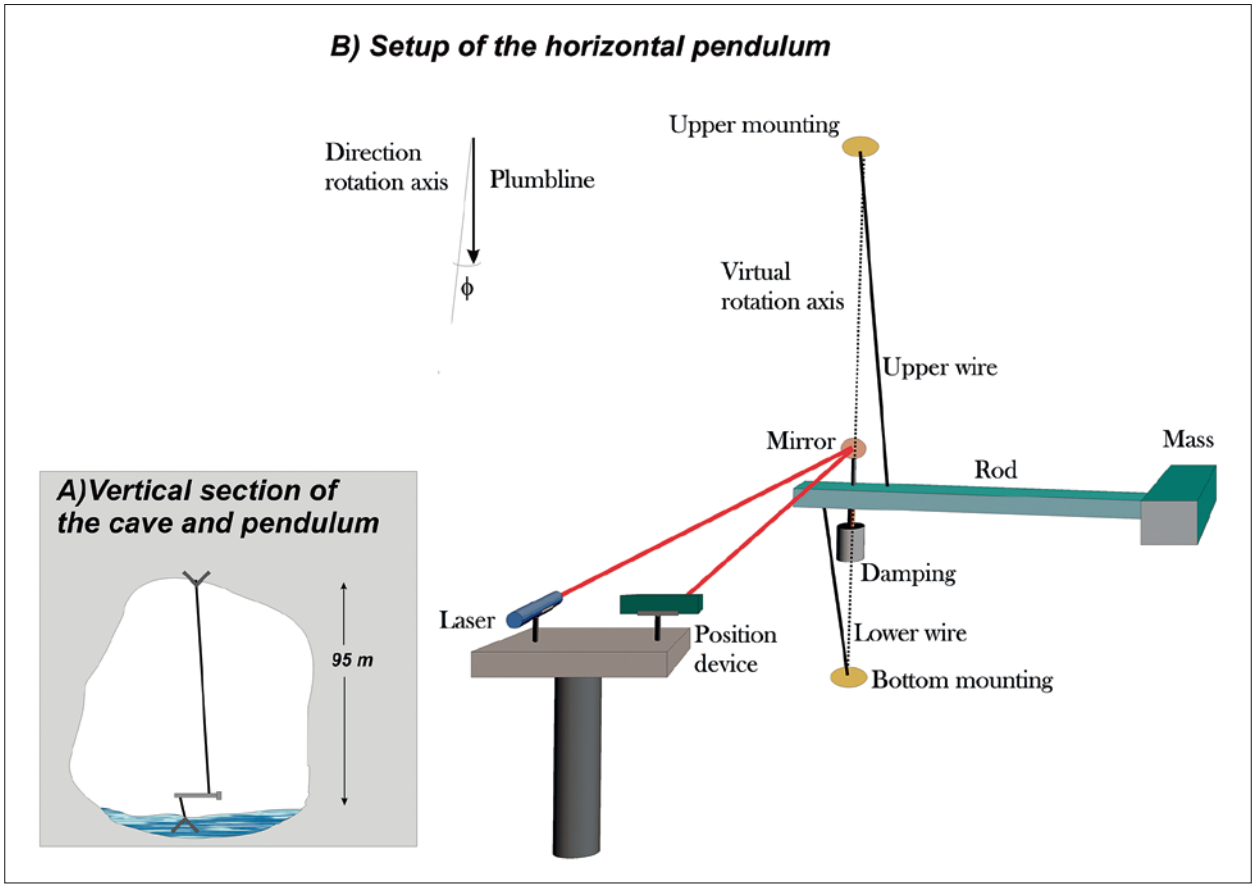

Fig. 3: Schematic drawing of the horizontal pendulum of Grotta Gigante. The rod with the mass rotates in the horizontal plane about the virtual rotation axis. The angle φ of the virtual rotation axis with the plumb line is essential for the amplification factor of the pendulum.

allows to have an instrument sensitive in both NS and EW directions. The movement of the rod is recorded by an optical device that records the light ray reflected by a mirror mounted on the rod (e.g. Braitenberg *et al.* 2006). The digital recording system is based on a solid-state acquisition system intercepting a laser light reflected from a mirror mounted on the horizontal pendulum beam. The sampling rate is 30 Hz, which makes this long-base instrument a ultra-broad- band tiltmeter, apt to record the tilt signal on a broad-band of frequencies, ranging from secular deformation rate through the earth tides to seismic waves. The smallest resolved tilt is 0.009 nrad (1 nrad = 10^{-9} radians). The digital data are transferred to the serial port of the PC, and the data are saved on hourly files of 109,600 samples by the acquisition software . The PC, running Linux, is accessible via ethernet, so the data are available in real time.

The first edition of the horizontal pendulums of the Grotta Gigante were built in 1959 by Antonio Marussi (Marussi 1959). The upper and lower wires of the horizontal pendulum-rod are fixed directly into the rock, at a vertical distance of 95 m. The oscillation period of the pendulum is near to 6 min. Next to tilt, the atmospheric pressure and temperature are measured at the station, as well as the tilting with a couple of traditional small scale tiltmeters.

THE DIFFERENT SIGNALS RECORDED BY THE GROTTA GIGANTE HORIZONTAL PENDULUMS

The complete time signal recorded by the pendulums is generated by many agents and when graphed, results in the superposition of oscillations of different frequencies, aperiodic variations and long term varia-

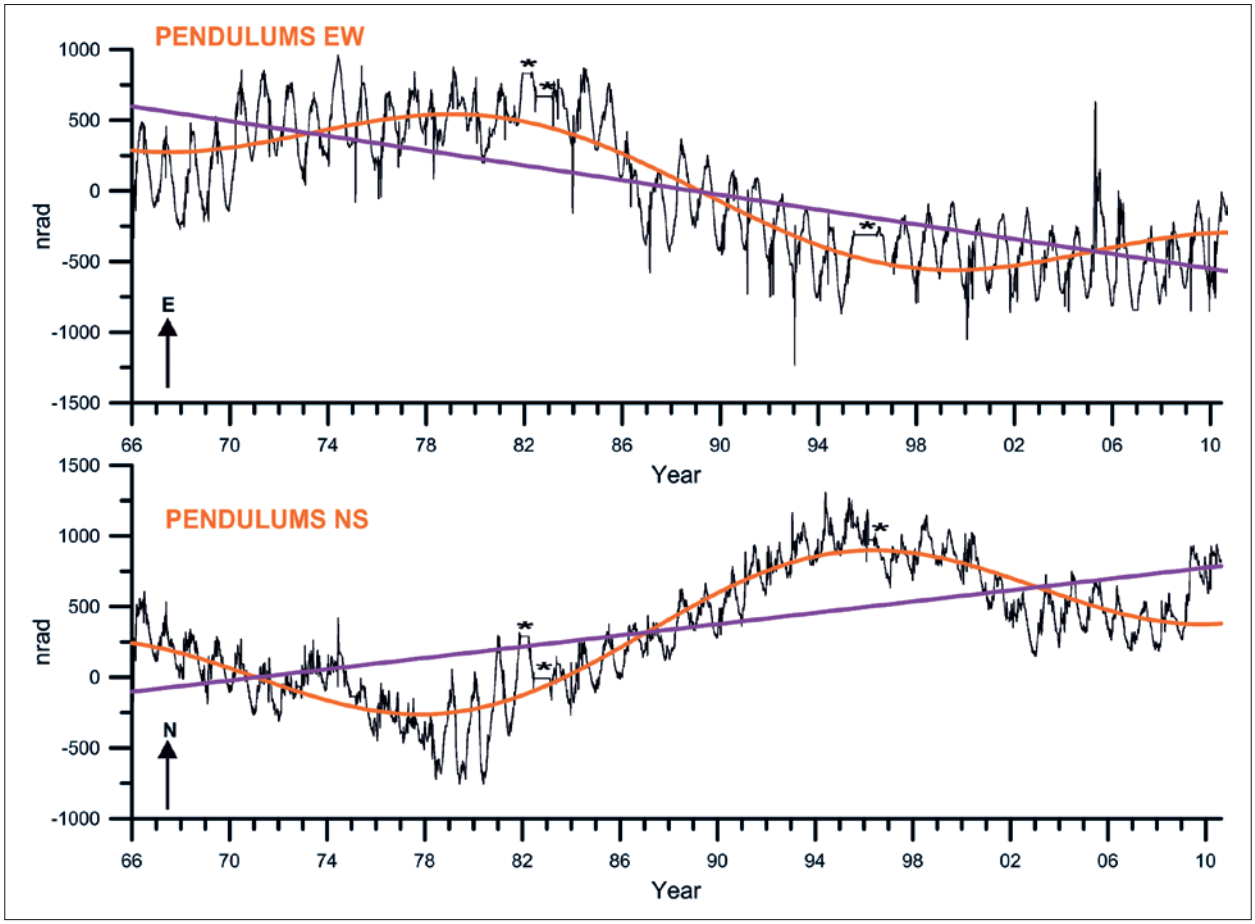

Fig. 4: Tilt observation(black) from 1966, secular variation (violet), secular variation and multi-decadal oscillation (orange).

tions. The main causes that make the Grotta Gigante deform are, from slow to fast movements: plate tectonic deformation, due to the fact that the station is on the north-eastern border of the Adria plate, which bends downwards and northwards below the sedimentary layers of North- Eastern Italy (Braitenberg *et al.* 2001). The movement generates the strong earthquakes of Friuli-Venetia and along the Dinarides mountain range. The pendulums record a steady north-westerly tilting of the cave over the last 48 years. The tidal movements are a perfectly regular oscillatory movement with the a package of diurnal and semi-diurnal periodicities of one day and half a day with a fortnightly modulation generated by the gravitational attraction of moon and sun. Near and far earthquakes are the expression of the rupture of a piece of rock, that gives way to the accumulation of deformation over decades of time. The fault can be in any place of the globe, and the seismic waves penetrate the globe as well as travelling along its surface before striking the cave. In the near field of the rupture a co-seismic deformation is observed, generated by the dislocation of the fault surface. The radius in which the co-seismic deformation is observed depends on the area of the fault plane and on the length of the dislocation. The amplitude of the deformation decays with the third power of distance and increases by a factor 31 for a unit increase in Magnitude (Wyatt 1988). Up to now the earthquakes were too distant to generate an observable coseismic permanent deformation at Grotta Gigante. The seismic waves generated by the breaking of the fault travel all over the globe. For very big earthquakes, greater magnitude 6, the pendulums measure the free oscillations of the earth, which are the series of well defined frequencies at which the earth oscillates. This signal is well defined due to the fact that the frequencies have been calculated with high precision (Dahlen & Sailor 1979). The lowest period is 54 minutes, and then the periods decrease up to fractions of a minute. The oscillations pursue for hours after the main shock and can be still recorded for days with decreasing amplitude (e.g. Braitenberg & Zadro 2007). Seismic waves caused by the rupture of the fault plane are propagating oscillations of the ground, that travel at a speed of 4–8 km/sec, and oscillate with frequencies between 1mHz and 50 Hz. A completely dif-

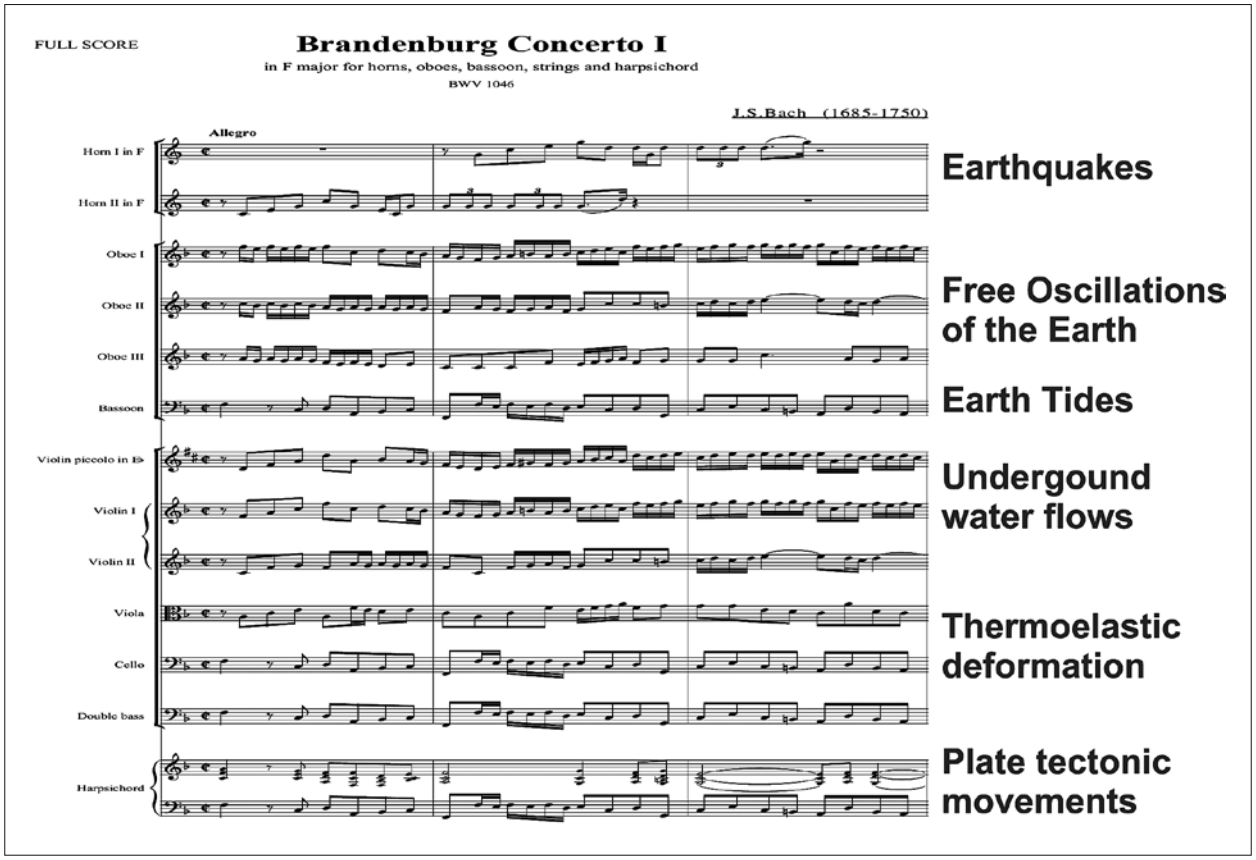

Fig. 5: The recorded movement is the sum of the effects of different agents, as in a score are acting different musical instruments for the final sound.

ferent type of tilting that is observed by the pendulums is due to the action of environmental effects, which are underground water flow (Grillo *et al.* 2011; Tenze *et al.* 2013; Braitenberg & Zadro 2001; Braitenberg 1999b), the ocean loading and the thermo-elastic deformation. The underground water flow is of general interest, as it could lead to trigger small earthquakes (Braitenberg 2000). The atmospheric pressure variations are hardly recorded in terms of deformation by the pendulums. All these deformations sum up and are the cause of the complete time varying tilting of the pendulums. In Fig. 4 the tilting from 1966 along the directions EW and NS can be seen as a graph. At the time scale of several decades only the slower movements can be appreciated, the faster movements as seismic waves and free oscillations having a much smaller amplitude.

In order to explain to the general public what the geophysical job is of interpreting the tilt signals, we choose the analogue to a piece of chamber music that has been written by the composer. The sheet music consists of the notes that the different instruments play at the same time (Fig. 5): The sheet scores give the deepest sounding at the bottom, and moving upward the higher-pitch instruments are found, grouped by type. In the example of Fig. 5 the score starts from the harpsichord, passing to the strings, and then to the wind instruments. Looking at an orchestra from right to left, we go from the double bass to the cellos and violins, and in second row from the flutes, trumpets back to the tuba on the right. The deep-sounding instruments usually play slowly, as the double bass, the higher instruments quickly. The deeper instruments are heard at great distance, the higher instruments only to close range. The sound that reaches the ear is the superposition of all the scores played by the single instruments. We could record it with a microphone and obtain a graph analogous to the one that we make for the tilt-observations. The musician will try to distinguish the scores played by the different instruments, and a skilled musician will even identify the size and type of instrument and qualities of the orchestral player. The job of the scientist in studying the records of the pendulum is analogous, in that from the complete record the goal is to define the different causes, their properties, the location, the evolution in time. It would correspond to writing down the sheet music by only listening to the orchestral piece.

We can also try to use our ear to understand the records of the pendulums better than representing it on a graph, by transforming it to the audible frequency range. A first audification of a 24h long sequence that covers the Earthquake of the Sumatra-Andaman islands of 2004 (Park *et al.* 2005) (Fig. 6) has been done by the composer Olga Neuwirth and Peter Plessas, IEM - Institut für Elektronische Musik und Akustik, Graz, Austria. Their experiments found that a direct transformation of 24^h observations to the 20Hz to 20 kHz audible frequency range of the human ear, resulting in a short piece of 10 sec, was not satisfactory for the ear, as the sound was too uniform, and only the main shock of the event gave an appreciable sound. Rather, the transformation was done mapping the amplitudes to frequencies of an instrument like the piano, in the sense that tilts to the East were mapped to low tones, tilts to West to high tones. The main shock of the event thus is transformed to a broad arpeggio that runs over the entire extent of the piano- keys. Smaller amplitude variations result in a twinkling sound of the piano. The final product was the composition "Kloing!" for computer-controlled piano, pianist and video, which was premiered in Weimar (Kunstfest 2008), with subsequent performances in Cologne (Philharmonie 2010), Paris (Festival d'Automne 2011) and Vienna (Wien Modern 2012) and gained lots of credits from the public. The aim of the experiment was to produce a piece that from the musical standpoint was valuable, so the scientific aspect of extracting the different geophysical signals was not pursued further. In the frame of the touristic caves it is a nice example of an innovative way to illustrate the different recorded signals to the general public and to illustrate the concept of a time series recorded by the geodetic pendulums. An example of the audification is given in an audio file (Audio 1), which is an excerpt from the composition Kloing! By Olga Neuwirth.

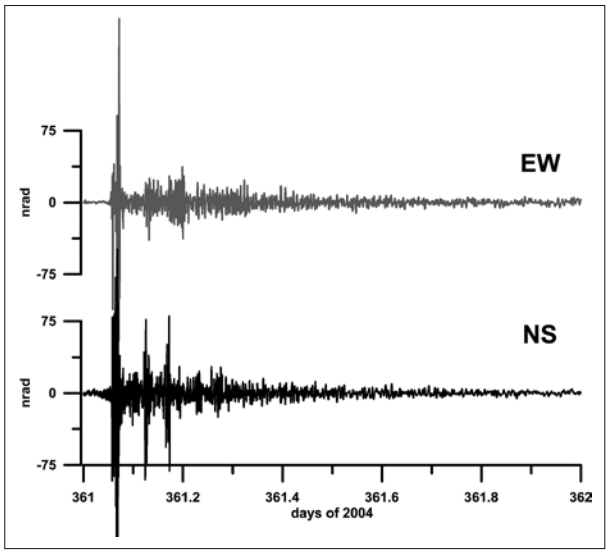

Fig. 6: Tilt records of the Earthquake Andaman-Sumatra Islands 2004, which was used for the sonification and transformed to music.

DISCUSSION AND CONCLUSIONS

The Grotta Gigante cave is a good example of a touristic unique cave being also the site of long lasting scientific measurements. Here we discuss the geodetic horizontal pendulums that measure deformation of the cave and mass changes. Next to these geodetic instruments, also seismometers and a Radon monitoring station are continuously producing data. The scientific measurements in the cave add value to the touristic attraction, because steadily new discoveries and results make multiple visits to the cave attractive. The scientists are then confronted with the problem of making the measurements understandable and fascinating to the general public of all ages and cultural background. It requires the illustration with hands on examples and intuitive transmission of information. An important concept in the geodetic measurements is the superposition of different signals each with characteristic frequencies, ranging from quasi-static movements to rapid aperiodic and periodic oscillations. The long history of scientific analysis has led us to be able to distinguish the different causes and associate them with their characteristic signals and frequencies. We find that this concept of associating a characteristic signal to its time variations, which can range from quasi-static to high frequencies, is not well understood by the public. It is for this reason that we find the analogue to a musical piece very useful. The concept of low and high tones, and the associated slow and fast movement is near to obvious to anyone. Musical groups have the slow and deep-sounding instruments and voices that complement the fast and high pitch soprano singer and instruments, and who listens to the music is well aware of being able to distinguish the different instruments and players. The other aspect of analogy of recorded sound to music, is to make the scientific records audible to the human ear, which in the case of the geodetic pendulums implies a mapping from the records to music. The ex-

periments resulted in a piece of music for pianos that has been successfully performed on stage. Concerning other caves, it could be thought of making also the droplets hearable, temperature variations, water level of the river forming the cave. The transformation to sound allows results to be more effective than the visual graph of a wiggly curve, and adds a dimension in human perception of the tourist visiting the cave, who can use eyes, nose, ear and feeling, only missing taste to use all five senses during the visit to the cave.

ACKNOWLEDGEMENTS

Peter Plessas and Olga Neuwirth are thanked for granting permission to publish an excerpt from the composition "Kloing!" for computer-controlled piano, pianist and video, which was premiered in Weimar (Kunstfest 2008). Giovanni Romeo and Quintilio Taccetti from INGV are thanked for the development of the digital acquisition system of the Grotta Gigante pendulums and the INGV is thanked for the support of the Grotta Gigante geodetic station.

REFERENCES

Braitenberg, C., 1999a: The Friuli (NE Italy) tilt/strain gauges and short term observations.- Annali di Geofisica ,42, 1–28.

Braitenberg, C., 1999b: Estimating the hydrologic induced signal in geodetic measurements with predicitive filtering methods.- Geophys. Res. Letters, 26, 775–778.

Braitenberg, C., 2000: Non-random spectral components in the seismicity of NE Italy.- Earth Planet. Science Lett., 179, 2, 379–390.

Braitenberg, C., 2011: Ultra broad band horizontal geodetic pendulums.- In: Harsh, K. Gupta (ed.) *Encyclopedia of Solid Earth Geophysics,* DOI :10.1007/978–90–481–8702–7, Springer Science-+Business Media.

Braitenberg, C. & M. Zadro, 1999: The Grotta Gigante horizontal pendulums instrumentation and observations.- Boll. Geof. Teor. Appl., 40, 3/4, 577–582.

Braitenberg, C. & M. Zadro, 2001: Time series modeling of the hydrologic signal in geodetic measurements.- Journal of the Geodetic Soc. of Japan, 47, 95–100.

Braitenberg, C., Nagy, I., Romeo, G. & Q. Taccetti, 2004: The very broad-band data acquisition of the long-base tiltmeters of Grotta Gigante (Trieste, Italy).- In: Zhu, Y. & Heping,S. (Eds.) *Progress in Geodesy and Geodynamics,* 457–462, Hubei Science and Technology Press, Wuhan, ISBN 7–5352–3194–2/P.10.

Braitenberg, C., Nagy, I., Negusini, M., Romagnoli, C., Zadro, M. & S. Zerbini 2001: Geodetic measurements at the northern border of the Adria plate, J. of Geodynamics, 32, 1/2, 267– 286.

Braitenberg, C., Romeo, G., Taccetti, Q. & I. Nagy, 2006: The very-broad-band long-base tiltmeters of Grotta Gigante (Trieste, Italy): Secular term tilting and the great Sumatra-Andaman Islands earthquake of December 26, 2004.- J. of Geodynamics, 41, 164–174.

Braitenberg, C. & M. Zadro, 2007: Comparative analysis of the free oscillations generated by the Sumatra-Andaman Islands 2004 and the Chile 1960 earthquakes.- Bulletin of the Seismological Society of America, 97, 1A, S6–S17, doi: 10.1785/0120050624.

Dahlen, F. A. & R. V. Sailor, 1979: Rotational and elliptical splitting of the free oscillations of the Earth.- Geophys. J. R. Astr. Soc., 58, 609–623.

Festival d'Automne a Paris, 2011: Festival d'automne a Paris, 41. edition, Music- Olga Neuwirth- Kloing! Computer programmed piano with live video [online] Available from: http://www.festival-automne.com/olga-neuwirth-show1498.html [Accessed 15 July 2013].

Grillo, B., Braitenberg, C., Devoti, R. & I. Nagy, 2011: The study of Karstic aquifers by geodetic mesurements in Bus de la Genziana station - Cansiglio Plateau (Northeastern Italy).- Acta Carsologica, 40/1, 161–173.

Marussi, A., 1959: The University of Trieste station for the study of the tides of the vertical in the Grotta Gigante. In Proceedings of the III Int. Symposium on Earth Tides, Trieste, 1960, pp. 45–52.

Marussi, A., 1960: I primi risultati ottenuti nella stazione per lo studio delle maree della verticale della Grotta Gigante, Boll. Geod. Sci. Affini, 19, 645–667.

Park J., Song T. A., Tromp J., Okal E., Stein S., Roult G., Clevede E., Laske G., Kanamori H., Davis P., Berger J., Braitenberg C., Van Camp M., Lei X., Sun H., Xu H. & S. Rosat, 2005: Earth's free oscillations excited by the 26 december 2004 Sumatra-Andaman earthquake.- Science, 308, 1139–1144.

Pinato Gabrieli, C., Braitenberg C., Nagy I. & D. Zuliani, 2006: Tilting and horizontal movement at and across the northern border of the Adria plate.- Gil A.J. & F. Sansò (Eds.) *Geodetic Deformation Monitoring: From Geophysical to Engineering Roles*, Springer Verlag, pp. 129–137. ISBN–10: 3–540–38595–9. (IAG Symposium Jaén, Spain, March 7–19,2005; Series: International Association of Geodesy Symposia , Vol. 131)

Plessas, P., 2008: "Olga Neuwirth – Kloing!" IEM Arbeitsbericht, September 2008.- [Online] Available from: http://old.iem.at/projekte/composition/neuwirth/kloing/bericht.pdf [Accessed 15 July 2013].

Spampinato C.R., Braitenberg, C., Monaco, C. & G. Scicchitano, 2013: Analysis of vertical movements in eastern Sicily and southern Calabria (Italy) through geodetic leveling data.- Journal of Geodynamics, 66, 1–12.

Tenze D., Braitenberg C. & I. Nagy, 2012: Karst deformations due to environmental factors: evidences from the horizontal pendulums of Grotta Gigante, Italy.- Bollettino di Geofisica Teorica ed Applicata, 53, 331–345, doi:10.4430/bgta0049.

Wien Modern 2012, 2012: Das Festival für Musik der Gegenwart.- [Online] Available from: http://www.wienmodern.at/Home/ARCHIV/Datenbank.aspx [Accessed 15 Juli 2013].

Wyatt, F.K. 1988: Measurements of coseismic deformation in Southern California: 1972–1982, J. Geophys. Res., 93, 7923–7942.

Zadro, M. & C. Braitenberg, 1999: Measurements and interpretations of tilt-strain gauges in seismically active areas.- EarthScience Reviews, 47, 151–187.

Audio 1: Sonification of the record of the Sumatra Andaman islands 2004 earthquake of magnitude 9.2. Music by Olga Neuwirth in cooperation with Peter Plessas (IEM – Institut für Elektronische Musik und Akustik, Graz, Austria.). Excerpt from Kloing! The original record of the geodetic pendulums is shown in Fig. 6. Available at: http://www2.units.it/geodin/Neuwirth- Kloing!(Excerpt)_PromotionOnly.mp3

COBISS: 1.01

TEMPORARY SEISMOLOGICAL MEASUREMENTS IN THE POSTOJNA CAVE SYSTEM

OBČASNE SEIZMIČNE MERITVE V POSTOJNSKEM JAMSKEM SISTEMU

Mladen ŽIVČIĆ [1], Giovanni COSTA [2], Peter SUHADOLC [3] & Stanka ŠEBELA [4]

Abstract UDC 551.435.84:550.34.016(497.471)

Mladen Živčić, Giovanni Costa, Peter Suhadolc & Stanka Šebela: Temporary seismological measurements in the Postojna Cave System

Karst caves are suitable places for seismological measurements because they are situated under the surface and often have lower seismic noise than locations on the surface. The idea to establish the first underground seismological station in Slovenia has led us to make preliminary seismic noise measurements in Črna Jama (part of the Postojna Cave System) in 2007. In search for further suitable stable places within the cave, we next performed seismic noise measurements, followed by a temporary accelerometer installation, near the highest point of the Velika Gora chamber in the first half of 2010. Since 7 May 2010, the seismic station is located inside the 9 m long artificial tunnel that was built for geophysical measurement purposes in Tartarus passage in 1931. From 27 January to 12 February 2010, the seismological station Velika Gora in Postojna Cave System (VGPJ) recorded 79 earthquakes with epicenters near Postojna. Records were especially important to determine the seismological characteristics of the $M_{LV} = 3.7$ Postojna earthquake (15 January 2010) aftershocks. The station in the Tartarus tunnel (TTPJ) operated from 7 May 2010 till 21 December 2010 and recorded more than hundred earthquakes of the sequence near Ilirska Bistrica that started on 15 September 2010, with two $M_{LV} = 3.5$ earthquakes and lasted till the end of the year 2010. The aim of this study is the installation of a permanent seismic station inside the Postojna Cave System and future real-time integration of the related seismological data within the Slovenian and Italian seismological networks.

Keywords: temporary seismological measurements, seismic noise, accelerometer, Postojna Cave System, Slovenia.

Izvleček UDK 551.435.84:550.34.016(497.471)

Mladen Živčić, Giovanni Costa, Peter Suhadolc & Stanka Šebela: Občasne seizmične meritve v Postojnskem jamskem sistemu

Kraške jame so primerna mesta za seizmološke meritve, saj se nahajajo pod površjem in imajo običajno nižji seizmični nemir kot mesta na površju. V želji, da bi postavili prvo podzemeljsko seizmološko postajo v Sloveniji, smo leta 2007 opravili predhodne meritve seizmičnega nemira v Črni jami (del Postojnskega jamskega sistema). Pri iskanju naslednjih ustreznih mest v jami smo v nadaljevanju v prvi polovici leta 2010 opravili meritve seizmičnega nemira ter začasno namestili pospeškometer v bližini najvišje točke podorne dvorane Velike Gore. Od 7. maja 2010 je potresna opazovalnica nameščena v 9 m dolgem umetnem tunelu, ki je bil zgrajen za geofizikalne meritve leta 1931 v Tartarusu. Od 27. januarja do 12. februarja 2010, je seizmološka postaja na Veliki Gori v Postojnskem jamskem sistemu (VGPJ) zabeležila 79 potresov z nadžarišči pri Postojni. Podatki so bili posebno pomembni za določitev seizmoloških značilnosti popotresnih sunkov potresa $M_{LV} = 3.7$ v Postojni 15. januarja 2010. Postaja v tunelu v Tartarusu (TTPJ) je delovala od 7. maja 2010 do 21. decembra 2010 ter zabeležila več kot sto potresov sekvence pri Ilirski Bistrici, ki se je začela 15. septembra 2010 z dvema $M_{LV} = 3.5$ potresoma in je trajala do konca leta 2010. Namen študije je namestitev stalne potresne opazovalnice v Postojnskem jamskem sistemu in njena vključitev v realnem času v slovensko in italijansko seizmološko mrežo.

Ključne besede: občasne seizmične meritve, seizmični nemir, pospeškometer, Postojnski jamski sistem, Slovenija.

[1] Slovenian Environment Agency, Seismology and Geology Office, Dunajska 47, Ljubljana, Slovenia, e-mail: mladen.zivcic@gov.si
[2, 3] Università degli Studi di Trieste, Dipartimento di Matematica e Geoscienze, via Weiss 2, 34128 Trieste, Italy, e-mail: costa@units.it, suhadolc@units.it
[4] Karst Research Institute ZRC SAZU, Titov trg 2, 6230 Postojna, Slovenia, e-mail: sebela@zrc-sazu.si

Received/Prejeto: 24.01.2013

INTRODUCTION

Within the framework of the agreement on scientific co-operation between *Agencija RS za okolje (Urad za seizmologijo in geologijo)* from Ljubljana, Slovenia (ARSO), the *ZRC SAZU (Inštitut za raziskovanje krasa)* from Postojna, Slovenia (IZRK ZRC SAZU) and the *Dipartimento di Matematica e Geoscienze Università degli Studi di Trieste*, Italy (DMG), the Italian partner proposed to install an accelerometric station in the Postojna Cave System. In Northern Italy there are already two underground seismic stations in continuous operation (station TRI in Grotta Gigante and station VINO in Grotta di Villanova). Karst caves are good places for such measurements due to the fact that seismic noise is lower underground than on the surface.

The aim of the study is to find a suitable place for installation of the permanent seismic station inside the

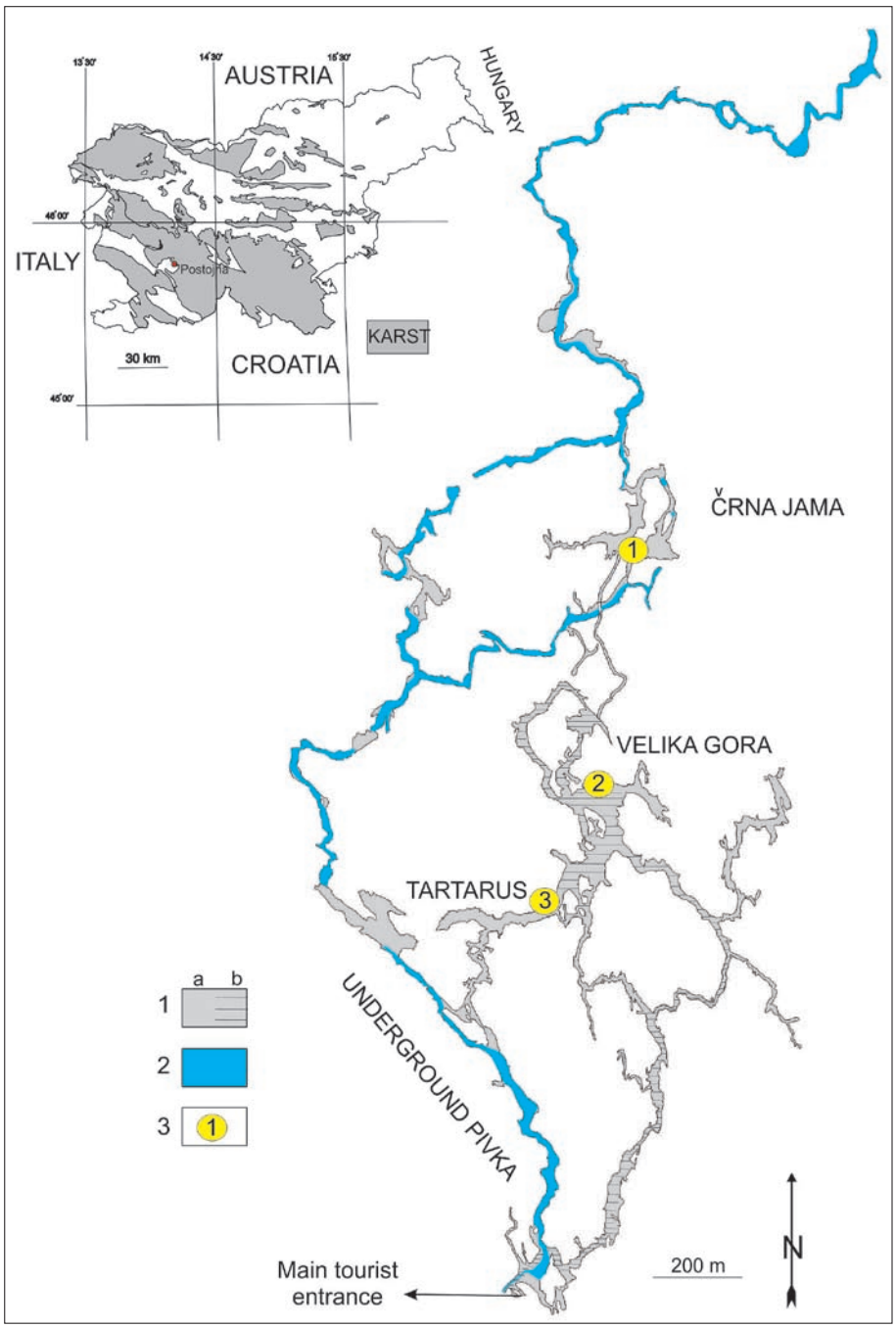

Fig. 1: The Postojna Cave System – locations of temporary seismological and seismic noise measurements.
1 – Dry cave passages (a-not frequently visited, b-tourist passages),
2 – Underground River Pivka passages,
3 – monitoring sites (1 = Črna Jama CJPJ, 2 = Velika Gora VGPJ and 3 = Tartarus tunnel TTPJ).

Postojna Cave System and to connect the instrument in the cave with GPS and GSM antennas outside the cave for accurate timing and for on-line flow of seismological data to the data centers of the Slovenian and Italian seismic networks.

The article describes the first results of seismic noise measurements in parts of the Postojna cave system named Črna Jama (being accomplished in 2007), Velika Gora and Tartarus (measured in 2012), and of the temporary seismological recordings on Velika Gora and in the artificial tunnel in Tartarus obtained since January 2010. The first analyses have shown low seismic noise in the cave, and proved that the artificial tunnel in Tartarus is appropriate for a permanent seismological station installation.

Geophysical studies in the Postojna Cave System started already in 1932 (R. R. Grotte Demaniali di Postumia 1933). Horizontal pendulums with photographic recording were the instruments used to detect minimal variations of the vertical. They were constructed at the Astronomic Observatory in Trieste and installed in the 9 m long artificial tunnel, built in 1931, in the Tartarus section of the Postojna Cave System (Fig. 1). During May 1932 these instruments detected the lowering (0.0003 mm) of the southern part of the rock mass due to the increased level of the underground river Pivka. The studies were important for understanding earth tides, underground karst hydrology and seismology (Carnera 1933).

In autumn of 1933 the underground river Pivka was very high and pendulum instruments in Tartarus were flooded and had to be moved to another place in the cave (R. R. Grotte Demaniali di Postumia 1934). The flood of 23 to 24 September 1933 affected a huge part of Slovenian territory. The level of the water in Tartarus reached more than 519.8 m above the sea. This was the highest flood in the cave in the last 100 years (Šebela 2011). Horizontal pendulums with photographic registration were removed from the cave before World War II.

DESCRIPTION OF THE STUDY AREA

Slovenia is located at the northern part of the Adriatic microplate, which is presently moving northward with a counter-clockwise rotation. A northward-oriented maximum principal stress direction has been also obtained from fault plane solutions. These reflect mostly strike-slip mechanisms along Dinaric (NW-SE) or cross-Dinaric (NE-SW) oriented faults (Poljak *et al.* 2010).

Slovenia is considered to have a moderate seismicity (Poljak *et al.* 2000). The last strong earthquakes occurred in 1998 ($M_w = 5.6$) and in 2004 ($M_w = 5.2$) in Krn Mountains in NW Slovenia (Živčić *et al.* 1999; Bajc *et al.* 2001; Pahor *et al.* 2006). In January 1926 (Ribarič 1982) the so-called Cerknica earthquake ($M_S = 5.6$) was well felt also in the Postojna Cave (Šebela 2010). The last strong earthquake ($M_{LV} = 3.7$) in Postojna was felt with intensity V (EMS-98) on 15 January 2010 (Jesenko *et al.* 2011).

The Postojna Cave System is located some 100 m north of the Predjama Fault zone and about 4–5 km southwest of the Idrija Fault. Both faults have a Dinaric orientation (NW-SE) and the Idrija Fault is presumably responsible for the strongest known earthquake in the area that happened on 26 March 1511 (Fitzko *et al.* 2005; Živčić *et al.* 2011a).

Being 20.570 m long and 115 m deep the Postojna Cave System is the second longest in Slovenia. The part of the cave open for visitors has electricity and other infrastructure facilities that are important and can be used for the installation of an underground seismological station.

STATION SITINGS (AND RELATED NOISE MEASUREMENTS)

The Earth is in a state of permanent shaking. Although such vibrations, called seismic noise, are imperceptible to human senses, they severely limit the sensitivity of seismic instruments and hamper their ability to record weak seismic signals. Since high-noise levels obscure weak seismic signals that we wish to record, the level of seismic noise is one of the main criteria when assessing the quality of a certain location to be used for seismological measurements. Seismic noise is present at all frequencies of interest for seismology and is caused by natural and human activity. Among the strongest natural generators of seismic noise are oceanic waves, fluctuations in barometric pres-

sure, and wind (Bormann 2002), and their effects cannot be avoided. On the other hand noise due to human activity contains higher frequencies and propagates to shorter distances compared to long-period oceanic waves (Webb 2002), but is high close to large urban agglomerations with lots of industrial facilities and traffic.

Fig. 2: Seismic noise measurements in Črna Jama in 2007 (Photo: S. Šebela).

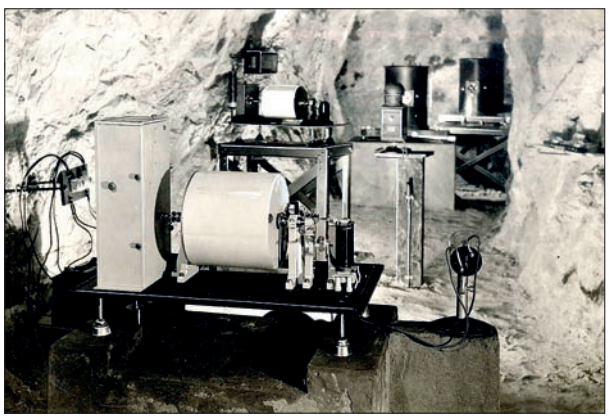

Fig. 4: Horizontal pendulums with photographic recording for the detection of minimal variations of the vertical direction, Tartarus artificial tunnel in 1932 (Carnera 1933).

The first idea was to install the subterranean seismic station close to one of the cave entrances. Thus, the Črna Jama section of the Postojna Cave System (Fig. 1) was selected for the first seismic noise measurements (Fig. 2). In order to find the best site for the seismic station installation, ARSO, IZRK ZRC SAZU and DST (now DMG), organized one-day-long seismic noise measurements in the Črna Jama cave in October 2007. Three sites have been selected, in advance, by IZRK ZRC SAZU colleagues. These sites are far enough from the part of the cave open for tourists, are near to an electric power connection, and are not far away from another cave entrance (not used for tourist visits) in order to have the possibility to install the GPS and GSM antennas necessary to synchronize the absolute time and to transmit the data to the data centers in Ljubljana and Trieste. The measurements were made on 18 October 2007 at several sites located 10 to 50 meters from the cave entrance. The

Fig. 3: Accelerometer installation at Velika Gora chamber in 2010 (Photo: S. Šebela).

Fig. 5: Accelerometer installation in the Tartarus artificial tunnel in 2010 (Photo: S. Šebela).

place with the lowest noise level has been selected for the sensor installation. The measurements were done using Guralp CMG-40T, Lennartz LE-3D/5s and Mark IV 1s seismometers.

The construction of the seismological station in Črna Jama was delayed for some time during which the manager of the *Postojnska jama d.d.* company that manages the cave installed an internet infrastructure within most parts of the cave accessible to tourists. This opened new possibilities in the search for sites suitable for a station installation since the internet infrastructure can be used to carry a GPS signal to the station deep inside the cave, where seismic noise is expected to be even lower, and also to connect the stations with the seismic data

centers in Ljubljana and Trieste for real time data transmission and station control.

In January 2010 a swarm occurred with numerous weak and moderate earthquakes having epicenters close to Postojna (Živčić *et al.* 2011b). Since there were no close-by seismic stations, a temporary station installation in the cave was immediately decided. On 27 January the accelerometer was installed on the top of Velika Gora at 559 m above sea level (Fig. 3). The position was selected in the close vicinity of a TM 71 extensiometer that has been detecting micro-tectonic displacements since 2004 (Gosar *et al.* 2009; Šebela *et al.* 2010) and where electricity was available.

On 7 May 2010 the instrument was moved to the old artificial tunnel in Tartarus (Fig. 4) at 519.8 m above sea level where electrical power is also available. The accelerometer with digitizer (Guralp CMG-5TD) was put on the concrete block built in 1931 (Fig. 5). The station in the tunnel (TTPJ) operated till the end of 2010.

Since the instrumental noise of the Guralp CMG-5-TD accelerometer used at the Velika Gora and Tartarus sites is higher than the natural seismic noise at these two locations, it was necessary to perform additional noise measurements with more sensitive instruments. On 23 March 2012 the measurements were performed at both locations using a Lennartz LE-3D/5s seismometer and a Kinemetrics Episensor accelerometer with Earth Data PR6 recorder.

RESULTS

For each series of noise measurements, a site having a good sensor-to-ground coupling has been chosen. All the measurements have lasted for at least half an hour long, in order to stabilize the sensors and to have a long enough time series for the analysis. From the computed power spectral densities (Fig. 6), it is possible to see that the seismic noise in Postojna Cave is very low, as expected for rock sites in a cave located far away from urban areas. This holds for all the investigated sites, which show a very similar PSD in the frequency range investigated. Fig. 6 shows comparison of seismic noise measured on three locations in the Postojna Cave. The measurements were made with the same sensor but not at the same time. Signal samples of 10 minutes are compared.

Comparison of the spectra of the seismic noise measured in Tartarus tunnel in Postojna Cave and the spectra of the noise on two nearby stations situated in the caves Trieste (TRI) station located in the Grotta Gigante Cave and Villanova (VINO) station located in the Villanova Cave is presented on Fig. 7. The measurements have been made at the same time. However, the seismometers were different: STS-1 at TRI, STS-2 at VINO and LE-3D/5s at TTPJ.

During the measurement at Site 1 in Črna Jama, an explosion occurred nearby at 09:00:01 and was well recorded. The records have been compared with the records of JAVS seismological station (ARSO network), located not far from the cave (Fig. 8). Site 1 looks less noisy

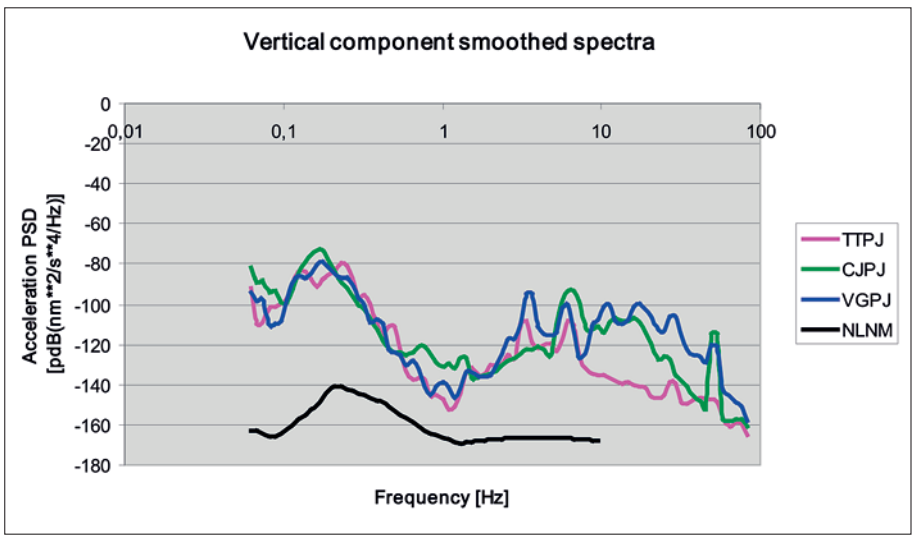

Fig. 6: Comparison of seismic noise spectra at three locations in the Postojna Cave: CJPJ – Črna jama, VGPJ – Velika Gora chamber and TTPJ – Tartarus tunnel. The measurements were made with the same sensor but not at the same time. Signal samples of 10 minutes are compared. The NLNM (Peterson 1993) is given for comparison.

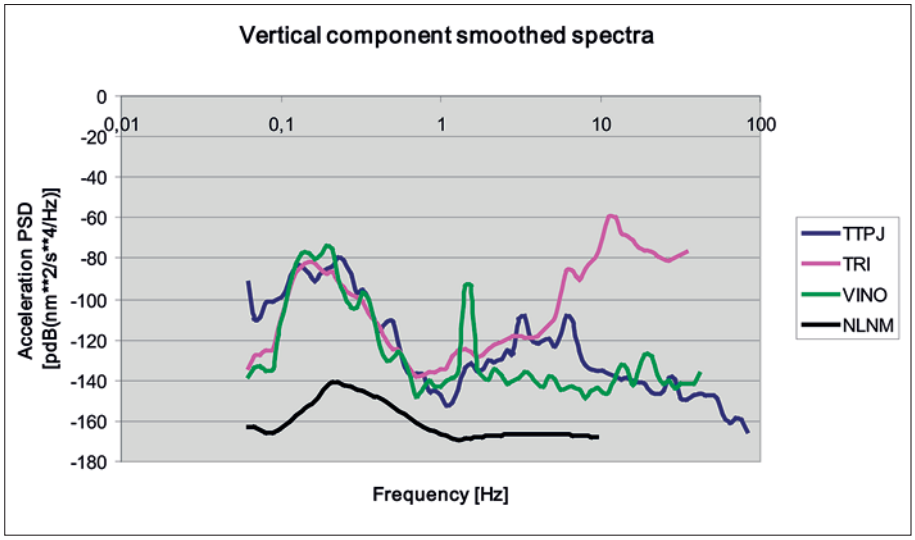

Fig. 7: Comparison of the spectra of the seismic noise measured in Tartarus tunnel (TTPJ) in Postojna Cave and the spectra of the noise at the Trieste (TRI) station located in the Grotta Gigante Cave and at the Villanova (VINO) station located in the Villanova Cave (both in Italy). The measurements were made at the same time. However, the seismometers were different: STS-1 at TRI, STS-2 at VINO and LE-3D/5s at TTPJ. The measurements were made on 23 March 2012 starting at 08:55 UTC. The NLNM (Peterson 1993) is given for comparison.

than JAVS station, although it is the noisiest site of the three considered.

During noise measurements at Velika Gora and Tartarus tunnel sites we also recorded the signal caused by the passage of the tourist train. The duration of the signal is about two minutes. The preliminary analyses show a low level of seismic noise in the cave and the artificial tunnel in Tartarus as appropriate site for permanent seismological station.

From January 27 to February 12, 2010, the seismological station VGPJ recorded 79 earthquakes with epicenters beneath Postojna (Fig. 9). The data was very useful to determine the seismological characteristics of the $M_{LV} = 3.7$ Postojna earthquake (15 January 2010) swarm sequence. The distribution of the differences in arrival times of transversal (S) and longitudinal (P) waves at the VGPJ station is presented in Figure 10. The majority (95%) of earthquakes had a Ts–Tp difference in the range of 0.07s (between 1.84 and 1.91s), which helped us to constrain the size of the activated volume to about 500 meters, which is in agreement with the source size determined from the corner frequency of the P-wave spectrum assuming Brune's circular source model (Brune 1970, 1971).

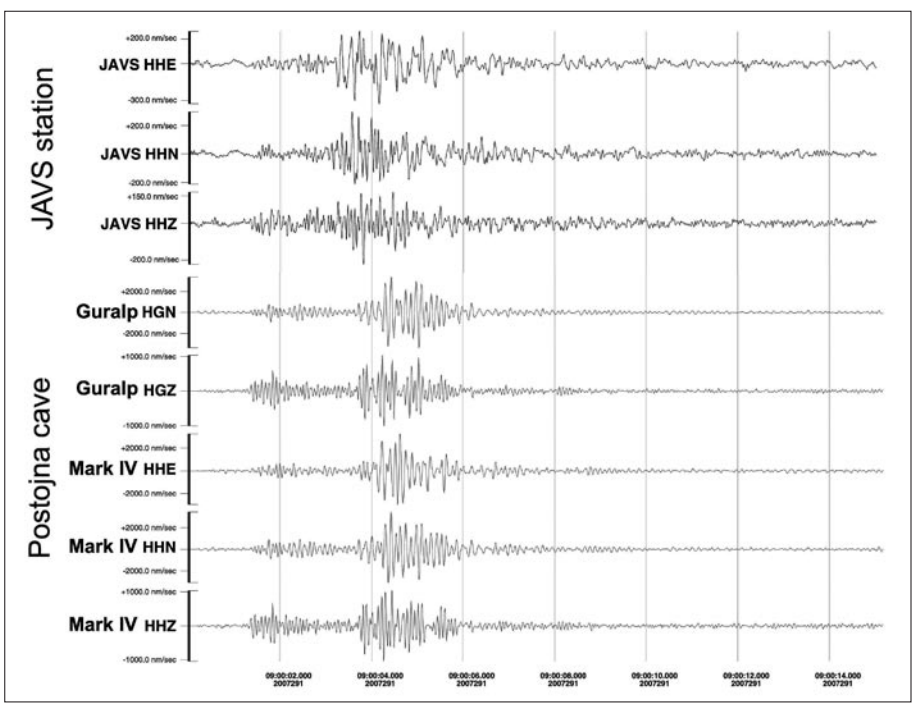

Fig. 8: Waveforms recorded by DST/DMG instruments in the Črna Jama and at the station JAVS of the Seismic Network of the Republic of Slovenia of an explosion happened during Site 1 noise measurement. For the instruments in the cave we do not have the absolute UTC time but from the Ts-Tp time difference it can be concluded that the explosion was somewhat closer to the JAVS station.

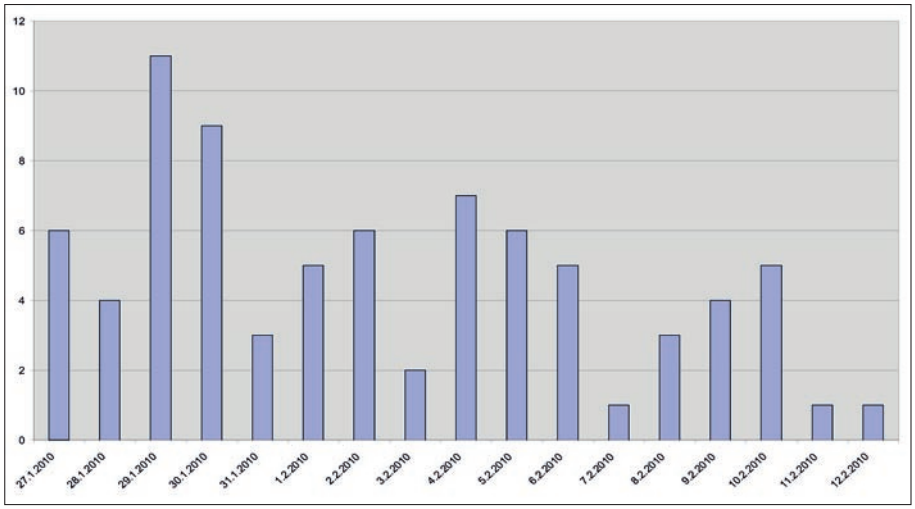

Fig. 9: Number of earthquakes with hypocenters in the vicinity of Postojna recorded on the temporary station VGPJ located in the Velika Gora chamber. On 15 January 2010 an earthquake of magnitude M_{LV} = 3.7 followed by numerous aftershocks happened essentially underneath Postojna.

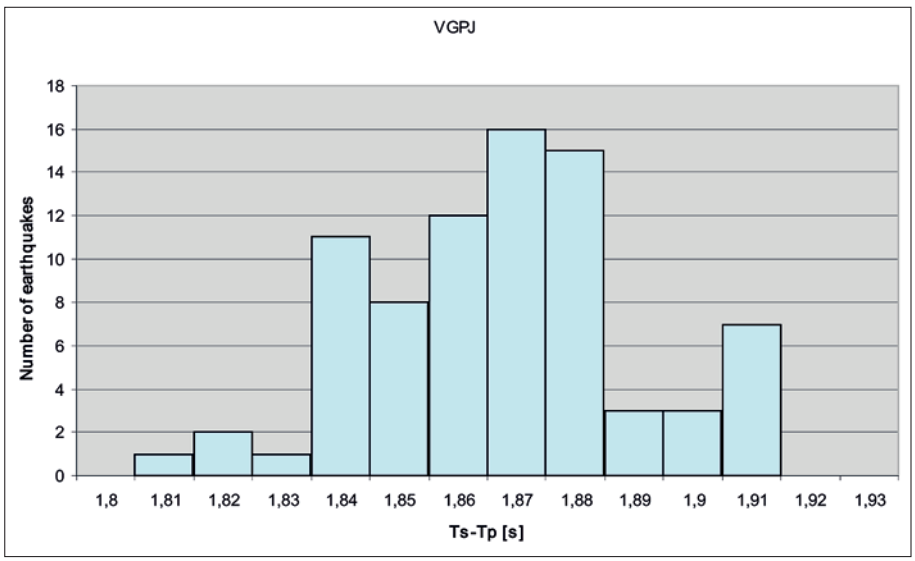

Fig. 10: Distribution of the differences in arrival times of transversal (S) and longitudinal (P) waves at station VGPJ in the Velika Gora chamber.

The TTPJ station in the Tartarus tunnel recorded more than hundred earthquakes of the sequence near Ilirska Bistrica, that started on 15 September 2010 with two M_{LV} = *3.5* earthquakes (Čarman *et al.* 2011) and lasted till the end of 2010.

CONCLUSIONS

The noise measurements performed and the temporary installations of seismic stations at various sites have shown that the location in the Tartarus artificial tunnel is appropriate and particularly suitable for the installation of a permanent seismic station. Although the site is sensitive to the high-frequency (above 20 Hz) noise caused by the train passage the noise in the rest of the frequency band is sufficiently low to provide good conditions for recording local seismicity. Also, this site is close to the internet installation in the cave and with electric power already at hand. The existing concrete pier built in 1931 can be used for the sensor placement. There is also enough space in the tunnel for the supporting equipment.

For these reasons ARSO and DMG propose the Tartarus tunnel as the best possible location for the installation of the permanent seismic station in the Postojna Cave System.

ACKNOWLEDGEMENTS

The authors are thankful to *Postojnska jama d.d.* (Marjan Batagelj, Ksenija Dvorščak and Stanislav Glažar) for their help. The field works of Janez Mulec (ZRC SAZU), Marko Mali and Luka Pančur (ARSO) and Lorenzo Furlan (DST) are much appreciated. This study was performed within the scientific cooperation between ARSO, IZRK ZRC SAZU and DMG. It is also part of the EPOS project (FP7 Preparatory Phase). We thank to anonymous reviewer for suggestions that have improved the paper.

REFERENCES

Bajc, J., Aoudia, A., Saraò, A. & P. Suhadolc, 2001: The 1998 Bovec-Krn mountain (Slovenia) earthquake sequence.- Geophys. Res. Lett., 28, 9, 1839–1842.

Bormann, P., 2002: Seismic Signals and Noise.- In Bormann, P. (ed.) *IASPEI New Manual of Seismological Observatory Practice (NMSOP)*. GeoForschungsZentrum, pp. 33, Potsdam.

Brune, J.N., 1970: Tectonic stress and the spectra of seismic shear waves from earthquakes.- J. Geophys. Res., 75, 4997–5009.

Brune, J.N., 1971: Correction.- J. Geophys. Res., 76, 5002.

Carnera, L., 1933: La stazione dei pendoli orizzontali nelle R.R. Grotte di Postumia.- Bollettino di Geodesia e geofisica, 9–10, 1933–XII, 1–13.

Čarman, M., Živčić, M. & M. Ložar Stopar, 2011: Potresi pri Ilirski Bistrici leta 2010.- In: Gosar, A. (ed.) *Potresi v letu 2010.* Agencija Republike Slovenije za okolje, pp. 97–109, Ljubljana.

Fitzko, F., Suhadolc, P., Aoudia, A. & G.F. Panza, 2005: Constraints on the location and mechanism of the 1511 Western-Slovenia earthquake from active tectonics and modeling of macroseismic data.- Tectonophysics, 404, 77–90.

Gosar, A., Šebela, S., Košťák, B. & J. Stemberk, 2009: Surface versus underground measurements of active tectonic displacements detected with TM 71 extensometers in western Slovenia.- Acta Carsologica, 38, 2–3, 213–226.

Jesenko, T., Cecić, I., Živčić, M. & M. Čarman, 2011: Potresi v Sloveniji leta 2010.- In: Gosar, A. (ed.) *Potresi v letu 2010.* Agencija Republike Slovenije za okolje, pp. 17–35, Ljubljana.

Poljak, M., Živčić, M. & P. Zupančič, 2000: The seismotectonic characteristics of Slovenia.- Pure and Applied Geophysics, 157, 37–55.

Pahor, J., Kolar, J., Živčić, M. & I. Cecić, 2006: Potres 12. julija 2004 v Krnskem pogorju (Zgornje Posočje) in opazovanje popotresne aktivnosti.- In: Vidrih, R. (ed.) *Potresi v letu 2004.* Agencija RS za okolje, pp. 88–94, Ljubljana.

Peterson, J., 1993: *Observations and modeling of seismic background noise*.- USGS Open-File Report, 93–322, pp. 42, Albuquerque

Poljak, M., Gosar, A. & M. Živčić, 2010: Active tectonics in Slovenia: GeoActa, 3, 15–24.

R. R. Grotte demaniali di Postumia, 1933: *Relazione del consiglio d'amministrazione alle loro eccellenze i ministri delle corporazioni e delle finanze sull'andamento dell'azienda dal 1° gennaio al 31 dicembre 1932*. R. R. Grotte demaniali di Postumia, XI, pp. 57, Postumia.

R. R. Grotte demaniali di Postumia, 1934: *Relazione del consiglio d'amministrazione alle loro eccellenze i ministri delle corporazioni e delle finanze sull'andamento dell'azienda dal 1° gennaio al 31 dicembre 1933*. R. R. Grotte demaniali di Postumia, XII, pp. 50, Postumia.

Ribarič, V., 1982: *Seismicity of Slovenia – Catalogue of Earthquakes (792 A.D. – 1981)*.- SZ SRS, Publication, A, 1–1, pp. 650, Ljubljana.

Šebela, S., 2010: Effects of earthquakes in Postojna cave system.- Acta Carsologica, 39/3, 597–604.

Šebela, S., Vaupotič, J., Košťák, B. & J. Stemberk, 2010: Direct measurement of present-day tectonic movement and associated radon flux in Postojna cave, Slovenia.- Journal of Cave and Karst Studies, 72, 1, 21–34.

Šebela, S., 2011: Exceptional natural events in Postojna and Predjama Cave Systems.- Annales (Ser. Hist. Nat), 21, 1, 87–94.

Webb, S. C., 2002: Seismic Noise on Land and on the Sea Floor.- In: Lee, W.H.K. et al. (eds.) *International Handbook of Earthquake and Engineering Seismology*. Part A, Academic Press, pp. 305–318, Amsterdam, London.

Živčić, M., Cecić, I., Gosar, A. & P. Zupančič, 1999: Potres 12. aprila 1998 v Zgornjem Posočju – osnove značilnosti.- In: Lapajne, J. (ed.) *Potresi v letu 1998.* Uprava RS za geofiziko, pp. 49–64, Ljubljana.

Živčić, M., Čarman, M., Gosar, A., Jesenko, T. & P. Zupančič, 2011a: Potresi ob Idrijskem prelomu.- Idrijski razgledi, LVI, 1, 119–126.

Živčić, M., Čarman, M. & M. Ložar Stopar, 2011b: Potres 15. januarja 2010 pri Postojni. In: Gosar, A. (ed.) *Potresi v letu 2010.* Agencija Republike Slovenije za okolje, pp. 76–86, Ljubljana.

COBISS: 1.01

CAVE INVERTEBRATES IN NORTHWESTERN MINAS GERAIS STATE, BRAZIL: ENDEMISM, THREATS AND CONSERVATION PRIORITIES.

JAMSKI NEVRETENČARJI V SEVEROZAHODNEM PREDELU MINAS GERAIS, BRAZILIJA: ENDEMIZEM, OGROŽENOST IN VIDIKI VAROVANJA

Matheus Henrique SIMÕES[1,2], Marconi SOUZA-SILVA[3] & Rodrigo Lopes FERREIRA[1].

Abstract UDC 551.435.84:502.17(815.1)

Matheus Henrique Simões, Marconi Souza-Silva & Rodrigo Lopes Ferreira: Cave invertebrates in northwestern Minas Gerais State Brazil: endemism, threats and conservation priorities

Due to their high economic value, karstic areas and caves have been affected for decades in Brazil. Accordingly, such systems have been receiving the attention of managers, environmental agencies and researchers, especially in recent years. The present study collected information regarding the cave invertebrate fauna of the Northwest region of Minas Gerais, Brazil, such as species richness and endemisms, besides the impacts and threats occurring in these environments, identifying caves and more vulnerable areas and proposing conservation actions. Three caves were identified as a priority for conservation: Lagoa Rica cave in Paracatu, and Lapa Nova and Lapa da Delza caves in Vazante. Another three areas were considered in need of conservation actions: regions of Arinos, Paracatu and Cabeceira Grande/Unaí. The main threat found in the area was the conversion of forests into pastures for cattle breeding, registered in the surroundings of 85% of the caves. The main recommendations were the recuperation of the surroundings, awareness raising of the population and biospeleological inventories in other caves of the area. The studied caves were very heterogeneous, presenting unique characteristics. Thus, the study of the highest possible number of caves of the region of interest is always recommended, to aid in conservation and action plans for cave fauna.

Key words: invertebrates, caves, conservation, endemisms.

Izvleček UDK 551.435.84:502.17(815.1)

Matheus Henrique Simões, Marconi Souza-Silva & Rodrigo Lopes Ferreira: Jamski nevretenčarji v severozahodnem predelu Minas Gerais, Brazilija: endemizem, ogroženost in vidiki varovanja

Kraška področja in jame v Braziliji so zaradi visoke gospodarske vrednosti že desetletja prizadeta. Posledično so, zlasti v zadnjih letih, pritegnila pozornost upravljalcev, okoljskih agencij in raziskovalcev. V pričujoči študiji so zbrani podatki o jamski favni severozahodnega območja Minas Gerais v Braziliji s poudarkom na bogastvu vrst in endemizmu, poleg ugotovljenih vplivov in nevarnosti, ki se pojavljajo v teh okoljih ter jam in drugih ranljivih predelov, za katere predlagamo ukrepe za njihovo ohranitev. Tri jame so bile opredeljene kot prednostne za ohranitev: jama Lagoa Rica v Paracatu in jami Lapa Nova in Lapa da Delza v Vazante. Poleg tega so bile prepoznane tri regije, kjer naj bi se izvajali ukrepi varovanja: Arinos, Paracatu in Cabeceira Grande/Unaí. Največja grožnja na teh območjih, kjer je registriranih 85% jam, je izsekavanje gozdov in sprememba v pašnike za vzgojo govedoreje. Glavna priporočila so zaščita področja, ozaveščanje prebivalstva in biospeleološke raziskave v drugih jamah na proučevanem območju. Vse raziskovane jame so heterogene, z edinstvenimi lastnostmi. Priporočene so raziskave v čim večjem številu jam, kot dodana vrednost pri načrtih za ohranjanje in varovanje jamske favne.

Ključne besede: nevretenčarji, jame, varovanje, endemizem.

[1] Laboratório de Ecologia Subterrânea, Setor de Zoologia/Departamento de Biologia, Universidade Federal de Lavras, Cx Postal 3037, Campus Universitário, CEP 37200-000 Lavras, Minas Gerais, Brasil, e-mail: drops@dbi.ufla.com.br

[2] Programa de Pós-Graduação em Ecologia Aplicada, Departamento de Biologia, Universidade Federal de Lavras, Cx Postal 37, Campus Universitário, CEP 37200 000, Lavras, Minas Gerais, Brasil, e-mail: matsimoes@hotmail.com

[3] Núcleo de Pesquisas em Ciências Biológicas (www.npcbio.org) /Centro Universitário de Lavras (UNILAVRAS), e-mail: marconisouza@unilavras.edu.bra

Received/Prejeto: 18.02.2013

INTRODUCTION

Caves are habitats for several species that use them for the most diverse purposes (Culver & Pipan 2009). The troglobites, a strictly cave species, stand out in function of the frequent evolutionary modifications of morphological, physiological and behavioral character that make them highly specialized to live in these environments (Culver & Wilkens 2000). As such, caves are places of great importance for the study of evolutionary processes moulded by the selective pressures typical of these environments, such as permanent absence of light, shortage of food resources, high moisture/humidity and constant temperatures, among others (Culver & Pipan 2009).

Many troglobitic species occur in a single cave or a small group of caves. Once these environments have been extensively altered, especially in recent decades, it is possible that many species have disappeared without even having been described (Elliott 2000). Furthermore, caves are important for the maintenance of the ecosystems where they are inserted, because they frequently possess drains that supply the surface and are shelters of species that provide recognized ecological services to the external ecosystem, as for instance, the bats (Elliott 2000).

Although the importance of the subterranean habitats is evident, caves have been threatened over the years by anthropic interventions (Watson *et al*. 1997). These interventions are resulting in negative effects, such as hydric resource pollution and reduction, changes in the hydrologic regime, habitat alterations and local species population decline, among others (Gillieson & Thurgate 1999; Parise & Pascali 2003; De Waele & Follesa 2003; Neill *et al*. 2004; Van Beynen *et al*. 2007). Given these threats, karstic areas and caves are receiving the attention of managers, environmental agencies and researchers, mainly in recent decades, due to the great importance of those areas to science (geology, paleontology, archeology and biology), as well as to human values (spiritual, religious, aesthetic, recreational and educational) (Watson *et al*. 1997).

Due to the socioeconomic importance of karstic areas and the consumption increase of natural goods and products it is unlikely that some caves do not come to be affected, even those that present rare species (Gibert & Deharveng 2002). As such, to recognize locals with conservation priority is an important step for the creation of preserved areas and maintenance of the subterranean biodiversity.

In Brazil, studies with the objective of proposing areas that need emergency action for subterranean fauna conservation have been conducted, especially in recent years (Souza-Silva 2008; Zampaulo 2010; Bento 2011; Souza 2012). Such studies are based mainly on three aspects: (I) presence of troglobite species considered relevant in function of the "evolutionary status", knowledge inadequacy, restricted distribution and fragility facing random habitat alteration events (Culver & Wilkens 2000; Culver & Pipan 2009), (II) species richness, by enabling complex ecological interactions and processes (Ferreira 2004) and (III) the conservational state of the cave surroundings and interiors, which can reveal the impact degree and the threats imposed to the fauna (Souza-Silva 2008).

Recently a National Action Plan was published (PAN) for the conservation of the speleological patrimony in the karstic areas of the São Francisco river basin (Cavalcanti *et al*. 2012), the third largest hydrographic basin and one of the most important in Brazil. Among the three karstic areas within the scope of PAN, the Region I, located in Middle San Francisco Basin (karstic areas of the Paranoá Group, Bambuí Group and Vazante Formation), can be considered the most lacking in studies related to the cave fauna. The few works regarding the subterranean fauna were only made at one cave, Lapa Nova, located in the municipal district of Vazante, state of Minas Gerais (Pellegrini & Ferreira 2012a, b; Souza & Ferreira 2012). As such, the present study gathered information of the cave invertebrate fauna, such as species richness and endemisms, and the impacts and the threats occurring to the environment, identifying caves and more vulnerable areas and proposing conservation actions.

MATERIALS AND METHODS

STUDY AREA

The study was carried out in 47 caves distributed in eight municipal districts of the Northwest area of Minas Gerais, Brazil. The caves are inserted in Region I of the National Action Plan for the conservation of the speleological patrimony in the karstic areas of the São Francisco river basin (PAN Caves of São Francisco) (Cavalcanti *et al*. 2012) (Fig. 1).

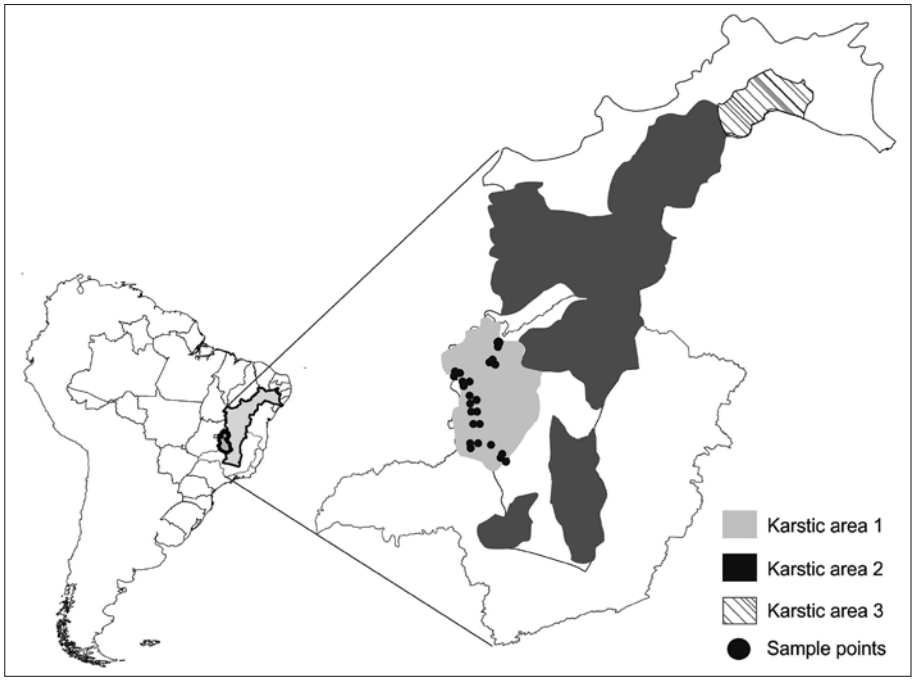

Fig. 1: Map of South America highlighting Brazil, Rio San Francisco hydrographic basin, and the state of Minas Gerais. Inside the San Francisco basin the karstic areas inserted in PAN San Francisco are highlighted. The caves of the present study are distributed through eight municipal districts of the Northwest area of Minas Gerais, belonging to the karstic area 1 of PAN Caves of São Francisco.

INVERTEBRATE SAMPLING

The collection of invertebrates was conducted through active searches throughout whole cave with the aid of tweezers, brushes and hand nets. During the collections, organic deposits were prioritized (plant debris deposits, carcasses, guano, etc.) and micro-habitats (under stones, moist soil, openings, speleothems, etc.). All of the collected specimens were conditioned in vials with 70% alcohol. The collection team was always composed of four biologists with experience in speleology and collection of invertebrates in caves, as recommended by Weinstein & Slaney (1995).

All of the organisms were identified until the lowest taxonomic level accessible and separated into morphospecies, as in other works (Souza-Silva 2011b; Oliver & Beattie 1996; Derraik *et al*. 2002; Ward & Stanley 2004; Derraik *et al*. 2010). All of the specimens are deposited in the subterranean invertebrate collection of Lavras (ISLA), at the Federal University of Lavras (UFLA).

The identification, in the specimens, of "troglomorphic" traits, was used for classification of potentially troglobitic species. Such characteristics vary among the groups, but are frequently represented by the reduction of pigmentation, reduction of ocular structures and appendage elongation (Culver & Wilkens 2000).

CAVE RATING TOOLS

The definition of the priority areas for conservation was based on the overlapping of the biological relevance, troglobitic species presence and impact degree in the caves as described below (modified from Souza-Silva 2008).

Biological relevance

The biological relevance categories were defined as extreme, high, medium and low, based on the total and relative species richness. The relative species richness in each cave was calculated through the ratio among the total richness, the horizontal projection of the cave and extension of the entrance (Souza-Silva 2008).

The highest value obtained for richness and relative richness was divided by four. Thus we obtained four categories of total and relative richness (extreme, high, medium and low) with intervals of number of species.

For the categorization of the biological relevance of the caves, weights were attributed to the total and relative richness categories. Caves with extreme total richness received Weight 8; high total richness Weight 6; medium total richness Weight 4 and low total richness Weight 2. Caves with extreme relative richness received Weight 4; high relative richness Weight 3, medium relative richness Weight 2 and low relative richness Weight 1.

It was defined that the total richness should receive the double the weight of the relative richness in function of the real and direct importance of the absolute number of species, as a parameter of preservation of a given system. In case only the relative richness was used, one would run the risk of preserving reduced caves, but with a relatively high number of species to the detriment of extensive caves and with high absolute richness (Souza-Silva 2008).

The biological relevance for each cave was determined through the sum of the weights of the total and relative richness for each cave. The highest biological

relevance served as a basis for the inclusion of the caves in the categories of extreme, high, medium and low final biological relevance. Caves with *extreme* biological relevance received Weight 4; *high* final biological relevance received Weight 3, *medium* final biological relevance received weight 2 and *low* final biological relevance received Weight 1.

Troglomorphic species categories

The highest values of troglomorphic species richness found served as the basis for classification of the caves as extreme (Weight 4), high (Weight 3), medium (Weight 2) and low (Weight 1) troglomorphic species richness.

Characterization of impacts

Environmental impacts were defined for each cave in function of the presence or absence of alterations in their internal and external environments. The surveyed alterations were classified in relation to *uses* and *impacts*. Tourism and religious activities were considered uses, impacts being trampling, illumination, and the consequent alterations by these activities.

From the identification of the impacts in the caves we proceeded to a second analysis concerning the magnitude of these impacts that can cause alterations in the communities. Such analysis considered from impacts that could cause minimum alterations to those that would considerably affect the cave fauna.

In the impact definitions, three types of modifications were considered (*depletion*, *enrichment* and *alteration*). The first modification type is that which can lead to depletion, in other words, the reduction of trophic resources or the fauna in function of the anthropic activities and the second type, the alterations that lead to the enrichment in the availability of organic resources for the fauna. The third type of modification is that which modifies, in space and time, the physical structure of habitats or micro-habitats in the caves, called *alteration* impacts. It is emphasized that the same impact can lead to more than one type of these three modifications.

For attribution of the weights, the impacts were classified according to the potential, into *intense* (potentially the cause of intense alterations in the fauna – Weight 2) or *tenuous* (potentially the cause of reduced alterations on the fauna – Weight 1). A second classification added to the impact analysis the deals with their permanence. The permanence refers to the period of time the impact persists. Thus, the impacts were considered of *short* (Weight 1) or *continuous* duration (Weight 3). We opted for a weight attribution three times higher for continuous impacts for the fact that the continuity of the impacts can cause much greater damage than those of short duration. The last impact classification refers to the range of the impact. *Punctual* impacts received Weight 1, while those that occur over a wide range (*systemic* impacts) received Weight 2. The impacts that presented more than

*Tab. 1: Valuation of the impacts to the caves. D: depletion, E: enrichment, A: alteration, I: intense; T: tenuous; CD: continuous duration; SD: short duration; GI: general impact; LI: localized impact; W: weigh of impacts; FIW: final impact weights (= $\Sigma w_{potencial} + \Sigma w_{permanence} + \Sigma w_{range}$); *: impacts inside the caves (Modified from Souza-Silva 2008).*

Impacts	*Modification*	*Potential*	*W*	*Permanence*	*W*	*Range*	*W*	*FIW*
Mining	D + A	I	2 + 2	CD	3	GI	2	9
Garbage	E + A	I	2 + 2	CD	3	GI	2	9
Bare soil	A	I	2	CD	3	LI	1	6
Roads surroundings	A	T	1	CD	3	LI	1	5
Trail	A	T	1	CD	1	LI	1	3
Erosion	A	I	2	CD	3	LI	1	6
Siltation	A	I	2	CD	3	LI	1	6
Area burned	A	I	2	SD	1	LI	1	4
Deforestation	D	T	1	SD	1	GI	2	4
Impermeability of the soil	A	I	2	CD	3	LI	1	6
Livestock	A	T	1	CD	3	LI	1	5
*Destruction of speleothems	A	T	1	CD	1	LI	1	3
* Mining tailings	D + A	I	2 + 2	CD	3	GI	2	9
*Silting of drainage	D + A	I	2	CD	3	LI	1	6
*Graffiti	A	T	1	SD	1	LI	1	3
* trampling	A	I	2	CD	3	GI	2	7
*Constructions	A	I	2	SD	1	LI	1	4
*Bonfires	A	T	1	CD	1	LI	1	3
*Burning tire	D + A	I	2 + 2	CD	1	LI	1	6

one of the three alterations (depletion, enrichment or alteration) had the intensity weights added.

Tab. 1 shows some examples of impacts that were registered for the interior and surroundings of the caves and the weights attributed to each one. Note that the final weight can vary among the caves, because the same impact can present intensity, permanence and different range for each cave.

The categorization of the caves regarding the impact degree was conducted starting from the sum of the values obtained in each cave. The highest sum of impacts served as the basis for the separation of the caves regarding the degree of impacts into extreme (Weight 4), high (Weight 3), medium (Weight 2) and low (Weight 1).

Vulnerability and priority caves for conservation

The degree of vulnerability of the invertebrate communities of each cave was obtained from the sum of the weights of the final biological relevance, richness of troglomorphic species and the impacts present in each cave. The highest vulnerability value was used for the inclusion of the caves in the vulnerability categories extreme, high, medium and low.

Caves classified as extreme vulnerability were considered as priority caves for conservation. Regions with caves with high vulnerability were highlighted as areas of secondary priority and that need some conservation action.

RESULTS

A total of 1,348 invertebrate species was registered distributed in at least 170 families. The average richness was 63 (±29) species. The Lapa Nova cave presented the highest richness (155 species) and the V01 cave presented the lowest species richness (15 species) (Tab. 2).

Among the 47 caves, 4.26% were classified as of extreme total richness (117–155 species), 19.15% as high (78–116 species), 59.57% medium (39–77 species) and 17.02% low (less than 39 species) (Tab. 2). The highest relative richness registered was at the Gruta Nove cave (3.822) and lowest in the Lapa Nova cave (0.001). Thus, 2.13% of the caves presented extreme (2.868 to 3.822), 2.13% high (1.913 to 2.867), 8.51% medium (0.956 to 1.912) and 87.23% low relative richness (under 0.956) (Tab. 2).

The highest sum obtained through the weights attributed to the caves starting from the total and relative richness classifications was nine. As such, 25.53% of the caves were classified as with extreme (7 to 9), 57.45% high (5 or 6) and 17.02% medium (3 or 4) biological relevance (Tab. 2). No cave presented low biological relevance.

Thirty six troglomorphic species were distributed throughout 19 caves, all with at least one endemic species, representing 80% of endemic species for a single cavity. Some troglomorphic species are presented in Fig. 2. The caves with the highest troglomorphic species richness were the Lagoa Rica cave, in Paracatu, with seven species and the Lapa Nova cave, in Vazante, with six species. Therefore, 4.26% of the caves were classified as of extreme (6 or 7 species), 2.13% high (4 or 5 species), 21.28% medium (2 or 3 species) and 72.34% low troglomorphic species richness (0 or 1 species) (Tab. 2).

The main use of the surroundings was the pastures, registered in 85.11% of the cave surroundings. The main use of the interior was tourist visitation, observed in 23.4% of the caves. The main impact found in the cave surroundings were trails, registered in 72.34% of the caves surroundings. The main impact observed inside the caves was the trampling, registered in 38.3% of the caves. Mining was considered as the main potential impact in the surroundings, being likely to occur in the future in 34% of the caves. The pollution of water bodies stood out as the main impact inside the caves, being likely in 27.6% of the caves. Some impacts are presented in Fig. 3.

The highest sum of the weights attributed to the caves regarding the observed impacts was registered for the Lapa do Campo de Futebol, located in the municipal district of Matutina (61), it being the only cave with extreme impact degree (46 to 61). 12.77% of the caves presented high (31 to 45), 38.3% medium (17 to 30) and 46.8% of the caves presented low degree of impact (below 16) (Tab. 2).

The highest sum of the weights attributed to the three items considered in this study regarding importance for cave conservation (biological relevance, troglobitic species presence and conservation state) was 11, registered for the Lapa Nova, municipal district of Vazante. As such, 6.38% (three caves) of the caves were classified as those of extreme vulnerability (9 to 11), 68.09% as high (6 to 8) and 25.53% of medium vulnerability (3 to 5). No cave presented low vulnerability (below 3) (Tab. 2).

The priority caves for conservation were the Lagoa Rica cave (Paracatu municipality), Lapa Nova cave and

Tab. 2: List of the caves studied in the municipal districts of the Northwest area of Minas Gerais, Brazil, between the years 2009 and 2011. Location in UTM (X, Y, Z), total number of species (S), classification as to total number of species (SC), relative richness (RR), classification as to the relative richness (RRC), biological relevance (BR), troglomorphic species richness (RT), classification as to the troglomorphic species richness (RTC), degrees of impact (DI), vulnerability (V), extreme (E), high (A), medium (M) and low (B), presence of water (PW) (R: rivers, P: pools; PP: phreatic pounds; D: dry).

Municipalities	*Caves*	*X*	*Y*	*Z*	*PW*	*S*	*SC*	*RR*	*RRC*	*BR*	*RT*	*RTC*	*DI*	*V*
Arinos	Camila	353310	8240506	23L	R	115	H	0.192	L	E	2	M	L	H
Arinos	Capa	357713	8236358	23L	R	113	H	0.014	L	E	0	L	L	H
Arinos	Marcela	354261	8240358	23L	R	94	H	0.002	L	E	0	L	M	H
Arinos	Suindara	354162	8240098	23L	D	55	M	0.021	L	H	0	L	M	H
Arinos	Salobo	369279	8287176	23L	P	50	M	0.188	L	H	2	M	M	H
Arinos	Taquaril	369401	8295327	23L	R	78	H	0.104	L	E	1	L	L	H
Arinos	Velho Juca	354106	8240266	23L	D	46	M	0.093	L	H	3	M	M	H
Cabeceira Grande	Caidô	259885	8206642	23K	D	70	M	0.006	L	H	1	L	M	H
Cabeceira Grande	Porco Espinho	257418	8206250	23K	D	35	L	0.529	L	M	0	L	L	M
João Pinheiro	Sapecado	350114	8015342	23K	D	26	L	0.867	L	M	0	L	L	M
João Pinheiro	Tauá	350312	8015352	23K	D	22	L	0.055	L	M	0	L	L	M
Matutina	Cachoeira	399044	7874960	23K	P	61	M	0.229	L	H	0	L	M	H
Matutina	Nove	399102	7874933	23K	D	48	M	3.822	E	E	0	L	H	H
Matutina	Campo de Futebol	398585	7874853	23K	D	42	M	0.112	L	H	0	L	E	H
Paracatu	Lagoa Rica	309267	8102836	23K	PP	55	M	0.055	L	H	7	E	H	E
Paracatu	Tamanduá II	311508	8070394	23K	D	41	M	0.539	L	H	0	L	M	H
Paracatu	Cava	297248	8132338	23K	D	48	M	0.383	L	H	0	L	M	H
Paracatu	Santa Fé	297342	8133601	23K	D	30	L	0.018	L	M	0	L	H	H
Paracatu	Brocotó	308134	8083657	23K	D	72	M	0.533	L	H	0	L	M	H
Paracatu	Brocotó II	308165	8083812	23K	D	73	M	0.243	L	H	0	L	M	H
Paracatu	Santo Antônio	306536	8105656	23K	P	51	M	0.055	L	H	0	L	H	H
Presidente Olegário	Caieira	385073	7974405	23K	D	61	M	0.014	L	H	0	L	L	M
Presidente Olegário	Juruva	385747	7973888	23K	R	112	H	0.030	L	E	1	L	L	H
Presidente Olegário	Vereda da Palha	380964	7981211	23K	R	119	E	0.034	L	E	1	L	L	H
Unaí	Abriguinho	256233	8206485	23K	D	34	L	0.654	L	M	0	L	L	M
Unaí	Barth Cave	279196	8183910	23K	D	47	M	0.021	L	H	1	L	M	H
Unaí	Cachoeira do Queimado	251574	8205653	23K	D	57	M	0.007	L	H	2	M	M	H
Unaí	Encosta	255335	8206050	23K	D	52	M	0.650	L	H	0	L	L	M
Unaí	Mata dos Paulista	278976	8183510	23K	R	64	M	1.422	M	H	0	L	L	M
Unaí	Frangas	279221	8183417	23K	D	41	M	1.051	M	H	0	L	L	M
Unaí	Deus Me Livre	279976	8182900	23K	D	106	H	0.236	L	E	0	L	L	H
Unaí	Rio Preto	259263	8205827	23K	D	56	M	0.320	L	H	2	M	L	H
Unaí	Malhadinha	257965	8206112	23K	D	108	H	0.311	L	E	3	M	L	H
Unaí	Sapezal	297937	8141547	23K	P	71	H	0.041	L	E	0	L	L	H
Vazante	Abrigo da Escarpa	307964	8016869	23K	D	36	L	0.900	L	M	0	L	M	M
Vazante	Escarpa	307911	8016928	23K	D	62	M	0.332	L	H	0	L	M	H
Vazante	Urtigas	308192	8017657	23K	D	70	M	0.006	L	M	2	M	M	H
Vazante	Urubus	307785	8016598	23K	D	93	H	0.063	L	E	3	M	L	H
Vazante	Não Cadastrada	308230	8017482	23K	D	49	M	1.332	M	H	1	L	M	H
Vazante	V01	306704	8017075	23K	D	15	L	1.500	M	M	0	L	L	M
Vazante	V02	306618	8017108	23K	D	37	L	2.467	A	H	2	M	L	H
Vazante	Delza	298146	8010447	23K	PP	46	M	0.008	L	H	5	A	H	E
Vazante	Mata Velha	299617	8007387	23K	P	61	M	0.054	L	H	0	L	L	M
Vazante	Guardião Severino	300039	8010088	23K	D	47	M	0.063	L	H	0	L	L	M
Vazante	Lapa Nova	299765	8010652	23K	PP	155	E	0.001	L	E	6	E	H	E
Vazante	Lapa Nova II	299691	8010585	23K	D	55	M	0.020	L	H	3	M	M	H
Vazante	Sumidouro da Vaca Morta	306446	8016811	23K	D	72	M	0.639	L	H	0	L	M	H

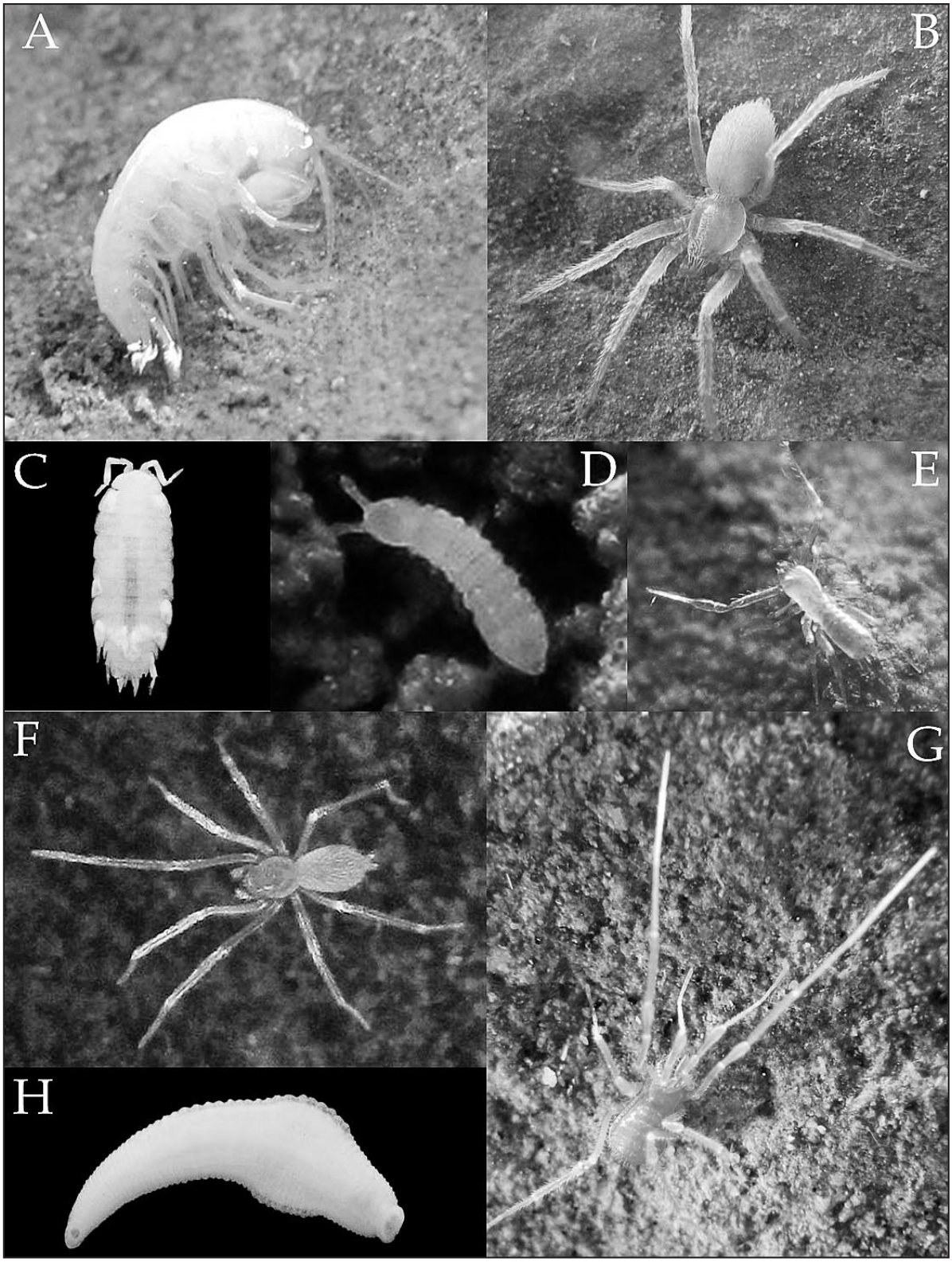

Fig. 2: Examples of troglomorphic species recorded in the Northwest region of the state of Minas Gerais, Brazil. A: Hyallela veredae (Hyallelidae). (Endemic to Vereda da Palha cave), B) Lygromma sp. (Prodidomidae) (Endemic to Cachoeira do Queimado cave); C) Trichorhina sp. (Endemic Camilo cave); D) Acherontides sp. and E) Chthoniidae sp. (Endemic to region of Vazante), F) Tetrablemmidae sp. and G) Speleoleptes sp. (Endemic Lagoa Rica cave), H) Hirudinea sp. (Endemic to Salobo cave).

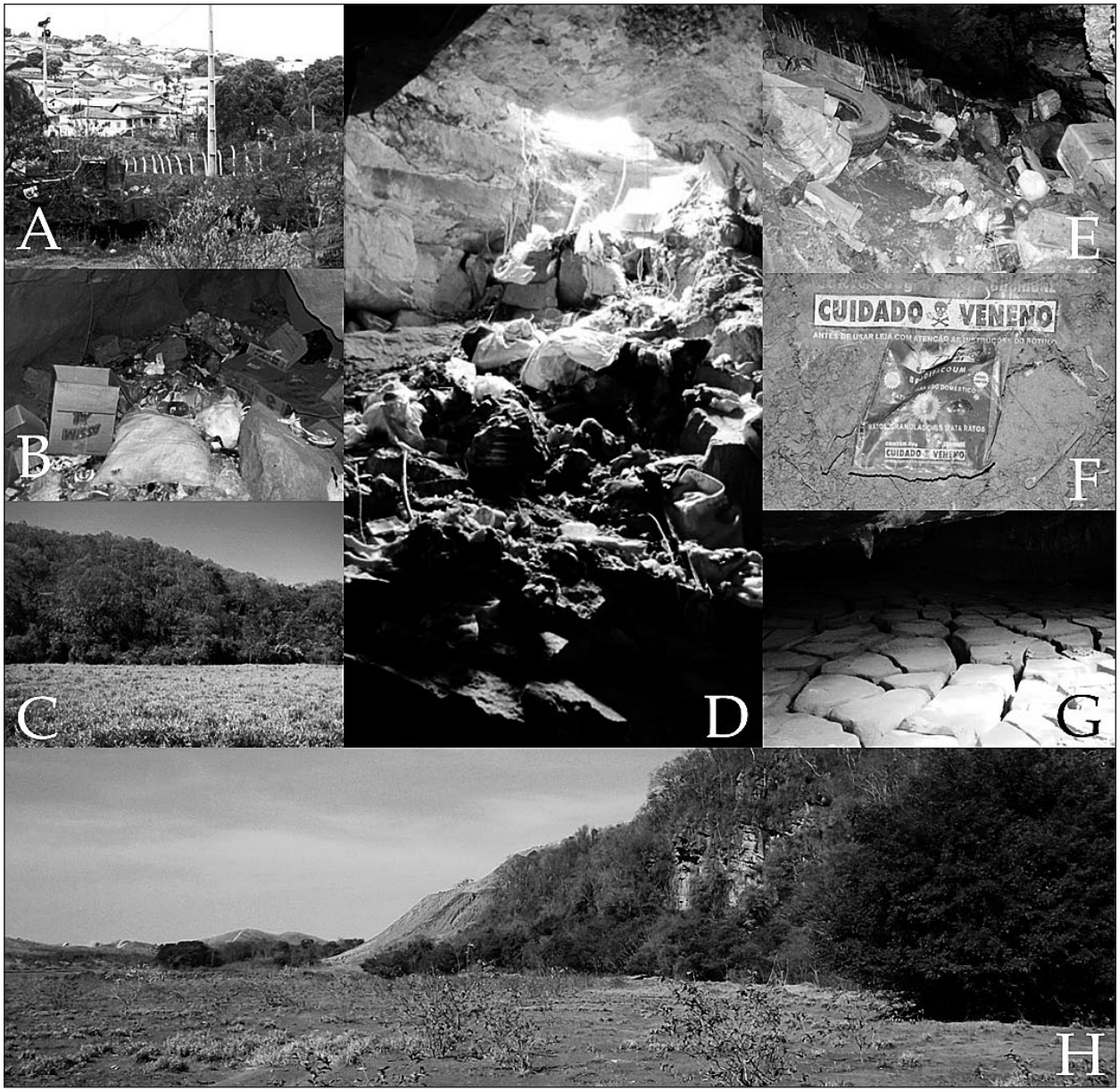

Fig. 3: Some impacts found in the surroundings and interior of the caves studied in the Northwest of the state of Minas Gerais, Brazil, between the years 2009 and 2011: A) Urban district on a cavity (Matutina); B) Discard of organic and veterinary trash (Paracatu); C) Removal of the external vegetation in the area of the surroundings (Paracatu); D) Discard of organic and veterinary trash (Paracatu); E) Discards of urban trash (Vazante); F) Discard of toxic waste (Paracatu); G) Silting of the cave by mining tailings; H) silting of the surrounding area by mining tailings (Vazante).

Delza cave, (both located in Vazante municipality) (Fig. 4, Tab. 3). Three regions were defined as priority for conservation: (1) the region of Arinos, (2) Cabeceira Grande and Unaí and (3) Paracatu (Fig. 4, Tab. 3). Table 3 summarizes the recommendations for the priority caves for conservation and the areas with need of conservation action, as well as the criteria used for indication.

Tab. 3: Caves and karstic areas in need of conservation action with the respective indication criteria, the main threats and the recommendations for conservation measures.

Site	*Indication criteria*	*Main threats*	*Recommendations*	*Endemic Species*
Lagoa Rica cave	High species richness and richness of troglomorphic species (seven species), six endemic to this cave.	Located in a mining area. Pollution of the groundwater lake.	Recovery of the cave surroundings. Constant supervision.	Tetrablemmidae sp.; Oonopidae sp.; Collembola sp.; Harpacticoida sp.; *Speleoleptes* sp. and Oniscodesmidae sp.
Lapa Nova cave	The biggest cave in this study and the higher observed richness (155 species); six troglomorphic species, two endemic to this cave.	Touristic cave, subject to impacts from such use.	Effective environmental protection of the reserve that exists around the cave and the execution of the management plan proposed by Pellegrini and Ferreira (2012).	Oonopidae sp. and Eukoenenia virgemdalapa Souza e Ferreira, 2012.
Delza cave	Five troglomorphic species, two endemic to this cave.	Inserted in the urban center of the municipality. Entrance used as a garbage dump by residents. Pollution of perennial water body.	Awareness of local residents not to throw garbage at the cave entrance.	*Lygromma* sp. and Oniscodesmidae sp.
Region of Arinos	Caves with great length, with rivers within, extreme biological relevance (25% of all species in the northwest of Minas Gerais studied), seven troglomorphic species recorded only in caves of this region.	Removal of native forest for pasture. Pollution of water bodies.	Recovery of the caves surroundings. Creation of a protected area in the region.	Hirudinea sp.; Collembola sp.; *Trichorhina* sp.; Styloniscidae sp.; Oniscodesmidae sp.; Polyxenida sp. and Turbellaria sp.
Region of Paracatu	Cave with the highest troglomorphic species richness registered in this study located in this region (Lagoa Rica cave) and other caves with high biological relevance and highly impacted.	Mining. Removal of native forest for pasture. Religious use.	Recovery of the caves surroundings. Biospelological inventories in other caves in the region.	Tetrablemmidae sp.; Oonopidae sp.; Collembola sp.; Harpacticoida sp; *Speleoleptes* sp. and Oniscodesmidae sp.
Region of Cabeceira Grande and Unaí	Caves with extreme biological relevance, seven troglomorphic species recorded only in caves of this region.	Removal of native forest for pasture. Construction of dams. Pollution of water bodies.	Recovery of the caves surroundings. Biospelological inventories in other caves in the region.	Trombidiformes sp.; Prodidomidae sp.; Ochiroceratidae sp. Pselaphidae sp.; Collembola sp.; *Trichorhina* sp.; and Oniscodesmidae sp.

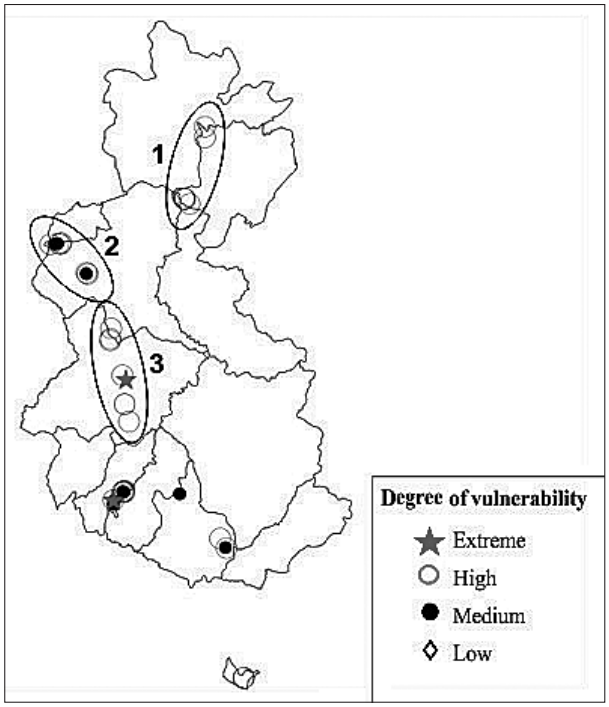

Fig. 4: Distribution map of the caves sampled in the Northwest area of the state of Minas Gerais, Brazil, between the years 2009 to 2011, and their respective classifications as to the vulnerability. The figure highlights the priority caves for conservation (red stars), as well as the regions in need of conservation actions (ellipses). 1: Region of Arinos, 2: Region of Cabeceira Grande and Unaí and 3: Region of Paracatu.

DISCUSSION

BIOLOGICAL RELEVANCE AND ENDEMISMS

Many studies regarding the subterranean fauna have been conducted in different regions of Brazil (Bento 2011; Bernardi *et al.* 2012; Cordeiro 2008; Ferreira 2004; Ferreira & Horta 2001; Ferreira *et al.* 2009; Ferreira *et al.* 2010; Santana *et al.* 2010; Souza 2012; Souza-Silva & Ferreira 2009; Souza-Silva *et al.* 2011a,b; Zampaulo 2010; Zeppelini Filho *et al.* 2003; Fundação Estadual do Estado de São Paulo 2010a,b,c,d). The average richness of those studies is 50 species (±20). In the present study the average found was higher than the general average for the Brazilian caves, but it is within the standard deviation. Therefore, the study area cannot be highlithed as one of the richer areas concerning cave fauna in Brazil. However, thirteen caves deserve prominence, because they present richness above average, plus the standard deviation, when compared to the other regions of Brazil (Tab. 2).

Regarding the troglobitic species, the distribution restricted to one or few caves, added to their potential low reproduction rate, make those organisms sensitive to alterations in the environment (Culver & Pipan 2009). Accordingly, they become an important tool for cave conservation (Elliott 2007; Borges *et al.* 2012). In the present study the troglobitis species presented a high degree of endemism and all of the caves that shelter troglobites possess at least one endemic species. Therefore, even if not being classified as the most vulnerable, these caves should be inserted in future conservation plans.

THREATS AND CONSERVATION STATUS OF THE AREA

The inadequate use of the land for agricultural activities, expansion of cities, surface and subterranean water use, mining activities, among others, have been the main threats imposed to the karstic areas (Watson 1997).

In the study region the main threat is the removal of forests for creation of pastures. Locally endemic cave species can become extinct if the surrounding area is deforested (Reboleira *et al.* 2011). Furthermore, the removal of the vegetation from the cave entrance surroundings can reduce the resource contribution and alter the environment in these areas, for instance, changing the local temperature and humidity/moisture. The entrances work as ecotones and they shelter a wide diversity of species that depend on the resource imported from the external environment (Prous *et al.* 2004).

The main potential threat for the caves of the studied region is the pollution of their water bodies, a fact

that can result in severe alterations to the environment and cave fauna. As an example, the agricultural practices carried out in the surroundings of the Tumbling Creek cave, (Missouri, USA), are affecting the water quality and they may be decreasing the population of aquatic species sensitive to these changes (*Antrobia culveri*) (Neill *et al.* 2004).

Although the region, as are all the karstic areas of the world, is subject to impacts of anthropic origin, there are still places that are preserved, as is the case of the northern portion of the region, like the municipal district of Arinos. The caves of this municipal district are considerably preserved if compared to other caves of the study. A good example is the Lapa da Capa, where no visible impact was found, to the surroundings as well as to the interior the cavity. Nevertheless, the area is inserted in the Cerrado biome, known for high diversity and constant threats (Myers *et al.* 2000), always in need of conservation actions.

LEGAL PROTECTION AND PUBLIC EDUCATION

The lack of laws specifically dedicated to the karst is very common all over the world. Even when the legislation considers these environments, the potential benefits do not indeed exists, mainly due to the lack of enforcement on the part of the authorities (Parise & Gunn 2007).

Throughout the world, there are only few countries that possess some type of specific legislation for cave protection; some that do for instance, are the United States, France, Slovenia, Australia and Brazil (Tercafs 1992; Kepa 2001; Restificar *et al.* 2006; Ferreira *et al.* 2007). There are examples of legally protected caves and areas, as is the case of regions considered as World Heritage sites due to the characteristics of their karstic landscapes (Williams 2008). However, karstic areas and caves have been sometimes protected in an indirect way, mainly by the establishment of reserves for reasons that do not include the importance of their karstic characteristics, as in the case of Central American countries (Day 1996; Kueny & Day 2002) and some countries of Southeast Asian (Day & Urich 2000).

Brazil is the only country that has an agency devoted specifically to the study, protection and management of caves, which comprises the Centro Nacional de Pesquisa e Conservação de Cavernas (CECAV) *(National Cave Research and Conservation Center (CECAV).* Historically, the Brazilian caves could not be destroyed for being patrimonies of the Union (Federal Constitution 1998; Decree 99556/1990). However in 2008, the caves started to be susceptible to supression (Decree 6640/2008), as long as they were previously studied during the enterprise licensing process. During the study the caves should be classified, according to their relevance, as maximum, high, medium and low, according to criteria proposed in the Instruction Normative Number 2 of 2009. Caves with maximum relevance are not able, under any circumstances, to be suppressed, and caves included in the other categories are susceptible to irreversible alterations, including suppression.

Such a decree has been severely criticized and considered a setback for cave conservation in the country (Figueiredo *et al.* 2010). However, the rigidity of the previous law caused, in cases of strong social and economical demand, caves´ suppression (Auler 2006), many times without there being previous study.

It is important to point out that protection based only in laws is not enough. Real and efficient protection should count on the support of the population and a continuous program of public education regarding the protection of resources (Watson 1997). Furthermore, the appropriate use of the land can increase the sustainable development of the economy in these areas (Linhua 1999).

CAVES CONSERVATION IN THE WORLD

Different strategies for conservation of caves and karstic areas have been used all over the world. Indices have been used to evaluate the impact degree and threats, seeking to identify karstic areas most threatened and/or that deserve priority attention for conservation strategies (Elliott 2007; Van Beynen & Townsend 2005; 2012).

Van Beynen & Townsend (2005) created a karstic area disturbance index with different indicators, including the subterranean fauna, which has been used in works that seek to propose priority areas for conservation (Calò & Parise 2006; Van Beynen *et al.* 2007; Borges *et al.* 2012). Van Beynen & Townsend (2005), however, affirmed that the selection of individual species as indicators would be problematic because of disagreements about which species to use. Therefore, only in Borges et al. (2012) was the biological component used as indicator, based on the troglobite richness, endemism and rarity. Recently a karst sustainability index was created (KSI) (Van Beynen & Townsend 2012). This index is based on indicators that incorporate measurements of the three resources use domains: the social, the environmental and the economic.

The species distribution was used to identify places with threatened species and to propose conservation priorities by Culver *et al.* (2000) and Lewis *et al.* (2003), both in areas of the United States, and by Ferreira *et al.* (2007) in karstic areas of France.

Elliott (2007) used the species richness, troglobite richness and endemism as indicators for an index used to rank biodiversity relevance of caves in Missouri, Unit-

ed States, for conservation plans. Such index uses the expression B = SR×T×SE, where, B is: biodiversity, SR: species richness, T: troglobites richness, SE: local endemism.

In several regions of Brazil, studies are using methodologies similar to those used in this work to propose priority areas and caves for conservation (Souza-Silva 2008; Zampaulo 2010; Bento 2011; Souza 2012). Good results have been obtained, as is the case of the creation of the Parque Nacional da Furna Feia, in the state of Rio Grande do Norte, where 36% (205 caves) of all of the caves known to the state are inserted and legally protected. That area had been pointed out by Bento (2011) as priority for conservation in the State of Rio Grande do Norte in function of his work that used the same methodology as employed here.

CONSERVATION ACTIONS

Although protected areas, in themselves, do not guarantee the preservation of nature, they are fundamental tools, separating elements of the biodiversity from the processes that threaten Nature (Margules & Pressey 2000). In karstic landscapes the creation of buffer zones in between the preservation area and the neighboring lands is important, reducing the influences and consequences of environmental damage to the adjacent lands (Barany-Kevei 1999).

In Brazil, the creation of reserves faces serious problems. Caves inserted in preservation areas suffer visitation impacts, as for instance, trampling, garbage and speleothem depredation, among others (Lobo 2008; Souza-Silva & Ferreira 2009). Thus, the creation of nature reserves for the protection of caves or cave species should be very well appraised and elaborated, besides possessing an effective site management plan, integrating scientists, managers and tourism professionals, besides specific studies on each cave used for tourist visitation (Lobo *et al*. 2013).

Although direct impacts (e.g. mining) are the most worrisome, because they can cause immediate losses, other impacts can create countless problems for the fauna, although over the long term. The pollution of water bodies is an example. Karstic land possess discontinuities through which potential pollutants can be transported to remote locations, such as springs and caves with groundwater and rivers (Parise & Gunn 2007). Therefore, to reduce the exploration and water pollution on karstic land would be important for the maintenance of caves that possess groundwater and rivers (De Waele & Follesa 2003).

FINAL REMARKS

To study the subterranean biodiversity in the maximum number of caves in the Cerrado is of addition importance, because it is a highly diverse environment and under constant threat (Myers *et al*. 2000). As such, the present study presented results that can aid conservation actions in a little studied region in this biome. Furthermore, other karstic areas in the São Francisco river basin should be investigated regarding their conservation priority, providing subsidies for the National Action Plan for conservation of caves and cave fauna of that region.

Caves and karstic areas are being affected all over the world, mainly by anthropic action. Although probable, it is impossible to determine if such impacts have been causing the loss of species in these environments, mainly through lack of information of the primary characteristics of the communities prior to the impacts.

Even facing the difficulty of quantifying the cave biodiversity loss before alterations in the environment, it is certain that loss exists. Although the impacts that cause irreversible alterations in the caves, such as mining, are the main targets for environmentalists, others are also highly troubling.

In the study region, as well as throughout the world, the removal of forests appears as one of the most disturbing alterations, not only for the epigean biodiversity, but also for the subterranean. Cave species depend, largely, on the importation of resources from the external environment (Culver 1982) and the removal of forests can reduce that importation.

Another important fact is that tropical forests shelter a great diversity of species and they are subject to various impacts of anthropic origin, mainly linked to agricultural activities, that provoke, in almost all cases, high epigean biodiversity loss (Gibson *et al*. 2011). Once the epigean biodiversity is decreased, possibly fewer species will be using the cave environment.

ACKNOWLEDGMENTS

To the Fundação de Amparo à Pesquisa e Extensão de Minas Gerais (FAPEMIG) for financial support, project APQ-01854-09. To friends of the Grupo de Estudos em Ecologia Subterrânea da Universidade Federal de Lavras. To Espeleo Grupo de Brasília for information about the caves in the region.

REFERENCES

Auler, A. S., 2006: *Relevância de cavidades naturais subterrâneas: contextualização, impactos ambientais e aspectos jurídicos*.- Ministério de Minas e Energia (MME), pp. 166, Brasília.

Australian Speleological Federation, 2010: Minimal Impact Caving Code (MICC).- [Online] Available from: http://www.caves.org.au/downloads/MICC2010.pdf [Accessed 3rd October 2012].

Australian Speleological Federation. Minimum Impact Code of Ethics for Scientific Investigation in Caves and Karst (Science MIC), 3pp, 2010. Available from: http://www.caves.org.au/downloads/ScienceCode-Jul2010.pdf [Accessed 3rd October 2012].

Balák, I. Janèo, J., Stefka, L. & P. Bosák, 1999: Agriculture and nature conservation in the Moravian karst (Czech Republic).- International Journal of Speleology, 28B, 71–88.

Barany-Kevei, I., 1999: Impacts of agricultural land use on some Hungarian karst regions.- International Journal of Speleology, 28B, 89–98.

Bento, D.M., 2011: *Diversidade de invertebrados em cavernas calcárias do oeste potiguar: subsídios para determinação de áreas prioritárias para conservação.*- M.D. Thesis. Universidade Federal do Rio Grande do Norte, pp. 160.

Bernardi, L.F.O., Pellegrini, T.G., Taylor, E.L.S. & R.L. Ferreira, 2012: Aspectos ecológicos de uma caverna granítica no sul de Minas Gerais.- Espeleo-Tema, 23, 5–12.

Borges, P.A.V., Cardoso, P., Amorim, I.R., Pereira, F., Constância, J.P., Nunes, J.C., Barcelos, P., Costa, P., Gabriel, R. & M.L. Dapkevicius, 2012: Volcanic caves: priorities for conserving the Azorean endemic troglobiont species.- International Journal of Speleology, 41, 101–111.

Calò, F. & M. Parise, 2006: Evaluating the human disturbance to karst environments in southern Italy.- Acta Carsologica, 35, 47–56.

Cavalcanti, L.F., Lima, M.F., Medeiros, R.C.S. & I. Meguerditchian, 2012: *Plano de ação nacional para a conservação do patrimônio espeleológico nas áreas cársticas da Bacia do Rio São Francisco, (Série Espécies Ameaçadas, 27)*.- Instituto Chico Mendes de Conservação da Biodiversidade, pp. 140, Brasília.

Constituição da República Federativa do Brasil, 1988: [Online] Available from: http://www.planalto.gov.br/ccivil_03/constituicao/ConstituicaoCompilado.htm [Accessed 3rd September 2012].

Cordeiro, L.M., 2008: *Fauna cavernícola da Serra da Bodoquena: revisão bibliográfica e um estudo de ecologia de comunidades*.- M.D. Thesis. Universidade Federal do Mato Grosso do Sul, pp. 119.

Culver, D.C. & H. Wilkens, 2000: Critical review of relevant theories of the evolution of subterranean animals.- In: Wilkens, H. et al. (eds.) *Ecosystems of the World Vol30: Subterranean Ecossystems*. Elsevier Press, p. 381–397, Amsterdam.

Culver, D.C. & T. Pipan, 2009: *The biology of caves and other subterranean habitats*.- Oxford University Press, pp. 254, Oxford.

Culver, D.C., 1982: *Cave life: Evolution and Ecology*.- Harvard University Press, pp. 189, Massachussets and London.

Culver, D.C., M.D. L.L., Christman M.C. & H.H. Hobbs, 2000: Obligate cave fauna of the 48 contiguous United States.- Conservation Biology, 14, 386–401.

Day, M. & P. Urich, 2000: An assessment of protected karst landscapes in Southeast Asia.- Cave and Karst Science, 27, 61–70.

Day, M.J., 1996: Conservation of Karst in Belize.- Journal of Cave and Karst Studies, 58, 139–144.

De Waele, J. & R. Follesa, 2003: Human impact on karst: the example of Lusaka (Zambia).- International Journal of Speleology, 32, 71–83.

Decreto Nº 6.640, 2008: [Online] Available from: http://www.planalto.gov.br/ccivil_03/_Ato2007-2010/2008/Decreto/D6640.html [Accessed 3rd September 2012].

Decreto Nº 99.556, 1990: [Online] Available from: http://www2.camara.gov.br/legin/fed/decret/1990/decreto-99556-1-outubro-1990–339026-normaatualizada-pe.html [Accessed 3rd September 2012].

Derraik, J.G., Closs, G.P., Dickinson, K.J., Sirvid, P., Barratt, B.I.P. & B.H. Patrick, 2002: Arthropod Morphospecies versus Taxonomic Species: a Case Study with Araneae, Coleoptera, and Lepidoptera.- Conservation Biology, 16, 1015–1023.

Derraik, J. G., Early, J.W., Closs, G.P. & K.J. Dickinson, 2010: Morphospecies and taxonomic species comparison for Hymenoptera.- Journal of Insect Science, 10, 1–7.

Elliott, W.R., 2004: Protecting caves and cave life.- In: Culver, D.C. & W.B. White, (eds.). *Encyclopedia of caves*. Elsevier Academic Press, pp. 458–467, San Diego.

Elliott, W.R., 2000: Conservation of the North American cave and karst biota.- In: Wilkens, H. *et al.* (eds.) *Ecosystems of the World Vol30: Subterranean Ecossystems*. Elsevier Press, pp. 665–689, Amsterdam.

Elliott, W.R., 2007: Zoogeography and biodiversity of Missouri caves and karst.- Journal of Cave and Karst Studies, 69, 135–162.

Ferreira, D., Malard F., Dole-Olivier, M.J. & J. Gibert, 2007: Obligate groundwater fauna of France: diversity patterns and conservation implications.- **Biodi**versity and Conservation, 16, 567–596.

Ferreira, R. L., 2004: *A medida da complexidade ecológica e suas aplicações na conservação e manejo de ecossistemas subterrâneos.*- PhD Thesis. Universidade Federal de Minas Gerais, pp. 158.

Ferreira, R.L. & L.C.S. Horta, 2001: Natural and human impacts on invertebrate communities in brazilian caves.- Revista Brasileira de Biologia 61, 7–17.

Ferreira, R.L., Bernardi, L.F.O., M. Souza-Silva, 2009: Caracterização dos ecossistemas das Grutas Aroê Jari, Kiogo Brado e Lago Azul (Chapada dos Guimarães, MT): Subsídios para o turismo nestas cavidades.- Revista de Biologia e Ciências da Terra, 9, 41–58.

Ferreira, R.L., Gomes, F.T.M.C. & M. Souza-Silva, 2008: Uso da cartilha "Aventura da vida nas cavernas" como ferramenta de educação nas atividades de turismo em paisagens cársticas.- Pesquisas em Turismo e Paisagens Cársticas, 1, 139–158.

Ferreira, R.L., Prous, X., Bernardi, L.F.O. & M. Souza-Silva, 2010: Fauna subterrânea do estado do Rio Grande do Norte: caracterização e impactos.- Revista brasileira de espeleologia, 1, p. 25–51

Figueiredo, L.A.V., Rasteiro, M.A. & P.C. Rodrigues, 2010: Legislação para a proteção do patrimônio espeleológico brasileiro: mudanças, conflitos e o papel da sociedade civil.- Espeleo-Tema, 21, 49–65.

Fundação Florestal do Estado de São Paulo, 2010a: Plano de manejo espeleológico: Caverna do Diabo.- **[On**line] Available from: http://www.ambiente.sp.gov.br/fundacaoflorestal/planos-de-manejo/planos-de-manejo-planos-espeleologicos (Accessed 1st November 2012).

Fundação Florestal do Estado de São Paulo, 2010b: Plano de manejo espeleológico: Gruta da Capelinha.- [Online] Available from: http://www.ambiente.sp.gov.br/fundacaoflorestal/planos-de-manejo/planos-de-manejo-planos-espeleologicos/ (Accessed 1st November 2012).

Fundação Florestal do Estado de São Paulo, 2010c: Plano de manejo espeleológico: Parque Estadual Turístico do Alto Ribeira (PETAR).- [Online] Available from: http://www.ambiente.sp.gov.br/fundacaoflorestal/planos-de-manejo/planos-de-manejo-planos-espeleologicos/ (Accessed 1st November 2012).

Fundação Florestal do Estado de São Paulo, 2010d: Plano de manejo espeleológico: Parque Estadual Intervales.- [Online] Available from: http://www.ambiente.sp.gov.br/fundacaoflorestal/planos-de-manejo/planos-de-manejo-planos-espeleologicos/ (Accessed 1st November 2012).

Gibert, J. & L. Deharveng, 2002: Subterranean Ecosystems: A Truncated Functional Biodiversity.- BioScience, 52, 473–481.

Gibson, L., Lee, T.M., Koh, L.P., Brook, B.W., Gardner, T.A., Barlow, J., Peres, C.A., Bradshaw, C.J.A., Laurance, W.F., Lovejoy, T.E. & N.S. Sodhi, 2001: Primary forests are irreplaceable for sustaining tropical biodiversity.- Nature, 478, 378–383.

Gillieson, D. & M. Thurgate, 1999: Karst and agriculture in Australia.- International Journal of Speleology, 28B, 149–168.

Gunn, J., Hardwick, P. & P.J. Wood, 2000: The invertebrate community of the Peak–Speedwell cave system, Derbyshire, England — pressures and considerations for conservation management.- Aquatic Conservation: Marine And Freshwater Ecosystems, 10, 353–369.

Hυppop, K., 2012: Adaptation to low food.- In: White, W.B. & D.C. Culver (eds) *Encyclopedia of Caves, 2nd edition*, Academic Press, p. 1–9, New York.

Instrução Normativa Nº 2, 2009: [Online] Available from: http://www.icmbio.gov.br/cecav/images/download/IN%2002_MMA_Comentada.pdf (Accessed 3rd Octuber 2012).

Kepa, T., 2001: Karst conservation in Slovenia.- Acta carsologica, 30, 143–164.

Kueny, J.A. & M.J. Day, 2002: Designation of protected karstlands in Central America: a regional assessment.- Journal of Cave and Karst Studies, 64, 165–174.

Lewis, J.J., Moss, P.H., Tecic, D. & M.E. Nelson, 2003: A conservation focused inventory of subterranean invertebrates of the southwest Illinois karst.- Journal of Cave and Karst Studies, 65, 9–21.

Linhua, S., 1999: Sustainable development of agriculture in karst areas, South China.- International Journal of Speleology, 28B, 139–148.

Lobo, H.A.S., 2008: Ecoturismo e percepção de impactos socioambientais sob a ótica dos turistas no Parque Estadual Turístico do Alto Ribeira – PETAR.- Pesquisas em Turismo e Paisagens Cársticas, 1, 67–75.

Lobo, H.A.S., Trajano, E., Marinho, M.A., Bichuette, M.E., Scaleante, J.A.B., Scaleante, O.A.F., Rocha, B.N. & F.V. Laterza, 2013: Projection of tourist scenarios onto fragility maps: Framework for determination of provisional tourist carrying capacity in a Brazilian show cave.- Tourism Management, 35, 234–243.

Margules, C.R. & R.L. Pressey, 2000: Systematic conservation planning.- Nature, 405, 243–253.

Myers, N., Mittermeier, R.A., Mittermeier, C.G., Fonseca G.A.B. & J. Kent, 2000: Biodiversity hotspots for conservation priorities.- Nature, 403, 853–858.

Neill, H., Gutiérrez, M. & T. Aley, 2004: Influences of agricultural practices on water quality of Tumbling Creek cave stream in Taney County, Missouri.- Environmental Geology, 45, 550–559.

Oliver, I. & A.J. Beattie, 1996: Invertebrate morphoespecies as surrogates for species: a case study.- Conservation Biology. 1, 99–109.

Parise, M. & J. Gunn, 2007: Natural and anthropogenic hazards in karst areas: an introduction.- Geological Society of London: Special Publications, 279, 1–3

Parise, M. & V. Pascali, 2003: Surface and subsurface environmental degradation in the karst of Apulia (southern Italy).- Environmental Geology, 44, 247–256.

Pellegrini, T.G. & R.L. Ferreira, 2012b: Management in a neotropical show cave: planning for invertebrates conservation.- International Journal of Speleology, 41, 361–368.

Pellegrini, T.G. & R.L. Ferreira,2012a: Sampling effort in mite communities associated with cave bat guano.- Speleobiology Notes, 4, 10–16.

Prous, X., Ferreira, R.L. & R.P. Martins, 2004: Ecótone delimitation: epigean-hypogean transition in cave ecosystems.- Austral Ecology, 29, 374–382.

Reboleira A.S., Borges P.A.V., Gonçalves, F., Serrano A.R.M. & P. Oromí, 2011: The subterranean fauna of a biodiversity hotspot region – Portugal: an overview and its conservation.- International Journal of Speleology, 40, 23–37.

Restificar, S.D.F., Day, M.J. & P.B. Urich, 2006: Protection of karst in the Philippines.- Acta Carsologica, 35, 121–130.

Santana, M.E.V., Souto, L.S. & M.A.T. Dantas, 2010: Diversidade de invertebrados cavernícolas na Toca da Raposa (Simão Dias – Sergipe): o papel do recurso alimentar e métodos de amostragem.- Scientia Plena, 6, 1–8.

Souza, M.F.V.R. & R.L. Ferreira, 2012: *Eukoenenia virgemdalapa* (Palpigradi: Eukoeneniidae): a new troglobitic palpigrade from Brazil.- Zootaxa, 3295, 59–64.

Souza, M.F.V.R., 2012: *Diversidade de invertebrados subterrâneos da região de Cordisburgo, Minas Gerais: subsídios para definição de cavernas prioritárias para conservação e para o manejo biológico de cavidades turísticas*.- M.D. Thesis. Universidade Federal de Lavras, pp. 149.

Souza-Silva, M. & R.L. Ferreira, 2009: Caracterização ecológica de algumas cavernas do Parque Nacional de Ubajara (Ceará) com considerações sobre o turismo nestas cavidades.- Revista de Biologia e Ciências da Terra, 9, 59–71.

Souza-Silva, M., 2008: *Ecologia e conservação das comunidades de invertebrados cavernícolas na Mata Atlântica Brasileira*.- PhD thesis. Universidade Federal de Minas Gerais, pp. 211.

Souza-Silva, M., Bernardi, L.F.O., Martins, R.P. & R.L. Ferreira, 2012: Transport and consumption of organic detritus in a neotropical limestone cave.- Acta Carsologica, 41, 139–150.

Souza-Silva, M., Martins, R.P. & R.L. Ferreira, 2011a: Cave lithology determining the structure of the invertebrate communities in the Brazilian Atlantic Rain Forest.- Biodiversity Conservation, 20, 1713–1729.

Souza-Silva, M., Nicolau, J.C. & R.L. Ferreira, 2011b: Comunidades de invertebrados terrestres de três cavernas quartzíticas no Vale do Mandembe, Luminárias, MG. Espeleo-Tema.- 22, 79–91.

Tercafs, R., 1992: The Protection of the subterranean environment: conservation principles and management tools.- In Camacho, A. (eds.) *The Natural history of bioespeleology*. Museo Nacional de Ciencias Naturales, pp. 485–522, Madrid.

Van Beynen, P. & K. Townsend, 2005: A Disturbance index for karst environments.- Environmental Management, 1, 101–116.

Van Beynen, P., Brinkmann, R. & K. Van Beynen, 2012: A sustainability index for karst environments.- Journal of Cave and Karst Studies, 74, 221–234.

Van Beynen, P., Feliciano, N., North, L. & K. Townsend, 2007: Application of a Karst Disturbance Index in Hillsborough County, Florida.- Environmental Manage, 39, 261–277.

Ward, D.F & M.C. Stanley, 2004: The value of RTUs and parataxonomy versus taxonomic species.- New Zealand Entomologist, 27, 3–9.

Watson, J., Hamilton-Smith, E., Gillieson, D. & K. Kiernan, 1997: *Guidelines for cave and karst protection*: IUCN, pp. 63, Gland/Cambridge.

Weinstein, P. & D. Slaney, 1995: Invertebrate faunal survey of Rope Ladder cave, Northern Queensland: a comparative study of sampling methods.- Journal of Australian Entomological Society, 34, 233–236.

Williams, P., 2008: World Heritage Caves and Karst.- IUCN, pp. 57, Gland.

Zampaulo, R.A., 2010: *Diversidade de invertebrados na província espeleológica de Arcos, Pains, Doresópolis (MG): Subsídios para a determinação de áreas prioritárias para a conservação*.- M.D. thesis. Universidade Federal de Lavras, pp. 190.

Zeppelini Filho, D., Ribeiro, A.C., Ribeiro, G.C., Fracasso, M.P.A., Pavani, M.M., Oliveira, O.M.P., Oliveira, S.A. & A.C. Marques, 2003: Faunistic survey of sandstone caves from Altinópolis region, São Paulo State, Brazil.- Papéis Avulsos de Zoologia, 43, 93–99.

COBISS: 1.01

NEXT STOP: UNDERGROUND. VARIABLE DEGREES AND VARIETY OF REASONS FOR CAVE PENETRATION IN TERRESTRIAL GASTROPODS

NASLEDNJA POSTAJA: PODZEMLJE. RAZLIČNE STOPNJE IN RAZLIČNI RAZLOGI PRODIRANJA KOPENSKIH POLŽEV V JAME

Alexander M. WEIGAND[1,2]

Abstract UDC 594.3:551.44

Alexander M. Weigand: Next Stop: Underground. Variable degrees and variety of reasons for cave penetration in terrestrial gastropods

Cave-dwelling animals can be classified based on their occurrence in and relationship to the subterranean environment. Subsurface distribution data and studies addressing the initial causes for animals to enter underground habitats are sparse. By retrieving occurrence data from two voluntary biospeleological collections in Central Germany, the degree of cave penetration in terrestrial gastropods was investigated, thus to infer potential evolutionary drivers. In total, 66 identified gastropod species entered the subterranean environment with 23 of the species also recorded from the dark zone. Gastropods possessed variable degrees of cave penetration and no obligate cave forms were observed. A decline of occurrence records from the entrance to the dark zone was the most prominent pattern. Nevertheless, several species were collected from all three light zones (i.e. entrance, transition and dark). A variety of potential reasons can be inferred to explain their subsurface appearance: exploitation of alternative food sources, aphotic above-ground movement, mating sites, temporal, seasonal and long-term refugia, and chance. Moreover, the results imply a frequent migration of species between the interconnected light zones and the surface. Consequently, terrestrial gastropods should be considered when investigating the origin and importation of allochthonous resources in caves.

Keywords: Gastropoda, subterranean environment, ecology, distribution data, cave colonization, speciation.

Izvleček UDK 594.3:551.44

Alexander M. Weigand: Naslednja postaja: podzemlje. Različne stopnje in različni razlogi prodiranja kopenskih polžev v jame

Podzemeljske živali lahko opredelimo glede na njihovo pojavljanje v podzemeljskem okolju in odnos do tega okolja. Podatki o razširjenosti živali v podzemlju in študije, ki obravnavajo vzroke za kolonizacijo podzemlja so redki. Stopnja prodiranja kopenskih polžev v jame in morebitni evolucijski vzroki so bili proučevani na podlagi dveh biospeleoloških zbirk v osrednji Nemčiji. Skupno je bilo določenih 66 vrst polžev, ki zaidejo v podzemlje, od tega 23 vrst iz temnih predelov podzemlja. Čeprav polži kažejo različne stopnje prodiranja v jame, podzemeljska oblika polžev ni bila ugotovljena. Najpogostejši vzorec razširjenosti je bil upadanje njihovega pojavljanja od vhoda proti notranjosti, čeprav je bilo po nekaj vrst vedno ugotovljenih v vseh treh conah: na vhodu, na prehodu med svetlo in temno cono ter v temni coni. Možnih je več razlogov, zaradi katerih se pojavijo v podzemlju: izkoriščanje alternativnih virov hrane, afotično gibanje na površju, paritvena mesta, začasno, sezonsko ali dolgotrajno zatočišče ter priložnost. Rezultati kažejo na pogosto migracijo vrst med posameznimi conami in površjem. Posledično bi bilo potrebno kopenske polže upoštevati pri raziskavah izvora in vnosa alohtonih virov v jame.

Ključne besede: Gastropoda (polži), podzemeljsko okolje, ekologija, podatki o razširjenosti, kolonizacija jam, speciacija.

[1] Goethe-University, Institute for Ecology, Evolution and Diversity, Department of Phylogeny & Systematics, Max-von-Laue Str. 13, 60438 Frankfurt am Main

[2] Croatian Biospeleological Society, Demetrova 1, 10000 Zagreb, Croatia, e-mail: weiganda@gmx.net

Received/Prejeto: 08.03.2013

INTRODUCTION

Since the first nominal description of a cave-dwelling animal, the blind cave salamander *Proteus anguinus* (Laurenti 1768), subterranean organisms have attracted people's attention. Possessing a life in permanent darkness, this curiosity immediately can be imagined. But even more so, the perception is frequently underscored by a strongly modified, sometimes bizarre morphology. Cave-dwelling adaptive features include the (often complete) reduction of eyes and body pigmentation (= reductive troglomorphies) resulting in 'blind albinos' or the elongation of body appendages and an improved extra-optical sensory system (= constructive troglomorphies; Protas & Jeffery 2012). However, not all cave species exhibit a troglomorphic appearance (Bichuette & Trajano 2003). Subterranean organisms can be ecologically classified depending on their occurrence in and relationship to the subterranean habitat (Sket 2008). Obligate cave forms (= eutroglobionts) are restricted and highly adapted to a life in darkness, whereas in some occasions, epigean animals may accidentally occur in the subterranean environment (= eutrogloxenes). Both extremes of this ecological continuum are connected by all levels of intermediate forms. Based on the formation of stable or temporal subterranean populations, they are commonly referred to as eutroglophiles or subtroglophiles, respectively.

To explain the initial phases of cave colonization and speciation between surface and subsurface populations, unsuitable environmental conditions on the surface (Climate Relict Hypothesis) and the exploitation of alternative resources (Adaptive Shift Hypothesis) have been discussed as evolutionary drivers (for a review see Juan *et al.* 2010). Subsequently, speciation of underground lineages may have been triggered by subsurface dispersal or vicariance events leading to the formation of allopatric populations. More recently, a combination of both non-exclusive processes has been considered (Culver *et al.* 2007; Weigand *et al.* 2013). Besides studies addressing speciation processes within the underground realm or to a surface population, causes for the initial phase of cave colonizations have been studied less intensively (Camp & Jensen 2007) although frequently reconstructed from phylogenetic patterns (Leys *et al.* 2003; Howarth & Hoch 2005; Cooper *et al.* 2007).

In this survey, the affinity of gastropod species to the subterranean environment is investigated with the aim to infer potential evolutionary drivers for their occurrence in underground habitats. Since gastropods are chemically oriented organisms, they do not have to overcome the disadvantage imposed by visual orientation in caves (Culver & Pipan 2009). As a consequence, a certain number of surface litter species are expected to occur in caves, thus representing multiple case studies.

VARIABLE DEGREES OF SUBTERRANEAN PENETRATION

Observation records of cave-dwelling terrestrial gastropods were retrieved from two voluntary collections: from the Biospeleological Register of the Hesse Federation for Cave and Karst Research (HES; Zaenker 2008; Reiss *et al.* 2009a) and for the region of Rhineland-Palatinate + Saarland (RP + SAR; Weber 2012) (Fig. 1). The geology of the study area is very heterogeneous but primarily consists of limestone, argillaceous shale, slate and red sandstone. In addition to natural objects (i.e. caves, deep fissures), species were recorded from artificial cavities (i.e. bunkers, tunnels, mines) totaling 3352 investigated terrestrial objects (i.e. without springs, groundwater samples). During each visit (N), terrestrial gastropods were recorded and classified based on their occurrence in the entrance (E), transition (T) or dark zone (D) of the subterranean environment. Thereby, species observations are qualitative records for a given zone rather than representing count data of specimens. In some occasions, specimens of a single species were collected in multiple zones during a visit (i.e. N = 1 but more than one light zone with an occurrence record). Taxonomic identification is based on conchological and/or anatomical characteristics and was primarily performed by S. Zaenker, D. Weber, K. Bogon and H. Kappes. Taxonomic nomenclature is according to Fauna Europaea (2012). For species with $N \geq 15$ and occurrence records from all three light zones, a Chi^2-test was conducted in SPSS 12.0 (IBM) to test for equal frequency distributions. In total, 66 gastropod species were found within the subterranean environment (Tab. 1, Fig. 2), i.e. at least penetrating the entrance zone. An amount of 58% (38/66) of the identified species was shared by both geographical regions (i.e. HES vs. RP + SAR). Notable exceptions refer to *Arion ater*, *Arion silvaticus*, *Ena montana* and *Pomatias elegans* only recorded from HES and *Arion rufus* and *Phenacolimax major*, which were only present in RP + SAR. *Daudebardia rufa* was almost en-

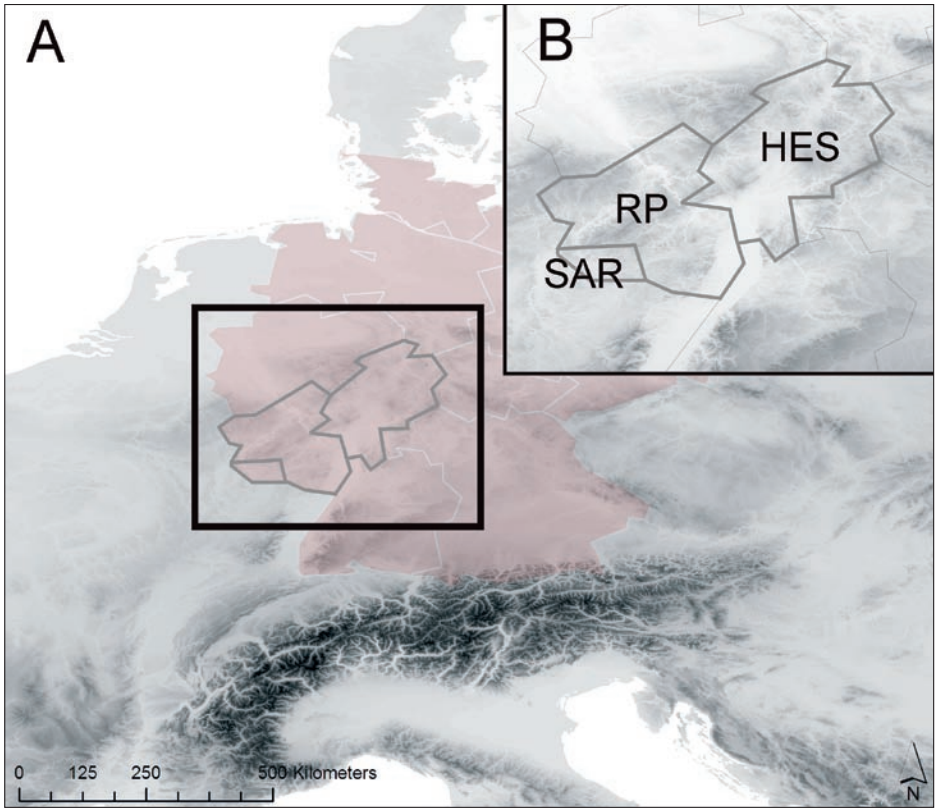

Fig. 1: Overview of the study area. A: The map indicates the geographical location of the two voluntary biospeleological collections for Hesse (HES) and Rhineland-Palatinate + Saarland (RP + SAR) in Germany (colored in red). B: Detailed geographical overview of the study area.

tirely restricted to HES (73 observations) with a single specimen found in SAR + RP. The dark zone was penetrated by 35% (23/66) of all species. Although they only constituted 13% of the total records (706/5589), *Boettgerilla pallens* and *Oxychilus* spp. accounted for 56% of all dark zone observations.

Fig. 2: Terrestrial gastropod species penetrating the subterranean environment. A: Discus rotundatus; B: Monachoides incarnatus; C: Pomatias elegans; D: Lehmannia marginata; E: Limax cinereoniger; F: Boettgerilla pallens; G: Oxychilus draparnaudi; H: Oxychilus cellarius. Copyright of the individual pictures: Klaus Bogon.

Tab 1: Subsurface distribution data of terrestrial gastropod species. Distribution records for the different light zones are separated for two voluntary collections: the biospeleological state register of Hesse (HES) and a private collection for the region of Rhineland-Palatinate + Saarland (RP + SAR). N: number of visits; S: surface record; E: entrance zone record; T: transition zone record; D: dark zone record. Species with records in the E + T + D zone (N ≥ 10) were tested by a Chi²-test.

#	taxon	morphospecies	N	S	E	T	D	N	E	T	D	p (Chi²)
					HES				RP + SAR			
1	Agriolimacidae	*Deroceras reticulatum* (O. F. Müller, 1774)	2	0	2	0	0	1	1	0	0	
2	Arionidae	*Arion* sp.	513	376	119	66	13	41	25	20	1	< 0.001
3		*Arion ater* (Linnaeus, 1758)	18	2	12	5	1					0.006
4		*Arion circumscriptus* Johnston, 1828	6	0	6	1	0	4	3	1	0	
5		*Arion distinctus* J. Mabille, 1868	3	0	3	0	0					
6		*Arion fasciatus* (Nilsson, 1823)	1	0	1	0	0	1	0	1	0	
7		*Arion fuscus* (O.F. Müller, 1774) / *A. subfuscus* (Draparnaud, 1805)	10	3	7	2	0	1	0	1	0	
8		*Arion cf. intermedius* Normand, 1852	4	0	3	2	0					
9		*Arion lusitanicus* J. Mabille, 1868	16	0	14	3	1	2	0	2	0	0.001
10		*Arion rufus* (Linnaeus, 1758)						38	13	25	2	< 0.001
11		*Arion silvaticus* Lohmander, 1937	16	1	11	4	1					0.007
12	Boettgerillidae	*Boettgerilla pallens* Simroth, 1912	92	24	27	32	34	14	5	6	4	0.717
13	Bradybaenidae	*Fruticicola fruticum* (O. F. Müller, 1774)	6	3	2	1	0					
14	Carychiidae	*Carychium tridentatum* (Risso, 1826) / *C. minimum* O. F. Müller, 1774	850	834	16	0	0	4	1	0	2	
15	Chondrinidae	*Chondrina avenacea* (Bruguière, 1792)	1	0	1	0	0					
16	Clausiliidae	*Alinda biplicata* (Montagu, 1803)	13	6	5	3	0	7	7	0	0	
17		*Balea perversa* (Linnaeus, 1758)	4	1	3	0	0					
18		*Clausilia bidentata* (Strøm, 1765)						19	18	1	0	
19		*Clausilia rugosa* (Draparnaud, 1801)	10	0	10	0	0	5	4	2	0	
20		*Cochlodina laminata* (Montagu, 1803)	8	2	6	0	0	10	8	1	1	
21		*Macrogastra attenuata* (Rossmässler, 1835)						2	2	0	0	
22		*Macrogastra ventricosa* (Draparnaud, 1801)						1	0	1	0	
23	Cochlicopidae	*Cochlicopa* sp.	84	73	10	9	0	4	2	2	0	
24		*Cochlicopa lubrica* (O. F. Müller, 1774)	9	9	0	0	0	9	8	1	0	
25		*Cochlicopa lubricella* (Rossmässler, 1834)	4	1	3	2	0					
26		*Azeca goodalli* (A. Férussac, 1821)	24	20	4	0	0					
27	Daudebardiidae	*Daudebardia rufa* (Draparnaud, 1805)	73	63	10	6	0	1	0	1	0	
28	Enidae	*Ena montana* (Draparnaud, 1801)	35	22	11	5	1					0.011
29		*Merdigera obscura* (O. F. Müller, 1774)	2	0	2	0	0	2	2	0	0	
30		*Zebrina detrita* (O. F. Müller, 1774)						1	1	0	0	
31	Euconulidae	*Euconulus* sp.	39	39	0	0	0					
32		*Euconulus fulvus* (O. F. Müller, 1774)	88	82	6	2	0	6	3	3	0	
33	Ferussaciidae	*Cecilioides acicula* (O. F. Müller, 1774)	10	9	1	0	0					
34	Helicidae	*Cepaea* sp.	49	17	28	12	2	12	10	2	0	< 0.001
35		*Cepaea hortensis* (O. F. Müller, 1774)	48	17	21	14	4	9	6	3	0	< 0.001
36		*Cepaea nemoralis* (Linnaeus, 1758)	48	11	28	13	5	34	18	13	4	< 0.001

#	taxon	morphospecies	N	S	E	T	D	N	E	T	D	p (Chi²)
37		*Arianta arbustorum* (Linnaeus, 1758)	21	15	6	3	0	2	2	0	0	
38		*Helicigona lapicida* (Linnaeus, 1758)	95	3	85	23	3	25	17	8	0	< 0.001
39		*Helix pomatia* Linnaeus, 1758	23	4	12	7	3	23	15	7	2	< 0.001
40		*Isognomostoma isognomostomos* (Schröter, 1784)	22	7	14	4	0					
41	Helicodontidae	*Helicodonta obvoluta* (O. F. Müller, 1774)	107	33	60	36	2	34	21	15	1	< 0.001
42	Hygromiidae	*Helicella* sp.						3	3	0	0	
43		*Trochulus* sp.	125	106	16	9	1	2	2	0	0	< 0.001
44		*Trochulus hispidus* (Linnaeus, 1758)	6	2	3	1	0	2	1	1	0	
45		*Trochulus plebeius* (Draparnaud, 1805)	4	4	0	0	0					
46		*Trochulus sericeus* (Draparnaud, 1801)						1	1	0	0	
47		*Monachoides incarnatus* (O. F. Müller, 1774)	511	399	95	50	7	49	39	10	0	< 0.001
48	Limacidae		191	148	39	18	4	26	14	15	1	< 0.001
49		*Lehmannia marginata* (O. F. Müller, 1774)	16	0	15	4	2	4	4	0	0	< 0.001
50		*Limax cinereoniger* Wolf, 1803	31	0	25	10	4	83	40	42	5	< 0.001
51		*Limax maximus* Linnaeus, 1758	59	21	30	21	5	23	12	16	3	< 0.001
52	Milacidae	*Tandonia rustica* (Millet, 1843)	6	2	3	1	1	2	1	0	1	
53	Orculidae	*Sphyradium doliolum* (Bruguière, 1792)	1	0	1	1	0	1	1	0	0	
54	Oxychilidae	*Oxychilus* sp.	67	24	29	23	10	31	10	18	4	0.001
55		*Oxychilus alliarius* (J. S. Miller, 1822)	6	3	2	0	1					
56		*Oxychilus cellarius* (O. F. Müller, 1774)	167	7	98	88	48	244	87	136	38	< 0.001
57		*Oxychilus draparnaudi* (H. Beck, 1837)	12	0	10	6	1	73	31	36	10	< 0.001
58		*Aegopinella nitens* (Michaud, 1831)	5	2	2	1	0	3	3	0	0	
59		*Aegopinella nitidula* (Draparnaud, 1805)	15	9	6	1	0	2	2	0	0	
60		*Aegopinella pura* (Alder, 1830)	15	11	4	1	0	1	0	1	0	
61		*Nesovitrea hammonis* (Strøm, 1765)	5	3	2	1	0	3	3	0	0	
62	Patulidae	*Discus rotundatus* (O. F. Müller, 1774)	655	386	226	108	19	299	174	132	14	< 0.001
63	Pomatiidae	*Pomatias elegans* (O. F. Müller, 1774)	13	2	11	3	0					
64	Pristilomatidae	*Vitrea crystallina* (O. F. Müller, 1774)	6	5	1	0	0	2	1	1	0	
65	Pupillidae	*Pupilla muscorum* (Linnaeus, 1758)	2	1	1	0	0					
66	Succineidae	*Oxyloma elegans* (Risso, 1826)	7	6	0	1	0					
67		*Succinella oblonga* (Draparnaud, 1801)	6	5	1	0	0					
68	Valloniidae	*Vallonia* sp.						1	1	0	0	
69		*Vallonia pulchella* (O. F. Müller, 1774)	13	12	1	0	0					
70		*Acanthinula aculeata* (O. F. Müller, 1774)	15	13	2	1	0					
71	Vitrinidae	*Eucobresia diaphana* (Draparnaud, 1805)	4	2	1	2	0					
72		*Phenacolimax major* (A. Férussac, 1807)						77	52	26	0	
73		*Vitrina pellucida* (O. F. Müller, 1774)	14	5	8	2	0	12	7	3	2	0.002
74		*Vitrinobrachium breve* (A. Férussac, 1821)						2	0	2	0	
		Σ	4331	2855	1181	608	173	1258	681	555	95	

VARIETY OF REASONS FOR SUBTERRANEAN PENETRATION

Knowledge about the occurrence of a species among different light environments (i.e. entrance, transition and dark zone) is important to understand the selective pressure of the subterranean environment imposed on the gene pool of the population. Numerous gastropod species were (sporadically) found within the subterranean environment. No true obligate cave forms were observed and only one third of all species possessed records in the dark zone. Those species were generally collected from other light zones as well. An unequal distribution of observation records with a peak in the entrance zone and decline to the dark zone was the most common pattern. One striking exception refers to the slug *Boettgerilla pallens*, for which an equal frequency distribution cannot be rejected (Chi^2-test, $p = 0.717$). The majority of observations for this species originated from the transition and dark zone. Typically known from soil samples, *B. pallens* demonstrates a rather limited mobility by ground-dwelling or moving in earthworm burrows (Gunn 1992). In the study area, however, it was found moving aboveground and climbing on walls in the subterranean environment. Supposedly, the species has recently spread from the Caucasus region over large parts of Central Europe. Even sightings from North- (Canada) and South-America (Columbia) exist (Reise *et al.* 2000; Hausdorf 2002). Although human-mediated dispersal is considered to explain the rapid pan-European colonization and transatlantic dispersal, this study points to a local aboveground movement within the more spacious, aphotic subterranean environment. This behavior may enable a faster establishment and spread after arrival.

Specimens of the carnivorous and omnivorous taxa *Oxychilus* and *Boettgerilla* constituted the majority of dark zone observations (56%). The penetration of non-surface habitats in those groups can be related to the exploitation of alternative food sources. Species of both taxa are known to prey on small gastropods and egg clutches. In particular, *Boettgerilla pallens*, *Oxychilus cellarius* and *Oxychilus draparnaudi* were recorded to feed on arionid eggs (Daxl 1967; Gunn 1992; von Proschwitz 1994). Their prey, juvenile slugs of the Arionidae and Limacidae, were frequently encountered in the subterranean environments of the studied region. The presence of juvenile slugs either suggests an underground colonization during infancy or a subsurface egg deposition with *in situ* hatching. Similar observations were recorded from caves in Luxembourg, including juvenile *Boettgerilla* for which egg-laying is known to occur below ground (Gunn 1992; Renker *et al.* 2012; Renker *et al.* 2013). Heller and Dolev (1993) hypothesized that "crevices might be a suitable habitat for land snails in which the hatching period, and period of juvenile growth, are very long". By implication, the prolonged development could be seen as a result of the less nutrient rich subsurface conditions.

Avoidance of unsuitable surface conditions must be seen as the most likely factor explaining the colonization of subterranean habitats by the majority of gastropod species. Local surface habitats are constantly changing and gastropod populations continuously feature the risk of extinction (Régnier *et al.* 2009). Because temperature and humidity levels in caves demonstrate rather low fluctuations and are generally buffered compared to the surface (Pipan *et al.* 2011), dwelling in the entrance zone may allow survival in patchy microhabitats (Poulson & White 1969). Hence, the risk of temporal or seasonal suffering from unsuitable environmental conditions can be locally decreased. By studying the Mediterranean helicid snail *Iberus gualtieranus gualtieranus*, Moreno-Rueda (2007) has found evidence for summer survival of this species in karstic crevices. Since slugs are particularly prone to desiccation, increased humidity levels in the subterranean milieu may ensure survival during droughts. Gunn (1992) showed that soil-dwelling is a common response of *Boettgerilla pallens* to escape direct light exposure and potentially heat. On the other site, winter freezing especially affects slugs and larger gastropods (Getz 1959; Biannic & Daguzan 1993; Ansart *et al.* 2001; Cook 2004). The frequent penetration of underground habitats by slugs (e.g. *Arion*, *Boettgerilla*, *Limax*) and helicids (*Cepaea* and *Helix*) in the study area may be best explained as a response to winter frost using the subterranean environment as a hibernation site.

Despite temporal or seasonal survival, subterranean habitats may act as long-term refugia at the edge of a species distribution range. The northern range limit of the Mediterranean snail *Pomatias elegans* is connected with the 2 °C January isotherm line. Hibernating specimens can withstand frost down to –6 °C for several days (Welter-Schultes 2012). In this study, several geographically restricted populations of *P. elegans* were found in the region of Treffurt at the NW-margin of the Thuringian Basin (i.e. at the NE-boarder of the HES state register). During a single visit, up to twelve individuals were collected from the soil populating the entrance and transition zone. More general, peripheral populations surviving in patchy subterranean microhabitats at the edge of a species distribution range can serve as an origin for future range expansion (thereby, significantly increasing the speed of colonization). Additionally, those populations are particularly susceptible to adapt to local environmental conditions because of an increased genetic isolation and/or enhanced/divergent selective pressures

(Sexton *et al.* 2009; Vergeer & Kunin 2013). Two other cave-penetrating gastropods possessed their range limits within the study area: the Scandinavian slug *Arion ater* (S-range limit) and *Phenacolimax major* (NE-range limit), the latter being rare east of the Rhine River (Renker *et al.* 2013).

Finally, one must be cautious to link species observations with their ecological requirements. As an example, frequent observations of living specimens in the dark zone do not necessarily reflect a cave-dwelling ecology of the species as best illustrated by the situation of *Discus rotundatus*. This abundant species was usually found above-ground or within in the entrance zone of subterranean environments comprising 20% of all records. However, and because of their sheer number, numerous specimens were also collected in the dark zone (12% of all dark zone observations). As a fungivorous species, *D. rotundatus* may be able to survive in the dark zone for a longer period of time (Renker *et al.* 2013). Nevertheless, their presence is most probably best explained by population density as some specimens of this highly abundant, cave-penetrating species (Reiss *et al.* 2009b) will "end up" in the dark zone. Because eco-classifications of cave-dwellers are inferred from the relationship of the animal to the subterranean environment (Sket 2008) and this relationship is reconstructed from observation and species abundance data, one might face a general problem.

CONCLUSIONS

Subsurface distribution data is paramount to reconstruct species affinities to subterranean habitats, since behavioral and ecological changes may precede morphological change. In this study, several gastropod species were observed from different subterranean light zones possessing a variety of reasons to explain their underground appearance (e.g. exploitation of alternative food sources, aphotic above-ground movement, mating site, temporal, seasonal and long-term refugia, and chance). These individual patterns are important to consider when reconstructing the evolutionary history of subterranean animals and addressing the question of what has caused animals to enter subterranean environments. Finally, the presented data imply the frequent migration of terrestrial gastropod species between the interconnected light zones and the surface. This knowledge may shed light on the origin and importation of allochthonous resources in cave environments (Souza-Silva *et al.* 2012; Boch *et al.* 2013). Cave-penetrating gastropods as well as their progeny (incl. deposited egg clutches and the newly hatched juveniles) may end up as nutrients for the cave community.

ACKNOWLEDGEMENTS

I thank Stefan Zaenker and Dieter Weber for providing the data of their biospeleological collections, Klaus Bogon for his pictures of gastropods and Hannah Schweyen as well as Peter Trontelj for valuable discussions on the topic.

REFERENCES

Ansart, A., Vernon, P. & J. Daguzan, 2001: Freezing tolerance versus freezing susceptibility in the land snail *Helix aspersa* (Gastropoda: Helicidae).- CryoLetters, 22, 3, 193–190.

Biannic, M. & J. Daguzan, 1993: Cold-hardiness and freezing in the land snail *Helix aspersa* Müller (Gastropoda; Pulmonata).- Comparative Biochemistry and Physiology Part A: Physiology, 104, 3, 503–506.

Bichuette, M.E. & E. Trajano, 2003: Epigean and subterranean ichthyofauna from the São Domingos karst area, Upper Tocantins River basin, Central Brazil.- Journal of Fish Biology, 63, 5, 1100–1121.

Boch, S., Prati, D., Werth, S., Rüetschi, J. & M. Fischer, 2011: Lichen Endozoochory by Snails. PLoS ONE 6, 4, e18770.

Camp, C.D. & J.B. Jensen, 2007: Use of twilight zones of caves by plethodontid salamanders.- Copeia, 2007, 3, 594–604.

Cook, R.T., 2004: The tolerance of the field slug *Deroceras reticulatum* to freezing temperatures.- CryoLetters, 25, 3, 187–194.

Cooper, S.J.B., Bradbury, J.H., Saint, K.M., Leys, R., Austin, A.D. & W.F. Humphreys, 2007: Subterranean archipelago in the Australian arid zone: mitochondrial DNA phylogeography of amphipods from central Western Australia.- Molecular Ecology, 16, 7, 1533–1544.

Culver, D.C., Pipan, T. & K. Schneider, 2007: Vicariance, dispersal, and scale in the aquatic subterranean fauna of karst regions.- Freshwater Biology, 54, 4, 918–929.

Culver, D.C. & T. Pipan, 2009: *Biology of Caves and Other Subterranean Habitats*.- Oxford University Press, pp. 276, Oxford.

Daxl, R., 1967: Ein Beitrag zur Biologie von *Boettgerilla vermiformis* Wiktor, 1959.- Zeitschrift für angewandte Zoologie, 54, 227–231.

Fauna Europaea, 2012: Fauna Europaea version 2.5.- [Online] Available from: http://www.faunaeur.org [Accessed 3rd March 2013].

Getz, L.L., 1959: Notes on the Ecology of Slugs: *Arion circumscriptus*, *Deroceras reticulatum*, and *D. leave*.- American Midland Naturalist, 61, 2, 485–498.

Gunn, A., 1992: The ecology of the introduced slug *Boettgerilla pallens* (Simroth) in North Wales.- Journal of Molluscan Studies 58, 4, 449–453.

Hausdorf, B., 2002: Introduced land snails and slugs in Colombia.- Journal of Molluscan Studies 68, 2, 127–131.

Heller, J. & A. Dolev, 1994: Biology and population dynamics of a crevice-dwelling landsnail, *Cristataria genezarethana* (Clausiliidae).- Journal of Molluscan Studies, 60, 1, 33–46.

Howarth, F.G. & H. Hoch, 2005: Adaptive shifts. In: D.C. Culver & W.B. White, eds. Encyclopedia of caves, pp. 492–495. Elsevier/Academic Press, Amsterdam, The Netherlands.

Juan, C., Guzik, M.T., Jaume, D. & S.J.B. Coopers, 2010: Evolution in caves: Darwin's 'wrecks of ancient life' in the molecular era.- Molecular Ecology, 19, 18, 3865–3880.

Leys, R., Watts, C.H.S., Cooper, S.J.B. & W.F. Humphreys, 2003: Evolution of subterranean diving beetles (Coleoptera: Dytiscidae: Hydroporini, Bidessini) in the arid zone of Australia.- Evolution, 57, 12, 2819–2834.

Moreno-Rueda, G. 2007: Refuge selection by two sympatric species of arid-dwelling land snails: Different adaptive strategies to achieve the same objective.- Journal of Arid Environments, 68, 4, 588–598.

Pipan, T., López, H., Oromí, P., Polak, S. & D.C. Culver, 2011: Temperature variation and the presence of troglobionts in terrestrial shallow subterranean habitats.- Journal of Natural History, 45, 3–4, 253–273.

Poulson, T.L. & W.B. White, 1969: The cave environment.- Science, 165, 3897, 971–981.

Protas, M. & W.R. Jeffery, 2012: Evolution and development in cave animals: from fish to crustaceans.- Wiley Interdisciplinary Reviews: Developmental Biology, 1, 6, 823–845.

Régnier, C., Fontaine, B. & P. Bouchet, 2009: Not Knowing, Not Recording, Not Listing: Numerous Unnoticed Mollusk Extinctions.- Conservation Biology, 23, 5, 1214–1221.

Reise, H., Hutchinson, J.M.C., Forsyth, R.F. & T. Forsyth, 2000: The ecology and spread of the terrestrial slug *Boettgerilla pallens* in Europe with reference to its recent discovery in North America.- The Veliger, 43, 4, 313–318.

Reiss, M., Zaenker, S. & H. Steiner, 2009a: The biospeleological register of the Hesse Federation for Cave and Karst Research (Germany).- Cave and Karst Science, 35, 1, 25–34.

Reiss, M., Zaenker, S. & G. Stein, 2009b: Höhlen als Lebensräume in Hessen – Erfassung, Bewertung und Schutz subterraner Ökosysteme.- Naturschutz und Landschaftsplanung, 41, 6, 165–172.

Renker, C., Weber, D. & A. Pohl, 2012: Gastropods of caves in the Grand Duchy of Luxembourg.- *American Malacological Society 78th Annual Meeting*. 16.–21.6.2012, Cherry Hill, New Jersey.

Renker, C., Weber, D. & A. Pohl, 2013: Schnecken (Mollusca, Gastropoda) aus Höhlen des Großherzogtums Luxemburg.- Ferrantia, 69, 96–107.

Sexton, J.P., McIntyre, P.J., Angert, A.L. & K.J. Rice, 2009: Evolution and Ecology of Species Range Limits.- Annual Review of Ecology, Evolution, and Systematics, 40, 415–436.

Sket, B., 2008: Can we agree on an ecological classification of subterranean animals?- Journal of Natural History, 42, 21–22, 1549–1563.

Souza-Silva, M., Ferreira de Oliveira Bernardi, L., Parentoni Martins, R. & R. Lopes Ferreira, 2012: Transport and consumption of organic detritus in a neotropical limestone cave.- Acta Carsologica, 41, 1, 139–150.

Vergeer, P. & W.E. Kunin, 2013: Adaptation at range margins: common garden trials and the performance of *Arabidopsis lyrata* across its northwestern European range.- New Phytologist, 197, 3, 989–1001.

Von Proschwitz, T., 1994: *Oxychilus cellarius* (Müller) and *Oxychilus draparnaudi* (Beck) as predators on egg-clutches of *Arion lusitanicus* Mabille.- Journal of Conchology, 35, 183–184.

Weber, D. 2012: Die Höhlenfauna und -flora des Höhlenkatastergebietes Rheinland-Pfalz/Saarland, 5. Teil.- Abhandlungen zur Karst- und Höhlenkunde, 36, 1–2367.

Weigand, A.M., Jochum, A., Slapnik, R., Schnitzler, J., Zarza, E. & A. Klussmann-Kolb, 2013: Evolution of Microgastropods (Ellobioidea, Carychiidae): Integrating taxonomic, phylogenetic and evolutionary hypotheses.- BMC Evolutionary Biology, 13, 18.

Welter-Schultes, F.W., 2012: *European non-marine molluscs, a guide for species identification*.- Planet Poster Editions, pp. 760, Göttingen.

Zaenker, S., 2008: Das Biospeläologische Kataster von Hessen.- Abhandlungen zur Karst- und Höhlenkunde, 32, updated till 12.04.2008.

COBISS: 1.01

SPECIES DIVERSITY OF BRYOPHYTES AND FERNS OF LAMPENFLORA IN GROTTA GIGANTE (NE ITALY)

VRSTNA RAZNOLIKOST MAHOV IN PRAPROTI LAMPENFLORE V VELIKI JAMI V BRIŠČIKIH (SV ITALIJA)

Miris CASTELLO[1]

Abstract UDC 582.3:551.442(450.361)

Miris Castello: Species diversity of Bryophytes and ferns of lampenflora in Grotta Gigante (NE Italy)

Lampenflora consists of phototrophic organisms which grow near artificial light. In caves with artificial lighting, a vegetation of aerophytic cyanobacteria and algae, bryophytes and ferns can be found around lamps; these communities represent an alteration of the underground environment and may cause damages both to speleothems and cave fauna. The development of lampenflora is a typical problem for show cave management. A floristic research of bryophytes and ferns (land plants) of lampenflora was carried out in 2012 in Grotta Gigante, a very well-known show cave of the Trieste Karst (NE Italy), in order to compile a species inventory. 26 sites near artificial lights of different kinds were sampled in the dark zone of the show cave. 16 moss species and 2 ferns were found; no liverworts were observed. The most common species are the mosses *Eucladium verticillatum, Fissidens bryoides, Oxyrrhynchium schleicheri, Rhynchostegiella tenella* and the fern *Asplenium trichomanes*; 7 moss species were found only in one to two sites. Some moss species belong to the flora of natural cave entrances of the Italian Karst, while other are typical of disturbed, open habitats. Various moss species and *A. trichomanes* are colonizing areas around LEDs and fluorescent lamps installed in 2009 along the cave's pathways for safety lighting. Species richness of bryophytes and ferns of lampenflora in Grotta Gigante is the highest compared to other recently investigated show caves in the neighbouring Slovenia. Lampenflora of Grotta Gigante conforms to that found in other Slovenian show caves studied starting from the '40. The main ecological factors affecting lampenflora identified in this work are: light intensity, water availability, type of substrate, morphological features of surfaces, presence of clay. Aspects of species ecology and distribution in the cave are discussed.

Keywords: bryophytes, ferns, lampenflora, show caves, Grotta Gigante, Italy.

Izvleček UDK 582.3:551.442(450.361)

Miris Castello: Vrstna raznolikost mahov in praproti lampenflore v Veliki jami v Briščikih (SV Italija)

Lampenfloro sestavljajo fototrofni organizmi, ki rastejo v bližini umetne svetlobe. V jamah z umetno razsvetljavo lahko okoli luči najdemo različno vegetacijo, od aerotrofnih cianobakterij in alg do mahov in praproti. Te skupnosti predstavljajo spremembo podzemnega okolja in lahko povzročijo poškodbe kapnikov in jamske favne. Razvoj lampenflore je tipičen problem pri upravljanju jam. Leta 2012 so bile izvedene floristične raziskave mahov in praproti (kopenske rastline) v Veliki jami v Briščikih, znani turistični jami Tržaškega Krasa v SV Italiji, da bi ugotovili vrstno raznolikost lampenflore. V temnem delu turistične jame je bilo vzorčevanih 26 lokacij v bližini različnih vrst umetnih luči. Najdenih je bilo 16 vrst mahu in dve vrsti praproti, medtem ko ni bilo opaženih nobenih jetrenjakov. Najbolj pogosti so mahovi *Eucladium verticillatum, Fissidens bryoides, Oxyrrhynchium schleicheri, Rhynchostegiella tenella* in praprot *Asplenium trichomanes.* Sedem vrst mahov je bilo najdenih le na dveh lokacijah. Nekatere vrste mahov pripadajo rastlinstvo naravnih jamskih vhodov na Italijanskem Krasu, medtem ko so druge značilne za površinske habitate. Različne vrste mahov in *A. trichomanes* naseljujejo območja okrog LED in fluorescentnih svetilk, v letu 2009 nameščenih ob jamskih poteh za varnostno razsvetljavo. Biodiverziteta mahov in praproti lampenflore v Veliki jami v Briščikih je najvišja v primerjavi z lampenfloro v drugih nedavno raziskanih turističnih jamamah v sosednji Sloveniji. Lampenflora iz Veliki jami v Briščikih ustreza tisti, najdeni v drugih slovenskih turističnih jamah, katerih proučevanja segajo v 40. Leta prejšnjega stoletja. Glavni ekološki dejavniki, ki vplivajo na lampenflora, opredeljenih v tem delu so: jakost svetlobe, razpoložljivost vode, vrsta podlage, morfološke značilnosti površin, prisotnost gline. Delo obravnava tudi različne vidike ekologije vrst in distribucijo v jami.

Ključne besede: mahovi, praproti, lampenflora, turistične jame, Veliki jami v Briščikih, Italija.

[1] Department of Life Sciences, University of Trieste, via Giorgieri 10, I-34127 Trieste, Italy, e-mail: castello@units.it,

Received/Prejeto: 15.02.2013

INTRODUCTION

The presence of phototrophic organisms in caves depends on the availability of light, essential for the photosynthetic process. In wild caves, aerophytic algae and land plants are naturally limited to the entrance parts, where there is at least some sunlight, while they can't grow in the dark, inner parts. In natural caves opened to the public and in artificial caves, the electrical lighting enables phototrophic organisms to grow in the underground: lit areas around lamps are colonized by cyanobacteria and algae, bryophytes, ferns, and exceptionally shoots of seed plants. They constitute what is called "lampenflora" (Dobàt 1963, 1998; Mulec 2012) or lamp flora, which includes all phototrophic organisms growing near artificial light sources in areas where they do not naturally occur because of the absence of sunlight.

These communities represent an alteration of the delicate cave environment and may cause damages both to speleothems and cave fauna.

Organisms of lampenflora influence lithogenic and litholitic processes. Biodeterioration of stony substrata caused by lampenflora is related to different, complex mechanisms involving the whole community of lit areas, both autotrophs and heterotrophs such as bacteria and fungi. Main mechanisms of biodeterioration of cave surfaces are: biofilm formation, colour changes and development of coloured patches, release of weak organic acids which in time can corrode limestone and formations, absorption of some chemicals from the substrate, proton–cation exchange, carbon dioxide and oxygen fluxes due to photosynthesis, respiration or fermentation, pH changes (acid or alkaline reactions), the possible formation of an amorphous mix of dead organisms and calcium carbonate which may alter substrate surfaces (e.g. Warscheid & Braams 2000; Mulec 2012).

Natural cave ecosystems are characterized by low levels of nutrients (Simon *et al.* 2007). The growth of primary producers provides an unnatural input of biomass, which is a source of nutrients available for both true cave-dwellers and occasional dwellers. Lampenflora may represent a threat to obligated cave-dwellers (troglobites), facilitating the proliferation of external opportunistic species which may compete with them and drive them to extinction (Mulec & Kosi 2009; Mulec 2012).

Different mechanical, physical and chemical methods to control lampenflora growth have been proposed; discussions and reviews can be found in Johnson (1980), Olson (2006), Mulec and Kosi (2009) and Mulec (2011, 2012).

A key aspect to limit lampenflora growth is represented by lighting design. Main guidelines for show cave management to control lampenflora by adequate lighting are available in the literature (Olson 2006; Mulec & Kosi 2009; Cigna 2012; Mulec 2012). According to them, great attention should be paid to type and power of lights and positioning of lamps, which should be installed at appropriate selected sites, at a distance from cave surfaces. Lighting time should be minimized, by switching lights on only when visitors are nearby. Lamp emission spectra should be poor in the wavelengths that are most effective for photosynthesis: in various caves, yellow-light or green-light were shown to prevent or limit lampenflora growth, although they may have an unaestethic effect in cave lighting. LEDs seem to represent an effective solution for cave lighting as they feature low power consumption, long life and selected narrow emission spectra.

Show caves are provided with artificial lighting systems to attract visitors and to ensure public access and safety, of both the visitors and the staff. The control of lampenflora is a typical problem for show cave management: besides the alteration of the underground environment, the unwanted growth of lampenflora causes the development of more or less wide unaesthetic coloured patches on speleothems, walls and other parts of the cave illuminated by sufficient light.

A well-known show cave of Italy is Grotta Gigante, a very large cave which opens in the Trieste Karst. Grotta Gigante has a long tradition as a tourist cave, being opened to the public in 1908, when carbide lamps and candles were used for illumination. The first electrical lighting system was installed in 1957 and completely replaced in 2009 by a new one in accordance with laws, safety and environmental protection measures. The new lighting system consists of floodlights of different power and colour temperature to light the cave, speleothems and other objects; an emergency and safety lighting system consisting of LED lights and fluorescent lamps was installed along cave's pathways. A set of UVC germicidal lamps, provided with the 2008 Green certificate, was installed in different parts of the cave to inhibit the development of lampenflora (Fabbricatore 2011); their effects are under investigation. No methods to control lampenflora growth were used in the past in the cave (A. Fabbricatore, Director of Grotta Gigante, pers. comm.).

Few published studies are available on the flora and vegetation of the cave. Bussani (1966) reported information on some species of cyanobacteria. Polli and Sguazzin (1998) surveyed the vascular plants and the bryophytes of the entrances and the inner part of Grotta Gigante, providing accurate notes on the distribution of lampenflora throughout the cave; 1 fern and 4 moss species were reported in this work around lamps in the inner part of the cave.

The present paper reports the results of a floristic study of the bryophytes and ferns (land plants) of lampen-

flora of Grotta Gigante. The main aims of the work are: a) to investigate bryophyte and fern diversity of lampenflora of the cave and compile a species inventory; b) to provide basic knowledge to monitor and control lampenflora growth in Grotta Gigante.

STUDY AREA

Grotta Gigante is situated in the Trieste Karst, in the municipality of Sgonico (NE Italy). The cave opens into ultrapure Cretaceous limestones at 274 m a.s.l. It consists of a large chamber (167.6 m long, 98.5 m high, 76.3 m wide) which may be accessed through two galleries; it reaches a maximum depth of 252 m referred to the entrance level (Fig. 1). Inside the cave, temperature is 11 °C and relative humidity is 98%.

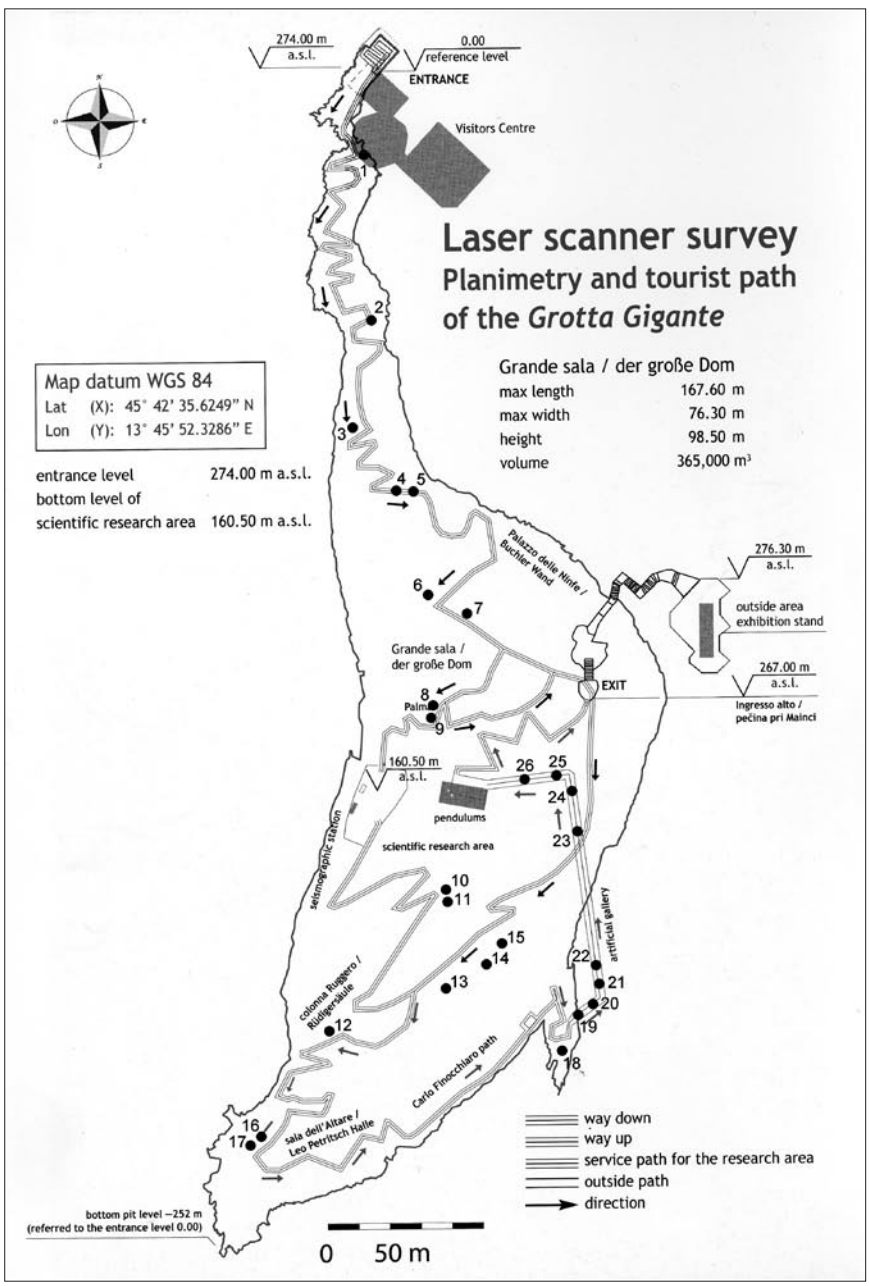

The lighting system installed in 2009 consists of metal halide and discharge lamp floodlights of different power (from 20W to 250W) and colour temperature (2,800 K and 3,000 K) to illuminate the cave interior and formations. The emergency and safety lighting system fitted along cave's pathways consists of 3W LED lights and 14W warm white fluorescent lamps. A set of UVC germicidal lamps (with 2008 Green certificate) was installed in different parts of the cave to control lampenflora growth; they are switched on every day during closing hours (Fabbricatore 2011).

The cave is open year round, with 7 daily hours of lighting (42 average hours/week) from October to March and 9 daily hours of lighting (57 average hours /week) from April to September. Annual illumination of the show cave is c. 2,580 hours. The average annual number of visitors over the last 30 years is 80,000, with peaks of 100,000.

Fig. 1: Map of the study area with location of sampling sites. Map courtesy of Grotta Gigante S.A.G. (Società Alpina delle Giulie); laser scanner survey and graphic processing by O.G.S. (National Institute for Oceanography and Applied Geophysics).

MATERIALS AND METHODS

Sampling was carried out in the dark part of the cave from January to July 2012. Bryophytes and ferns were surveyed near lights of different kind (floodlights, LEDs, fluorescent lamps) in microhabitats related to different ecological conditions: type of substrate, inclination, light intensity, water availability (Figs. 2, 3, 4 & 5). In order to get a comprehensive study of floristic diversity, all safely reachable lit areas with bryophyte and fern cover of speleothems, other cave surfaces and clastic deposits were investigated. As for LEDs and fluorescent lamps along the pathways, all betwen largest vegetated patches found in the different environmental conditions and those spots with species not yet recorded for a particular microhabitat were sampled. Each sampled lamp corresponds to a sampling site, in which one or more relevés were carried out, depending on the variability of ecological conditions occurring at the lamps (e.g. different types or inclination of substrate present at a same lamp, different distance from lamps). 26 sites were sampled in the show cave (Fig. 1, Tab. 1), for a total of 50 relevés of species.

Tab. 1: Number of sampling sites grouped by main type of lights and substrate. Each site corresponds to a lamp, but it may include one or more types of substrate colonized by lampenflora. For light, F: floodlights; FL: fluorescent lamps; LE: LEDs.

Substrate	***Light***		
	F	***FL***	***LE***
Speleothems	10		
Main stalagmites	2		
Rock walls	3	8	
Clastic sediments, highly degraded rock (debris slopes)	5		
Clay (also as thin layer on solid surfaces)	6		
Concrete	1		3

Identification was performed in the field and in the laboratory. For the study of bryophytes, in the laboratory general morphological characters were observed using a stereomicroscope and anatomical characters were studied by light microscopy on hand-cut sections mounted in water. Identification and ecological features of bryophytes were based on Cortini Pedrotti (2001, 2005), Smith (2004) and Atherton *et al.* (2010). Nomenclature of bryophytes follows Aleffi *et al.* (2008). Collected specimens are deposited at the University of Trieste Herbarium (TSB).

RESULTS AND DISCUSSION

A total of 16 moss species (9 acrocarps and 7 pleurocarps) and 2 ferns were found around the lamps in the cave; no liverworts were observed (Tab. 2). Seed plants were not noticed inside the cave. The comparison with 8 show caves and 2 mines equipped with electric illumination of the neighbouring Slovenia investigated in recent years by Mulec and Kubešová (2010) shows that, at present, Grotta Gigante hosts the highest number of species (18); in the most species-rich site of Slovenia, Mežica lead and zinc mine, in areas lit 24 hours/day and with an annual illumination of 8,760 hours/sector, 16 taxa were found (Mulec & Kubešová 2010). The high species diversity of Grotta Gigante may be explained by two main factors: a) high annual illumination hours (c. 2,580), which is a rather high value compared to those of the show caves and mines investigated by Mulec and Kubešová (2010), all below 500 hours/sector with the exception of Mežica lead and zinc mine (8,760) and Postojnska jama (1,000); b) absence of interventions to remove or control lampenflora in the past.

The composition of lampenflora of Grotta Gigante agrees with that found in other Slovenian artificially lit caves and mines investigated starting from the ’40 (Mulec & Kubešová 2010). This confirms a substantial homogeneity of lampenflora of caves in the same geographical area.

The most common and widespread mosses found in Grotta Gigante, occurring in more than 50% of sites, are *Eucladium verticillatum, Fissidens bryoides, Oxyrrhynchium schleicheri* and *Rhynchostegiella tenella;* 7 moss species are rare, being found only in 1 to 2 sampling sites (Tab. 2).

Some mosses are known for the flora of wild cave entrances of the Italian Karst (e.g. Polli & Sguazzin 2002; Sguazzin 2011; Castello & Strazzaboschi 2013) or favour moist and sheltered places, such as *Eucladium verticillatum, Rhynchostegiella tenella*, *Orthothecium intricatum, Oxyrrhynchium schleicheri*. Other mosses are typical of disturbed or open to slightly sheltered habitats, such as *Barbula unguiculata*, *Funaria hygrometrica*, *Tortula muralis*. Almost all mosses are sterile, but *F. hygrometrica* was often found with well-developed sporophytes, and few sporophytes of *R. tenella* were observed at one site.

Tab. 2: Synthetic table of results of the floristic survey of lampenflora bryophytes and ferns in Grotta Gigante. Species list, number and frequency of occurrence in sites and relevés, main type of lights and substrate. For light, F: floodlights; FL: fluorescent lamps; LE: LEDs. For substrate, S: speleothems; MS: main stalagmites; W: rock walls; CS: clastic sediments and highly degraded rock (landslides); CL: clay (also as thin layer on solid surfaces); CO: concrete along pathways.

Species	Occurrence				Light			Substrate					
	Sites		Relevés										
	No.	%	No.	%	F	FL	LE	S	MS	W	CS	CL	CO
BRYOPHYTES: MOSSES													
Amblystegium serpens (Hedw.) Schimp.	1	4	2	4	x			x				x	
Barbula unguiculata Hedw.	4	15	4	8	x			x			x	x	
Bryum sp.	6	23	8	16	x	x	x	x		x		x	x
Didymodon vinealis (Brid.) R.H. Zander	3	12	3	6	x	x		x		x			x
Eucladium verticillatum (With.) Bruch & Schimp. var. verticillatum	23	88	43	86	x	x	x	x	x	x	x	x	x
Fissidens bryoides Hedw. var. *bryoides*	14	54	24	48	x	x	x	x		x	x	x	x
Funaria hygrometrica Hedw.	4	15	6	12	x			x			x	x	
Hygroamblystegium varium (Hedw.) Mönk.	2	8	2	4	x			x				x	
Orthothecium intricatum (Hartm.) Schimp.	1	4	1	2	x			x					
Oxyrrhynchium pumilum (Wilson) Loeske	1	4	1	2	x			x				x	
Oxyrrhynchium schleicheri (R. Hedw.) Röll.	14	54	22	44	x	x	x	x		x		x	x
Ptychostomum pallens (Sw.) J.R. Spence	1	4	1	2	x			x					
Rhynchostegiella tenella (Dicks.) Limpr. var. tenella	15	58	24	48	x	x		x		x	x	x	x
Rhynchostegium murale (Hedw.) Schimp.	1	4	1	2	x			x					
Tortula muralis Hedw.	4	15	4	8	x	x		x		x		x	
Weissia sp.	1	4	1	2	x			x				x	
FERNS													
fern prothallus	6	23	8	16	x	x		x		x	x	x	
Asplenium trichomanes L.	12	46	19	38	x	x	x	x		x	x	x	x
Asplenium scolopendrium L. subsp. *scolopendrium*	1	4	1	2	x			x					

As for ferns, *Asplenium trichomanes* is common throughout the cave; small plants are usually found around lamps, but well-developed individuals occur in highly lit sites wet by continuous dripping water. *Asplenium scolopendrium* in development in one site is a new record for the inner part of the cave. According to Polli and Sguazzin (1998), the species, which has been decreasing and disappearing from many Karst caves in the past decades probably due to climatic changes, grew in the past at the cave's entrance but it went extinct some decades ago. These authors did not observe the species inside the cave. A few plants were later re-introduced in the outer part of the cave near the exit (archive of Grotta Gigante), where they are still present.

Fig. 2: A well developed lampenflora community dominated by mosses in Grotta Gigante.

The most common species inside the cave is the moss *Eucladium verticillatum*, which occurs in 88% of sites and 86% of relevés (Tab. 2). This is one of the most important tufa-forming mosses; it promotes calcium carbonate deposition and lower parts of stems are often encrusted with calcium carbonate (Glime 2007; Atherton *et al.* 2010). In Grotta Gigante this moss favours moist surfaces of different kind; it was collected over a wide range of substrates and light intensities, from very well lit to deep shaded areas around the lamps, as found by Mulec and Kubešová (2010) in show caves of Slovenia.

All moss and fern species reported in the previous study of lampenflora by Polli and Sguazzin (1998) (*Amblystegium serpens*, *Bryum* sp., *Eucladium verticillatum*, *Fissidens bryoides* and the fern *Asplenium trichomanes*) were found in this survey.

As for main ecological factors influencing lampenflora in the cave, no particular zonation of bryophyte and fern vegetation was observed along decreasing light gradient around lights, as found by Mulec *et al.* (2008) for aerophytic algal communities in Slovenian caves. Various mosses and *Asplenium trichomanes* were observed growing over a relatively wide range of light intensity, in accordance with the findings by Mulec and Kubešová (2010). The poorly lit, most distant areas from lamps are characterized by the constant occurrence of *Eucladium verticillatum*; sometimes some reduced plants of *A. trichomanes* are present there as well.

Fig. 3: Small mosses around LED lamps installed along the pathways in 2009.

The influence of the main types of lights (floodlights, LEDs and fluorescent lamps) on species occurrence could not be fully assessed, as lamps of different type are positioned in different ecological conditions. LEDs were installed in 2009 as step lights for pathways and stairs and they lit mainly concrete areas (Fig. 3); fluorescent lamps were fitted in 2009 at the base of the rock walls of an artificial gallery (Fig. 4); floodlights are positioned on various cave formations and substrata in areas illuminated at different starting times. LEDs and fluorescent lamps were all installed in 2009 in new positions, therefore investigated sites around them correspond to the first stages of ecological succession. All species observed around LEDs and fluorescent lamps were found near the other lights (Tab. 2); this shows that in Grotta Gigante at least a set of species are not affected by types of lights. The reduced number of species found near LEDs and fluorescent lamps compared to floodlights could be influenced by different light features, but also simply by the shorter time available for community development. However, it is evident that in areas lit by LEDs lampenflora growth is limited both in number of species and biomass in comparison to fluorescent lamps.

Substrate type seems to play a minor ecological role for some species, such as *Eucladium verticillatum* and *Asplenium trichomanes*, but it influences the occurrence of others. *Tortula muralis*, for instance, was mainly found on the rock walls of the artificial gallery. The permanently wet, lit surfaces of cave speleothems are dominated by *E. verticillatum* and avoided by other mosses: lit parts of the main stalagmites of the show cave, the "Palma" and the "Colonna Ruggero", are colonized by patches of this species. *Fissidens bryoides* thrives on clay, even if present as a thin layer on rocks and formations. Clay influences both moisture and mineral nutrient content of the substrate, promoting plant growth: in Grotta Gigante surfaces with clay support the growth of extensive patches of mosses, up to c. 4 m^2 wide (Fig. 5), as reported in the literature (e.g. Johnson 1980).

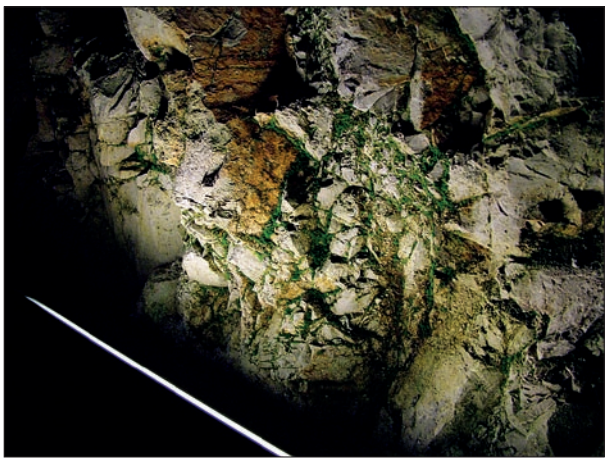

Fig. 4: Lampenflora colonizing the wet walls of an artificial tunnel around fluorescent lamps fitted in 2009.

Surface morphology is a relevant ecological factor for species growth. Surface topography and roughness, and porosity of the substrate strongly influence bioreceptivity of materials. They influence water and nutrients availability for organisms; furthermore, they affect the settlement of spores, cells and vegetative propagules and the attachment of the plants (e.g. Warscheid & Braams 2000; Mulec 2012). This was also observed for substrata of Grotta Gigante: surface irregularities, rough or porous materials promote the colonization by organisms and the proliferation of dense patches of lampenflora, and affect its distribution near the lamps.

The survey of safety lights installed along the pathways in 2009 shows that a colonizing process is in act, involving microalgae, which are typical pioneer species in lampenflora ecological succession, but also mosses

and ferns, which usually appear in later stages (Mulec & Kubešová 2010). Near various LED lamps installed along the steps of the downwards pathway, green patches of microalgae were found, but near some LEDs small, very scattered individuals of *Bryum* sp., *Eucladium verticillatum, Fissidens bryoides, Oxyrrhynchium schleicheri,* sometimes accompanied by single small shoots of *Asplenium trichomanes* were observed, extending up to a distance of 15 cm from the lights (Tab. 2, Fig. 3). In the artificial tunnel along the Carlo Finocchiaro path, opened to the public in 1996, lampenflora is colonizing the moist calcareous walls around almost all the fluorescent lamps, with *Bryum* sp., *Didymodon vinealis*, *Eucladium verticillatum*, *Fissidens bryoides*, *Oxyrrhynchium schleicheri*, *Rhynchostegiella tenella*, *Tortula muralis* and small plants of *A. trichomanes*, forming large patches extended up to c. 60 cm from the lights (Tab. 2, Fig. 4). Previous work by Polli and Sguazzin (1998) confirms the ongoing colonizing process: along the steps of the downwards staircase mosses or ferns were not observed by these authors, while in the artificial gallery a reduced zone with mosses was noticed around just one single lamp.

Fig. 5: Clastic deposits and clay promote the growth of large patches of mosses.

The present study provides further evidence that established lampenflora is able to survive for long periods of darkness, as reported in the literature (e.g. Johnston 1980; Eliot 2006; Mulec & Kosi 2009; Mulec 2011; Cigna 2011). Shortly before the survey, a lamp failed leaving the surrounding area completely dark and it was replaced after c. 7 months; the site was investigated two months later. Mosses did not show particular damages; many patches of calcified filamentous cyanobacteria, several prothalli and small shoots of *Asplenium trichomanes* were observed. The ability to withstand long periods of darkness may be linked to particular physiological features of plants of lampenflora, which are mainly shade-adapted, stress-tolerant organisms, able to survive under adverse environmental conditions even over long periods. Control of lampenflora growth based on periodical closing of show caves lasting some weeks or months to reduce lighting time is likely to have no particular advantage, as prolonged periods without illumination do not seem to reduce established lampenflora, may favour the development of some organisms as cyanobacteria, and may be very problematic for the economic management of show caves (see also Mulec & Kosi 2009; Cigna 2011).

CONCLUSIONS

In the inner part of Grotta Gigante 16 mosses and 2 ferns were found around the artificial lights, for a total of 18 land plants. Species richness of the cave is the highest compared to other recently investigated show caves and mines of the neighbouring Slovenia (Mulec & Kubešová 2010). Only some species are common throughout the cave, while many other occur in one or few sites. The high number of species found in the cave may be mainly explained by the light regime, with a rather high number of annual lighting hours (c. 2,500 hours/year) and by the absence of interventions to remove lampenflora in the past. The moss *Eucladium verticillatum* is the most common and abundant species in the cave; it favours wet rock surfaces and it shows a remarkable ecological plasticity, being able to grow over a wide range of substrates and light intensities.

The main ecological factors affecting lampenflora in Grotta Gigante identified in this work, and corresponding to the results of studies from other caves, are: light intensity, water availability, type of substrate, morphological features of surfaces, presence of clay.

Observations on the distribution of bryophytes and ferns in Grotta Gigante support many guidelines recommended in the literature to control lampenflora growth. In particular, light installation should be avoided or limited on damp and moist surfaces, as simultaneous availability of water and light greatly promotes lampenflora growth. Similarly, areas with mud or clay should not be directly lit.

An environmentally sustainable strategy to control lampenflora growth should mainly rely on an ecological approach based on minimizing the energy input of arti-

ficial lighting in the underground ecosystems. Cleaning methods are able to control lampenflora only for short periods and may have negative effects on other cave organisms, speleothems and on the staff and visitors as well: if artificial lighting is kept, lampenflora will reappear, as propagules are constantly present inside a cave (Mulec 2012). Lampenflora can be ecologically controlled in the long term by limiting light eutrophication of caves, which promotes the growth of phototrophs. This may be achieved by an adeguate cave lighting design and regime, thoughtfully planned to reduce intensity and duration of illumination and with particular attention to type, power and installation sites of lights (e.g. Olson 2006; Mulec & Kosi 2009; Cigna 2012; Mulec 2011, 2012). The development of microalgae, mosses and small ferns around LEDs in a few years time observed in Grotta Gigante highlights that LED lighting is not sufficient by itself to prevent lampenflora growth: in any case, great attention must be paid to intensity and emission spectrum of LED lights. This ecologically-based approach to control lampenflora could reduce the frequency and the costs of cleaning interventions, resulting advantageous for both the environment and the economic management of a show cave.

Thanks to the long history as a show cave, the absence of interventions to control lampenflora in the past and the possibility to date new installation of several lamps, Grotta Gigante represents an interesting case study for research on lampenflora.

ACKNOWLEDGEMENTS

The author would like to thank Michele Codogno and Andrea Nardini (University of Trieste) for valuable discussions and suggestions, Salvatore Branca and Luca Strazzaboschi for their help in field work. Special thanks go to the director of Grotta Gigante, Alessio Fabbricatore, and to the staff of the cave for their kind support and collaboration. The research was carried out within a collaboration framework between Grotta Gigante S.A.G. and the University of Trieste.

REFERENCES

Aleffi, M., Tacchi, R. & C. Cortini Pedrotti, 2008: Checklist of the Hornworts, Liverworts and Mosses of Italy.- Bocconea, 22, 1–256.

Atherton, I., Bosanquet, S. & M. Lawley (eds.), 2010: *Mosses and Liverworts of Britain and Ireland. A field gui*de.- British Bryological Society, Latimer Trend & Co., pp. 848, Plymouth.

Bussani, M., 1966: Le Cianoficee nelle cavità carsiche.- Atti e Memorie Commissione Grotte "E. Boegan", 5 (1965), 107–109.

Castello, M. & L. Strazzaboschi, 2013: Le briofite della Grotta dell'Orso (33-7VG, Carso Triestino, NE Italia).- Atti e Memorie Commissione Grotte "E. Boegan", 44, 55–71.

Cigna, A.A., 2011: The problem of lampenflora in show caves.- In: Bella, P. & P. Gažík (eds.) *ISCA 6th Congress Proceedings*, 18th–23rd October 2010, Demänovská Dolina, Liptovský Mikuláš, Slovakia. State Nature Conservancy of the Slovak Republic, Slovak Caves Administration, 201–205, Slovakia.

Cigna A.A., 2012: Show caves. In: White, W.B. & D.C. Culver (eds.) *Encyclopedia of Caves, Second Edition*. Academic Press, pp. 690–697, Chennai.

Cortini Pedrotti, C., 2001: *Flora dei muschi d'Italia. Sphagnopsida, Andreaeopsida, Bryopsida (I parte).*- Antonio Delfino Editore, pp. 832, Roma.

Cortini Pedrotti, C., 2005: *Flora dei muschi d'Italia. Bryopsida (II parte).*- Antonio Delfino Editore, pp. 432, Roma.

Dobàt, K., 1963: "Höhlenalgen" bedrohen die Eiszeitmalereien von Lascaux.- Die Höhle, Wien, 14, 2, 41–45.

Dobàt, K., 1998: Flore de la lumiére artificiélle (lampenflora-maladie verte).- In: Juberthie, C. & V. Decu (eds.) *Encyclopaedia biospeleologica*, Tome 2, Société de Biospéologie, 1325–1335, Moulis-Bucarest.

Elliott, W. R., 2006: Biological Dos and Don'ts of Cave Restoration and Conservation.- In: Hildreth-Werker, V. & J.C. Werker (eds.) *Cave Conservation and Restoration.* National Speleological Society, pp. 33–46, Huntsville, Alabama U.S.A.

Fabbricatore, A., 2011: The new electrical system of the Grotta Gigante: compliance with the laws in force and lighting study – The Grotta Gigante as a tourist and scientific centre.- In: Bella, P. & P. Gažík (eds.) *ISCA 6th Congress Proceedings*, 18th–23rd October 2010, Demänovská Dolina, Liptovský Mikuláš, Slovakia. State Nature Conservancy of the Slovak Republic, Slovak Caves Administration, 62–70, Slovakia.

Glime, J.M., 2007: Light: cave mosses.- In: *Bryophyte ecology, Volume 1, Physiological ecology*. Ebook sponsored by Michigan Technological University and the International Association of Bryologist.- [Online] Available from: http://www.bryoecol.mtu.edu/ [Accessed 10th September 2012].

Johnson, K., 1980: Control of lampenflora at Waitomo Caves, New Zealand.- In: Robinson A. C. (ed.) *Cave Management in Australia III: Proceedings of the third Australian Conference on cave tourism and management*, 30th April–4th May 1979, Mount Gambier, South Australia. National Parks and Wildlife Service, Adelaide and Australian Speleological Federation, 105–122, Adelaide.

Mulec, J., 2011: Lampenflora in show caves in Slovenia. - In: Prelovšek, M. & N. Zupan Hajna (eds.) *Pressures and Protection of the Underground Karst – Cases from Slovenia and Croatia*. Karst Research Institute ZRC SAZU, 64–73, Postojna.

Mulec, J., 2012: Lampenflora. In: White, W.B. & D.C. Culver (eds.) *Encyclopedia of Caves, Second Edition*. Academic Press, pp. 451–456, Chennai.

Mulec, J. & G. Kosi, 2009: Lampenflora algae and methods of growth control.- Journal of Cave and Karst Studies, 71, 2, 109–115.

Mulec, J. & S. Kubešová, 2010: Diversity of bryophytes in show caves in Slovenia and relation to light intensities.- Acta Carsologica, 39, 3, 587–596.

Mulec, J., Kosi, G. & D. Vrhovšek, 2008: Characterization of cave aerophytic algal communities and effects of irradiance levels on production of pigments.- Journal of Cave and Karst Studies, 70, 1, 3–12.

Olson, R., 2006: Control of lamp flora in developed caves.- In: Hildreth-Werker, V. & J.C. Werker (eds.) *Cave Conservation and Restoration*. National Speleological Society, pp. 343–348, Huntsville, Alabama U.S.A.

Polli, E. & F. Sguazzin, 1998: Aspetti vegetazionali della Grotta Gigante (2 VG): le piante vascolari ed il componente briologico. Atti e Memorie Commissione Grotte "E. Boegan", 35 (1997), 63–80.

Polli, E. & F. Sguazzin, 2002: Felci e briofite rinvenute in recenti esplorazioni speleobotaniche sul Carso triestino.- Pagine Botaniche, 27, 3–20.

Sguazzin, F., 2011: Check-list delle Briofite del Friuli Venezia Giulia (NE Italia).- Gortania, 32 (2010): 17–114.

Simon, K.S., Pipan, T. & D.C. Culver, 2007: A conceptual model of the flow and distribution of organic carbon in caves.- Journal of Cave and Karst Studies, 69, 2, 279–284.

Smith, A.J.E., 2004: *The Moss flora of Britain and Ireland*.- Cambridge University Press, pp. 1026, Cambridge.

Warscheid, Th. & J. Braams, 2000: Biodeterioration of stone: a review.- International Biodeterioration & Biodegradation, 46, 343–368.

COBISS: 1.01

LETTER:

CALCITE DISSOLUTION UNDER TURBULENT FLOW CONDITIONS: A REMAINING CONUNDRUM

PROBLEM NASTANKA FASET IN RAZTAPLJANJA KALCITA V TURBULENTNEM TOKU

Matthew D. COVINGTON[1]

UDK 551.435.8:549.742.111

INTRODUCTION

A significant body of experimental and theoretical work has examined the dissolution rates of calcite, and other carbonate minerals, under varying chemical and hydrodynamic conditions (see Morse & Arvidson (2002) for a comprehensive review). The relationships derived from this work have been applied extensively to the development of mechanistic models of speleogenesis (e.g. Dreybrodt 1996; Dreybrodt *et al.* 2005; Birk e*t al.* 2005; Rehrl *et al.* 2008; Kaufmann 2009; Szymczak & Ladd 2011). However, the primary focus of these models has been on the early stages of cave formation, with less attention toward the later stages of cave evolution and turbulent flow conditions. Recent efforts have begun to develop mechanistic models for processes governing later stages of cave evolution, considering factors such as turbulent flow structures (Hammer *et al.* 2011) and open channels (Perne 2012). However, such studies remain limited, in part due to significant quantitative uncertainties in a variety of processes that become important beyond the incipient speleogenesis stage (Covington *et al.* 2013).

While speleogenetic models have not typically been run much beyond the transition from laminar to turbulent flow conditions, experimental and theoretical studies of carbonate dissolution have constrained dissolution rates and rate-controlling mechanisms under turbulent flow (e.g. Rickard & Sjöberg 1983; Dreybrodt & Buhmann 1991; Liu & Dreybrodt 1997). However, a direct application of these results and comparison to field observations leads to an apparent conundrum. According to the theory, solutional forms such as scallops and flutes should not exist in limestone; however, they clearly do exist at a wide variety of sites and scales. This conundrum suggests that there may be problems with the theory, problems with our understanding of scallop formation, or both.

THE CONUNDRUM

Dissolution rates under turbulent flow conditions are typically calculated by dividing the fluid into two regions, a turbulent core that is well-mixed, and a diffusion boundary layer (DBL) that lies between the turbulent core and the dissolving wall (Dreybrodt & Buhmann 1991). Within the DBL, flow is presumed to be laminar and species cross the layer via the process of molecular diffusion. There are two end-member regimes in which overall dissolution rates are limited by either diffusion rates (the transport-limited regime),

[1] University of Arkansas Department of Geosciences Fayetteville, Arkansas, USA, e-mail: mcoving@uark.edu
Received/Prejeto: 26.11.2013

$$F_D = \frac{D(C_{eq}-C_b)}{\epsilon}, \quad (1)$$

or surface reaction rates (the reaction-limited regime),

$$F_s = k_1(1 - C_b/C_{eq}), \quad (2)$$

where F_D and F_s are the transport-, and reaction-limited fluxes, respectively, D is the diffusion constant, C_{eq} is the equilibrium concentration of calcium, C_b is the concentration of calcium in the bulk solution, ϵ is the DBL thickness, and k_1 is the kinetic rate constant for calcite dissolution in the linear kinetic regime. The mixed kinetic regime occurs when the diffusion-limited and surface-reaction-limited rates are similar (Rickard & Sjöberg 1983). In this case, both processes are important. For simplicity, I only consider linear dissolution kinetics

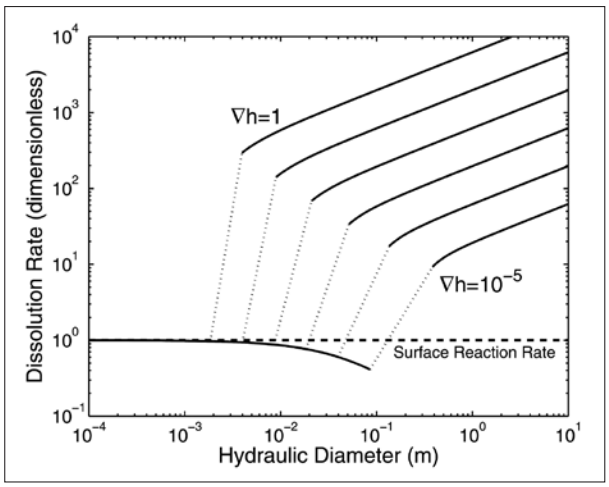

Fig. 1: Diffusional (solid) and surface reaction (dashed) dissolution rates as a function of hydraulic diameter, D_H, depicted for different hydraulic head gradients, ∇h. Sharp jumps in diffusion rates occur at the onset of turbulent flow. The laminar/turbulent transition is indicated with dotted lines. For the parameter space shown, the theory suggests that diffusional rates only control dissolution for low-gradient conduits just below the laminar/turbulent transition. Elsewhere, diffusional rates are much higher than surface reaction rates. Figure reproduced with permission from Covington et al. (2012).

here, as is common below about 80% saturation, though our conclusions are not sensitive to this choice. In the case of a sufficiently thick DBL, or a sufficiently thin turbulent core, conversion of CO_2 can also be rate-limiting (Dreybrodt & Buhmann 1991). Though non-linear kinetics and CO_2 conversion limitation are not explicitly considered here, if anything, they would exacerbate the presented conundrum by providing further means to reduce surface reaction rates.

In order to determine the typical conditions under which rates were limited by either reaction or transport, Covington *et al.* (2012) calculated surface reaction and diffusion rates for a wide variety of head gradients and hydraulic diameters using the Darcy-Weisbach equation and Colebrook-White relation. For these calculations, the fiducial parameter values given in Dreybrodt *et al.* (2005) were used, with $k_1 = 4 \times 10^{-11}$ mol cm^{-2} s^{-1}, $D = 10^{-5}$ cm^2 s^{-1}, and $C_{eq} = 2 \times 10^{-6}$ mol cm^{-3}. For ease of comparison, Covington *et al.* (2012) converted the "surface" rate law to the form

$$F_s = \alpha_s(C_{eq} - C), \quad (3)$$

where $\alpha_s = 2 \times 10^{-5}$ cm s^{-1} was determined by dividing k1 by C_{eq}. Here I have slightly modified the notation of Covington *et al.* (2012), replacing α with α_s to clarify that the constant applies to the chemical reaction rate at the surface. In many previous manuscripts (e.g. Buhmann & Dreybrodt 1985) α without a subscript represents the combined effects of diffusion and reaction.

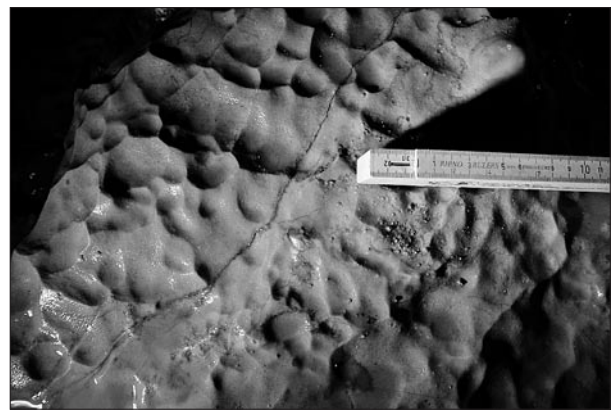

Fig. 2: Scallops formed on a limestone surface within a cave, indicating contrasts in dissolution rates as a result of turbulent flow structures. Major divisions on the ruler are in cm (Photo: Matija Perne).

Covington *et al.* (2012) compared the rates predicted by Equations 1 and 3 by nondimensionalizing the two equations by dividing by the term $\alpha_s(C_{eq} - C)$, such that the dimensionless dissolution rates are independent of chemistry and become

$$F_s^* = 1, \quad (4)$$

and

$$F_D^* = \frac{D}{\alpha_s \epsilon}, \quad (5)$$

where the stars denote dimensionless rates. Then ϵ was calculated for a wide variety of head gradients and hydraulic diameters to examine the relative magnitude of the reaction-and transport-limited equations. The DBL thickness was calculated using equations 2.13 and 2.14 from Dreybrodt *et al.* (2005), which are equivalent to Equations 9 and 10 of this manuscript. For these calculations a fractional roughness of 0.05 was assumed. The results of this calculation (Fig. 1) show that, according to the equations used above, the surface reaction rate is almost always limiting, and no cases in the turbulent flow

regime show transport-limited rates. In fact, diffusion rates under turbulent flow are typically several orders of magnitude larger than the surface reaction rate. This conclusion leads to the conundrum. The model suggests that dissolution rates should almost always be controlled by the surface reaction rate in the turbulent flow regime, and, therefore, that dissolution rates should be independent of any spatial variations in DBL thickness. On the contrary, caves and channels formed in limestone frequently contain scallops (Fig. 2) and flutes that apparently form as the result of systematic contrasts in DBL thickness as a result of turbulent flow structures (Curl 1966; Goodchild & Ford 1971; Blumberg & Curl 1974; Curl 1974). The remainder of this note will explore this conundrum in more detail, and discuss possible resolutions.

SURFACE RATES FROM THE PWP EQUATION

The above analysis makes use of fiducial kinetic constants from Dreybrodt *et al.* (2005). However, these constants are motivated by typical values from experiments, where the effects of transport and reaction are both present. Therefore, a more accurate approach is to use the full Plummer-Wigley-Parkhurst (PWP) equation (Eqn. 6, Plummer *et al.* 1978) to calculate true theoretical surface rates. If the PWP rates were high enough, then they could explain away the conundrum.

For comparison, I calculate PWP rates that result from a temperature and partial pressure of CO_2 that approximately reproduce the fiducial value of $C_{eq} = 2 \times 10^{-6}$ mol cm^{-3} used above. This equilibrium concentration is roughly obtained (for an open system) with $T = 10$ °C and $P_{CO_2} = 0.01$ atm, values which are also quite typical in the cave environment. The PWP rates are depicted in Fig. 3, alongside the simplified linear relationship with two different values of α_s.

The form of the PWP equation over the relevant range is approximately linear for this example, except for the highly undersaturated end, suggesting that use of a linear function is reasonable in this case, except at nearly zero dissolved Ca. However, comparing the fiducial value of α_s used to create Fig. 1 above, with the best-fit value for the linear region of the PWP equation (Fig. 3), suggests that the value of α_s from Dreybrodt *et al.* (2005) is too small by about a factor of 3 to 4 in order to approximate the PWP rate. Consequently, the surface reaction line in Fig. 1 should be shifted up by a similar factor of 3 to 4. While this does imply that the surface rates are higher than would be predicted by the equation and parameter values given in Tab. 2.1 of Dreybrodt *et al.* (2005), the more accurate surface rates obtained from PWP are still much lower than the diffusive rates are predicted to be for the majority of the turbulent region of the parameter space (Fig. 1). For the convenience of future studies, a fitting function for PWP rates as a function of temperature and P_{CO_2} is provided in the Appendix. This relation is not used explicitly here, but provides a quick means of estimating PWP rates in a given setting.

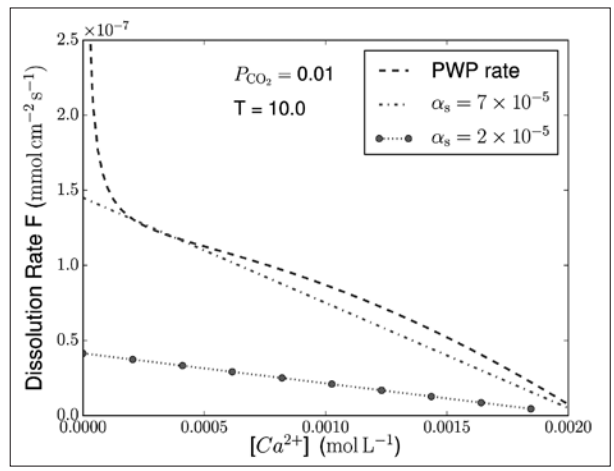

Fig. 3: The dissolution rate as a function of Calcium concentration for PCO$_2$ = 0.01 atm and T = 10 °C. This example is constructed to have a similar value of C_{eq} and temperature to the fiducial case from Dreybrodt et al. (2005).

COMPARING SURFACE-REACTION AND DIFFUSION RATES

The equations given above for diffusion-limited (Equation 1) or surface-limited rates (Equation 3) are only valid under conditions where dissolution is truly limited by the respective process. In steady state, diffusion and sur-

face reaction rates must be equal, and the rate of diffusion is given by

$$F_D = \frac{D(C_S - C_b)}{\epsilon}, \quad (6)$$

where C_s is the concentration at the surface, and C_b is the concentration in the bulk flow. For the diffusion-limited case $C_s \to C_{eq}$, and we recover Equation 1 above. Similarly, surface reaction rates are dependent on the concentration at the surface and are given by

$$F_s = \alpha_s(C_{eq} - C_s). \quad (7)$$

Again, if dissolution is reaction-limited $C_s \to C_b$ and we recover Equation 3. Setting diffusion and reaction rates equal, solving for C_s, and plugging this back into Equation 7, one can see that the dissolution rate accounting for both reaction and diffusion is given by

$$F = \frac{\alpha_s \alpha_d}{\alpha_s + \alpha_d}(C_{eq} - C_b), \quad (8)$$

where $\alpha_d = D/\epsilon$. The lines depicting the diffusion-limited rates in Fig. 1 are equivalent to α_d/α_s, so the analysis and conclusions of Covington *et al.* (2012) can also be cast in terms of the relative magnitudes of α_d and α_s. Therefore, if dissolution rates are well-represented by the linear relation in Equation 7, then the relative importance of diffusion and reaction in determining the overall rates can be quantified by comparing α_d and α_s. A critical diffusion boundary layer thickness, at which diffusion and reaction are equally important can be calculated by setting $\alpha_d = \alpha_s$, leading to

$$\epsilon_{crit} = D/\alpha_s. \quad (9)$$

When $\epsilon \gg \epsilon_{crit}$ then rates are diffusion-limited, and when $\epsilon \ll \epsilon_{crit}$ rates are reaction-limited. If $\epsilon \sim \epsilon_{crit}$ then dissolution will occur via mixed kinetics. At $\epsilon = \epsilon_{crit}$ diffusion surpresses dissolution rates to half of what they would be from surface reaction alone.

The above analysis relies on a surface reaction rate of the linear form given by Equation 7. However, it can be generalized using the full PWP dissolution rate. In the limit of a thick DBL the diffusion-limited equation can be applied, while in the limit of thin DBL the PWP surface rate can be applied. An estimate of ϵ_{crit} can be obtained by extrapolating the diffusion-limited equation until it intercepts the PWP surface rate (Fig. 4). Quantitatively, this results in the relation

$$\epsilon_{crit} = \frac{D(C_{eq} - C)}{F_{pwp}}. \quad (10)$$

When the DBL thickness is near this critical value, dissolution will occur via mixed kinetics, but when the DBL is much larger or smaller than ϵ_{crit} then dissolution rates will be limited by either diffusion or surface reaction, respectively. Using this relation, and the full PWP equation, one can calculate critical DBL thicknesses for a range of temperatures, P_{CO_2} values, and calcium concentrations. This calculation (Fig. 5) shows that the critical DBL thickness is on the order of magnitude of 1 mm for essentially the entire range of temperature, P_{CO_2}, and dissolved load found in natural karst systems, except in highly undersaturated conditions where $C \to 0$ and $\epsilon_{crit} \ll 1$ mm.

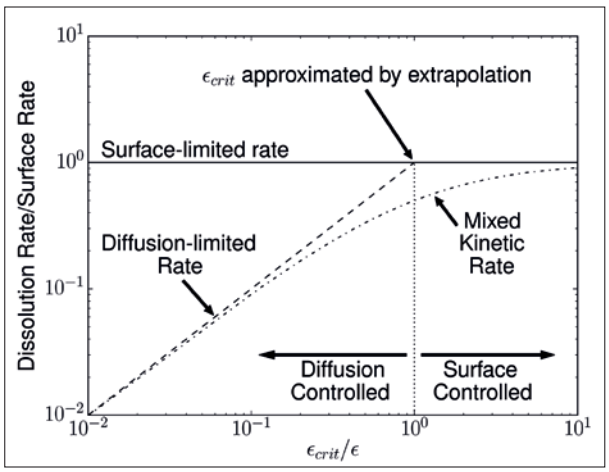

Fig. 4: The critical DBL thickness, below which dissolution rates are surface reaction-limited, can be estimated by extrapolating the diffusion-limited rate until it intersects the surface-limited rate determined by the PWP Equation. This leads to the relation in Equation 10. Though this approximation scheme can be employed more generally, the lines plotted in this figure represent exactly the case where the rates can be approximated using α_D and α_s.

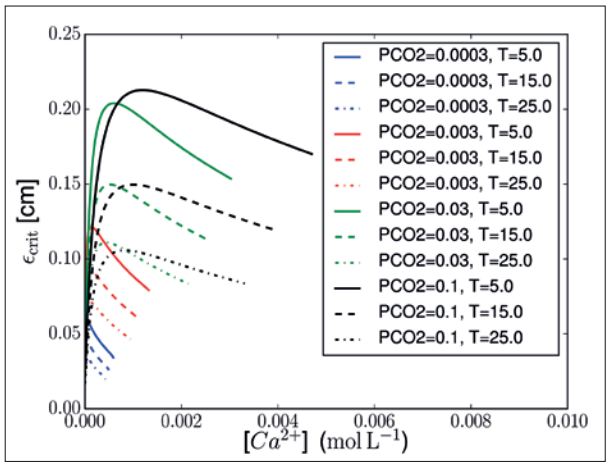

Fig. 5: The critical DBL thickness, below which dissolution rates are surface reaction-limited, shown for a wide range of temperature, P_{CO_2} values, and dissolved loads. Lines terminate on the right-hand side at saturation.

The approximation $\epsilon_{crit} \sim 1$ mm can also be reproduced using a rough estimate of PWP rates. In most natural settings, the forward reaction rate is dominated by reaction III (κ_3 in the PWP equation) (Dreybrodt 1988). This rate is simply a function of temperature and is on the order of 10^{-10} mol cm^{-2} s^{-1} (Dreybrodt 1988, p. 127). Critical DBL thickness can then be estimated as

$$\epsilon_{crit} \sim \frac{DC_{eq}}{\kappa_3} = \frac{(10^{-5}\ \mathrm{cm^2\ s^{-1}})(2\times10^{-6}\ \mathrm{mol\ cm^{-3}})}{10^{-10}\ \mathrm{mol\ cm^{-2}}} = 0.2\ \mathrm{cm} \quad (11)$$

which is quite similar to the result of 1 mm obtained from the larger parameter study (Fig. 5).

Within speleogenesis models DBL thickness is usually estimated from a relationship for pipe flow that employs the Sherwood Number (Sh),

$$\epsilon = D_H/\mathrm{Sh}, \quad (12)$$

where Sh is given by an empirical relationship such as

$$\mathrm{Sh} = \frac{(f/8)(\mathrm{Re} - 1000)\mathrm{Sc}}{1+12.7\sqrt{f/8}(\mathrm{Sc}^{2/3} - 1)} \quad (13)$$

(Dreybrodt *et al.* 2005). Here, Re is the Reynolds number, Sc is the Schmidt number, and f is the Colebrook-White friction factor. Using these relations, one can calculate typical values of DBL thickness, (ϵ), for a selection of head gradients and hydraulic diameters (Fig. 6). Again, for this calculation a relative pipe roughness of 0.05 is assumed, though the result is not particularly sensitive to this choice. Typical values of the DBL thickness under turbulent conditions, as calculated from Sherwood Number, are much less than the order of magnitude estimate of a critical DBL thickness of 1 mm. This is true for all turbulent flow cases except those at very low head gradients (i.e. 10^{-5}).

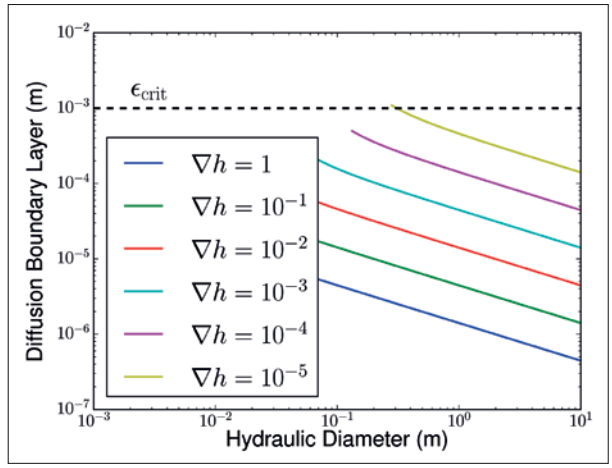

Fig. 6: DBL thickness (ϵ) under turbulent flow conditions as estimated from Sherwood number for a wide range of hydraulic parameters. Each line represents a choice of head gradient. The lines terminate on the left at Re = 4000, where the Colebrook-White formulation breaks down. Typical values of DBL thickness as estimated from Sherwood Number are much less than the 1 mm magnitude of the critical value determined from the PWP equations.

CONCLUDING THOUGHTS AND POTENTIAL RESOLUTIONS

A more careful analysis reinforces the conundrum. The theory suggests that limestone dissolution rates under turbulent flow conditions should be typically limited by surface reaction rates. However, field observations of scallops and other solutional forms clearly suggest otherwise. A recent model developed using PWP dissolution equations and computational fluid dynamics also found that limestone dissolution flutes were unstable under the calculated dissolution rates, though flutes in gypsum, which has much higher surface rates, proved to be somewhat more stable (Hammer *et al.* 2011). Superficially, this result is in agreement with the analysis presented here, and may provide further evidence of difficulties with the current theory. The central purpose of this letter is to clearly state the problem, rather than to solve it, in hopes of stimulating some discussion on the subject. However, I here discuss a few potential resolutions.

Perhaps the most suspicious component of the turbulent dissolution model is the semi-empirical equation used to calculate Sherwood Number (Eqn. 13), and consequently DBL thickness (Eqn. 12). This equation is based on experiments in smooth pipes, and therefore ought to be used with caution when calculating DBL thickness for the rough and irregular surfaces found on natural bedrock channel walls. However, the experiments of Blumberg & Curl (1974) provide a means of checking this as a potential resolution. Mass transfer data from their experiments with flutes in gypsum suggest a typical DBL thickness of $\epsilon = 0.0089\ \mathrm{L\ Sc^{-1/3}}$, where L is the flute length and Sc is the Schmidt Number, with Sc $\gtrsim$ 1000 for water at the relevant temperatures. This results in a DBL thickness that is roughly $\lesssim$0.1% of the flute length. In combination with the estimate of critical DBL thickness of 1 mm for limestone, this result suggests that such solutional forms should develop, but only on length scales of a meter or greater. This again is in conflict with field observations, where scallops and flutes often form on length scales of centimeters (Fig. 2).

Another possibility is that the rates estimated by the PWP equation are significantly lower than rates on natural surfaces. In fact, several studies of dissolution rates measured on rotating disks produce rates that are approximately twice those given by the PWP equation (Dreybrodt & Buhmann 1991; Liu & Dreybrodt 1997). These studies have suggested that increased surface roughness, and therefore surface area, on the disks may result in the higher apparent dissolution rates. Similarly, roughness on natural limestone surfaces on a smaller scale than the DBL thickness could result in an apparent increase in surface reaction rates that would reduce the critical DBL thickness. However, the observed discrepancy of a factor of two is not sufficient to explain away the conundrum by itself. If natural surfaces are still significantly rougher at scales below the DBL thickness than the disks used in experiments, this could potentially resolve the problem. Other factors, such as microbial films, could also influence surface reaction rates, and perhaps in some cases increase them.

One might ask whether a very small contrast in dissolution rates would be sufficient to form flutes and scallops. However, flute experiments show that dissolution rates vary by roughly a factor of two over the length of a flute (Blumberg & Curl 1974), a number that is thought to be relatively constant across the parameter space (Curl 1966). A constrast in dissolution rates of a factor of two requires that the thickest portion of the DBL within the scallop is greater than or equal to the critical thickness, as this is the DBL thickness when surface rates are suppressed by roughly a factor of two. A thinner DBL would not allow sufficient contrast in rates.

Forms somewhat similar to scallops (mechanical erosion flutes) also are found in bedrock channels in relatively insoluble rocks, though the variety and prevalence of such forms is greatest in highly soluble rocks (Richardson & Carling 2005). One possible explanation is that so-called solutional forms, such as scallops and flutes, actually form by a combination of solutional and mechanical processes. For example, chemical processes could loosen individual grains that are later plucked from the surface by mechanical processes.

Finally, it could be that scallops form only in highly aggressive waters, where the critical DBL thickness is sufficiently small (Fig. 5). However, the author's experience would suggest that scallops are also present in locations without such highly aggressive water. Little systematic attempt has been made to study the locations in which scallops form, and whether forms differ according to hydrological or lithological settings. Such studies might also provide clues as to the correct resolution of the current conundrum.

ACKNOWLEDGMENTS:

I would like to acknowledge Franci Gabrovšek, Matija Perne, Joe Myre, Wolfgang Dreybrodt, and Douchko Romanov for stimulating discussions and useful comments. This material is based upon work supported by the National Science Foundation under Grant No. EAR 1226903. Any opinions, findings, and conclusions or recommendations expressed in this material are those of the author and do not necessarily reflect the views of the National Science Foundation.

REFERENCES

Birk, S., Liedl, R., Sauter, M. & G. Teutsch, 2005: Simulation of the development of gypsum maze caves.- Environmental Geology, 48, 3, 296–306.

Blumberg, P. & R.L. Curl, 1974: Experimental and theoretical studies of dissolution roughness.- Journal of Fluid Mechanics, 65, 4, 735–751.

Buhmann, D. & W. Dreybrodt, 1985: The kinetics of calcite dissolution and precipitation in geologically relevant situations of karst areas: 1. Open system.- Chemical Geology, 48, 1–4, 189–211.

Covington, M.D., Luhmann, A.J., Wicks, C.M. & M.O. Saar, 2012: Process length scales and longitudinal damping in karst conduits.- Journal of Geophysical Research, 117, F1, 1–19.

Covington, M.D., Prelovšek, M. & F. Gabrovšek, 2013: Influence of CO_2 dynamics on the longitudinal variation of incision rates in soluble bedrock channels: Feedback mechanisms.- Geomorphology, 186, 85–95.

Curl, R.L., 1966: Scallops and Flutes.- Transactions of the Cave Research Group of Great Britain, 7, 2, 121–160.

Curl, R.L., 1974: Deducing flow velocity in cave conduits from scallops.- National Speleological Society Bulletin, 36, 2, 1–5.

Dreybrodt, W., 1988: *Processes in Karst Systems: Physics, Chemistry, and Geology.*- Springer, pp. 288, New York, USA.

Dreybrodt, W., 1996: Principles of early development of karst conduits under natural and man-made conditions revealed by mathematical analysis of numerical models.- Water Resources Research, 32, 9, 2923.

Dreybrodt, W. & D. Buhmann, 1991: A mass transfer model for dissolution and precipitation of calcite from solutions in turbulent motion.- Chemical Geology, 90, 1–2, 107–122.

Dreybrodt, W., Gabrovšek, F. & D. Romanov, 2005: *Processes of Speleogenesis: A Modeling Approach.*- ZRC Publishing, pp. 376, Ljubljana, Slovenia.

Goodchild, M. & D. Ford, 1971: Analysis of scallop patterns by simulation under controlled conditions.- Journal of Geology, 79, 1, 52–62.

Hammer, Ø., Lauritzen, S.E. & B. Jamtveit, 2011: Stability of dissolution flutes under turbulent flow.- Journal of Cave and Karst Studies, 73, 3, 181–186.

Kaufmann, G., 2009: Modelling karst geomorphology on different time scales.- Geomorphology, 106, 1–2, 62–77.

Liu, Z. & W. Dreybrodt, 1997: Dissolution kinetics of calcium carbonate minerals in H_20–CO_2 solutions in turbulent flow: the role of the diffusion boundary layer and the slow reaction $H_2O + CO_2 \leftrightharpoons H^+ + HCO_3^-$.- Geochimica Cosmochimica Acta, 61, 14, 2879–2889.

Morse, J. & R. Arvidson, 2002: The dissolution kinetics of major sedimentary carbonate minerals.- Earth-Science Reviews, 58, 51–84.

Perne, M., 2012: *Modelling speleogenesis in transition from pressurised to free surface flow.*- Ph.D. thesis, University of Nova Gorica.

Plummer, L., Wigley, T. & D.L. Parkhurst, 1978: The Kinetics of Calcite Dissolution in CO_2- Water Systems at 5° to 60 °C and 0.0 to 1.0 ATM CO_2.- American Journal of Science, 278, 179–216.

Rehrl, C., Birk, S. & A.B. Klimchouk, 2008: Conduit evolution in deep-seated settings: Conceptual and numerical models based on field observations.- Water Resources Research, 44, 11, 1–13.

Richardson, K. & P. Carling, 2005: *A typology of sculpted forms in open bedrock channels. Special Publication 392.*- Geological Society of America, pp. 108, Boulder, Colorado.

Rickard, D. & E. Sjöberg, 1983: Mixed kinetic control of calcite dissolution rates.- American Journal of Science, 283, 815–830.

Szymczak, P. & A.J. Ladd, 2011: The initial stages of cave formation: beyond the one-dimensional paradigm.- Earth and Planetary Science Letters, 301, 3–4, 424–432.

APPENDIX: AN APPROXIMATION FOR THE PWP EQUATION

The PWP equation is roughly a linear function of $(C_{eq} - C)$ between 10% and 90% of saturation for a wide range of temperatures and P_{CO_2} values. To facilitate future work with PWP rates, I present a fitting function for the rate constant α_s,

$$\log(\alpha_s) \approx A + B_1 T + B_2 \log(P_{CO_2}) + C_1 T_2 + C_2[\log(P_{CO_2})]^2 , \quad (14)$$

where the best fit values of the parameters are given in Tab. 1. To determine this relationship, I calculated PWP rates for 100 calcium concentration values from 10% to 90% saturation for each of 100 different values of P_{CO2} sampled evenly in log space in the range $3\times10^{-4} \leq P_{CO2} \leq 0.1$ and for 11 different values of temperature in the range 0 °C ≤ T ≤ 24 °C. For each choice of T and P_{CO2} a best fit value of α_s for the relation $F_{pwp} = \alpha_s(C_{eq} - C)$ was calculated using least squares. This resulted in 1100 values of α_s for a range of T and P_{CO2} conditions. Typical residuals between the linear relation and the full PWP equation are about 10%. The maximum residuals for any of the fits are around 70% and occur near saturation for cases with high P_{CO2} .

Parameter	Best fit value
A	−4.30
B_1	1.40×10^{-2}
B_2	0.150
C_1	-2.83×10^{-5}
C_2	8.76×10^{-2}

Table 1: Best fit parameters for the equation for the linear approximation to the PWP dissolution rate equation.

The parameters in the best fit relation above (Eqn. 14) were determined via least squares fitting of these 1100 values of α_s. Eqn. 14 reproduces the best fit values of α_s within 10%. Therefore, this relation is not intended for precision work, but can allow quick estimation of PWP rates according to a simpler relation. In addition to the fitting relation, the Python code used to calculate PWP rates is available online at http://www.speleophysics.com. All calculations shown above employed the full PWP equation rather than the approximation given by Eqn. 14.

Acta carsologica

43, 1 (2014)

Izdala in založila / Published by
Slovenska akademija znanosti in umetnosti / Slovene Academy of Sciences and Arts
in / and
Znanstvenoraziskovalni center SAZU / Scientific Research Centre of the SASA
v Ljubljani / in Ljubljana

Grafična priprava in tisk / Layout and print
Inženiring grafičnih storitev, d.o.o., Ljubljana

Naklada 500 izvodov / Printed in 500 copies

Organizacija Združenih narodov za izobraževanje, znanost in kulturo

United Nations Educational, Scientific and Cultural Organization

Slovenska nacionalna komisija za UNESCO

Slovenian National Commission for UNESCO

ACTA CARSOLOGICA

ISSN 0583-6050 · LETNIK/ VOLUME 43 · ŠTEVILKA/NUMBER 1 · LJUBLJANA 2014

ISSN 0583-6050